A Comparative Study of the Evolution of Mammalian High-Frequency Hearing and Echolocation

Betkowska-Davies, Kalina

A Comparative Study of the Evolution of Mammalian High-Frequency Hearing and Echolocation

Kalina Bętkowska-Davies
School of Biological & Chemical Sciences
Queen Mary University of London
Mile End Road, London, E1 4NS

A thesis submitted to the
University of London for the
Degree of Doctor of Philosophy
February 2012

Declaration

I certify that the research presented in this thesis is the product of my own work, and all ideas and quotations of the work of other people, published or otherwise, are fully acknowledged in accordance with standard referencing practices of the biological sciences.

I acknowledge the particular data acquisition and analytical contributions of my supervisors and advisors as follows:

Stephen Rossiter allowed access to unpublished assembled short read Solexa data for use in Chapters 2 and 3.
James Cotton performed the branch-wise convergence significance tests in Chapter 2.
Georgia Tsagkogeorga performed genomic blast searches for Chapter 2 and 3, and also wrote and executed Perl scripts to estimate missing data and individual CNE rates of substitution in BASEML.
Norman MacLeod wrote and provided programs to perform Eigenshape analyses and construct models in Chapters 4 and 5.
Richie Abel and Stig Walsh aided with μCT scan acquisition for Chapters 4 and 5.

All views expressed in the thesis, unless otherwise referenced, are those of the author and do not express the views of Queen Mary, University of London.

Kalina Bętkowska-Davies

Acknowledgments

I would firstly like to thank my supervisor, Stephen Rossiter, for all his guidance, encouragement and support throughout my study. I am also grateful to Emma Teeling and James Cotton for all their help and advice relating to data acquisition and analysis. Also I thank Greg Elgar for initiating the CNE study, and the members of his lab who helped with the lab work and provided useful discussion during the data collection stage. I am especially grateful to Norman MacLeod, who first introduced me to geometric morphometrics and enabled the morphological study to take place.

I would especially like to thank all the members, past and present, of the lab: Matt Struebig, Lee-Sim Lim, Hao-Chih Kuo, Helen Ward, Georgia Tsagkogeorga and Joe Parker. Also all the members of SBCS who were always on hand for help and advice; in particular: Elizabeth McCarthy, Anja Nenninger, Giulia Mastroianni and Kofan Chen. I am grateful to all the members of the UCD bat lab - thank you for looking after me in Dublin! In particular, I thank Alisha Goodbla, Michael Beckaert, Sebastian Peuchmaille, and Serena Dool. I am especially grateful to Serena Dool for taking me out in the 'field' and some truly memorable experiences of Ireland! Also, I thank Katherine Brown for numerous pearls of wisdom and sharing the joys of phylogenetics. Also thanks to Richie Abel and Stig Walsh; who introduced me to CT scanning and answered all my questions. I am especially grateful to Paul Bates and everyone at the Harrison Institute, who were very generous with their time and specimens.

Throughout the last few years I feel exceptionally lucky in being able to have visited many different institutions and met many enthusiastic and motivational researchers. It would be impossible to list everyone who has provided me with the motivation and encouragement I needed to pursue my PhD – but thank you all. My project was possible due to generous funding from NERC, CRF, CEE and SRF; and additional support from the Teeling lab. I also thank Dr Anjali Goswami and Dr Nick Mundy for their consideration of my work.

Finally, I thank my friends and family who have provided much support and encouragement throughout my PhD.

Abstract

The lineage that gave rise to mammals split from other basal amniotes, approximately 300 million years ago. Since then, mammals have evolved many sensory novelties, including high-frequency hearing and echolocation. Sensitivity to high frequencies is particularly well developed in many echolocating mammals; for example, the upper hearing limit of several laryngeal echolocating bat species are estimated to be approximately ten times that of humans. In order to process the high frequency sounds produced during echolocation, the inner ears of laryngeal echolocating bats have undergone substantial modifications. Despite the evolutionary significance of laryngeal echolocation, it is unknown how many times it evolved within bats. Its occurrence on most, but not all, bat lineages suggests it either evolved once with secondary loss, or independently on multiple lineages. Distinguishing between these possibilities is complicated by morphological diversity and convergence. Furthermore, the genetic basis underpinning echolocation remains largely unknown.

To elucidate the evolutionary history of this key trait in bats, a combined molecular and morphological approach was taken. Firstly, for two mammalian 'hearing genes' sequence convergence, phylogenetic signal and selection pressures were examined across echolocating and non-echolocating mammal species. Secondly, substitution rates of Conserved Non-coding Elements associated with genes regulating ear development were compared across mammals. Finally, as mammalian inner ear development is controlled by many genes, the gross structure of the bony labyrinth was studied in order to examine the combined genetic effect. Structural variation of bat cochleae and vestibular systems was examined using micro-computed tomography reconstructions, and related to ecological data.

Subsequent analyses found evidence of convergence at the molecular level, in terms of amino acid substitutions, and also the morphological level, in terms of inner ear morphology. No evidence of degeneration, supporting loss-of-function in Old World fruit bats was found. Conversely, evidence of differential evolution pressures acting on the two echolocating bat lineages was found, which supports multiple origins of laryngeal echolocation in bats.

Contents:

List of figures

List of tables

Abbreviations

AIC	-	Akaike information criterion
BEB	-	Bayes empirical Bayes
BP	-	Base pair
BPP	-	Bayesian posterior probability
BS	-	Bootstrap
CF	-	Constant frequency
CNE	-	Conserved non-coding element
CVA	-	Canonical variates analysis
DIC	-	Deviance information criterion
d_n	-	Rate of nonsynonymous substitutions
d_s	-	Rate of synonymous substitutions
d_n/d_s	-	Omega (ω)
DSC	-	Doppler shift compensation
ESA	-	Eigenshape analysis
FA	-	Forearm length
FM	-	Frequency modulated
IHC	-	Inner hair cell
KB	-	Kilo-base
(k)Hz	-	(kilo)hertz
LRT	-	Likelihood ratio test
µCT	-	Micro-computed tomography
Ma	-	Mega-annum
MB	-	Mega-base
ML	-	Maximum likelihood
NSHL	-	Non-syndromic hearing loss
OHC	-	Outer hair cell
OLS	-	Ordinary least squares
PCA	-	Principal component analysis
PCR	-	Polymerase chain reaction
PI	-	Prediction interval
PJVK	-	Pejvakin (Autosomal recessive deafness type 59 protein)
R	-	Radius of curvature
RMA	-	Reduced major axis
SCC	-	Semicircular canal
TMC1	-	Transmembrane channel-like protein 1
WAR	-	Wing aspect ratio
WL	-	Wing loading
WTS	-	Wing tip shape index
VOR	-	Vestibulo-ocular reflex

Gene Nomenclature

Human gene capitalised – e.g. *TMC1*
Mammalian orthologs lowercase – e.g. *Tmc1*
Gene symbols italicised – e.g. *Tmc1*
Encoded protein non-italicised – e.g. Tmc1

CHAPTER ONE

General Introduction

Phylogenetics and our understanding of adaptations

Mammals have been very successful in terms of species number and global distribution, with representatives currently found on all continents including Antarctica. They have become highly adapted to diverse environmental niches and, therefore, selection pressures have resulted in some extreme morphological adaptations, for example, the flight membranes of flying lemurs, and the loss of limbs in aquatic cetaceans.

In the earlier days of systematics and taxonomy only morphological characters were available to classify organisms, which, as described above, can often be highly sculpted by an animal's niche. Despite this, using relationships based on morphological features it was possible to form the basic backbone of mammalian evolutionary history (as reviewed in Novacek 1992). However, with the onset of molecular evidence, much of the early understanding of mammalian systematics has been shown to be incorrect (e.g. Murphy *et al.,* 2001a). The principal reason for many of the former erroneous relationships is the evolution of similar phenotypic features in unrelated taxa, that have arisen due to convergent evolution and not common descent (e.g. Luo 2007). Conversely, there are numerous cases of related taxa that show very divergent phenotypes. As such, molecular tools have not only greatly increased our confidence in mammalian systematics, but perhaps more importantly have also enhanced our understanding of the power of ecological selection in driving morphological change.

The proliferation of molecular sequence data has led to a dramatic improvement in our knowledge of higher mammal classification, and also brought about radical changes to the established view. Examples of reorganisations include paraphyly of the former order Insectivora, with some members joining the newly recognised monophyletic superorder Afrotheria (Springer *et al.,* 1997; Stanhope *et al.,* 1998; Malia Jr. *et al.,* 2002). This rearrangement illustrates how morphologically similar species can be taxonomically divergent, and thus highlights parallel adaptive radiations within two mammalian superorders (Table 1.1) (Madsen *et al.,* 2001).

Table 1.1 Phenotypic convergence between members of Laurasiatheria and Afrotheria.

Laurasiatheria		Afrotheria	Adaptation / Niche
Pangolins	and	Aardvarks	Digging / Myrmecophagy
Cetaceans	and	Sirenians	Loss of limbs, fully aquatic
True moles	and	Golden moles	Subterranean insectivores
Shrews	and	Shrew tenrecs	Terrestrial insectivores
Hedgehogs	and	Madagascar hedgehog tenrec	Spiney terrestrial insectivores
Otters	and	African otter shrews	Semi-aquatic carnivores

Another example of when phenotypic convergence led to the incorrect grouping of unrelated taxa is the former superorder Archonta, which included primates, treeshrews (Scandentia), flying lemurs (Dermoptera) and bats (Chiroptera). The erroneous association of bats and flying lemurs was based on convergent features associated with flight and gliding, respectively (as discussed in Simmons and Geisler 1998). Despite contradictory morphological characters resulting in considerable debate, the correct relationships were only resolved with the addition of molecular information (e.g. Miyamoto *et al.,* 2000; Murphy *et al.,* 2001b).

Gradually a consensus for the ordinal and superordinal relationships of mammals is now being approached (Kriegs *et al.,* 2006; Nishihara *et al.,* 2006; Murphy *et al.,* 2007) and, as future genome sequencing projects and analytical methods advance, it seems likely that an undisputed phylogeny will soon be established. Such information will not only provide a key insight into the evolutionary past of mammal species, but perhaps more importantly, will provide a key tool with which to study the many adaptations of the 5,000, or so, currently known species.

Evolutionary history of bats

Bats belong to the order Chiroptera, derived from the two Greek words - *cheir* meaning "hand" and *pteron* "wing". This refers to their forelimbs that are uniquely modified into wings, with bats being the only mammals to have ever evolved true powered flight. Colloquially, the bat has received many labels, from ‘the little evening one’ - due to their primarily nocturnal habits - to the wholly misconceived ‘blind mouse’ – being neither blind, nor closely related to rodents. Throughout history bats have remained enigmatic in popular views, and frequently misunderstood, and it is only within the last century that major advances in our understanding of their ecology and taxonomy have been made (e.g. Pierce and Griffin 1938; Hutcheon *et al.,* 1998). Yet many questions

concerning the taxonomy and evolution of bats remain unanswered. Therefore, our understanding of the group is set to benefit further as more molecular data become available. The sheer number of bat species - a total of 1,133 extant species have so far been documented (Reeder *et al.,* 2007) - makes them a hugely significant and important group for biological and evolutionary research. Moreover, once their many key innovations, behavioural traits, morphological specialisations, ecosystem roles and adaptive radiations have been considered, they become a truly exceptional group.

Bats are first known from the fossil record of the Early Eocene (Simmons *et al.,* 2007). Since the Eocene they radiated to exploit a range of niches, resulting in correspondingly disparate morphologies and ecologies (Fenton 2010). For example, the insectivorous bumblebee bat, *Craseonycteris thonglongyai*, is arguably the world's smallest mammal at 2 g (Pereira *et al.,* 2006), while the frugivorous Indian flying fox, *Pteropus giganteus,* weighs 1.2 kg and has a wingspan of 1.25 m (Norberg and Rayner 1987). The vast majority of bat species are insectivorous, but the order also includes frugivorous, nectarivorous (including pollen eaters), carnivorous (feeding on small vertebrates, including fish) and sanguinivorous members (Neuweiler 2000). Dietary niches are often accompanied by adaptations in hunting or foraging strategy, tooth and skull morphology, and, in echolocating species, echolocation call-structure. Some of the best examples of these adaptations are within the New World leaf-nosed bats (Phyllostomidae), which show a particularly wide range of diets (Bogdanowicz *et al.,* 1997; Baker *et al.,* 2011). More broadly, there are numerous examples of convergent phenotypes (e.g. Teeling *et al.,* 2002), cryptic species (e.g. Thabah *et al.,* 2006), adaptive radiations (e.g. Freeman 2000), resource partitioning (e.g. Kingston *et al.,* 2000), character displacement (e.g. Russo *et al.,* 2007) and possible cases of sympatric speciation (e.g. Kingston and Rossiter 2004). Bats are also commercially important; species such as *Eonycteris spelaea* pollinate crops (Bumrungsri *et al.,* 2009) while others, such as *Tadarida brasiliensis* control pests (Cleveland *et al.,* 2006).

The two key innovations of bats

Bats are remarkable vertebrates for two reasons: flight and echolocation. These highly specialised mammals are one of only three vertebrate groups to have evolved powered flight, with a modified forelimb, two-layered membrane and cutaneous muscles forming the wing (Neuweiler 2000). Bats also exhibit one of the most highly-developed systems of echolocation (Pye 1983), which is used by all echolocating species for orientation,

and by most species for additional purposes, such as prey detection (Schnitzler and Kalko 2001). Together these two features are recognised as the key innovations that likely account for the global success of bats (Jones and Teeling 2006). Indeed, among mammals, these two adaptations have allowed bats to occupy the previously unexploited niche of nocturnal flying insects, which other competitors, such as most birds, could not due to visual limitations (Fenton 1974).

The basic bat body plan was established early in their evolutionary history, as documented by Early Eocene fossils. For example, two of the earliest known bat fossils, *Onychonycteris finneyi* and *Icaronycteris index,* dated from approximately 52.5 million years (Ma) ago, show forelimb anatomy indicative of powered flight (Gunnell and Simmons 2005; Simmons *et al.,* 2008). Interestingly, *O. finneyi* has intermediate limb proportions between modern bats and non-volant mammals, with reconstructed wing parameters suggesting undulating gliding–fluttering flight (Simmons *et al.,* 2008). Based on wing morphology the ecology of the younger Messel fossil bats, (*Archaeonycteris*, *Hassianycteris* and *Palaeochiropteryx*) dated at around 40-50 Ma ago, have been reconstructed (Habersetzer and Storch 1989). Each species putatively occupied different levels of the canopy, with species such as *Palaeochiropteryx* predicted to hunt close to the ground or within vegetation. Therefore, it can be assumed that flight evolved some time prior to the late-Early Eocene (Gunnell and Simmons 2005).

To date, the inner ear dimensions of 7 fossil bat genera have been examined (Simmons *et al.,* 2008). Typically cochlear diameter relative to either skull length (e.g. Novacek 1987; Habersetzer and Storch 1989) or basicranial width (e.g. Habersetzer and Storch 1992) is used as a measure of size. Relative cochlear size can then be used to infer the echolocation capability of extinct taxa, as there is little documented overlap (see below) in cochlear size between laryngeal echolocating bats and Old World fruit bats. Cochleae size of *Hassianycteris messelensis*, *Tachypteron franzeni* and *Tanzanycteris mannardi* has been shown to be comparable to laryngeal echolocating bats (Habersetzer and Storch 1992; Simmons and Geisler 1998; Gunnell *et al.,* 2003). *Tanzanycteris mannardi* and *Tachypteron franzeni* have been dated to the early Lutetian (46 Ma ago), with the latter assigned to the Emballonuridae (Storch *et al.,* 2002; Gunnell *et al.,* 2003). *Tanzanycteris mannardi* possesses the largest cochlea size of all Eocene bats so far measured. It is comparable in size to those of extant rhinolophids, which may indicate it

was capable of sophisticated high-duty-cycle constant frequency (CF) echolocation (Gunnell *et al.,* 2003). Whereas, *H. messelensis* and *T. franzeni* have been hypothesised to possess echolocation comparable to the extant Emballonuridae (Storch *et al.,* 2002). For the remaining Messel species, cochlear size of *Palaeochiropteryx spp.* fall between Old World fruit bats and laryngeal echolocating bats, and *Icaronycteris index* and *Archaeonycteris spp*. fall closer to the Old World fruit bat distribution (Habersetzer and Storch 1992; Simmons *et al.,* 2008). However, an analysis using cochlea width and skull length, recovered *Icaronycteris* and *Palaeochiropteryx* within laryngeal echolocating bats (Novacek 1987). Furthermore some laryngeal echolocating bats, including members of Phyllostomidae and Megadermatidae, posses relative cochleae more similar in size to those of non-echolocating Old World fruit bats than the remaining laryngeal echolocating bats (Habersetzer and Storch 1992). This documented overlap in cochlear size between Old World fruit bats, *I. index, Archaeonycteris spp,* and some laryngeal echolocating bats, has been taken by some as evidence of residual features of early echolocation in the former group (Springer *et al.,* 2001).

In addition to cochlear enlargement, two osseous characters (orbicular process on malleus and cranial expansion of stylohyal) are said to indicate laryngeal echolocation (Simmons and Geisler 1998). Both characters are present in *Icaronycteris, Archaeonycteris, Hassianycteris* and *Palaeochiropteryx* (Simmons *et al.,* 2008). Unfortunately, these characters could not be recorded in *Tanzanycteris* and *Tachypteron*. Gross cochlea structure of two Messel bats, *Palaeochiropteryx* and *Hassianycteris,* indicate 2.5 turns without enlargement of the basal turn (Habersetzer and Storch 1989). Therefore, based on all these features it has been concluded that *Icaronycteris*, *Archaeonycteris* and *Palaeochiropteryx* were most likely capable of a primitive form of echolocation e.g. short multi-harmonic pulses or frequency modulated (FM) calls (Habersetzer and Storch 1992; Simmons and Geisler 1998). Furthermore, fragmented insect remains have been found in the stomach contents of some Messel bats indicating they were capable of catching adequate prey, and thus further supporting the hypothesis that echolocation was likely (Habersetzer *et al.,* 1994; Simmons and Geisler 1998).

The measured cochlear width of *Onychonycteris finneyi* falls cleanly within the Old World fruit bat distribution (Simmons *et al.,* 2008). Furthermore, both additional echolocation osseous characters, mentioned above, are absent. It has thus been

concluded that *O. finneyi,* the most primitive bat discovered so far, was most likely capable of powered flight but not laryngeal echolocation (Simmons *et al.,* 2008). Thus it seems probable that powered flight evolved prior to echolocation in bats. Therefore, in combination, fossil evidence provides the possible time period during which echolocation evolved. However, as a robust phylogeny indicating the correct placement of the fossil taxa in relation to extant taxa is currently lacking (e.g. Eick *et al.,* 2005), ancestral echolocation state reconstructions alone cannot reveal how many times laryngeal echolocation has evolved.

Several intriguing fossil finds have further implications for the origins of bat echolocation. A notable case is the discovery of a fossilised moth egg, putatively assigned to the Noctuidae; these moths possess hearing organs hypothesised to have evolved as a defence against predation by echolocating bats (Gall and Tiffney 1983). However, this fossil egg considerably predates the supposed timing of the origin of echolocation. Another case is the earliest known bat fossil from Murgon, Australia, which is dated at 54.6 Ma old (Hand *et al.,* 1994), this raises questions regarding early bat diversification across the globe. Problems of reconstructing bat evolution are complicated by the absence of Palaeocene fossils, and also transitionary forms between either non-volant to volant or non-echolocating to echolocating taxa. This probably reflects the depauperate fossil record, recent estimates suggest up to 88% of all bat genera that ever existed are absent from the fossil record (Eiting and Gunnell 2009). Therefore, the timing and mechanism involved in the acquisition of echolocation currently remains unclear, with the fossil record alone unlikely to be able to provide the answers.

What is echolocation?

Echolocation is summarised as an active process by which an animal uses the echoes of its own emitted sound-waves to build a 'sound picture' of its immediate environment (Altringham 1996). Among mammals, sophisticated echolocation, utilising ultra-sonic sounds, have evolved independently in bats and toothed cetaceans (Thomas *et al.,* 2004). The Old World fruit bat genus, *Rousettus,* has also evolved a different kind of echolocation which utilises audible tongue-clicks (Pye and Pye 1988), it has also been postulated that the cave roosting fruit bat, *Eonycteris spelaea*, may use echoes in the roost by clapping its wings during flight (Gould 1988). In birds, echolocation has evolved independently at least twice, in cave swiftlets, *Aerodramus spp.,* (Griffin and

Thompson 1982) and oilbirds, *Steatornis caripensis* (Konishi and Knudsen 1979). However, in these birds and Old World fruit bats, it is almost certain that echolocation has no role in prey detection (Iwaniuk *et al.,* 2006).

Theoretical and empirical research has linked echolocation to the demands of occupying a three dimensional aerial niche, and as such it is currently debated as to whether echolocation occurs in any terrestrial vertebrates. However, there is some evidence of the use of echo derived information in shrews (e.g. Forsman and Malmquist 1988; Siemers *et al.,* 2009) and Tenrecs (Gould 1965).

Call production

In bats, all but one of the 19 recognised families produce echolocation vocalisations with the larynx (so-called 'laryngeal echolocation'). As with other mammal vocalisations, bat ultrasound is generated by vibrations of the vocal chords (Fenzl and Schuller 2007). Although the bat vocal tract itself has been described as typical of other modern mammals (Fenzl and Schuller 2007), there have been several modifications. For example, the larynx of echolocating bats is displaced to allow bats to breathe through the nose even when swallowing (Neuweiler 2000). Furthermore, the supporting structures of the larynx are highly modified (Fenzl and Schuller 2007), and in all echolocating bats studied to date, articulation between the stylohyal and tympanic bones has been found, which may provide additional support during echolocation call emission (Simmons *et al.,* 2010; Veselka *et al.,* 2010a). As mentioned, the only Old World fruit bat genus known to echolocate is *Rousettus*, which produces tongue-clicks which are audible to man, and, therefore are not ultrasonic (Pye and Pye 1988; Giannini and Simmons 2003).

Call emission

Bats emit echolocation calls through the mouth or nose (Pedersen 1993; Neuweiler 2000). Nasal emitters include Rhinolophidae, Hipposideridae, Rhinopomatidae, Megadermatidae, Phyllostomidae and Nycteridae, and can be distinguished by the presence of a noseleaf (see Fig.1.1). Noseleaves are fleshy protrusions located around the nostrils, and are made up of two main parts – the horseshoe and spear. Although the precise role noseleaves play in call emission is unclear, some studies suggest they focus the emitted sound into a directional beam (Zhuang and Muller 2006). Correlations have

been found between noseleaf width and echolocation calls in members of the horseshoe and roundleaf bats (Rhinolophidae and Hipposideridae, respectively) (Robinson 1996), and also between noseleaf width and diet in members of the New World leaf-nosed bats (Phyllostomidae) (Bogdanowicz *et al.,* 1997). Oral emission of echolocation calls is found in a greater number of bat families, and it is generally thought of as the ancestral state for bats capable of echolocation (Pedersen 2000; Jones and Teeling 2006). Echolocation emission in the mono-specific family Craseonycteridae remains somewhat undetermined, however, despite the presence of narial pads, it has been documented as an oral emitter (Hill 1974; Pedersen 1993).

Echo perception

In bats the returning echoes are received and processed by the peripheral auditory system, including the cochlea and auditory nerve (Neuweiler 2003). Many bat species possess specific modifications, such as the 'auditory foveae' found in members of Rhinolophidae and the mustached bat *Pteronotus parnellii* (Schuller and Pollak 1979; Russell *et al.,* 2003). These are collections of auditory nerves fibres that are sharply tuned to a particular frequency, in this case the dominant frequency of the echolocation call. The gross morphology of the cochlea of laryngeal echolocating bats is very characteristic, appearing hypertrophic with 2.5 – 3.5 turns, compared to only 1.75 turns in non-echolocating Old World fruit bats (Altringham 1996). The different requirements posed by different modes of echolocation have also produced a series of different adaptations in the mechanics of the inner ear (Kossl *et al.,* 2004).

Call types and frequencies used

The calls of laryngeal echolocating bats are characterised as ultra-sonic because they are typically higher than the auditory range of humans (the typical upper limit of which is 20 kHz). However, the upper frequency hearing limit of some bat species is potentially over 200 kHz (Fenton and Bell 1981; Schmieder *et al.,* 2010). High frequency sounds are more rapidly attenuated, i.e. become weaker as they travel, and so echolocating bats that hunt using high frequencies can get closer to hearing prey without being detected. Additional benefits of high frequency sounds are shorter wavelengths which enables bats to discriminate small targets, such as insects, and also better perception of directionality (Obrist *et al.,* 1993; Houston *et al.,* 2004).

Bat echolocation calls can be divided into three broad types; narrowband frequency modulated (FM), broadband FM, and long constant frequency (CF) with Doppler shift compensation (DSC) (Schnitzler *et al.,* 2003; Jones and Teeling 2006). However, most bat species use a combination of CF and FM elements (Altringham 1996). Frequency modulated broadband calls cover a range of frequencies over a short time interval (Jones and Teeling 2006). On the other hand, some CF species use DSC, in which a bat lowers the emitted call frequency in order to compensate for the effects of its own flight speed thus, keeping the returning echoes at the optimum frequency (Jones and Teeling 2006).

Echolocation call types are generally phylogenetically consistent; however there are exceptions to this pattern, and several examples of convergent call types exist (Jones and Teeling 2006; Jones and Holderied 2007) (see Fig.1.1). Comparative studies have shown that ecology, as well as phylogeny, has a strong effect on a species call type (Schnitzler and Kalko 2001).

Figure 1.1 Echolocation call and emission type mapped onto the bat phylogeny. Family level echolocation call type (1): Narrowband, dominated by fundamental harmonic (orange); Narrowband, multiharmonic (green); Short, broadband, multiharmonic (yellow); Long, broadband, multiharmonic (blue); Constant frequency (red); Polymorphic (white and purple); Equivocal (?). Ancestral reconstructions of echolocation call type: branch colours as above, with Equivocal (grey). Following Figure 1 from Jones and Teeling (2006). Echolocation call emission (2): none (black); nasal (grey); oral (white); following those proposed by Pedersen (1993).

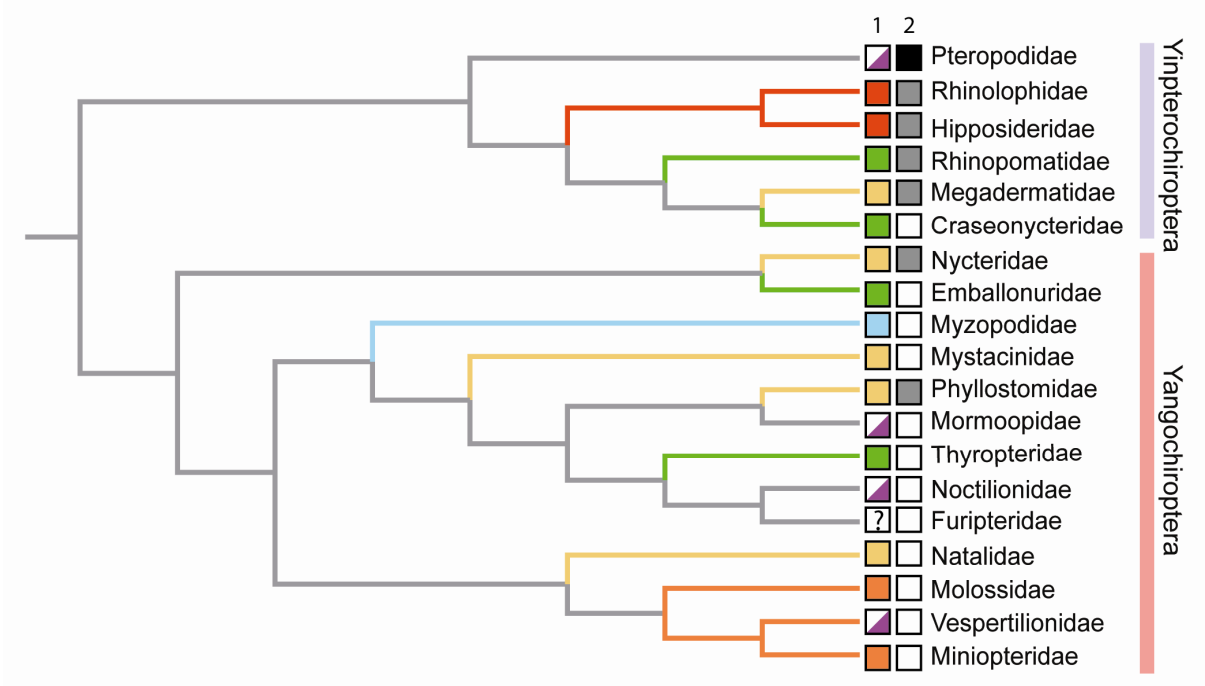

Many bat species also show variation in call duty cycle, i.e. the ratio of time of signal presence to the length of time from the onset of a call to the next (Neuweiler 2000). The average duty cycle in most species is 4-20%, however, it can be much higher, for example ~50% in some horseshoe bats (Neuweiler 2000). Calls also vary in intensity and harmonic composition (Jones and Teeling 2006). Use of DSC is particularly associated with bats that use long pure tones to locate moving insects within cluttered habitats (Jones and Teeling 2006), and is one example of the strong link between hunting/foraging strategy and call type used. External morphological features associated with echolocation call audition include pinnae shape (Fenton 1984) and size (Zhao *et al.,* 2003), and those with call emission include facial structures such as noseleaves, exemplified by horseshoe bats and also New World leaf-nosed bats (Bogdanowicz *et al.,* 1997; Zhuang and Muller 2006).

Debated scenarios for the evolution of bat echolocation

For a considerable period it was debated as to whether all bats were in fact bats, as based on morphological features of the brain and eyes, it was suggested that Old World fruit bats (Pteropodidae) were in fact more closely related to primates than insectivorous bats (Pettigrew 1986; Dell *et al.,* 2010; Kruger *et al.,* 2010). However, following increased molecular evidence, there has been an overwhelming rejection by most mammalogists of the so-called 'flying primate' theory, in favour of bat monophyly (e.g. Bailey *et al.,* 1992; Stanhope *et al.,* 1992; Murphy *et al.,* 2001a). Prior to the 'flying primate' hypothesis, there was an accepted putative alliance between bats, primates, flying lemurs and tree shrews, which together were placed in the old superorder Archonta (Gregory 1910), which continued to receive support until relatively recently (e.g. Shoshani and McKenna 1998). However, based on molecular evidence, bats are now placed within the new superorder Laurasiatheria, with carnivores and odd-toed ungulates suggested to be the most likely sister groups (Pumo *et al.,* 1998; Nishihara *et al.,* 2006; Murphy *et al.,* 2007).

Until the last decade, bats were split into two suborders: the echolocating bats (Microchiroptera) and the Old World fruit bats (Megachiroptera). Laryngeal echolocation was therefore considered to have evolved just once, in the former group, in accordance with the phylogeny supported by morphological characters (see Fig. 1.2a). Thus echolocation and associated features were considered to be the defining synapomorphies of the Microchiroptera (Simmons and Geisler 1998). However, this

relationship has now been widely disproved by a large number of molecular studies (e.g. Murphy *et al.,* 2001b; Teeling *et al.,* 2002; Eick *et al.,* 2005). Instead molecular evidence has led to the new intra-ordinal classification of Yinpterochiroptera and Yangochiroptera (and this is the scheme followed throughout this study), which replaces the former long standing 'Mega/Microchiroptera' divisions (see Fig. 1.2b). In this new classification scheme, the superfamily Rhinolophoidea and three other families of echolocating bats are more closely related to Old World fruit bats than to the remaining echolocating bats. This arrangement has been shown to be supported by DNA hybridisation (Hutcheon *et al.,* 1998; Hutcheon and Kirsch 2004) and sequence data from mitochondrial and nuclear genes (e.g. Teeling *et al.,* 2000; Teeling *et al.,* 2002; Van den Bussche and Hoofer 2004; Teeling *et al.,* 2005) and FISH analyses of chromosomes (Volleth *et al.,* 2002).

Intriguingly, however, so far not a single morphological character supporting this classification scheme has been found, which might highlight the extreme nature of convergent evolution shown by echolocating bats (for examples see Fenton 2010). This re-organisation is now widely accepted, and has important implications concerning the evolution of echolocation across the order.

As mentioned, in accordance with the morphological phylogeny, echolocation was assumed to have evolved once at the base of Microchiroptera. However, given the newly accepted phylogeny, two equally parsimonious evolutionary scenarios can explain the evolution of laryngeal echolocation in bats. Firstly, that echolocation evolved independently at least twice in insectivorous bats, and secondly, that it evolved once at the base of all bats and was subsequently lost in Old World fruit bats (see Fig. 1.2b). In both cases, *Rousettus spp.* would have to have secondarily evolved a different kind of echolocation that uses tongue-clicks. Both hypotheses are supported and opposed by a variety of sources of evidence, which have previously been reviewed in detail (for example Arita and Fenton 1997; Jones and Teeling 2006; Teeling 2009), and which are briefly summarised below.

Figure 1.2 The phylogenetic relationship between bat families based on (a) morphological and (b) molecular evidence. The hypothesised evolutionary gains of echolocation are indicated with stars, and a loss by a line (each colour scheme represents a different scenario). The six proposed superfamilies [Pteropodidae, Rhinolophoidea, Emballonuroidea, Noctilionoidea and Vespertilionoidea following Teeling *et al.* (2003)] are indicated with the coloured branches; orange, blue, purple, yellow and green, respectively.

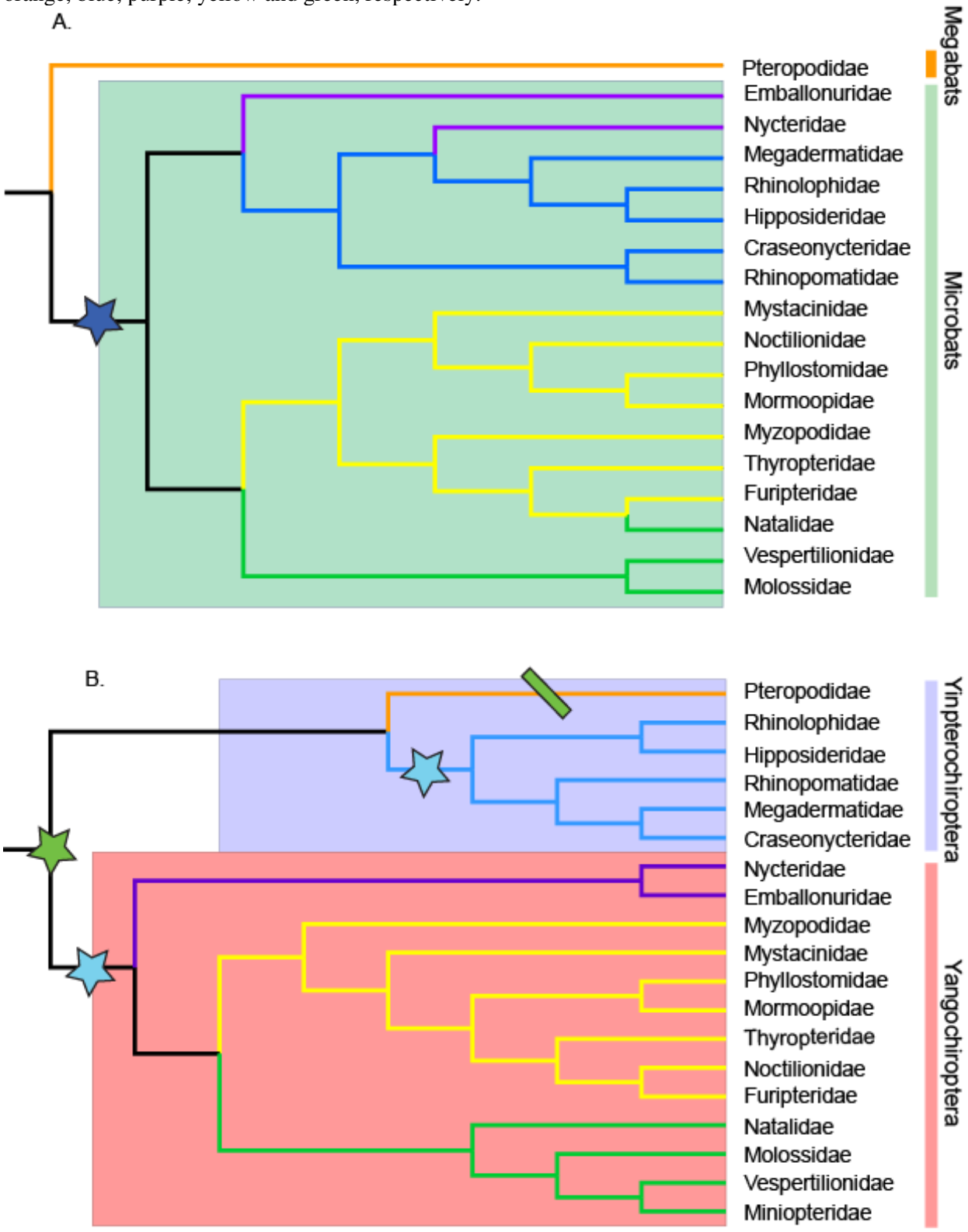

Morphological evidence for the origins of echolocation:

Micro-computed-tomography (μCT) scans of fluid preserved bats recently revealed that all laryngeally echolocating species have proximally articulated stylohyal and tympanic bones; whereas this feature was not found in the Old World fruit bats (Simmons *et al.,* 2010; Veselka *et al.,* 2010a; Veselka *et al.,* 2010b). It was therefore suggested that this trait may be necessary for coordination between vocalisation and auditory systems (Veselka *et al.,* 2010a). Direct comparisons of the skeletal remains of *Onychonycteris finneyi,* the oldest currently known bat fossil, initially suggested that this bat also possessed this feature and thus was capable of echolocation. This led to the suggestion that the shared features associated with echolocation, including contact between the stylohyal and tympanic bones should be considered the ancestral state, and not derived (Fenton 2010). However, after clarification of the preservation state of the original *O. finneyi* specimen it was determined that the articulation character state could not be accurately determined, and, therefore, it seems unlikely that *O. finneyi* could in fact echolocate (Simmons *et al.,* 2010).

Phylogenetic analyses of fossil taxa further illustrate the contention surrounding the evolution of echolocation, as surprisingly, instead of elucidating the situation, the currently known early Eocene bat fossils continue to provide a source of conflict. Four previous studies have combined molecular, morphological, and fossil evidence to reconstruct the evolutionary history of laryngeal echolocation (Simmons and Geisler 1998; Springer *et al.,* 2001; Eick *et al.,* 2005; Simmons *et al.,* 2008). Simmons and Geisler (1998) concluded, based on morphological characters, the four Eocene bat genera represent consecutive sister-taxa to extant echolocating bats, thus supporting a single origin of echolocation. However, they also stated "exclusion of soft-tissue and molecular characters resulted, at least in this case, in a biased topology that does not provide an adequate basis for inferring relationships" (Simmons and Geisler 1998). Springer et al. (2001) mapped 195 morphological features onto the molecular scaffold tree, and by applying a maximum parsimony analysis, claimed that a single origin would require two steps (i.e. one gain followed by one loss), while two independent origins would require four steps (i.e. 4 gains). A basal placement of *Icaronycteris*, *Archaeonycteris, Palaeochiropteryx* and *Hassianycteris* was again recovered and it was concluded that the common bat ancestor could echolocate and this trait was then lost in Old World fruit bats (Springer *et al.,* 2001). Finally, Eick *et al.* (2005) analyzed wider taxa and only included non-homoplasious morphological characters and ultimately

concluded that the placement of the fossil taxa could not currently be resolved. Although some support was given to a possible independent origin of echolocation in the Rhinolophoidea (Eick *et al.,* 2005). Furthermore, some early fossil bats have cochlea widths similar to those of extant echolocating bats (Simmons and Geisler 1998; Simmons *et al.,* 2008), which has been taken by some as support for a single origin of echolocation (Jones and Teeling 2006).

One argument against a single origin of echolocation is that, despite the associated energetic costs and physical constraints of echolocating, it confers such an adaptive advantage that it is highly unlikely that Old World fruit bats would have subsequently lost the ability (Speakman 2001). Indeed this argument seems particularly compelling given that *Rousettus spp.* then independently evolved a form of echolocation utilising tongue clicks. On the other hand, since around one sixth of all bat species are Old World fruit bats and they are able to obtain a wide range of diets (Courts 1998) the lack of echolocation does not seem to have been particularly detrimental to their evolutionary success.

Molecular evidence for the origins of echolocation:

To date, two genes, *Forkhead box protein P2* (*FoxP2)* and *Prestin,* have shown interesting signatures of molecular evolution that may be related to the acquisition of echolocation. The transcription factor *Foxp2*, previously thought to be highly conserved across mammals, has been shown to be highly diversified in echolocating bats (Li *et al.,* 2007). *Foxp2* has been implicated in the development of language in humans, based on species specific mutations and deleterious mutations associated with deficits in speech and orofacial coordination (Lai *et al.,* 2001; Enard *et al.,* 2002); therefore, the variation in *Foxp2* seen in bats could be associated with the orofacial demands of echolocation call emission. At the same time, however, this gene has several other critical roles in mammals, such as lung development (Shu *et al.,* 2007), which could account for it being under strong purifying selection in Old World fruit bats and other mammals. Despite higher levels of nonsynonymous mutations in echolocating bats, positive selection was not detected, but rather changes in selection pressure (termed ‘divergent selection’) was determined between the two main clades of echolocators rather than relaxation in the Old World fruit bats.

The protein Prestin, known as the 'motor protein of the outer hair cells', drives the mechanical changes of the outer hair cells (OHC) in order to amplify vibrations in the cochlea (Zheng *et al.,* 2000). *Prestin* was also once thought to be highly conserved across mammals (He *et al.,* 2006), however, surveys of echolocating bats (Li *et al.,* 2008) and whales (Liu *et al.,* 2010b) have shown this not to be the case. Perhaps the most striking feature of the sequence variation shown by groups of echolocating taxa is that they share several convergent amino acid substitutions, which are possibly related to the high-frequency hearing necessary for echolocation (Li *et al.,* 2010; Liu *et al.,* 2010a). Moreover, evidence of positive selection in both cetacean and bat species suggests that the numerous convergent changes were adaptive. The fact that not all 'hearing' genes show increased diversification in bats e.g. *Gja1* (Wang *et al.,* 2009), suggest that adaptations may be limited to certain aspects of the auditory system, such as the OHCs, which are unique to mammals. In summary, evidence that some 'echolocation' genes in both clades of echolocating bats are highly variable compared to homologues seen in non-echolocating mammals, coupled with the lack of evidence of relaxed selection in non-echolocating Old World fruit bats, gives some support to two independent origins of laryngeal echolocation in bats.

Morphological and molecular considerations

No conclusive morphological character linking Old World fruit bats and echolocating Yinpterochiroptera has so far been found. Similarly, no molecular or morphological evidence unequivocally supports the loss of echolocation in Old World fruit bats, although it is not easy to predict what the signal of a loss of echolocation might look like. Typically, the loss of a sense or organ is linked with structural degeneration; for example the eyes of blind cavefish (Jeffery 2005) or the human appendix (Smith *et al.,* 2009). These cases, and many others, are frequently linked with a change of environment such as loss of light or a change in diet (Zhao *et al.,* 2009b; Cui *et al.,* 2011).

However, the putative loss of echolocation in Old World fruit bats would represent a special case, as it involves the loss of a highly derived sensory trait not seen in most mammals. As such, the loss of echolocation could see reversion to a typical mammalian hearing system; that is completely functional with no signs of vestigiality. Yet, because bats have highly modified bodies, it becomes difficult to directly compare the allometry of organs and physical features between bats and non-volant and/or non-echolocating

mammals (Jones 1999). Furthermore, it is unclear how a return to 'normal' morphological features (e.g. non-enlarged cochlea) would differ to the one expected in Old World fruit bats, under the model of multiple independent origins of echolocation. Known examples of trait loss that might provide clues are island birds that have lost the ability to fly, or mammals that have become secondarily aquatic (McNab 1994; Thewissen *et al.,* 2001). However, different flightless bird species display different resultant morphologies; for example some have completely lost their wings (kiwi) while others' wings remain intact but non-functional (penguins). Cetaceans and squamate reptiles have independently evolved highly modified bodies to allow them to occupy aquatic and fossorial niches respectively. These adaptations include markedly absent or reduced limbs. Therefore, limb reduction in this case could be viewed as part of the process of functional evolutionary adaptation (Bejder and Hall 2002; Wiens *et al.,* 2006).

If the underlying genetic mechanism of echolocation were known, it might be considerably easier to ascertain which of the two above scenarios, i.e. multiple origins or loss, is correct in the context of bat evolution. For example, if many small changes in a number of independently regulated genes were necessary then identical multiple origins of echolocation would seem unlikely. On the other hand, if a small number of regulatory control genes are responsible for the 'echolocation complex', then multiple origins could be considered more plausible – with the possibility of a number of switches over time. However, it cannot be ruled out that laryngeal echolocation could arise via different underlying genetic mechanisms in different clades. In blind cave fish, out-breeding experiments have been shown to restore sight, indicating that several different molecular pathways are responsible for loss of sight in different populations (Borowsky 2008). Typically, if a gene is neither functional nor required, then pseudogenization is ultimately expected to occur (e.g. Zhao *et al.,* 2010). If we assume that echolocation involved the co-option of genes previously involved in hearing, then it would seem unlikely that in these genes loss of function would arise. Possibly a more reasonable scenario would be a return to ancestral states followed by purifying selection.

Although, evidence suggesting the oldest known bat did not echolocate does not directly support either single or multiple origins of echolocation, it does raise important considerations. It suggests that powered flight evolved prior to laryngeal echolocation,

and this agrees with the assertion that it is energetically favourable for echolocation call emissions to be linked with flapping flight (Simmons *et al.,* 2008). Indeed, some studies suggest that echolocation call emission and the wing-beat upstroke are tightly coupled to reduce the associated energetic cost, though examples whereby echolocation calls are emitted at different stages of the wing stroke are also known, suggesting flexibility in the system (Suthers and Suthers 1972; Speakman and Racey 1991; Wong and Waters 2001; Moss *et al.,* 2006).

As direct observations of echolocation and its associated features have so far proved inconclusive in determining its evolutionary origins, a large body of work has been directed towards indirect measures, and in particular searching for evidence of a 'sensory trade-off'. This is based on the assumption that, due to neuronal constraints, it might be expected that major advances in one sense would lead to a reduction in another. However, one study to test this found no evidence of a trade-off between visual and olfactory brain elements in bats (Barton *et al.,* 1995), although it did not include echolocation parameters, and also used the incorrect phylogeny. An earlier study carried out a multiple discriminant analysis across bats based on body size and five brain centres (Baron and Jolicoeur 1980), with the effects of body size removed by regression, and with the bat species subdivided into seven categories that approximated to the currently accepted families (albeit with the exception that *Desmodus rotundus* was in its own group outside of the other Phyllostomidae). The results of this study suggested that the three Old World fruit bats were spatially separated from the echolocating bats along an 'acoustico-visual gradient' (Baron and Jolicoeur 1980). The grouping together of echolocating members of Yinpterochiroptera and Yangochiroptera in this analysis can be attributed to phenotypic convergence, which also appears to account for the intermediate placement of the seven frugivorous phyllostomids between the Old World fruit bats and the remaining echolocating bats. More recently, a detailed molecular study that examined hundreds of olfactory receptor genes did not detect any evidence to suggest that the acquisition of echolocation was associated with a loss of olfaction capabilities (Hayden *et al.,* 2010). Another study examined a crucial gene of the vomeronasal system, *Trpc2*, and based on if it was functional or a pseudogene suggest that whereas all Yinpterochiroptera have lost vomeronasal sensitivity, some Yangochiroptera retain sensitivity (Zhao *et al.,* 2011).

Perhaps the most expected sensory trade-off in bats would be between vision and audition (Speakman 2001). The extent to which bat species rely on visual spatial cues is highly variable; several echolocating species are known to use visual inputs for orientation and prey detection (Bell 1985; Winter *et al.,* 2003). Most mammals possess two cone photopigments responsible for colour vision: the M/LWS (middle/long-wavelength sensitive) opsin and the SWS1 (shortwave length sensitive type 1) opsins (Lukats *et al.,* 2005). While M/LWS are functional in all bats studied to date, SWS1 has been shown to be non-functional in two echolocating Yinpterochiroptera families (Rhinolophidae and Hipposideridae) and in some Old World fruit bats (Zhao *et al.,* 2009a; Shen *et al.,* 2010). Furthermore, the acquisition of stop codons and indels in the former bat families appear to have coincided with episodes of positive selection in the hearing gene *Prestin*. Therefore, there is some evidence to suggest a trade-off between vision and echolocation, with loss of function in SWS1 coinciding with the acquisition of high-duty-cycle echolocation (Zhao *et al.,* 2009a). Meanwhile, the rod photopigment, rhodopsin, which enables vision in dim-light, has been shown to have undergone some spectral tuning within different groups of bats (Zhao *et al.,* 2009b; Shen *et al.,* 2010). Therefore, it seems that there have been multiple adaptive stages throughout the development of echolocation in different bat clades.

Supporters of the hypothesis that echolocation evolved once argue that such a complex trait could not have evolved twice. However, as echolocation has evolved independently in several taxonomically diverse groups, multiple origins might not be out of the question (Griffin and Suthers 1970; Au and Simmons 2007; Siemers *et al.,* 2009). Indeed given that 'tongue-click' echolocation has independently evolved in the genus *Rousettus,* there may be some aspects of the biology of bats that has facilitated the acquisition of echolocation. Simplifying the evolution of complex traits to the minimum number of steps is unrealistic, because evolution is not a simple process which rarely takes the optimum path. Applications of parsimony to bat evolution have previously led to erroneous conclusions (e.g. the aforementioned grouping of bats and flying lemurs in order to facilitate a single origin of flight in mammals). In reality, all of the proposed scenarios might oversimplify the case, and there instead could be many stages of acquisition and refinement of echolocation and high-frequency hearing across bats.

Thus the persisting question regarding the evolution of bat echolocation is as follows: is it more likely that either there has been a loss of a highly advantageous trait in some

lineages (Old World fruit bats) accompanied with complete morphological reversal, or has selection led to extreme phenotypic convergence, to the extent that few morphological features can distinguish Yangochiroptera from echolocating Yinpterochiroptera?

AIMS AND OBJECTIVES

Echolocation imposes great sensory demands on bats orofacial, auditory and neuronal processing systems. It has necessitated the evolution of character complexes to meet a suite of sensorimotor challenges, such as the requirement to emit sonar pulses, interpret the echoes, and adjust the flight, all with timeframes of just a few milliseconds. In this project, I applied a range of powerful analytical methods to test whether laryngeal echolocation is likely to have evolved just once in bats with a subsequent loss in Old World fruit bats, or whether there have been multiple evolutionary origins of bat echolocation. My approach was based on characterising and reconstructing evolutionary change that may have taken place in several genes and morphological structures thought to be linked to echolocation. This thesis comprises four separate yet related studies, summarised below.

i. Functional 'hearing genes'

The principal aim of the first study was to identify putative 'hearing' genes that have become co-opted for the high-frequency hearing required by some echolocating bat species. Candidate 'echolocation genes' involved in hearing and ear development; in particular those linked to non-syndromic deafness, cochlea development, high-frequency hearing loss or stereocilia structure - were identified by a literature survey of mammalian models. In addition, a literature search of published known pathogenic and non-pathogenic mutations in the genes under study was carried out. The mutations were mapped onto the gene, and regions characterized by high numbers of substitutions were then targeted for in-depth study. If single point mutations, or the regions in which these mutations occur, are implicated in deafness, then they will be important for hearing, and thus might have been targets for selection in taxa (i.e. bats) that evolved highly developed hearing. I examined two candidate genes across a wide range of echolocating and non-echolocating species using phylogenetic and molecular evolution methods to investigate the phylogenetic signal, selection pressures and, where applicable, presence of convergence. Detailed knowledge of sites under selection in putative hearing genes

will not only have implications for evolutionary studies, but could also lead to a greater understanding of human hearing disorders.

ii. Conserved Non-coding Elements

Auditory processing in echolocating bats is highly complex; their auditory systems have undergone many structural changes and have become highly modified in order to cope with the demands of echolocation. To gain a wider understanding of the evolutionary processes that occurred during the acquisition of echolocation, the molecular evolution of non-coding regulatory regions was investigated. Given that many of the regions regulate gene expression of crucial developmental genes we might expect that taxa with phenotypic changes of sensory organs would have divergent regulatory regions. The sequence variation of conserved non-coding elements (CNEs) found in genomic regions in the vicinity of 28 genes involved in regulating the developing mammalian auditory system were investigated in a range of bats and mammals. In particular, variations in substitution rates were compared between laryngeal echolocating and non-echolocating bat species.

iii. Cochlear morphology

Given that inner ear development and function is controlled epistatically by a large number of genes, a single genic approach cannot document the complete evolutionary history. The evolution of echolocation in bats is known to be associated with enlargement of the cochlea. Therefore, in order to study the overall phenotypic variation of the cochlea of echolocating bats, a morphological approach was also conducted. Computed-tomography scans were used to digitally reconstruct the minute internal structures of bat inner ears so that variation in cochlear architecture could be studied in more detail and related to functional changes. In particular, the gross morphology of the cochlea was studied in terms of size and number of turns, and also certain specific functional details, such as basilar membrane length. These values were then related to aspects of auditory and echolocation ability as well as ecology.

iv. Semicircular canal morphology

As well as evolving sophisticated echolocation, bats are also proficient fliers, and as these two traits are undeniably related, their evolution will have had profound effects on the vestibular system. In birds, flight has been shown to be associated with enlargement

of the semicircular canals of the vestibular system. In echolocating bats, however, the morphology of the semicircular canals will be under selection associated with flight, but its size and shape might also be constrained by the cochlea with which it shares the confined space of the petrosal bone. In order to study how echolocation may have affected the bat vestibular system, I conducted a detailed morphological study of bat semicircular canals using computed-tomography scans of bat skulls. By studying the interactions of the inner ear, echolocation and flight capabilities it is aimed to better understand the selection pressures that have acted on bats throughout their evolution.

CHAPTER TWO

Parallel Signatures of Sequence Evolution among Hearing Genes in Echolocating Mammals: an Emerging Model of Genetic Convergence*

SUMMARY

Recent findings of sequence convergence in the *Prestin* gene among some bats and cetaceans suggest that parallel adaptations for high-frequency hearing have taken place during the evolution of echolocation. To determine if this gene is an exception, or instead similar processes have occurred in other hearing genes, I examined *Tmc1* and *Pjvk*, both of which are associated with non-syndromic hearing loss in mammals. These genes were amplified and sequenced from a number of mammalian species, including echolocating and non-echolocating bats and whales, and were analysed together with published sequences. Sections of both genes showed phylogenetic signals that conflicted with accepted species relationships, with coding regions uniting laryngeal echolocating bats in a monophyletic clade. Bayesian estimates of posterior probabilities of convergent and divergent substitutions provided more direct evidence of sequence convergence between the two groups of laryngeal echolocating bats as well as between echolocating bats and dolphins. I found strong evidence of positive selection acting on some echolocating bat species and echolocating cetaceans, contrasting with purifying selection on non-echolocating bats. Signatures of sequence convergence and molecular adaptation in two additional hearing genes suggest that the acquisition of high-frequency hearing has involved multiple loci.

*Publication information: This chapter contains content similar to that published, together with additional background information and analyses.

Citation: Davies, KTJ, Cotton, JA, Kirwan, J, Teeling, EC, Rossiter, SJ (2011). Parallel signatures of sequence evolution among hearing genes in echolocating bats: an emerging model of genetic convergence. *Heredity* doi: 10.1038/hdy.2011.119

INTRODUCTION

Convergent and parallel sequence evolution

Examples of adaptive phenotypic convergence are widespread in nature and are usually considered to arise from similar selection pressures acting on unrelated taxa (e.g. Packard 1972; Nevo 1979). Yet given the relative plasticity of the phenotype, it is perhaps surprising that there are few documented cases of convergence acting at the sequence level. The recent proliferation of genetic and genomic data has seen a rise in the number of convincing examples (as reviewed in Wood *et al.,* 2005; Christin *et al.,* 2010). Some of the earliest and best examples of convergent sequence evolution include the stomach lysozymes of langurs and cows (Stewart *et al.,* 1987), and the peptide-binding regions of MHC class Ib genes in primates and rodents (Yeager *et al.,* 1997; Yeager and Hughes 1999). More recently, the mitochondrial genomes of snakes and agamid lizards have also been found to contain numerous convergent sites distributed across all protein-coding genes, leading to a conflict with the true species phylogenetic signal obtained from nuclear genes (Castoe *et al.,* 2009).

The 'hearing gene' *Prestin* was recently shown to have undergone unprecedented levels of sequence convergence between lineages of echolocating mammals (Li *et al.,* 2008; Li *et al.,* 2010; Liu *et al.,* 2010a). *Prestin* encodes a motor protein expressed in the outer hair cell (OHC) and is thought to drive the cochlear amplifier that gives mammalian hearing its characteristically high sensitivity and selectivity (Zheng *et al.,* 2000). Phylogenetic analysis of *Prestin* sequences grouped unrelated lineages of echolocating bats suggesting a link with high-frequency hearing (Li *et al.,* 2008), which was supported by evidence of sequence convergence between echolocating bats and some cetaceans (Li *et al.,* 2010; Liu *et al.,* 2010a; Liu *et al.,* 2010b) as well as associations between numbers of replacements and hearing sensitivity (Liu *et al.,* 2010b; Rossiter *et al.,* 2011). Recorded signatures of positive selection in bats (Li *et al.,* 2008) and toothed whales (Liu *et al.,* 2010b) reinforce the adaptive significance of these changes.

Molecular basis of mammalian hearing

The molecular basis of mammalian hearing is becoming increasingly well characterised (e.g. Fekete 1999; Ficker *et al.,* 2004; Frolenkov *et al.,* 2004; Accetturo *et al.,* 2010; Dror and Avraham 2010). An extensive literature survey identified 152 candidate genes thought to play a role in mammalian hearing or ear development. From these, 51 were

identified from studies of mutagenesis and human epidemiology as being associated with non-syndromic hearing loss (NSHL). Of the remaining genes, 29 were associated with syndromic hearing loss (SHL) and 72 with abnormal ear development.

The mammalian hearing apparatus has evolved for over 200 million years into the wide range of specialised auditory systems, of which echolocating bats and whales arguably possess the most highly derived forms (Vater and Kossl 2004). Well-supported phylogenies have revealed that bats comprise two divergent suborders: the Yinpterochiroptera that contains echolocating species plus non-echolocating Old World fruit bats, and the Yangochiroptera that contains other echolocating bats (e.g. Teeling *et al.,* 2002; Eick *et al.,* 2005; Miller-Butterworth *et al.,* 2007). This uneven distribution of echolocation and associated ultrasonic hearing has initiated a debate as to whether these traits evolved more than once, or were lost in the Old World fruit bats. Notwithstanding this debate, bats undoubtedly do show convergence in particular forms of echolocation, such as constant frequency echolocation seen in horseshoe bats and the Neotropical species *Pteronotus parnellii* (e.g. Jones and Teeling 2006).

Results from Prestin all suggest that echolocating mammals might be an especially useful group in which to test for evidence of genetic convergence. Here I extend the study of the evolution of echolocation in bats to investigate whether *Prestin* is exceptional, or whether signatures of convergent sequence evolution can also be detected more widely in other putative hearing genes implicated in deafness. I focused on two genes that have specific roles in hair cell function: *Tmc1* (Transmembrane cochlear-expressed gene 1) and *Pjvk* (Pejvakin). *Tmc1* encodes a transmembrane protein of the inner and outer hair cells that might either traffic molecules to the plasma membrane or act as an intracellular regulatory signal during hair cell maturation (Marcotti *et al.,* 2006). In mice, *Tmc1* is expressed from early development and is needed for normal hair cell function (Marcotti *et al.,* 2006), whereas the human gene (*TMC1*) is associated with several types of NSHL with over 20 documented pathogenic mutations, including deletions, nonsense and splice mutations (Kurima *et al.,* 2002; Kitajiri *et al.,* 2007). The gene *Pjvk* (also known as *Dfnb59*) encodes a protein called pejvakin. Missense and stop mutations in the human form have both been linked to deafness - in the former case caused by auditory neuropathy (Delmaghani *et al.,* 2006) - whereas in mice, premature stop codons disrupt hair cell activity and also cause vestibular defects (Schwander *et al.,* 2007).

From the initial 152 candidate genes, this study focused on the two genes, *Tmc1* and *Pjvk,* for the following reasons. Firstly, I decided to focus only on nuclear genes associated with NSHL or ear abnormalities. Genes associated with SHL (i.e. when affected individuals display a specific pattern of additional clinical features not related to audition) were excluded. The genetic basis of syndromes may involve several mutations at different loci, or by a single mutation with a pleiotropic effect, therefore it would be impossible to relate the published mutations, or genes, directly to hearing. Following a detailed survey of the associated literature of mutations and the gene structure of the 51 NSHL genes it was decided to limit further study to the following 13 genes: Cochlin (*Coch*), Connexin 30 (*Gjb6*), Myosin VI (*Myo6*), Solute carrier family 26 member 4/Pendrin (*SLC26A4/Pds*), Transmembrane cochlear-expressed gene 1 (*Tmc1*), Transmembrane protease serine 3 (*Tmprss3*), KIAA1199 (*Kiaa1199*), Otoancorin (*Otoa*), Pejvakin (*DFNB59/Pjvk*), Pou domain class 4, transcription factor 3 (*Pou4F3*), Espin (*Espn*), Otoferlin (*Otof*) and Transmembrane inner ear-expressed gene (*Tmie*). Also six genes associated with ear development: Otoraplin (*Otor*), Goosecoid (*Gsc*), Retinoic acid receptor α (*Rarα*), SRY (sex determining region Y)-box 2 (*Sox2*) and Paired box gene 2 (*Pax2*) and Transforming growth factor β 2 (*Tgfb2*), were selected.

The above 19 genes were then further reduced based on the following considerations. It was attempted to design universal primers for each of the above genes using 'Uniprime' (Bekaert and Teeling 2008). 'Uniprime' identifies and uses conserved areas to design sets of degenerate primers to meet a range of user-specified criteria. For example, in this case primers were chosen to amplify PCR products ~1 kilo-base (KB) in length with genomic DNA. Due to this criterion, *Gjb6* was excluded from further study. Priority was then given to genes with primers that were predicted to maximize amplification of exonic regions using cross species data from Ensembl (www.Ensembl.org). Therefore, potential genes were further limited to *Otof, Pou4F3, Pjvk* and *Tmc1*. An exhaustive literature search of published known pathogenic and non-pathogenic mutations in the remaining genes of interest was also carried out. All mutations were then mapped onto the gene structure and the overall distribution assessed to identify regions of interest characterised by high numbers of substitutions. The rationale behind this being, that if a single point mutation was pathogenic, as with regards deafness, then this region is likely to be crucial in normal hearing and so may be under selection in groups, such as bats,

that display highly developed hearing. Finally, the specific function of each gene in mammalian hearing was investigated. As *Tmc1* and *Pjvk* encode proteins thought to be vital for the normal function of OHCs, and given that OHCs are known to be, at least in part, responsible for the high-frequency specificity of mammalian hearing they became the logical choice.

Aims and objectives of this study

In this study, I examined and compared sections of both genes in a range of mammals. Given that Tmc1 and Pejvakin are - like Prestin - thought to be important for the normal function of OHCs, I undertook a comparative analysis to test whether these proteins showed evidence of convergence and/or molecular adaptation associated with the independent evolution of high-frequency hearing.

Hypothesis 1: I used a phylogenetic approach to test whether, if present, sequence convergence would cause unrelated echolocating taxa (i.e. divergent lineages of bats, and bats and cetaceans) to group together, as previously reported for *Prestin*. It was predicted that, if adaptive, any gene-species tree conflicts would be more evident in coding DNA.

Hypothesis 2: I predicted that within the species tree, greater support for convergent changes between branches would correspond to the inferred origins of echolocation and high-frequency hearing. Stronger evidence of convergence between the ancestral branches of two main groups of laryngeal echolocators would support multiple independent origins of echolocation (and high-frequency hearing) in bats.

Hypothesis 3: Finally, I predicted that both candidate hearing genes would show evidence of positive selection in key branches and clades. In particular it was predicted that the occurrence of positive selection would coincide with detected sequence convergence, and the inferred origins of high-frequency hearing in the divergent lineages of bats, and cetaceans.

MATERIALS AND METHODS

In Silico study

Complete *Tmc1* and *Pjvk* coding region sequences were downloaded from Ensembl and GenBank for all available mammals. MegaBLAST was used to identify these genes from published genome data from the bat species *Myotis lucifugus* and *Pteropus vampyrus,* as well as from assembled short read Solexa data from the bats *Eidolon helvum, Pteronotus parnellii* and *Rhinolophus ferrumequinum* [that are available as part of ongoing genomic work (Rossiter S. J. Unpublished data)]. Complete coding regions from the alpaca, *Vicugna pacos,* were used as the reference sequence and expected value thresholds of 10^{-6} were used for sequences of approximately 100 base pairs (bp) or more. Taxa with incomplete sequences were pruned from the dataset so as to maximise sequence and taxonomic coverage. The final *Tmc1* dataset contained 23 species and covered 2,139 bp, corresponding to 713 out of the total 760 amino acids (i.e. from amino acid 25 to 736 using human TMC1 as a reference). For *Pjvk*, sequences from 21 species were collated, which covered the entire 1,059 bp or 352 amino acids. Both datasets contained three echolocating bats (two from the suborder Yangochiroptera and one from the suborder Yinpterochiroptera), two non-echolocating Old World fruit bats (from the suborder Yinpterochiroptera) and one echolocating cetacean (see Fig.2.1). The remaining mammals incorporated a range of auditory thresholds; for example, species with relatively low-frequency hearing such as an elephant and primates, and high-frequency hearing such as rodents (Table A1).

Wider taxonomic study

To test for signatures of convergence and selection in *Tmc1* and *Pjvk* across a much wider range of taxa, for which published genetic data were unavailable, I amplified and sequenced new data from 64 mammal species, including 39 echolocating bat species (12 families) and 10 species of non-echolocating Old World fruit bat (one family). I also obtained additional published sequences from 29 species from 13 mammalian orders. Total coverage comprised 93 mammal species from 14 orders, and included numerous bats, three species of echolocating toothed whale, one non-echolocating baleen whale, and 11 other mammal species from six orders (Table A2).

Figure 2.1 Simplified phylogenetic tree of the families included in this study (based on Csorba *et al.,* 2003; Nishihara *et al.,* 2006; Miller-Butterworth *et al.,* 2007; Murphy *et al.,* 2007; McGowen *et al.,* 2009; Khan *et al.,* 2010). Bats include the Yinpterochiroptera, which are subdivided into the Pteropodidae (orange), that do not possess laryngeal echolocation, and laryngeal echolocating families (green); and the laryngeal echolocating Yangochiroptera (blue). Other mammalian clades (brown) and echolocating and non-echolocating cetacean species (grey clade) were also included. In particular this study aimed to document levels of sequence convergence between echolocating Yinpterochiroptera (green) and Yangochiroptera (blue), as well as each of these clades with the odontocetes.

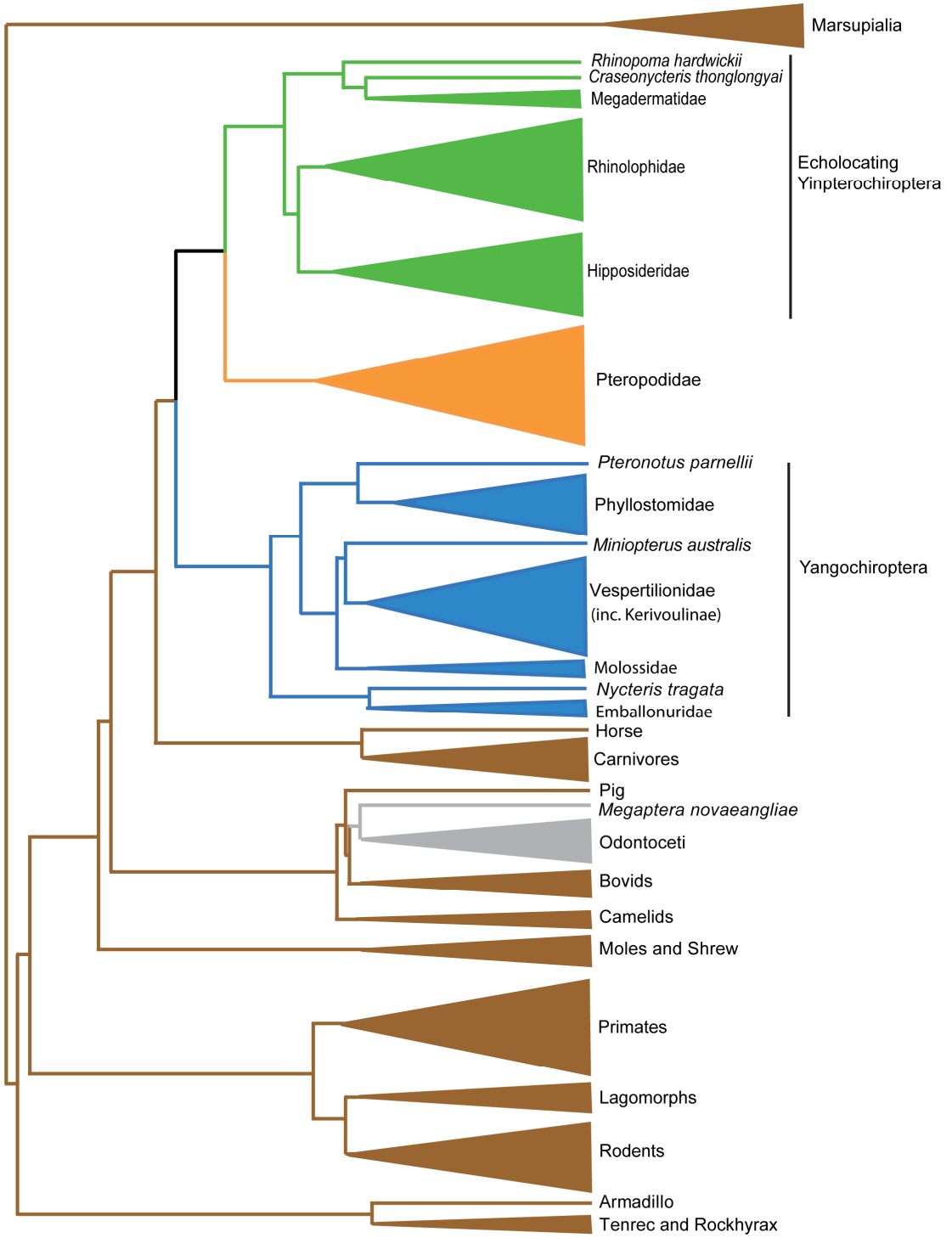

Included bat species represented a range of echolocation call types and associated auditory characteristics (Jones and Teeling 2006) and belonged to both suborders (Yinpterochiroptera and Yangochiroptera). From the former suborder, members of all six families, with contrasting call types, were included as follows: Old World fruit bats (Pteropodidae) that do not possess laryngeal echolocation, horseshoe bats (Rhinolophidae) and roundleaf bats (Hipposideridae) that have evolved narrowband pure constant frequency (CF) echolocation, and representatives of the other families (Megadermatidae, Rhinopomatidae and Craseonycteridae) that all possess more broadband echolocation calls with a range of bandwidths. From Yangochiroptera, bats from seven families were sampled, all characterised by broadband FM echolocation calls, with the exception of *Pteronotus parnellii* that has independently evolved narrowband CF echolocation (Table A3).

DNA isolation, primer design, amplification and sequencing

For new sequences generated in this study, DNA was extracted using DNeasy kits (Qiagen, UK). 'Uniprime' (Bekaert and Teeling 2008) was used to design degenerate primers based on the multi-species alignment of the genomic sequence for *Homo sapiens, Bos taurus, Mus musculus, Macaca mulatta, Pan troglodytes, Canis familiaris,* and *Rattus norvegicus* for *Tmc1* to amplify the predicted product of the 459 bp around exons 16-17. This region corresponds to human exons 16-17 and has been implicated in deafness in mice (Kurima *et al.,* 2002). The forward primer sequence was 5'-CCT CCT NGG GAT GTT CTG TC-3' and the reverse 5'-TGN CCC ACC ATT GTT TCC-3'. Degenerate primers to amplify the predicted product of 798 bp around Exon 5-6 for *Pjvk* were based on the multi-species alignment of *H. sapiens, B. taurus, C. lupus familiaris* and *Equus caballus.* The forward primer sequence was 5'- AAA GGA GGA TTT GAA AGG GAA G-3', and the reverse 5'- TAA AGT TCC CCA TTC CAC AGA G -3'. This region corresponds to human exons 5-6, and contains the functionally important putative nuclear localization signal and zinc-binding motif (Delmaghani *et al.,* 2006), and also contains the site identified by a forward genetics screen as containing a premature stop codon in mutant mice (Schwander *et al.,* 2007).

The desired fragments of gDNA were amplified using a touch-down polymerase chain reaction (PCR) with the following steps; 95°C for 5 minutes activation of taq, 95°C for 30 seconds, 60-50°C for 30 seconds, 72°C for 1 minute for 45 cycles run on a MJ Research PTC225 Peltier thermocycler. Total volume of each reaction mix was 15 μL,

which included approximately 25ng of gDNA, 1.5 μL 10x PCR buffer, 1.2-1.5 μL (25mM) $MgCl_2$, 0.5 μL (10μM) dNTPs, 1 μL (10μM) each forward and reverse primers, 0.1 μL (FastStart Taq DNA polymerase (Roche) and 4.4-4.7 ddH_20. PCR products were run on a 2% agarose gel and visualized using SYBR Safe DNA gel stain (Invitrogen). Successfully amplified products were then purified using ExoSap and sequenced using Sanger sequencing by either Macrogen, GATC or at the Genome Centre of Barts and The London, Queen Mary's School of Medicine and Dentistry. Products were sequenced with the same primers, using BigDye v3.1, and visualized on an ABI 3700 automated DNA sequencer. In the case of multiple bands, specific PCR products were isolated either using a 'touch-prep' (Murphy and O'Brien 2007) where a pipette tip was used to stab the desired product on an agarose gel or cloned prior to sequencing using TOPO TA Cloning Kit for subcloning from Invitrogen.

Analytical approach:

To test for adaptive sequence convergence associated with the acquisition of high-frequency hearing, I undertook analyses that comprised three steps, described below. For both genes, each analysis was repeated separately for the alignments of complete and partial sequences.

1. Tests of phylogenetic signal and hypotheses
2. Examination of sequence convergence
3. Examination of selection using i) Site ii) Branch-site and iii) Clade models

Tests of phylogenetic signal and hypotheses

Nucleotide sequences were aligned using ClustalW2 (Larkin *et al.,* 2007) and checked by eye. Published sequences for *Homo sapiens* (EMBL-EBI) were used to identify the exon-intron boundaries and identify open reading frames for generating alignments of in-frame exons only. To compare phylogenetic signals in the datasets, maximum-likelihood (ML) and Bayesian trees were constructed with RAxML-7.0.3 (Stamatakis 2006) and MrBayes v3.1.2 (Ronquist and Huelsenbeck 2003), respectively. Prior to analysis jModelTEST.0.1 (Posada 2008) was used to suggest the most appropriate substitution models under the Akaike Information Criterion (AIC) for each dataset (see Table 2.1 for model details).

Table 2.1 Model settings and phylogenetic analyses implemented in RAxML and MrBayes for all datasets. * As it is not possible to implement the HKY+G model of substitution in RAxML the next best model was selected.

	Pjvk partial	*Pjvk* complete	*Tmc1* partial	*Tmc1* complete
RAxML model	GTR+G*	GTR+G+I	GTR+G+I	GTR+G+I
Bootstrap samples	1,000	1,000	1,000	1,000
MrBayes model	HKY+G	GTR+G+I	GTR+G+I	GTR+G+I
Number of generations	1,000,000	2,000,000	1,000,000	2,000,000
Number of chains	6	6	6	6
Sample frequency	100	100	100	100
Burn-in	2,500	500,000	2,500	500,000
Sumt burn-in	2,500	5,000	2,500	5,000

To test the confidence of any conflicting topological hypotheses, site-wise log-likelihood values were calculated for trees with the observed topologies constrained as well as the constrained species tree. These site-wise log-likelihood values were then used these to implement Shimodaira's Approximately Unbiased Test (AUT) (Shimodaira 2002) in CONSEL (Shimodaira and Hasegawa 2001). For the complete coding regions and partial gene sequences nucleotide site-wise log-likelihood values were calculated, a heuristic search (tree-bisection-reconnection branch-swapping) from neighbour-joining starting trees using GTR+I+G for *Tmc1* and HKY+G for *Pjvk*, with 5 replicates was used in PAUP* (Swofford 2003), with other model parameters estimated from the data. Site-wise log-likelihoods were calculated for all datasets of both genes, for a fully constrained species tree (see Fig. 2.1), as well as a convergent tree, which only differed from the species tree by enforced monophyly of laryngeal echolocating bats. Relative support along each site for the convergent topology was calculated as the difference between the 'Species topology' and the 'Convergent topology', with positive values indicating more support for the convergent topology.

In order to investigate further the origin of the multiple phylogenetic signals, reduced sequence alignments, for the shorter dataset, were converted into a series of taxonomic splits, and the support and conflict values for each of these splits were then visualized as Lento-Plots in SPECTRONET (Huber *et al.,* 2002). For these analyses, datasets consisted of all bat species plus horse, dog, cow and mole sequences, and were divided between exons and introns. All splits consistent with phenotypic convergence (i.e. containing at least one member of each of the echolocating bat clades) were highlighted.

Tests for sequence convergence

For each gene, I tested for evidence of sequence convergence between the two clades of laryngeal echolocating bats, as well as between these echolocating bats and the dolphin following the approach developed by Castoe et al. (2009). I predicted greatest levels would occur between taxa known to have independently evolved echolocation or particular types of echolocation; in the case of Yangochiroptera versus Yinpterochiroptera, evidence of convergence would add weight to the hypothesis that laryngeal echolocation in bats has evolved multiple times. In this method, the posterior probabilities of all possible amino acid substitutions were calculated along each branch in the species phylogeny, under the JTT+F+G model of amino acid substitution. The species tree topology was fixed and based on several published trees (Csorba *et al.,* 2003; Nishihara *et al.,* 2006; Miller-Butterworth *et al.,* 2007; Murphy *et al.,* 2007; McGowen *et al.,* 2009; Khan *et al.,* 2010), I estimated branch lengths using sequence divergence of the exons with MrBayes v3.1.2 and the same model of substitution as used previously for phylogenetic reconstruction. For all pair-wise branch comparisons where both branches followed divergent paths, the sum of the joint probabilities of all possible pairs of substitutions that are either convergent (same amino acid) or divergent (different amino acid) was calculated. Following this analysis convergent sites were then classified as "parallel" if they arose from the same ancestral state. Levels of convergence for pairs of branches of interest were examined. As a measure of what could be regarded as 'false positives' i.e. a measure of sequence convergence that might be expected aside from that associated with phenotypic convergence, convergence levels between the Pteropodidae and the Yangochiroptera were measured.

I also examined the distribution of sites showing high probabilities of convergence in relation to the functional domains of each protein. Protein domains were taken from literature sources (Kurima *et al.,* 2002; Delmaghani *et al.,* 2006; Schwander *et al.,* 2007) and also confirmed using SMART (Schultz *et al.,* 1998).

Finally, to test whether the branch-wise posterior probabilities of convergence were significantly greater than an expected distribution based on simulations I generated an expected distribution of values for branch-pair comparisons of interest, using simulated sequences generated with EVOLVER in PAML (Yang 2007). This analysis used a constrained species tree, with codon substitution models, and other parameters set to the ML estimates reported by codeml. For the complete coding sequences 10,000 codons,

and for the partial 5,000 codons were generated. These sequences were then analyzed with CodeML Ancestral as previously described. From the site-wise values of convergence, 1,000 random datasets, with the same number of sites as the observed date were sampled. These 1,000 simulated datasets were used to create a null distribution of expected convergence levels with which the observed convergence levels were compared to, these calculations were performed in the R package (R Development Core R Development Core Team 2011).

Tests for selection

Where I found evidence of convergent substitutions, I determined whether these were due to molecular adaptation or neutral evolution. The strength of selection can be detected by comparing the rates of non-synonymous (d_N) and synonymous substitutions (d_S). A d_N/d_S ratio (termed omega, ω) of greater than one signifies positive selection, a value of ω around one signifies neutrality, and an ω value less than one signifies purifying selection. I derived ML estimates of d_N, d_S and ω for each site under different codon models (Yang and Swanson 2002) implemented in the Codeml package within PAML 4.4 (Yang 2007). For these analyses I used exon data with gaps removed, and the accepted species trees as previously described.

(i) Site models of selection

Before testing for molecular adaptation in high-frequency hearing mammals, I first characterised the signature of selection acting along each of the two focal genes regardless of lineage specific adaptation. For this, I estimated site-wise ω values across all branches in the phylogeny for the complete alignments. These ω values were assigned to predefined site classes according to each site model (e.g. M0 had one class and M3 had three). The mean ω of each site class, and the proportions of sites falling into each class, were estimated. To test where and how ω varied among sites, three model comparisons were carried out. Firstly, I assessed whether ω varied among sites by comparing a model with a single free ω (M0) to one in which ω fell into three discrete classes (M3). Secondly, to test for positive selection, I compared model M1a (Nearly Neutral) in which site classes were neutral (ω=1) and purifying (0<ω<1) to model M2a (Positive Selection) that had a third site class corresponding to positive selection (ω>1). For a second test of adaptation, I compared model M7 (beta) to M8 (beta&ω), in which the latter had an additional site class in which ω could exceed one.

Likelihood ratio tests (LRT) were used for all model comparisons, and, where relevant, I identified positively selected sites using Bayesian Empirical Bayes (BEB) inference (Yang *et al.,* 2005).

(ii) Branch-site models of selection

To examine associations between convergent or parallel substitutions with molecular adaptation, I determined the selection pressures acting at particular sites along seven focal branches (i.e. *T. truncatus*, ancestral Yinpterochiroptera branch, *R. ferrumequinum,* ancestral Pteropodidae branch, and all three Yangochiroptera branches) using branch-site models (Zhang *et al.,* 2005). Site-wise ω values were calculated for the foreground branch of interest and across the remaining background branches of the species phylogeny. The ω values were assigned to four predefined site classes under Model A. In the first site class, ω_0 was estimated from the data but constrained ($0 < \omega_0 < 1$), in the second class ω_1 was fixed at 1, in the third class ω_{2a} was allowed to exceed 1 (positive selection) on the branch of interest but constrained to be under purifying selection on the background, and in the final class ω_{2b} could exceed one on the foreground but was not under selection on the background. This model was compared to the null Model A in which only purifying or neutral evolution were permitted i.e. ω_2 on the focal branch is fixed at 1, with a LRT with 1 degree of freedom. Where the alternative model was a better fit (i.e. positive selection was detected along a focal branch), BEB was used to quantify the probability that particular sites were under positive selection.

Whereas, clade models are used to detect divergent selection that has acted over all branches in particular clades, it is also possible that shorter bursts of positive selection may have acted over a smaller number of branches. Therefore, in certain instances where divergent selection was detected across whole clades more specific branch-site models were then used to detect specific episodes of positive selection.

(iii) Clade-wise models of selection

Using the larger taxonomic coverage obtained by sequencing it was possible to estimate selection pressures acting across key groups of echolocating taxa. Thus to test for divergent selection between non-echolocating and echolocating bats and whales, I compared ω averaged across branches within focal clades (foreground) to ω estimated

for the rest of the tree (background) (Bielawski and Yang 2004). For both foreground and background, three site classes were modeled (model C), in two classes ω was constrained ($0< \omega_0 < 1$ and $\omega_1 = 1$) and in the third class, separate foreground and background (ω_2, ω_3) values were modeled, which were allowed to differ from each other. Site-wise mean ω estimates were obtained by multiplying the resulting ω within each class by its corresponding posterior probability. The likelihood values of Model C were compared to model M1a (Nearly Neutral) using a LRT.

Further clade models were used to estimate the selection pressure acting on families repeatedly involved in associations of high probability of convergence. In these models, I removed all other echolocating bats and cetaceans from the background, to avoid underestimating divergent selection.

RESULTS

In silico study

Tests of phylogenetic signal and hypotheses

Bayesian and ML trees based on nearly complete *Tmc1* and *Pjvk* coding regions recovered consistent topologies that showed similarities to previous results reported for *Prestin,* i.e. all laryngeal echolocating bats formed a monophyletic clade with the exclusion of Pteropodidae. Support for this node was relatively high (*Tmc1*: Bayesian posterior probability (BPP) 0.83, Bootstrap (BS) 63; *Pjvk*: BPP 0.91, BS 51) (see Fig. 2.2). For both genes neither "convergent tree" topology (*Tmc1*: $P = 0.291$; *Pjvk*: $P = 0.136$, AUT) was significantly less supported than either the unconstrained tree (*Tmc1*: $P = 0.804$; *Pjvk*: $P = 0.295$, AUT), or the constrained "species tree" (*Tmc1*: $P = 0.102$; *Pjvk*: $P = 0.830$, AUT). This suggests there is mixed phylogenetic signal in both datasets.

Figure 2.2 Tree topologies recovered by Bayesian and ML analyses for 2,139 bp of *Tmc1* (left) and 1,059 bp of *Pjvk* (right). Node support values are BPP and bootstrap values, 1000 replicates, (- indicates topology differed in ML, so no bootstrap value shown; *before / indicates BPP > 0.95, * after / indicates BS > 95%). Branch colours: non-bat species (black), Old World fruit bats (red), laryngeal echolocating Yinpterochiroptera (green) and Yangochiroptera (blue).

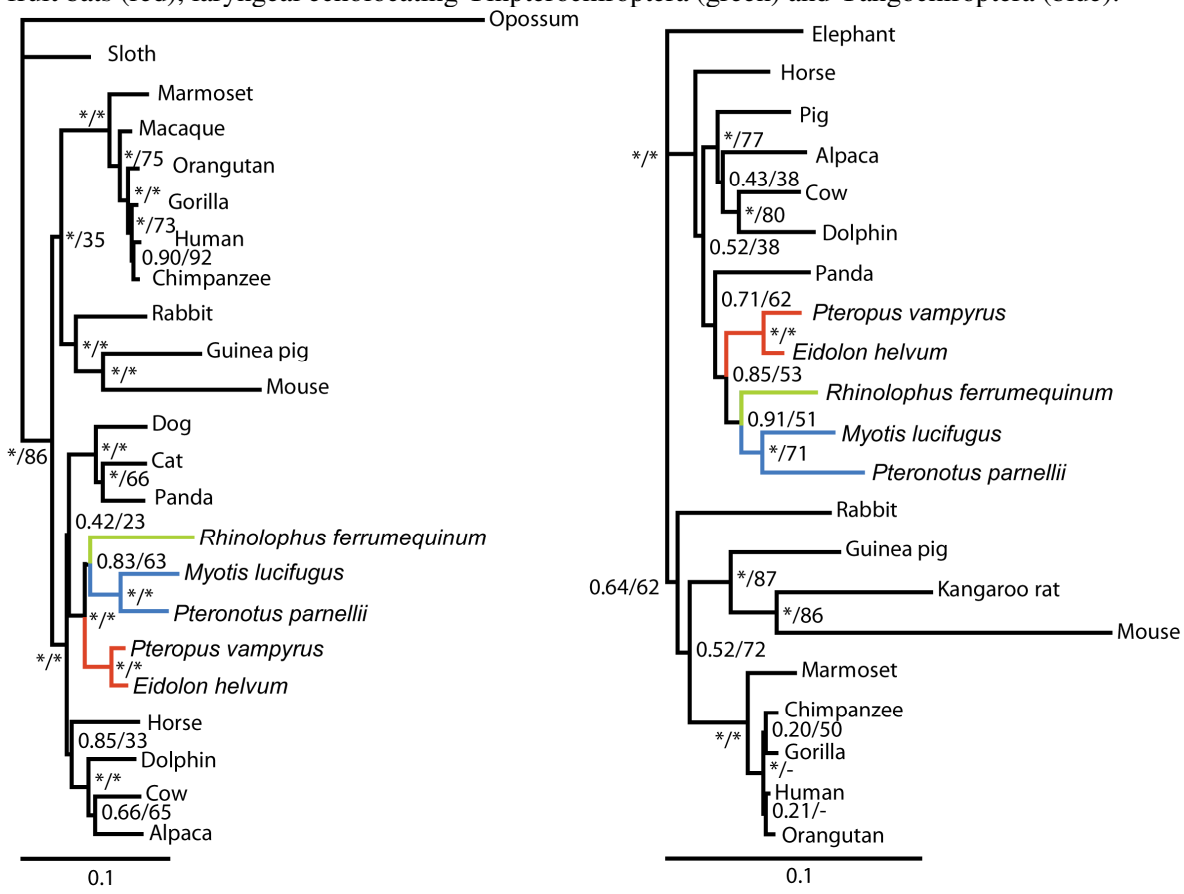

Tests for sequence convergence

To test levels of sequence convergence associated with the acquisition of high-frequency hearing, I compared posterior probabilities of convergence between the dolphin and bat branches, as well as branches between *R. ferrumequinum* and Yangochiroptera branches (Fig. 2.3). Inspection of the probability of convergence in *Tmc1* for comparisons of placental mammal branch-pairs (i.e. with marsupial branch comparisons removed), found that the three branch-pairs with the highest probability of convergence are between divergent echolocating taxa (Fig. 2.3b). The branch-pair with the highest overall probability of convergence was between *R. ferrumequinum* and *P. parnellii*, two bat species which have independently evolved CF echolocation. The other two comparisons were between the dolphin, *T. truncatus*, with firstly, the ancestral Yangochiroptera branch and secondly, *R. ferrumequinum*. Closely below these three comparisons, was the branch comparison between the ancestral Yangochiroptera and *R. ferrumequinum*. In contrast, comparisons between the dolphin and all branches of the Old World fruit bats had very low probabilities of convergence, as did comparisons between the dolphin and the ancestral Yinpterochiroptera. The comparison between the dolphin and the ancestral bat branch also suggested low levels of sequence convergence.

Sites with probabilities of convergent substitutions, greater than 0.5, are listed in Table 2.2, for branch comparisons of interest. A total of four sites with high probability of convergence were identified between *R. ferrumequinum* and *P. parnellii,* this level of branch-wise convergence was found to be highly significant compared to expected levels based on simulations (P <0.001). Three sites with high probabilities of convergence were found between *T. truncatus* and *R. ferrumequinum*, and also between *T. truncatus* and the ancestral Yangochiroptera, again these levels of branch-wise convergence were significantly higher than expected (P <0.001). Two sites with high probability of convergence were found between *R. ferrumequinum* and *M. lucifugus,* as well as *R. ferrumequinum* and the ancestral Yangochiroptera branch. Only a single site was found with high probability of convergence between *T. truncatus* and either *P. parnellii,* or with the ancestral bat. No sites with PP > 0.5 were found between the dolphin and either the ancestral Yinpterochiroptera branch or the Old World fruit bats branches.

Plots of site-wise probability of convergent substitutions (greater than 0.10) between bats and the dolphin, in relation to functional domains, revealed several interesting patterns (Fig. 2.4). Firstly, very few of the predicted convergent substitutions between

taxa that have independently evolved echolocation were found within the six transmembrane domains and are, therefore, either intra- or extra-cellular residues. The single convergent site between the ancestral bat branch and the dolphin was located within the 6th transmembrane domain. Several sites show repeated association of convergence in different taxa; for example amino acids 154 and 613 showed high probability of convergence in all three groups of echolocating taxa (dolphin, echolocating Yinpterochiroptera and Yangochiroptera). Amino acid 613 is particularly interesting in this respect as it is located within the highly conserved TMC domain of this peptide. Eight sites with high probabilities of convergence were found between the single species of echolocating Yinpterochiroptera and the two species of Yangochiroptera (3 branch comparisons), compared to only three between the two species of non-echolocating Yinpterochiroptera and the Yangochiroptera (totalling 9 branch comparisons). This further highlights the association of sequence convergence with the phenotypic convergence of laryngeal echolocation.

For *Pjvk,* pair wise comparisons between the dolphin and the echolocating bats (*R. ferrumequinum* and *M. lucifugus*) showed among the highest probability of convergence across all mammals studied (Fig. 2.3c). Within bats, the comparison between *R. ferrumequinum* and the ancestral Yangochiroptera branch showed the highest level of convergence, followed by the comparison with *M. lucifugus.* Two sites had high probability of sequence convergence between *T. truncatus* and *R. ferrumequinum*, *T. truncatus* and *M. lucifugus,* and also between *R. ferrumequinum* and the ancestral Yangochiroptera (Table 2.2b). The majority of branch-wise comparisons between taxa that are thought to have evolved echolocation independently are found to have significantly higher than expected levels of sequence convergence, while none of the comparisons between the dolphin and the Old World fruit bats were found to be higher than expected (P = 0.07, 1.00 and 1.00). As can be seen from Figure 2.4b, the majority of dolphin-echolocating bat convergent substitutions occur within the highly conserved Gasdermin domain. In fact, one of the sites (193) had a high probability of convergence between the dolphin with both *R. ferrumequinum* and *M. lucifugus.* The convergent substitution between *T. truncatus* and *P. parnellii* occurs within the predicted zinc-binding motif. Three sites were identified with a high probability of convergence between the two echolocating bat suborders (193, 262 and 282), whereas, only a single site was identified between Yangochiroptera and the Old World fruit bats.

Table 2.2 Sites along a) Tmc1 and b) Pjvk with > 0.5 PP total convergence along key branch pairs. Significance levels of branch-wise convergence are based on 1,000 simulated datasets. Amino acid numbers refer to the human peptide.

a) *Tmc1*

Branch pairs			Convergent Substitution (BPP)	Branch-wise convergence
R. ferrumequinum	vs.	*P. parnellii*	N 50 S (0.84), S 128 N (0.98), A 154 V (0.83), M 269 L (0.99),	<0.001
T. truncatus	vs.	*R. ferrumequinum*	A 154 V (0.98), C 613 G (0.97), K 691 M (1.00)	<0.001
T. truncatus	vs.	Ancestral Yangochiroptera	K 76 R (0.93), L 192 M (0.97), C 613 G (0.96)	<0.001
R. ferrumequinum	vs.	*M. lucifugus*	K 263 Q (0.97), K 298 Q (0.99)	<0.001
R. ferrumequinum	vs.	Ancestral Yangochiroptera	P 501 A (0.85), C 613 G (0.93)	<0.001
T. truncatus	vs.	*P. parnellii*	A 154 V (0.84)	0.072
T. truncatus	vs.	Ancestral bat	A 710 V (0.66)	<0.001
T. truncatus	vs.	Ancestral Yinpterochiroptera	None	<0.001
T. truncatus	vs.	Ancestral Pteropodidae	None	0.067
T. truncatus	vs.	*E. helvum*	None	<0.001
T. truncatus	vs.	*P. vampyrus*	None	<0.001
T. truncatus	vs.	*M. lucifugus*	None	0.079
Ancestral Pteropodidae	vs.	*M. lucifugus*	I 204 V (0.88)	NA
Ancestral Pteropodidae	vs.	*P. parnellii*	L 481 I (0.87)	NA
P. vampyrus	vs.	*P. parnellii*	V 358 I (0.92)	NA

b) Pjvk

Branch pairs			Site (BPP Convergence)	Branch-wise convergence
T. truncatus	vs.	*R. ferrumequinum*	I 72 V (0.99), K 193 R (0.98)	0.007
T. truncatus	vs.	*M. lucifugus*	A 181 S (0.99), K 193 R (0.96)	0.002
R. ferrumequinum	vs.	Ancestral Yangochiroptera	A 262 V (0.73), L 282 F (0.55)	<0.001
R. ferrumequinum	vs.	*M. lucifugus*	K 193 R (0.96)	<0.001
T. truncatus	vs.	*P. parnellii*	I 346 V (0.94)	0.028
T. truncatus	vs.	Ancestral bat	I 110 V (0.89)	<0.001
T. truncatus	vs.	Ancestral Yangochiroptera	None	0.057
R. ferrumequinum	vs.	*P. parnellii*	None	0.031
T. truncatus	vs.	Ancestral Yinpterochiroptera	None	<0.001
T. truncatus	vs.	Ancestral Pteropodidae	None	0.066
T. truncatus	vs.	*E. helvum*	None	1.000
T. truncatus	vs.	*P. vampyrus*	None	1.000
Ancestral Pteropodidae	vs.	*M. lucifugus*	None	NA
Ancestral Pteropodidae	vs.	*P. parnellii*	T 105 A (0.69)	NA
P. vampyrus	vs.	*P. parnellii*	None	NA

Figure 2.3 Branch-pair plots of total BPP divergence vs. total BPP convergence. In b) *Tmc1* and c) *Pjvk,* bat branches vs. dolphin (diamonds), and *Rhinolophus ferrumequinum* vs. Yangochiroptera branches (circles) are colour coded according to the species tree (a), remaining points (grey circles) correspond to comparisons between the remaining non-echolocating mammal species.

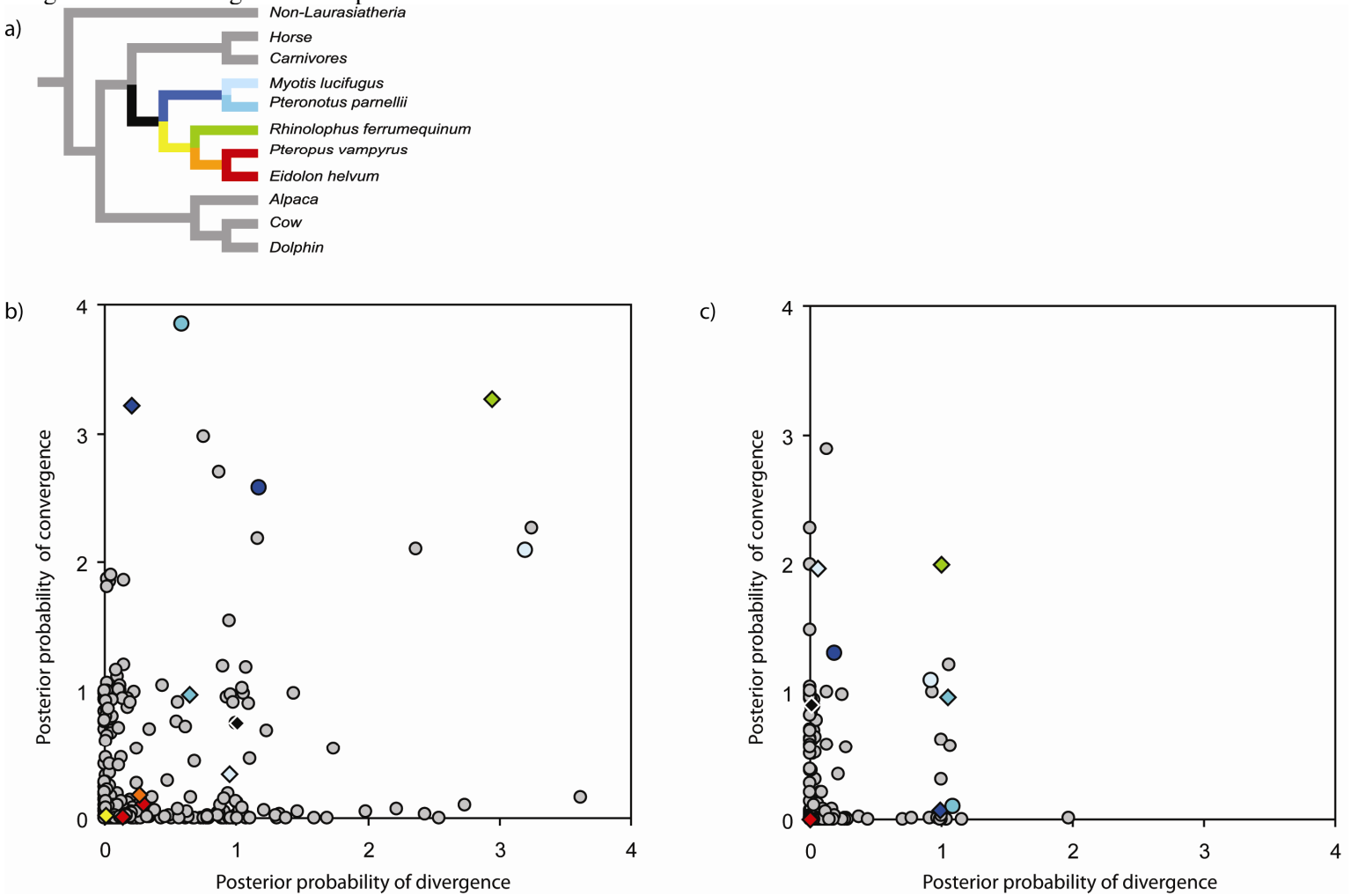

Figure 2.4 Site-wise posterior probability of convergent substitution against functional peptide domains for TMC1 and PJVK proteins. Only sites with PP convergence greater than 0.1 are shown, and bat branches vs. dolphin (diamonds), and *Rhinolophus ferrumequinum* vs. Yangochiroptera branches (circles) are colour coded according to Figure 2.3. a) The six TMC1 transmembrane domains are numbered (i-vi), and their locations are indicated with pale grey shaded regions, and the highly conserved TMC domain (TMC) is indicated with the dark grey shaded region. b) The location of the highly conserved Gasdermin domain (i), the putative nuclear localization signal (ii) and the zinc-binding motif (iii) of PJVK are indicated with the dark grey shaded regions.

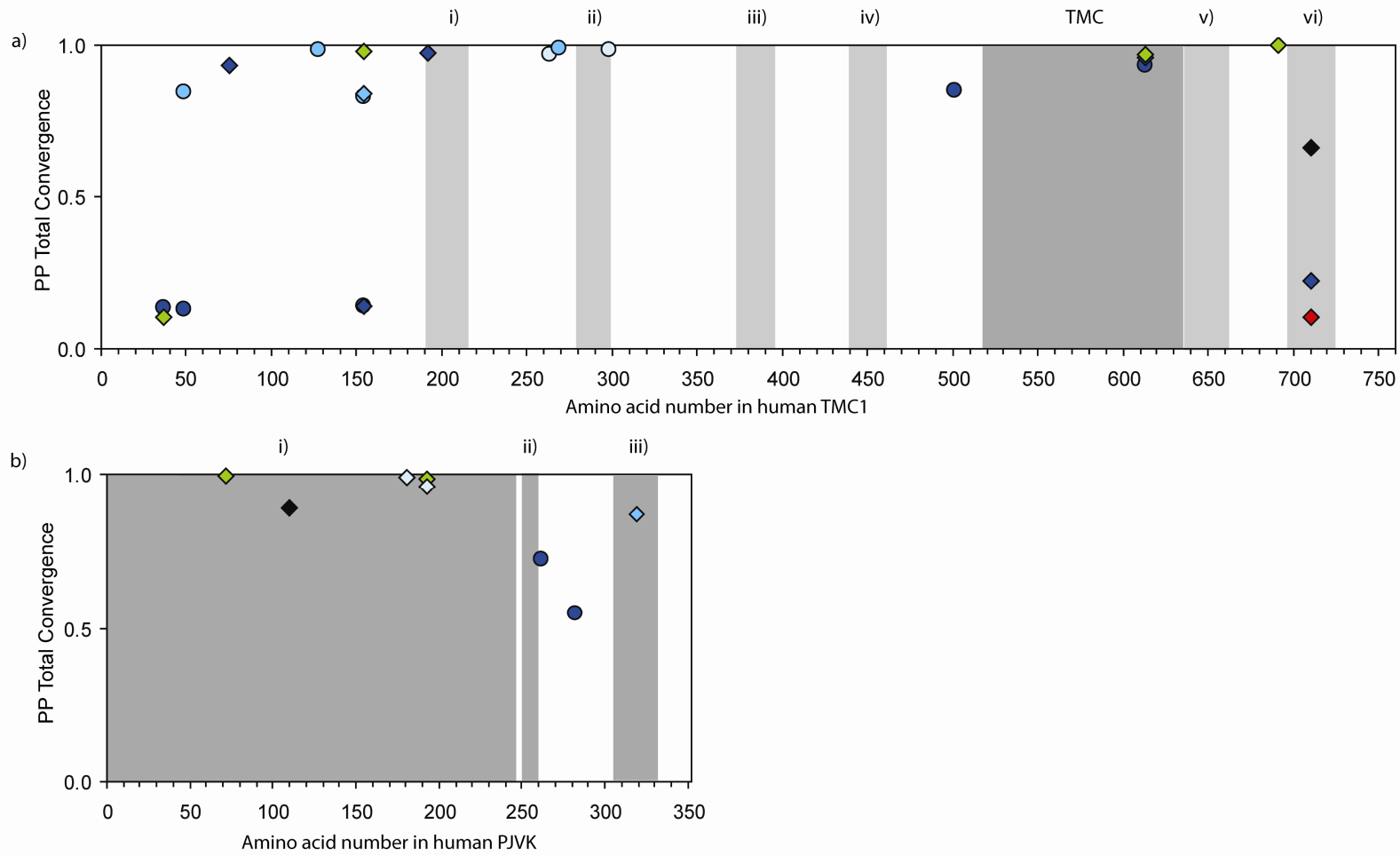

Tests for selection

(i) Site models of selection

Site models undertaken to estimate selection pressures along the nearly complete coding regions of both genes, did not find evidence of positive selection in either gene (Table A4). For both genes, model M3 with three ω classes (all ω<1), fitted the data better than model M0 (*Tmc1*: LRT = 193.99, $P < 0.001$; *Pjvk*: LRT = 61.00, $P < 0.001$). Furthermore in both pair-wise model tests for positive selection (M1a vs. M2a and M7 vs. M8) the alternative hypotheses were rejected (Table 2.3). Therefore, it can be concluded that these genes are typically under purifying and neutral evolution across the majority of mammals included in this study.

Table 2.3 Site-wise model LRT for *Tmc1* and *Pjvk*

Gene	LRT	df	$2(l_0-l_1)$	*P*
Tmc1	M0 vs. M3	4	193.989	<0.001
	M1a vs. M2a	2	0.000	1.00
	M7 vs. M8	2	2.039	0.36
Pjvk	M0 vs. M3	4	61.00	<0.001
	M1a vs. M2a	2	0.00	1.00
	M7 vs. M8	2	1.25	0.54

(ii)Branch-site models of selection

Branch-site tests of selection based on the nearly complete coding sequence of *Tmc1* detected positive selection in both clades of echolocating bats. Firstly positive selection was found on the branch leading to echolocating Yangochiroptera (ω = 9.36, LRT = 4.83, DF = 1, $P = 0.028$), with a total of 16 positively selected sites identified from BEB analyses (Table A5). Positive selection was also detected on the *M. lucifugus* branch (ω = 33.36, LRT = 5.53, DF = 1, $P = 0.019$) with eight positively selected sites based on BEB analysis (Table A5), but not on the *P. parnellii* branch. Secondly, positive selection was detected on the branch leading to the echolocating Yinpterochiroptera, *R. ferrumequinum,* (ω = 3.88, LRT = 5.20, DF = 1, $P = 0.023$), with a total of 25 positively selected sites identified. Positive selection was not detected on either the branch leading to all Yinpterochiroptera or the dolphin. Similarly, no evidence of positive selection was detected along the ancestral Pteropodidae branch; instead the majority of sites were found to be under purifying selection (Table 2.4 and Table A5).

In contrast to above, branch-site tests of selection based on the full coding sequence of *Pjvk* revealed no evidence of positive selection on any of the bat or dolphin branches tested (Table 2.4).

Table 2.4 LRT results of branch-site models for *Tmc1* and *Pjvk*.

LRT (Null vs. Alt)	df	$2(l_0-l_1)$	*P*
Tmc1			
I Yangochiroptera	1	4.83	0.028
II *Myotis lucifugus*	1	5.53	0.019
III *Pteronotus parnellii*	1	0.00	1.000
IV Yinpterochiroptera	1	0.00	1.000
V Pteropodidae	1	0.00	1.000
VI *Rhinolophus ferrumequinum*	1	5.20	0.023
VII *Tursiops truncatus*	1	0.00	1.000
Pjvk			
I Yangochiroptera	1	0.00	1.000
II *Myotis lucifugus*	1	0.00	1.000
III *Pteronotus parnellii*	1	0.00	1.000
IV Yinpterochiroptera	1	0.00	1.000
V Pteropodidae	1	0.00	1.000
VI *Rhinolophus ferrumequinum*	1	0.00	1.000
VII *Tursiops truncatus*	1	0.13	0.720

Association between convergence and positive selection

Sites identified with high probabilities of convergent substitutions, in *Tmc1* and *Pjvk*, between taxa that are thought to have independently evolved echolocation are shown by Figure 2.5. Sites found to be under positive selection in either focal branch are also highlighted. In *Tmc1*, eight of the sites identified as undergoing convergent substitutions between echolocating taxa were also found to be under positive selection in at least one of the taxa concerned. In *Pjvk,* no significant positive selection was detected so it is not possible to associate the convergent substitutions with positive selection in these taxa.

Figure 2.5 Positive selection and convergent substitutions, in (a) *Tmc1* and (b) *Pjvk*. Sites with high probability of convergent substitutions, in parenthesis, are shown in black text; arrows indicate branches which share the convergence. Significant branch-site models are indicated by coloured text, sites are listed if identified as undergoing convergent substitutions and positive selection. For each gene the upper tree displays convergence between echolocating Yinpterochiroptera and Yangochiroptera, and the lower between the dolphin and echolocating bats.

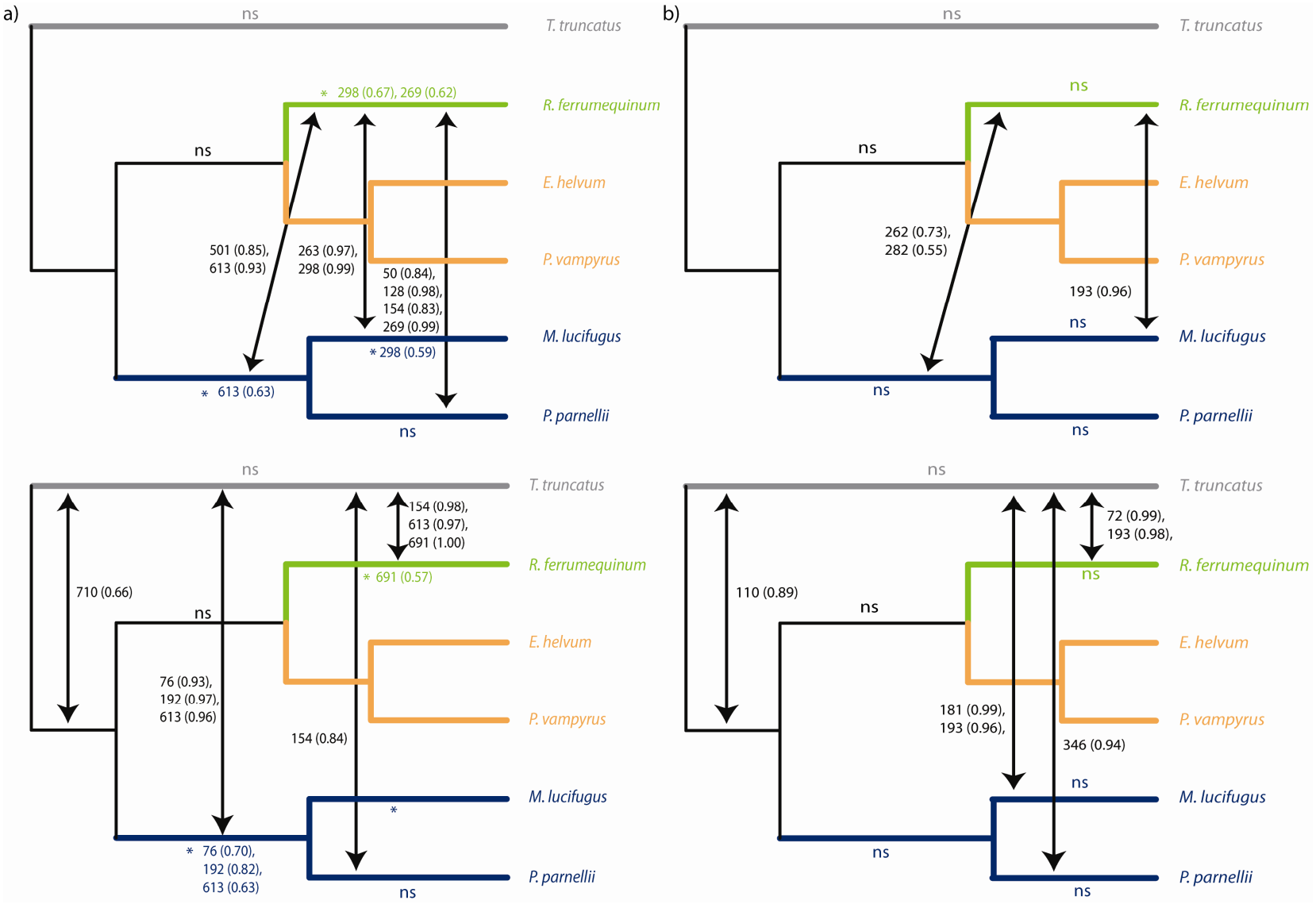
a)
ns
T. truncatus
* 298 (0.67), 269 (0.62)
R. ferrumequinum
ns
E. helvum
501 (0.85),
613 (0.93)
263 (0.97),
298 (0.99)
P. vampyrus
50 (0.84),
128 (0.98),
154 (0.83),
269 (0.99)
M. lucifugus
* 298 (0.59)
* 613 (0.63)
P. parnellii
ns
b)
ns
T. truncatus
ns
R. ferrumequinum
ns
E. helvum
262 (0.73),
282 (0.55)
P. vampyrus
193 (0.96)
ns
M. lucifugus
ns
ns
P. parnellii
ns
ns
T. truncatus
154 (0.98),
613 (0.97),
691 (1.00)
R. ferrumequinum
* 691 (0.57)
710 (0.66)
ns
E. helvum
76 (0.93),
192 (0.97),
613 (0.96)
P. vampyrus
154 (0.84)
M. lucifugus
*
* 76 (0.70),
192 (0.82),
613 (0.63)
P. parnellii
ns
ns
T. truncatus
72 (0.99),
193 (0.98),
R. ferrumequinum
ns
110 (0.89)
ns
E. helvum
181 (0.99),
193 (0.96),
P. vampyrus
346 (0.94)
ns
M. lucifugus
ns
ns
P. parnellii
ns

Wider taxonomic study dataset

Tests of phylogenetic signal and hypotheses

Using the dataset of newly generated shorter sequences from a greater range of taxa, trees based on intron+exon and exon sequence data showed different topologies for both *Tmc1* and *Pjvk* (Fig. 2.6). Specifically, in the intron+exon dataset for *Tmc1* (455 bp) and *Pjvk* (509 bp), the phylogenetic signal was generally congruent with the accepted relationships among mammalian orders. Focusing on bats, the intron+exon trees of both genes supported bat monophyly (*Tmc1*: BPP 0.92, BS 86; *Pjvk*: BPP 0.99, BS 94). However, while the *Tcm1* tree recovered the Yinpterochiroptera and Yangochiroptera suborders, the *Pjvk* tree did not. By comparison, in the exon-only trees for *Tmc1* (291 bp) and *Pjvk* (206 bp) all laryngeal echolocating bat species were monophyletic (*Tmc1*: BPP 0.73, BS 36; *Pjvk*: BPP 0.71, BS 25), whereas the main mammalian orders were retained. Furthermore, the nature of conflict was seen using both Bayesian and ML methods, and was consistent across both genes and showed similarities to previous results reported for *Prestin* i.e. trees based on coding regions resulted in the monophyly of laryngeal echolocators. For the exon data of both genes, the "convergent tree" was not significantly less supported (*Tmc1*: $P = 0.884$; *Pjvk*: $P = 0.628$, AUT) than either the unconstrained tree (*Tmc1*: $P = 0.884$; *Pjvk*: $P = 0.592$, AUT) or the constrained "species tree" (*Tmc1*: $P = 0.116$; *Pjvk*: $P = 0.125$, AUT) and, therefore, could not be rejected.

The weakly supported monophyly of laryngeal echolocators combined with AUT results suggest conflicting phylogenetic signal within *Tmc1* and *Pjvk* coding regions. This was supported by Lento-Plots for all splits, which revealed that intron data contained fewer bifurcating splits than exon data (Fig. 2.7). The smaller number of supported splits in the intron data points to a clearer phylogenetic signal compared to the exons. Relative site-wise likelihoods along the *Tmc1* exon alignment (Fig. 2.8a), showed strong support for the convergent tree topology at first positions of codons 423, and 501, whereas support for the species tree was distributed more widely across the alignment. Along the whole intron+exon alignment, it seems that most nucleotides supporting the species topology occurred in the intron (Fig. 2.8b). Strong support for the convergent tree was found at the first position of *Pjvk* codon 282, whereas relatively weaker support for the species topology was found at the third positions of codons 294 and 302 (Fig. 2.8c). Inspection of the intron+exon alignment revealed that many sites, albeit with low support, for the species tree were concentrated within the intron (Fig. 2.8d).

Figure 2.6 Tree topologies recovered by Bayesian analyses. Nodal support - Bayesian posterior probabilities, and bootstrap values (1000 replicates) based on ML analyses (*before / indicates BPP > 0.95, * after / indicates BS > 95%, - indicates node not recovered by ML analysis). Clades as follows: outgroup species (brown), cetaceans (grey), Old World fruit bats (orange) and echolocating Yinpterochiroptera (green), Yangochiroptera (blue).

(a) *Tmc1* main tree based on 291 bp of exons 16 – 17, inset shows the simplified tree topology recovered from 455 bp of exons 16 – 17 plus intron XV1.

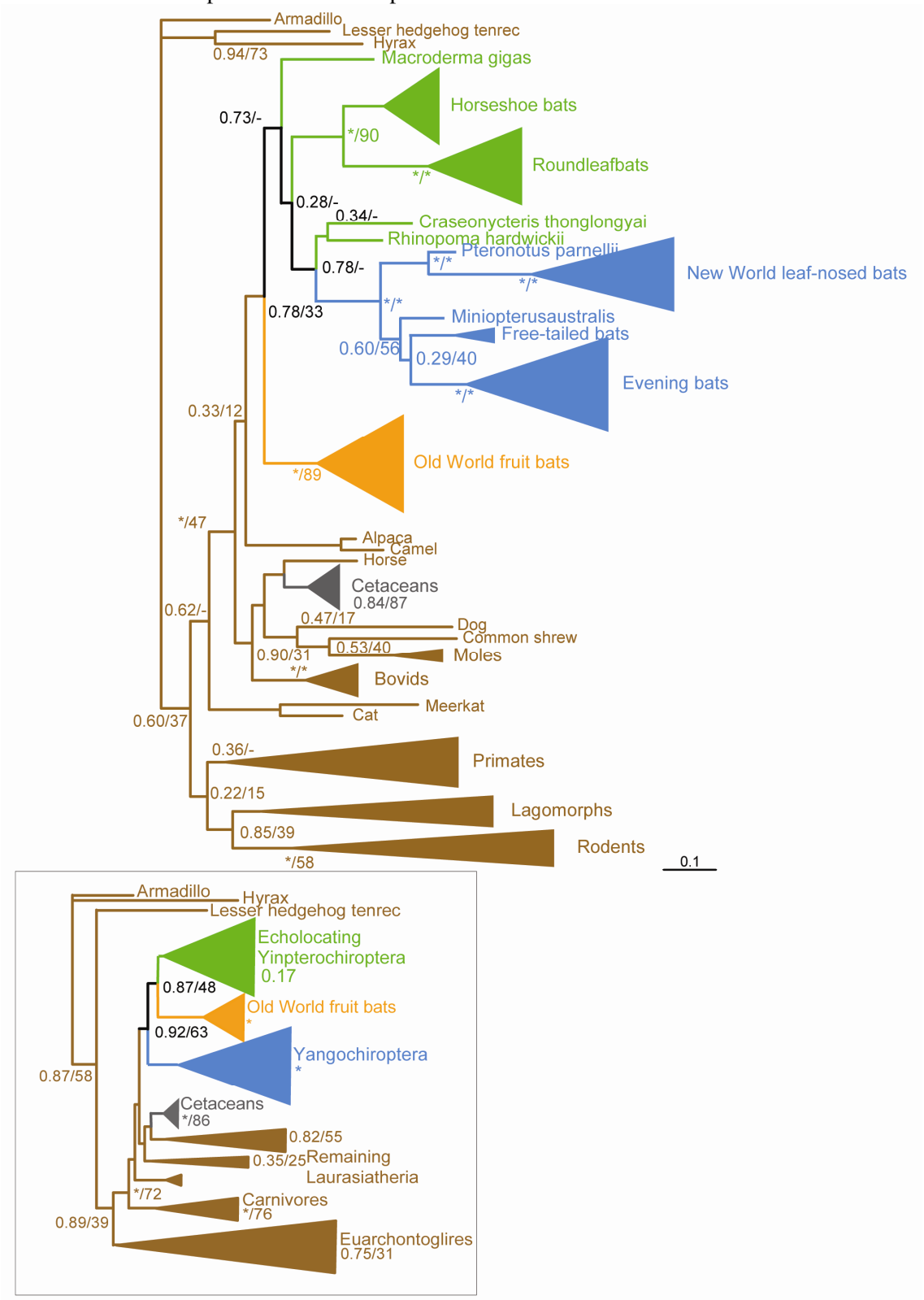

(b) *Pjvk* main tree based on 206 bp of exons 6 – 7, and the inset shows the simplified tree topology recovered from 509 bp of exons 6 – 7 plus intron V1.

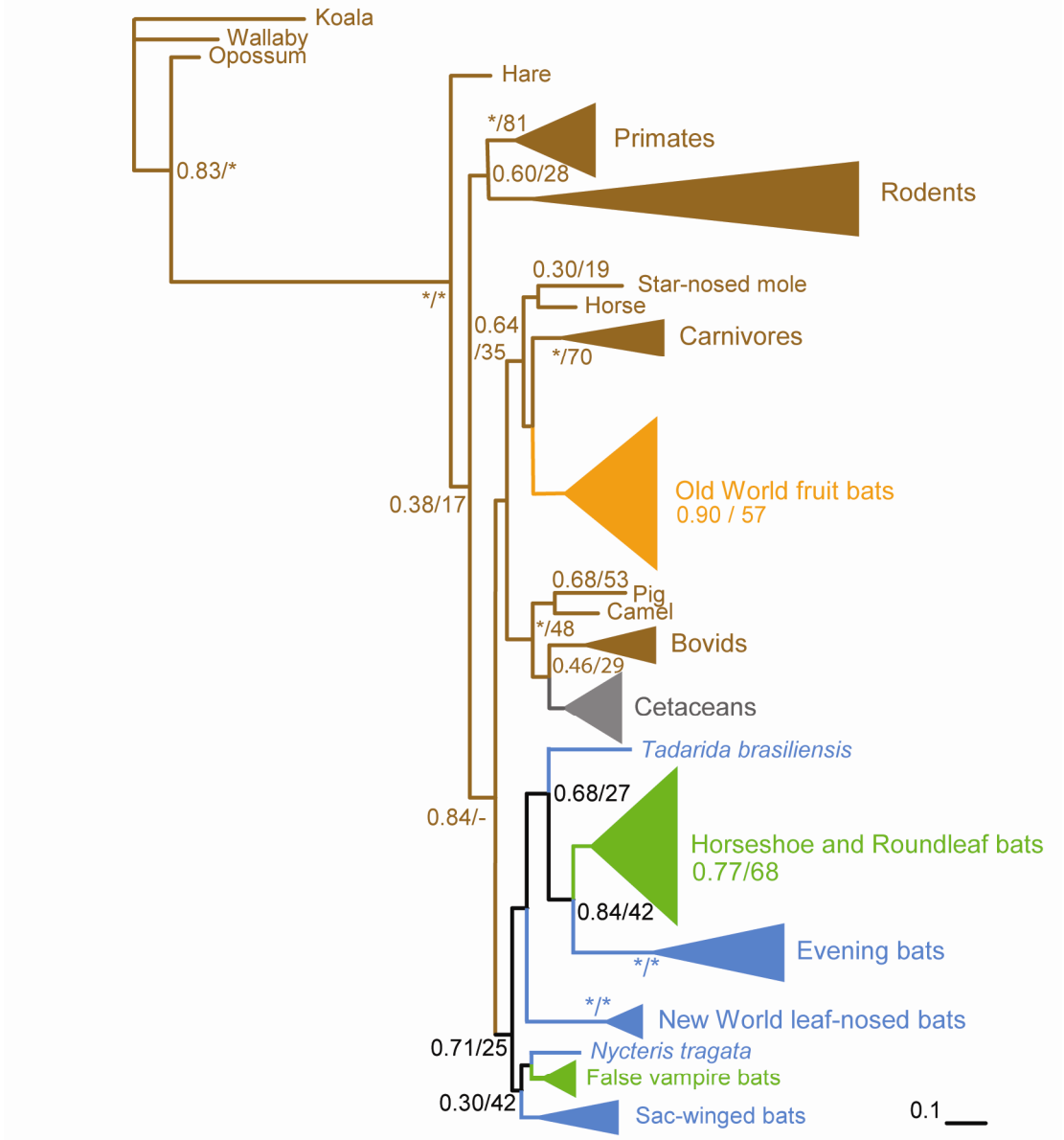

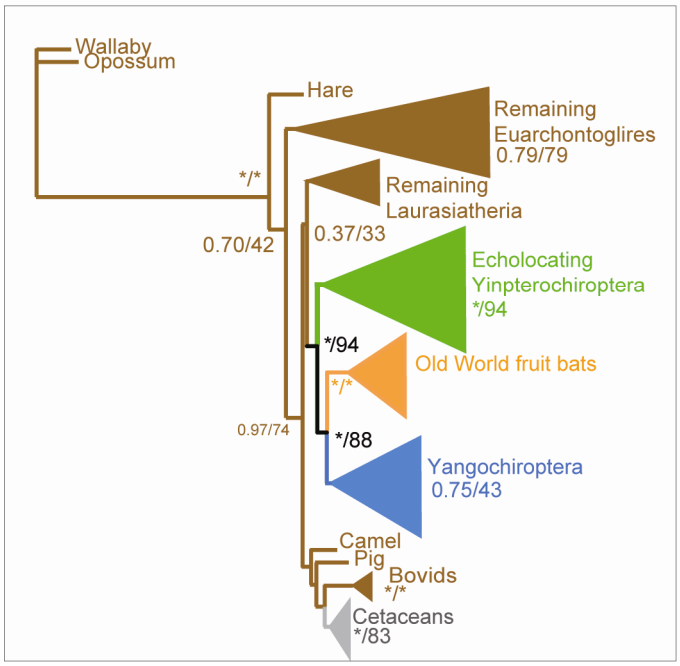

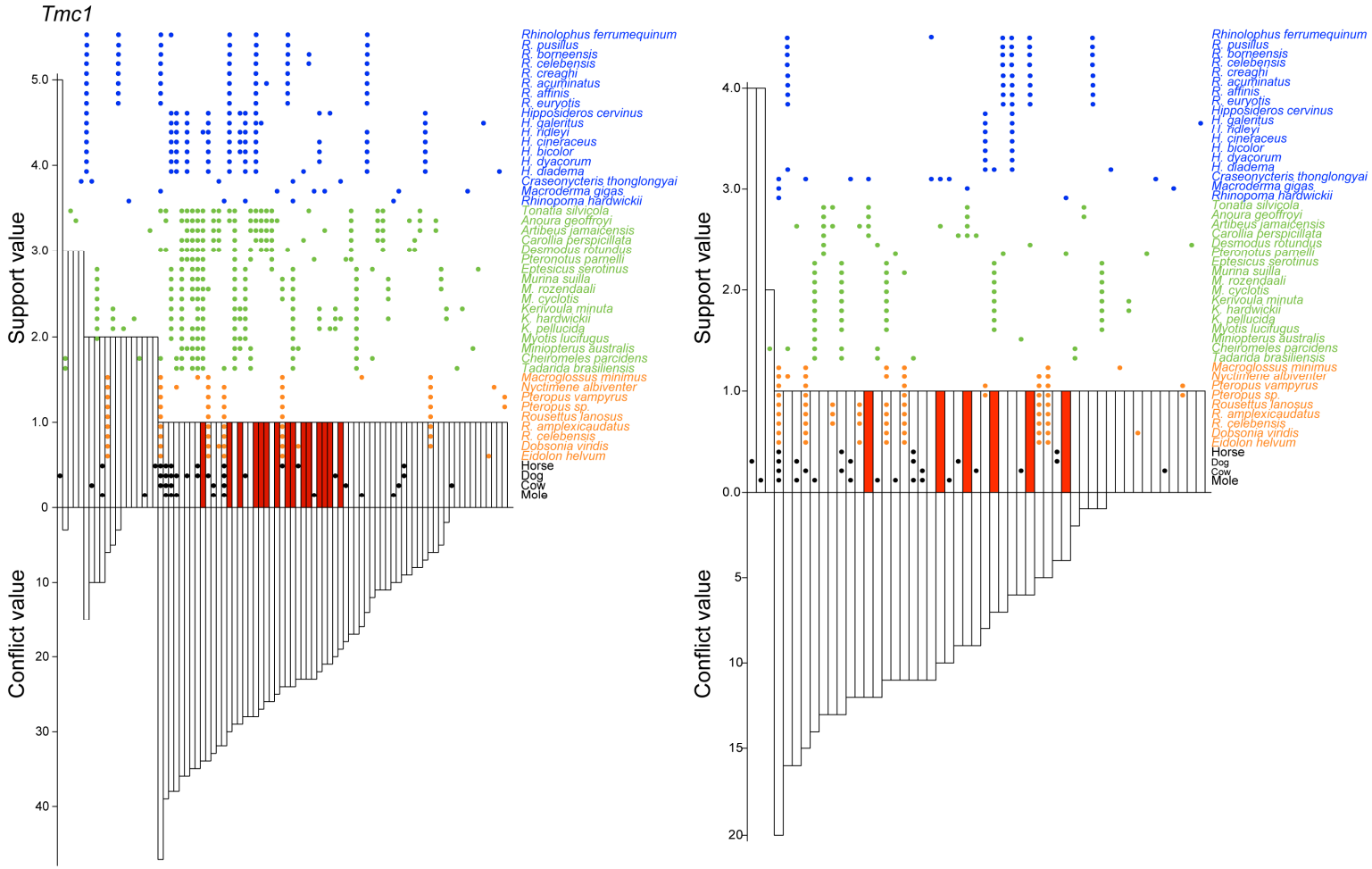

Figure 2.7 Lento-plots of support and conflict values for all splits for *Tmc1* and *Pjvk*. For exons (left) and introns (right), splits consisting of at least one species of each of the echolocating bat clades are shaded red. Echolocating Yinpterochiroptera species (blue); Yangochiroptera (green); Old World fruit bats (orange) and outgroup taxa (black). Support values for each split (the number of sites resulting in the split) are shown above the x-axis, and conflict values (the sum of the support for all incompatible splits) are shown below.

Pjvk

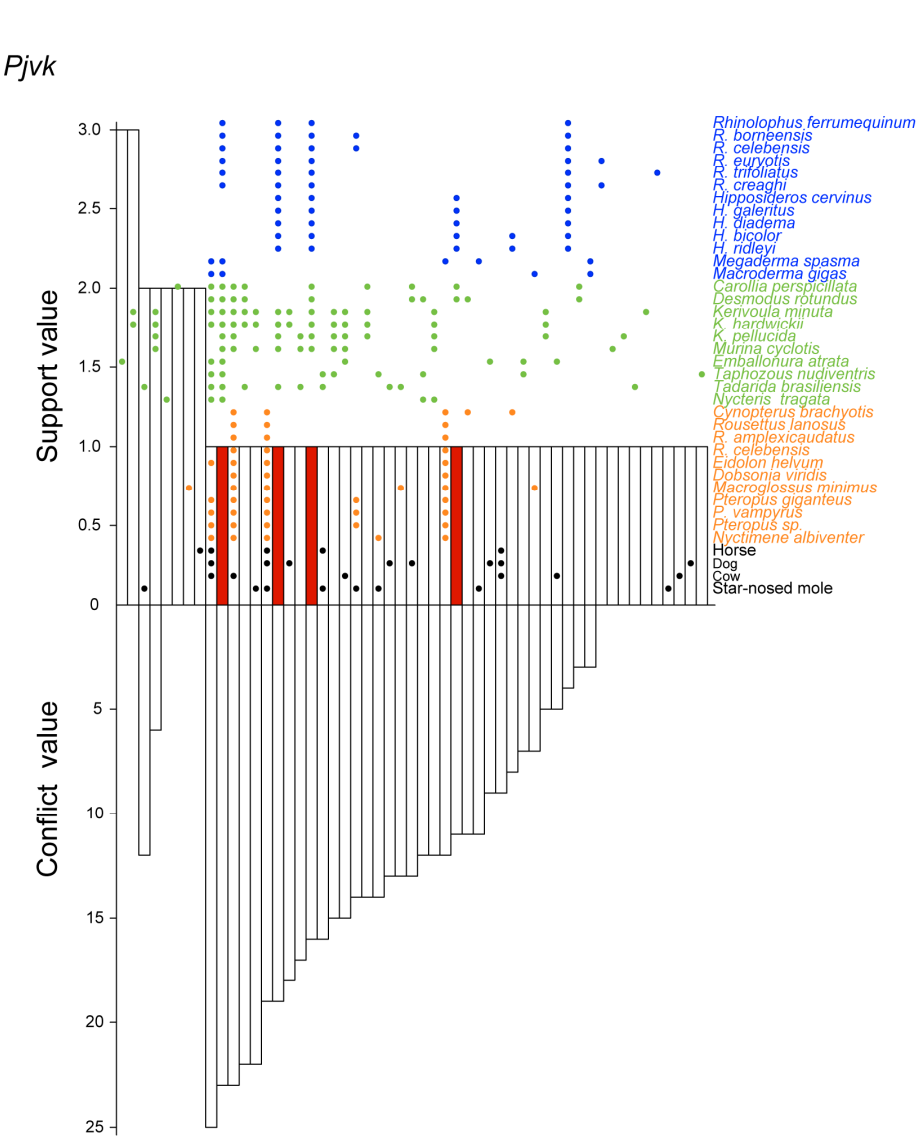
Support value
Conflict value
3.0
2.5
2.0
1.5
1.0
0.5
0
5
10
15
20
25
Rhinolophus ferrumequinum
R. borneensis
R. celebensis
R. euryotis
R. trifoliatus
R. creaghi
Hipposideros cervinus
H. galeritus
H. diadema
H. bicolor
H. ridleyi
Megaderma spasma
Macroderma gigas
Carollia perspicillata
Desmodus rotundus
Kerivoula minuta
K. hardwickii
K. pellucida
Murina cyclotis
Emballonura atrata
Taphozous nudiventris
Tadarida brasiliensis
Nycteris tragata
Cynopterus brachyotis
Rousettus lanosus
R. amplexicaudatus
R. celebensis
Eidolon helvum
Dobsonia viridis
Macroglossus minimus
Pteropus giganteus
P. vampyrus
Pteropus sp.
Nyctimene albiventer
Horse
Dog
Cow
Star-nosed mole

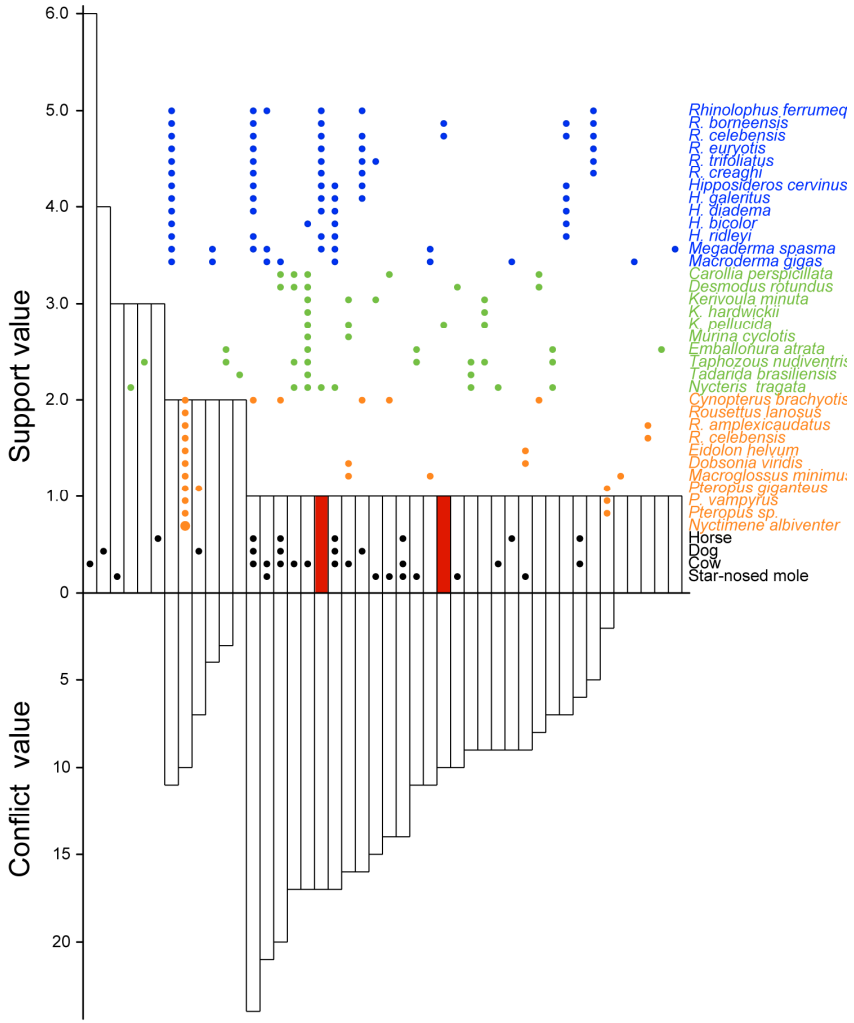
Support value
Conflict value
6.0
5.0
4.0
3.0
2.0
1.0
0
5
10
15
20
Rhinolophus ferrumeq
R. borneensis
R. celebensis
R. euryotis
R. trifoliatus
R. creaghi
Hipposideros cervinus
H. galeritus
H. diadema
H. bicolor
H. ridleyi
Megaderma spasma
Macroderma gigas
Carollia perspicillata
Desmodus rotundus
Kerivoula minuta
K. hardwickii
K. pellucida
Murina cyclotis
Emballonura atrata
Taphozous nudiventris
Tadarida brasiliensis
Nycteris tragata
Cynopterus brachyotis
Rousettus lanosus
R. amplexicaudatus
R. celebensis
Eidolon helvum
Dobsonia viridis
Macroglossus minimu
Pteropus giganteus
P. vampyrus
Pteropus sp.
Nyctimene albiventer
Horse
Dog
Cow
Star-nosed mole

Figure 2.8 Relative site-wise support for constrained species topology vs. convergent topology (monophyly of echolocating bats enforced). For *Tmc1* data are based on (a) exons 16–17, and (b) exons 16-17 plus intron XVI. For *Pjvk* data are based on (c) exons 6–7, and (d) exons 6-7 plus intron VI. Relative support was calculated as the difference between site-wise negative log likelihoods for convergent tree minus those of the species tree. Negative values (red area) indicate more support for the convergent topology and positive values (blue area) indicate more support for the species tree. In Figs. a. and c., the 1st codon positions are coloured red, the 2nd in blue and the 3rd in black, the vertical black line corresponds to the transition from one exon to the next. In Figs. b. and d. the intron is denoted by the shaded region.

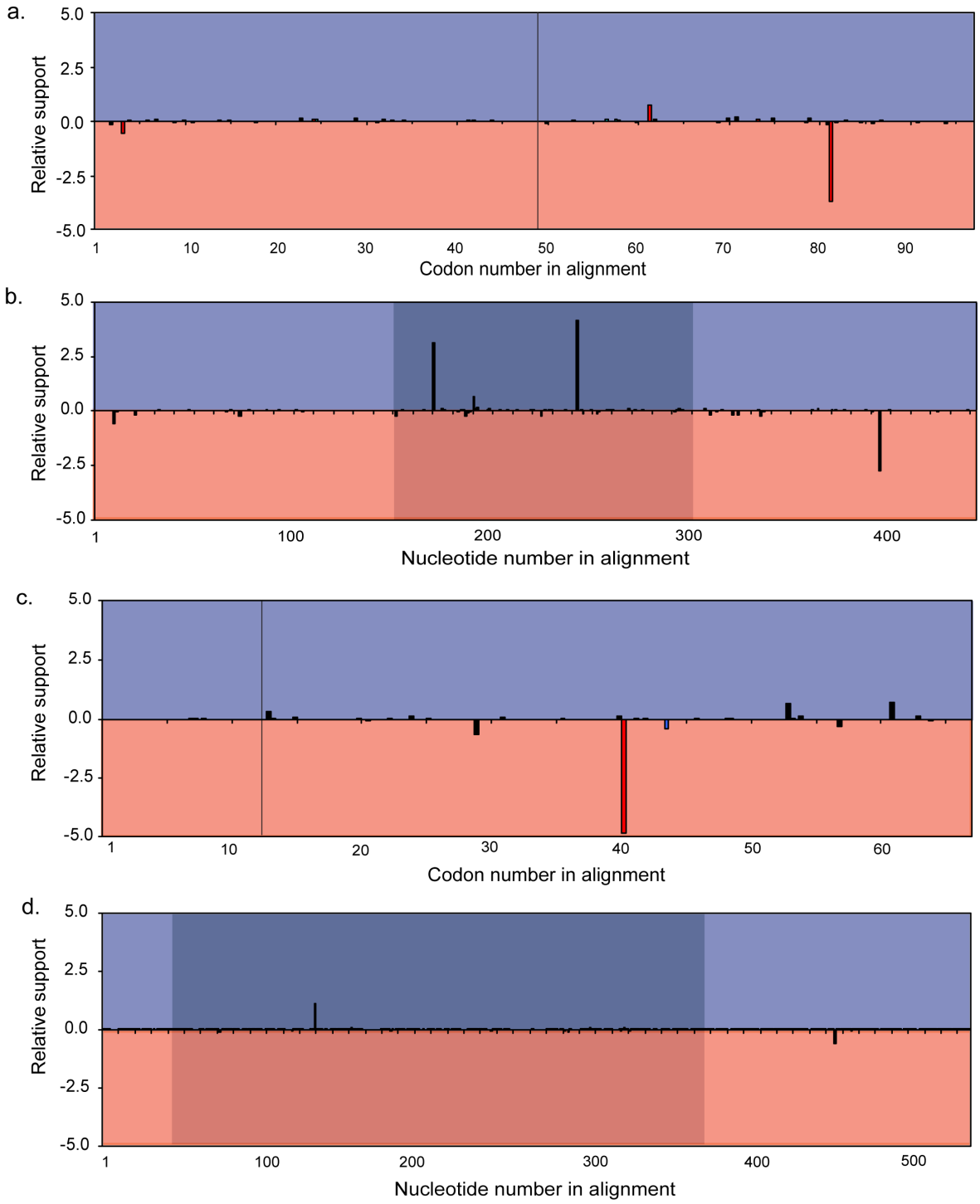

Tests for sequence convergence

Using the wider taxonomic dataset, I repeated the calculations of the posterior probabilities of convergent and divergent substitutions for all ancestral branch pairs. This analysis clearly identified some branch pairs with high probabilities of convergent substitutions, but not all of these are restricted to comparisons between the two clades of echolocating bats (Fig. 2.9). However, for *Tmc1*, posterior probabilities of convergence for pairs of branches were greater for comparisons corresponding to phenotypic convergence (i.e. echolocation across clades) than for comparisons both within these clades and those involving non-echolocating Old World fruit bats (Mann–Whitney $U = 37460$, $n_1 = 272$, $n_2 = 426$, $P < 0.0001$, two-tailed). However, for the *Pjvk* gene, sequence convergence probabilities did not differ between these groups (Mann–Whitney $U = 16820$, $n_1 = 117$, $n_2 = 298$, $P = 0.56$, two-tailed).

I found several sites within each gene that showed strong evidence, in the form of high probabilities, of convergence between certain members of echolocating Yinpterochiroptera and Yangochiroptera. Specifically, for *Tmc1*, amino acid sites with high probabilities of convergence were 481, 500 and 504, whereas for *Pjvk*, sites identified as convergent were 245, 262 and 282. All branch-wise significance tests of convergence revealed that the branch-pairs that the above convergent substitutions occurred on were significantly greater compared to the null distribution of expected values (Table 2.5). No sites in *Tmc1* were identified as having high probabilities of convergence between Yangochiroptera and the Old World fruit bats (see Fig. 2.9). However, in *Pjvk* one site, 282, was identified as having high probability of convergence between the Old World fruit bats and the Kerivoulinae.

Figure 2.9 Plots of posterior probabilities of divergence and convergence for branch comparisons (with all tip comparisons removed). Comparisons between the two main echolocating bat clades (red); within each echolocating clade or those involving Old World fruit bats (blue); with one non-bat (grey) and involving two non-bat mammals (black).

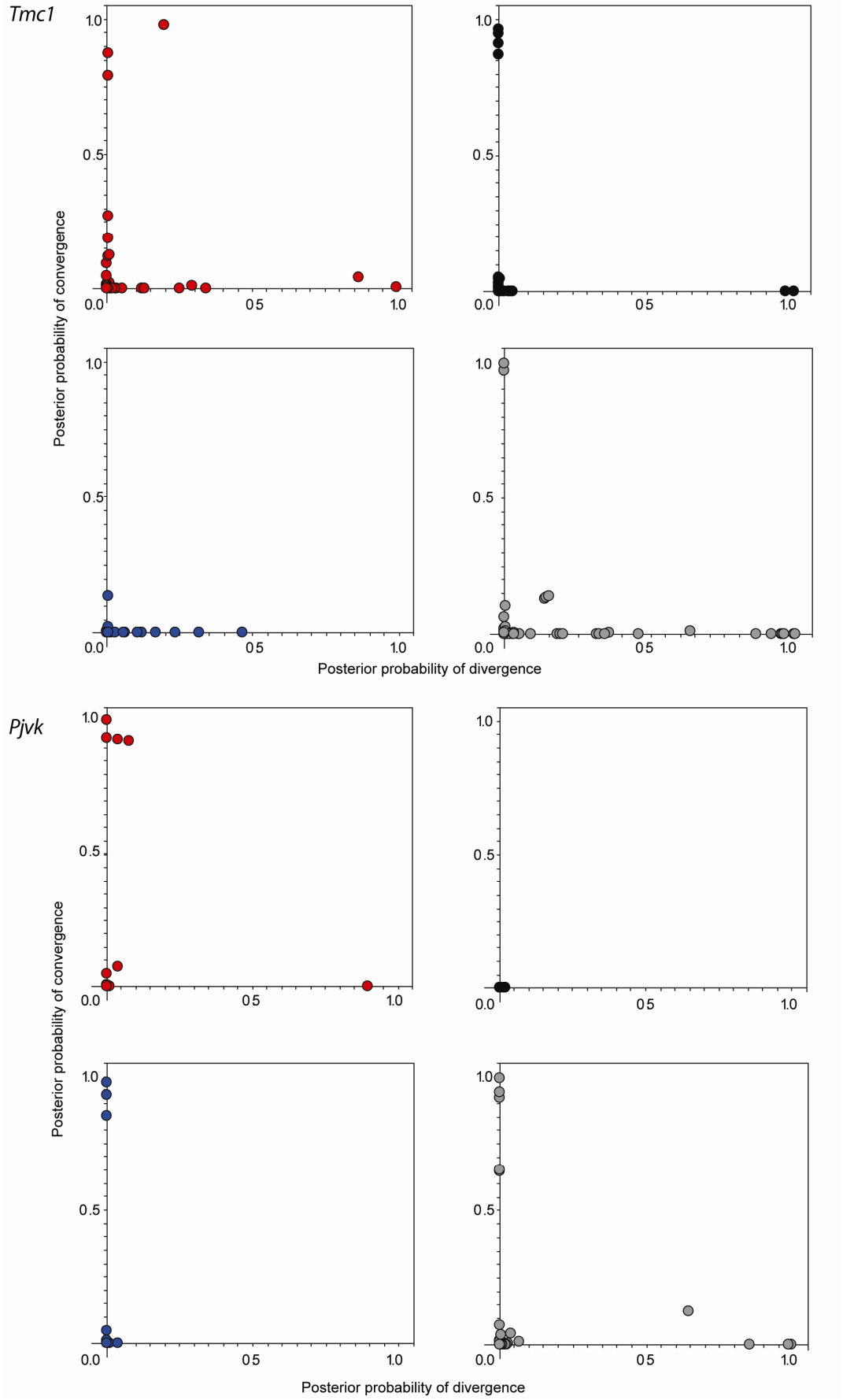

Table 2.5 Amino acid sites identified as undergoing convergent substitutions. Again only sites PP >0.5 are shown, branch-wise significance levels are also shown. Estimated ω values are calculated using clade models and the posterior probability of the site being in the 3rd site class are shown in brackets.

a) *Tmc1*

AA site	Yinpterochiroptera	Est. ω (PP 3rd site class)	Yangochiroptera	Est. ω (PP 3rd site class)	PP Conv.	Branch-wise
I 481 L	Hipposideridae	4.49 (0.93)	Vespertilionidae	1.17 (0.94)	0.88	0.036
G 500 A	Rhinolophidae and Hipposideridae	2.39 (0.96)	Internal Phyllostomidae	0.82 (0.93)	0.98	<0.001
F 504 Y	Internal Hipposideridae	4.70 (0.99)	Internal Kerivoulinae	2.09 (0.77)	0.79	<0.001

b) *Pjvk*

AA site	Yinpterochiroptera	Est. ω (PP 3rd site class)	Yangochiroptera	Est. ω (PP 3rd site class)	PP Conv.	Branch-wise
L 245 F	Hipposideridae	1.02 (0.93)	Phyllostomidae	0.63 (0.89)	0.99	0.002
A 262 V	Rhinolophidae and Hipposideridae	0.94 (0.92)	Phyllostomidae	0.64 (0.89)	0.92	0.018
A 262 V	Rhinolophidae and Hipposideridae	0.94 (0.92)	Vespertilionidae	0.62 (0.88)	0.92	0.014
F 282 L	Hipposideridae	1.04 (0.90)	Internal Kerivoulinae	0.54 (0.83)	0.94	0.012

Tests for selection

(iii) Clade models of selection

For both genes, clade models conducted to test hypotheses of divergent selection between echolocating and non-echolocating taxa were significant for all groups examined, as indicated by better fit than their corresponding M1a models (Table A6 and 2.6). Moreover, for *Tmc1*, estimates of ω were >1 (positive selection) for ~16% of sites when the foreground clade was defined as either all echolocating species of Yinpterochiroptera (ω = 1.37), or all Rhinolophidae and Hipposideridae (ω = 2.48). By comparison, the foreground ω was around zero (purifying selection) in the Pteropodidae and 0.86 (purifying selection) in the Yangochiroptera. In echolocating cetaceans, clade model showed evidence of positive selection (ω = 1.13) at 16% of sites.

For *Pjvk,* analyses of the same bat clades revealed either purifying selection or neutral evolution (0>ω>1). In the Old World CF bats, ω values were around 1 (Rhinolophidae and Hipposideridae ω = 0.97; Hipposideridae ω = 1.05), this could be due to a past short burst of positive selection. Indeed a branch-site model of the Rhinolophidae and Hipposideridae branch detected positive selection (ω = 115.81, LRT = 4.28, df = 1, $P <$ 0.05), with two amino acid sites (244 and 262) identified to be under positive selection (Table A7). A clade model undertaken for echolocating whales revealed strong positive selection (ω = 7.40), detected at 16% of sites.

Table 2.6 Results of LRT for clade parameters of *Tmc1* and *Pjvk*. The *Tmc1* null model had 158 parameters and the alternatives 161, the *Pjvk* null model had 127 parameters and the alternatives 130, therefore, all LRT were performed with 3 DF.

Gene	Model comparisons:			$2(l_0-l_1)$	*P*
Tmc1	Null	vs.	I Rhinolophidae and Hipposideridae	61.31	<0.0001
	Null	vs.	II Hipposideridae	62.69	<0.0001
	Null	vs.	III Pteropodidae	37.51	<0.0001
	Null	vs.	IV Yangochiroptera	46.06	<0.0001
	Null	vs.	V Kerivoulinae	45.57	<0.0001
	Null	vs.	VI Vespertilionidae	41.64	<0.0001
	Null	vs.	VII Phyllostomidae	36.36	<0.0001
	Null	vs.	VII Odontoceti	33.44	<0.0001
Pjvk	Null	vs.	I Rhinolophidae and Hipposideridae	19.74	<0.005
	Null	vs.	II Hipposideridae	19.57	<0.005
	Null	vs.	III Pteropodidae	16.33	0.001
	Null	vs.	IV Yangochiroptera	20.19	<0.005
	Null	vs.	V Kerivoulinae	18.31	<0.005
	Null	vs.	VI Vespertilionidae	20.90	<0.005
	Null	vs.	VII Phyllostomidae	18.92	<0.005
	Null	vs.	VII Odontoceti	26.77	<0.0001

Association between convergence and positive selection

Estimated site-wise ω values for the sites in *Tmc1* and *Pjvk* found to have high probabilities of convergence are listed in Table 2.5. All *Tmc1* sites identified with high posterior probabilities of convergent substitutions were seen to be under positive selection in at least one of the clades involved. *Tmc1* clade models comparing four focal bat clades to non-bats were used to estimate site-wise ω values without the confounding effect of other echolocating taxa in the background branches (Fig. 2.10). The highest values of ω occurred in the Hipposideridae (ω = 5.70) and the subfamily of Vespertilionidae, Kerivoulinae (ω = 3.09), in which multiple sites showed signatures of positive selection. Again, sites identified as undergoing convergent substitutions were shown to be under positive selection.

For *Pjvk*, two sites in the Hipposideridae were estimated to have ω values marginally above one (Table 2.5b). However, no sites were found to be under positive selection in any Yangochiroptera species, although all clade comparisons had revealed divergent selection in these species. None of the alternative reduced *Pjvk* clade models were found to fit the data significantly better than the null model (results not shown). However, of the two amino acid sites (244 and 262) shown to be under positive selection along the Rhinolophidae and Hipposideridae branch in a branch-site model (Table A7), the latter was identified as convergent between Rhinolophidae and Hipposideridae with Vespertilionidae.

Figure 2.10 Estimated site-wise omega along *Tmc1*. Grey shaded sites indicate sites with high probabilities of convergence.

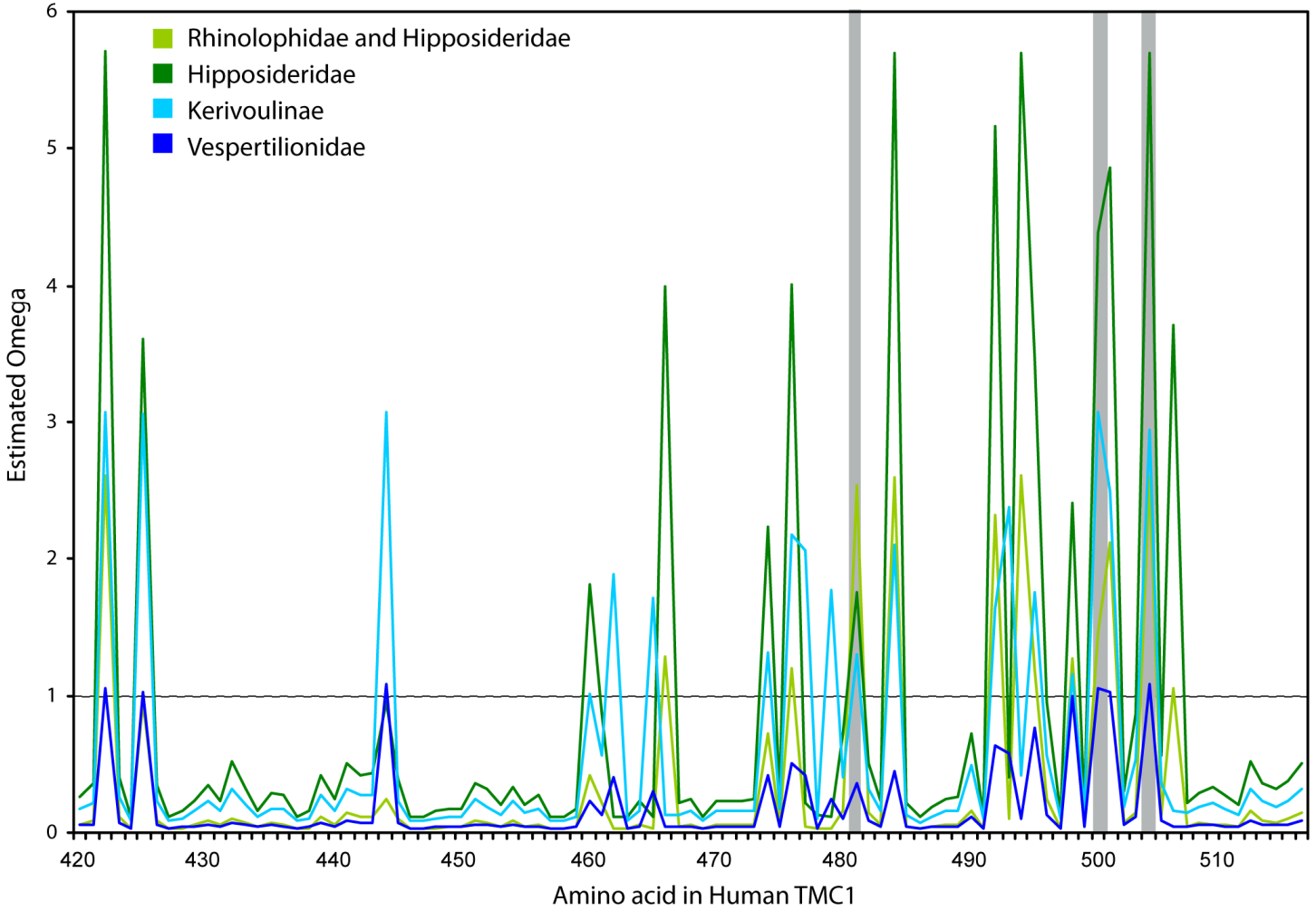

Figure 2.11 Positive selection and convergent substitutions, in *Tmc1* (upper) and *Pjvk* (lower). Sites with high probability of convergent substitutions, in parentheses, are shown in black text; the arrows indicated the two branches which share the convergence. Significant clade models are indicated by coloured text, sites are listed when they were identified as undergoing convergent substitutions and positive selection was detected.

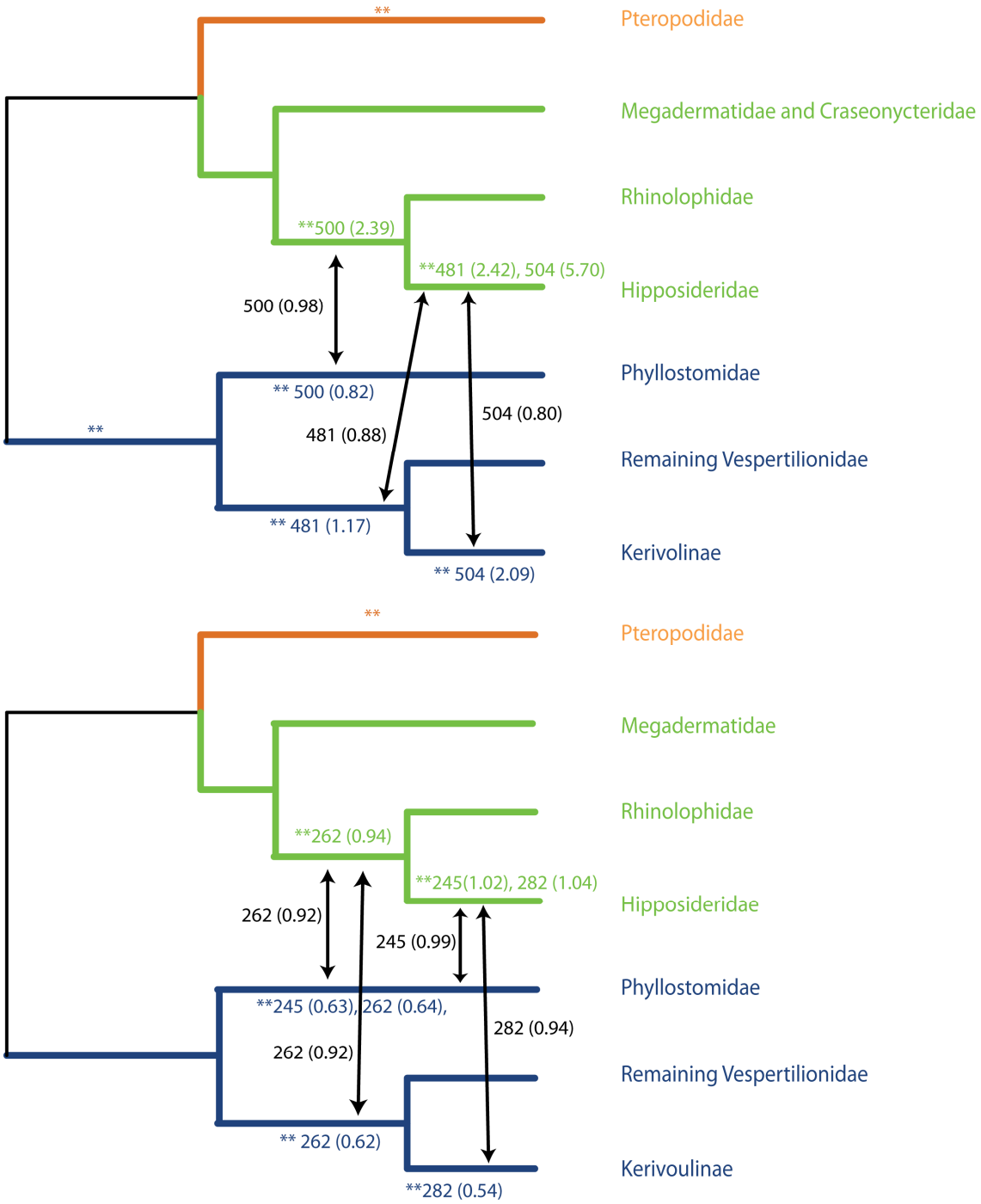

Discussion

Results from two independent hearing genes, *Tmc1* and *Pjvk*, revealed strong evidence of positive selection in echolocating whales, and also in some echolocating bats. Positive selection in *Tmc1* was detected along the branch leading to Yangochiroptera, and also echolocating Yinpterochiroptera. In contrast, no evidence of positive selection acting on the ancestral bat branch was found in either gene. I also detected signatures of parallel sequence evolution between the *Tmc1* gene in dolphin and echolocating bats, which was not seen to occur between dolphin and non-echolocating fruit bats. Taken together, these results from *Tmc1* indicate that functional adaptations for high-frequency hearing associated with echolocation arose after the split between the Yangochiroptera and Yinpterochiroptera. While the data appear to support multiple independent origins of echolocation, at least of the form seen in extant lineages of bats, I am unable to rule out the possibility that ancestral bats could echolocate. Nonetheless, no evidence of relaxed selection, perhaps expected with a loss of echolocation, was seen in the non-echolocating Old World fruit bats. Although the functional significance of these parallel substitutions in *Tmc1* is currently unknown, several of the observed substitutions appear to have involved amino acids with subtly different physicochemical properties. All regions of TMC proteins, other than the transmembrane domains, are predicted to be either intra- or extra-cellular residues (Keresztes *et al.,* 2003), and thus these substitutions may have an adaptive role.

High levels of positive selection were found in the echolocating cetacean clade in *Pjvk*, however, within bats positive selection was restricted to the Old World CF bats. This provides additional support for the hypothesis that functional adaptations arose after the Yinpterochiroptera and Yangochiroptera split. Although the exact function of Pjvk remains unknown, it has been predicted to contain a zinc binding motif and also the highly conserved Gasdermin domain and, therefore, of the two proteins studied this protein may be under higher structural constraints.

In addition to observed parallel changes between bats and cetaceans, both genes showed strong evidence of parallel sequence evolution between different clades of echolocating bats. Patterns of sequence convergence appeared to be concentrated in some families. In particular, comparisons of Hipposideridae versus the subfamily Kerivoulinae, and also Rhinolophidae versus Phyllostomidae, showed increased levels of sequence convergence. These results are especially intriguing given that species of *Hipposideros*

and *Kerivoula* possess the highest echolocation call frequencies recorded to date (Fenton and Bell 1981; Schmieder *et al.,* 2010). Additionally, along *Tmc1* some of the highest levels of sequence convergence were seen between *Rhinolophus ferrumequinum* and *Pteronotus parnellii*, two bats that are known to have independently evolved CF echolocation.

In *Tmc1* several sites exhibited an association between high posterior probabilities of convergent substitutions and positive selection. However, several sites identified with a high probability of convergent substitutions were not associated with positive selection; for example all branch-site models for *Pjvk* were not significant. Conversely, several sites along key branches were identified as being under positive selection but were not found to have undergone convergent substitutions. There are several potential reasons for these results. Previous analyses of *Prestin* found a correlation between nonsynonymous substitutions and inferred hearing-frequency ability, and suggested this might indicate key sites especially important for high-frequency hearing tuning (Liu *et al.,* 2010b). This suggests that amino acids in different lineages may be under different functional constraints. Therefore it might be expected that not all sites under positive selection lead to a convergent substitution. Additionally, mutation rates are affected by global genomic location and local sequence context of a site (Schmidt *et al.,* 2008). For example, in mammals CpG context leads to substantially increased mutation rate (e.g. Schmidt *et al.,* 2008). Furthermore, I used branch-site models with BEB inference of positively selected sites to detect selection regime. Branch-site tests of positive selection have been described as more powerful in detecting episodic positive selection compared to branch-based tests (Yang and dos Reis 2011). However, it has been shown, with the use of simulations, it is common for branch-site tests of positive selection to be significant, yet no sites shows posterior probability >0.95% according to BEB (Zhang *et al.,* 2005). Therefore, it is suggested that it is intrinsically more difficult to identify sites under positive selection than it is to detect if positive selection is present (Zhang *et al.,* 2005). This may be the case for the *Tmc1* sequence data presented here, where several sites were identified by BEB as being under positive selection, yet few had >0.95% probability. The addition of sequence data from additional species may serve to increase the power of tests for positive selection.

Several life history traits, such as body size, metabolic rate, generation time and effective population size (N_e), are thought to affect mutation rate (Martin and Palumbi

1992; Li *et al.,* 1996; Welch *et al.,* 2008; Charlesworth 2009; Bromham 2011). These factors not only influence non-synonymous and synonymous substitution rates, but also d_n/d_s. For example, species with smaller N_e are more likely to accumulate non-synonymous mutations than synonymous mutations (Popadin *et al.,* 2007). Certain taxonomic groups included in this study have documented rate differences, for example cetaceans, primates and rodents (Martin and Palumbi 1992). However, differences in selection pressures were found acting on different clades of bats, and though there are some differences in life history traits between Old World fruit bats and laryngeal echolocating bats, they should have comparable generation times and N_e. Therefore, overall the sampled differences in generation time and N_e across the species included in this study should not greatly influence the results.

In both genes, a small number of convergent changes were sufficiently abundant to cause conflicts between gene trees (in which all echolocating bats cluster together) and the known species tree, in which they are paraphyletic. However, in all analyses levels of convergence were not sufficient to result in the incorrect placement of toothed whales. Phylogenetic incongruence between datasets is not uncommon, particularly where sequence length is limited as is the case for the wider taxonomic study. However, the specific nature of conflict reported here supported the *a priori* hypothesis, was consistent across genes, and, from Lento-plots, appeared not simply to be due to a lack of power. These results endorse the utility of intronic DNA as putative neutral markers for recovering species relationships (e.g. Corte-Real *et al.,* 1994), but at the same time add weight to previous warnings about the potential pitfalls of using loci under selection for phylogenetic reconstruction (Li *et al.,* 2008; Castoe *et al.,* 2009). Furthermore, these results show remarkable similarities with published findings from the *Prestin* gene. All three genes encode proteins that are expressed in cochlea and implicated in mammalian hearing, and all have mutant forms that have been linked to NSHL in human and/or mice. The proteins Tmc1 and Pjvk have vital roles in hair cell development and function, respectively, whereas Prestin is thought to specifically drive the motility of the outer hair cells on the basilar membrane (Zheng *et al.,* 2000; Marcotti *et al.,* 2006; Schwander *et al.,* 2007).

Echolocating mammals as potential molecular models of hearing

Echolocating mammals arguably possess the most specialised auditory systems of all mammals with greater sensitivity to higher frequencies than non-echolocating species,

and associated anatomical adaptations in their inner ears such as highly coiled cochleae and shortened hair cells (Vater and Kossl 2004). Given these specialisations, it is not surprising that echolocating mammals have long served as important models for understanding the neurophysiology of auditory processing (e.g. Kossl *et al.,* 2003). The data of sequence convergence between taxa with ultrasonic hearing abilities in two separate cochlear genes, combined with similar findings from *Prestin*, strongly suggest that echolocating mammals might be equally useful for unravelling the molecular basis of hearing and deafness, both of which are controlled by hundreds of independent genes.

Bats promise to be an especially valuable group for studying hearing because of the mounting evidence from large-scale multi-gene phylogenies that echolocation and related high-frequency hearing have either evolved at least twice in bats, or been lost in one lineage (Old World fruit bats) (Teeling *et al.,* 2000). Thus amino acids that show evidence of molecular adaptation and/or convergence among echolocating taxa could be of particular interest as a starting point for studies of protein structure and function. Although this study did not aim to tackle the specific issue of whether echolocation evolved more than once in bats, the detected convergent adaptations for high-frequency hearing between echolocating bats, and also between the dolphin and the Yangochiroptera, could be considered as favouring a scenario of multiple origins of modern echolocation. Moreover, selection models of *Tmc1* and *Pjvk* found positive selection acting on only echolocating Yinpterochiroptera species and Yangochiroptera, in the former case, with no evidence of relaxation on Old World fruit bats, a result similar to that found in *Prestin* (Li *et al.,* 2008). Indeed in all three genes, the Old World fruits bats appear to have experienced purifying selection.

Previous studies that amplified the same sections of *Tmc1* gene, and its paralogs, have found high levels of sequence conservation across mammals (Kurima *et al.,* 2002), probably partly reflecting the inclusion of a transmembrane domain (amino acids 436–458 of the human peptide) that is likely to be under purifying selection due to functional constraint (Franchini and Elgoyhen 2006). Furthermore, codons 515 onwards correspond to the start of the highly conserved TMC domain (Kurima *et al.,* 2002). Yet despite these segments, other parts of Tmc1 were variable in bats. An insertion of three amino acids was seen in two species of *Hipposideros* (X497E, X498M and X499A) and was also present, albeit comprising different residues, in the five representatives of the

family Phyllostomidae (X497Q, X498L and X499S). The same positional insertion (S, G and L) also occurs in the mouse (*Mus musculus*), and it is noteworthy that this region falls within mouse exon 14 which is deleted in mutant mice with recessive deafness (*dn*) (Kurima *et al.,* 2002). Homozygote mutant mice (*dn/dn*) never hear, as both inner and outer hair cells completely deteriorate within 45 days after birth (Keats *et al.,* 1995). In fact, most of the variable sites among the bat sequences were located within the stretch of 51 amino acids amplified from this exon. These comparative data from mice and bats suggest that this region of Tmc1 is likely to be important both in basic hearing, as well as acting as a target for evolutionary adaptations for high frequency processing. Like *Tmc1*, published *Pjvk* gene sequences from four mammals also show strong amino acid conservation (Schwander *et al.,* 2007). I amplified a region of the protein that is predicted to be exposed, composed of a putative nuclear localization signal and the beginning of the zinc-binding motif (Delmaghani *et al.,* 2006). Within these sections, all amino acids considered to be of particular functional or structural importance (Delmaghani *et al.,* 2006) were conserved across all bat protein sequences studied. On the other hand, several nucleotide regions were identified as showing sequence convergence, divergence or conservation across echolocating bats when compared to non-echolocating mammals.

This study indicates that identifying sections of 'hearing genes' that have undergone changes in selective constraint in mammals with ultrasonic audition could also provide insights into regions of functional importance in normal and/or defective mammalian hearing, and *vice versa*. Both genes studied here show considerable genetic diversity, even between closely related bat species despite previously being regarded as highly conserved across mammals. Moreover, evidence of sequence convergence in three independent loci, raises the possibility that, in terms of molecular change, the number of evolutionary routes to high-frequency hearing in mammals might be rather limited. It is therefore remarkable that given this tight regulation such variable phenotypes can be seen.

Sequence convergence across multiple functional genes

To my knowledge, the occurrence of parallel signatures of adaptive sequence convergence across three independent loci that encode similar gene products (i.e. hair cell proteins) is unique. Reported cases of convergent sequence evolution in which changes appear related to gene function are uncommon, and have nearly always focused

on single loci, often involving only a few amino acids. Examples of these include the convergent homologous sites in the visual pigments of squid and primates (Morris *et al.,* 1993), and also in the myoglobin gene of seals and cetaceans (Romeroherrera *et al.,* 1978). More extensive sequence convergence operating across several loci has been documented in the mitochondrial genomes of snakes and agamid lizards, however, mtDNA genes cannot be considered to represent independent loci, and the suggested potential adaptive role of such convergence in metabolism remains speculation (Castoe *et al.,* 2009). Several different toxin protein genes have also been shown to have undergone convergent evolution, among different frog species (Roelants *et al.,* 2010), as well as between shrews and lizards (Aminetzach *et al.,* 2009), although the latter is structural as opposed to sequence convergence. In general, surprisingly few studies that have described sequence convergence have also tested for selection and, therefore, have not explicitly been able to rule out non-adaptive homoplasy that is widespread in nature. Indeed, such homoplasy could account for limited convergence seen in *Pjvk* between Old World fruit bats and a few echolocating species, particularly given that purifying selection was recorded in the former, so reducing the number of possible mutations (Rokas and Carroll 2008).

Further work:

The occurrence of parallel sequence evolution in multiple proteins expressed in OHCs in echolocating taxa is intriguing (this study and e.g. Liu *et al.,* 2010a). In order to investigate if sequence convergence is restricted to OHC proteins, or if in fact it occurs in other loci involved in different stages of auditory processing a genome wide approach could be used. For example, components of the basilar membrane would be candidate loci as this structure is known to be modified in both of the main clades of echolocating bats. Genomic approaches would also be useful to provide an estimate of the overall sequence convergence that occurs in different types of genes due to neutral processes such as homoplasy.

Furthermore, the functional significance of these amino acid substitutions is unknown, and it remains a conjecture that they confer meaningful adaptations. Through structural protein analysis it may be possible to explore at least how the substitutions affect protein folding.

Conclusions

The finding that the monophyly of echolocating bats was recovered by coding regions highlights the adaptive nature of the observed convergence. Examination of the relative site-wise log likelihood values along the alignment, as well as Lento-plots, indicated most support for the 'convergent topologies' was concentrated within exonic regions, whereas phylogenetic signal for the true species relationships was more obvious in intronic sections. Together with other very recent research (Li *et al.,* 2008; Rokas and Carroll 2008; Castoe *et al.,* 2009; Li *et al.,* 2010; Liu *et al.,* 2010a) the data suggest that sequence convergence might be much more common than previously thought. Taken together, results from *Tmc1* and *Pjvk*, indicate that functional adaptations for high-frequency hearing associated with echolocation arose after the split between the Yangochiroptera and Yinpterochiroptera. Therefore, this supports at least two independent origins of high-frequency hearing (and possibly echolocation) in bats.

CHAPTER THREE

Conserved Non-Coding Elements and the Development of Bat Auditory Systems

SUMMARY

Approximately 98% of the DNA in mammalian genomes is non-coding. Despite this, surprisingly little is known about the role this component plays in an organism's development. Non-coding DNA has been found to contain numerous short highly conserved regions termed Conserved Non-coding Elements (CNEs). These elements show a spatial and functional association with key developmental genes. The highly conserved nature of these regions and the fact that many are transcription factor binding elements suggest they play crucial roles in the regulation of gene expression and hence cellular patterning.

In this study, CNEs located near ear development genes were screened across all mammal genomes currently available, including five bat species. Rates of evolution were compared across species to search for evidence of accelerated evolution in bat CNEs putatively associated with morphological adaptation of the auditory system. Results found that all five bat species tested had significantly higher rates of substitution across concatenated sequences of 3,110 CNEs compared to the horse. When restricted to CNEs found in genomic regions containing genes linked to auditory system development, statistically different rates of substitution were found in echolocating and non-echolocating taxa. Four CNEs associated with the Homeobox genes *Hmx2* and *Hmx3* were sequenced in a range of taxonomically diverse bat species. Rates of substitution were relatively consistent across Yinpterochiroptera. However, in the Yangochiroptera there was family-wise variation. In particular, members of Vespertilionidae were shown to have high substitution rates with considerable sequence divergence from the other bats examined. The majority of sequence variance occurred at the ends of the CNE, although functional significance of the substitutions found in the bat sequences remains unclear.

INTRODUCTION

Organisation of the mammalian genome

The beginning of the 21st century saw a dramatic rise in the number of sequenced and publically available genome projects. In a little over ten years after the first draft mammalian genome was made available, approximately 40 additional species have been completed and published (Benson *et al.,* 2007; Hubbard *et al.,* 2007), and this number is set to rise rapidly in the near future (Haussler *et al.,* 2009). This increase in available information has radically altered the type and number of evolutionary questions that could be addressed. For example, the publication of the human and chimpanzee genome projects promised to finally provide answers to the questions concerning the fundamental genetic differences that account for the traits that separate humans from other primates. Early upper predictions estimated approximately 120,000 coding genes in the human genome (Liang 2000), and it was therefore assumed that there would be numerous genetic differences between the two species, with even the possibility of the discovery of novel human specific genes (e.g. Chen *et al.,* 2002). As the project neared completion however, it became apparent that this number was hugely inflated, and in fact recent estimates suggest that there are only 23,000 protein coding genes, which account for only 1.5% of the whole human genome (Mikkelsen *et al.,* 2005). Moreover, comparisons with the chimpanzee genome revealed that, despite having diverged approximately 5 million years ago, the two genomes are approximately 96% identical (Mikkelsen *et al.,* 2005). Together these facts suggested that as well as amino acid changes in protein-coding genes, point mutations in non-coding regions may have equally large phenotypic and developmental effects. Therefore, it became necessary to reconsider the importance of the non-coding DNA that had previously been referred to as 'junk DNA'. This also confirmed the earlier hypothesis that it must be a small number of mutations in regulatory regions that affect gene expression, which then in turn accounts for phenotypic differences (King and Wilson 1975).

Non-coding conserved regions and gene regulation

As genomic information from diverse taxa became available, combined with increased analytical methods it became easier to study and identify the putative regulatory regions of genes. Comparisons of sequence variation of key developmental genes, such as *Hox-4.4* and *Hox-4.5,* between mice and humans revealed that protein-coding regions were

highly conserved (Renucci *et al.,* 1992). Surprisingly, it was noticed that the high levels of sequence conservation extended to the non-coding inter-genic regions, and from this it was possible to identify the key regulatory regions controlling the spatial expression of the genes during development (Renucci *et al.,* 1992). As genomic alignments continued to grow, by including more diverse taxa, it was revealed that many non-coding regions showed remarkably high levels of conservation, and that these were frequently associated with essential genes (Duret *et al.,* 1993). Another approach adopted to identify yeast DNA regulatory motifs associated with changes in gene expression, involved comparisons of expressions levels in different yeast strains in altered environmental conditions (Roth *et al.,* 1998). Using this approach it was possible to identify non-coding DNA motifs, located upstream of the up-regulated genes in differing conditions, and then deduce that these were the regulatory regions. Eventually these regions became known as conserved non-coding elements (CNEs or CNCs). Currently, the function of many CNEs remains unclear, but some have been shown to act as cis-regulatory modules and, therefore, are essential for the correct spatial and temporal expression of early developmental regulators (Wolfe et al 2005).

Amniotic and mammalian CNEs

As the number of completed vertebrate genomes rose it became possible to identify more CNEs, and, using different outgroup taxa, group specific CNEs. For example, alignments of the pufferfish, *Takifugu rubripes,* and human genomes were used to identify the complement of vertebrate specific CNEs, and with the addition of the chicken, *Gallus gallus domesticus,* genome it has been possible to document amniote specific CNEs (Hillier *et al.,* 2004; Siepel *et al.,* 2005). The grey, short-tailed opossum, *Monodelphis domestica*, was the first marsupial to have its genome published (Mikkelsen *et al.,* 2007), and for the first time this allowed eutherian specific CNEs to be identified. This was particularly important for understanding many of the morphological novelties of higher mammals, as it became possible to identify the specific genomic changes that had occurred in this lineage since the split with metatherians. Alignment of the opossum and chicken genomes allowed the identification of ~133,000 amniote conserved CNEs; and of these 97.5% were also found to be conserved in the human genome (Mikkelsen *et al.,* 2007). Given the highly conserved nature of CNEs across all vertebrates, it is perhaps surprising that attempts to find the corresponding elements within invertebrates have so far failed (Woolfe *et al.,* 2005). It has therefore been concluded that although invertebrate species do possess

CNEs, these are not orthologues of the vertebrate CNEs. It is therefore fascinating that invertebrate CNEs have undergone a parallel radiation, similar to those of vertebrates, in terms of their distribution and putative association with developmental genes (Siepel *et al.,* 2005; Vavouri *et al.,* 2007).

Association with developmental genes

From some of the earliest studies, the frequent association between highly conserved regions, regulating gene expression, with genes that played an essential role in cell life was noted (Duret *et al.,* 1993). As more genes were discovered and annotated it became possible to more accurately map the distribution of CNEs, and it has successively been shown that the majority of CNEs are located in clusters that are associated with genes governing development (Woolfe *et al.,* 2005; Mikkelsen *et al.,* 2007). Interestingly, in humans CNEs are found on all chromosome with the exception of Y and 21 (Woolfe *et al.,* 2005).

CNEs can typically be unequivocally assigned to their most proximate gene (Woolfe *et al.,* 2005). However, this association is not based on absolute close proximity, given that the average distance between a subset of 1,400 CNEs and their nearest gene was calculated to be 182 KB away, with 12 CNEs found to be over 1 MB away from their nearest gene (Woolfe *et al.,* 2005). Therefore, it has been necessary to empirically demonstrate the mode of action of certain CNEs. One method that achieved this was an *in vivo* Zebrafish, *Danio rerio*, embryo assay (Woolfe *et al.,* 2005). This system makes it possible to monitor and identify the tissue-specific enhancer activity of particular CNEs. Also several interactive databases have been developed that allow users to identify CNEs that are associated with the development of particular regions, such as the otic capsule, (Woolfe *et al.,* 2007) or by proximity to key developmental genes across a wide range of evolutionary diverse taxa (Woolfe *et al.,* 2007; Engstrom *et al.,* 2008). By detailed mapping of the location of CNEs it has been possible to confirm their proximity to developmental genes, and it has been suggested that, conversely, the clustering of high numbers of CNEs may be used to identify the location of previously unknown developmental controlling genes.

Results of an *in vivo* reporter assay identified several CNEs that were found to strongly enhance GFP expression in the sense organs of zebrafish (Woolfe *et al.,* 2005). Of these, many were associated with *SOX21*, and certain CNEs were found to significantly

enhance expression in either developing ears or eyes. In particular the *SOX21* associated element, known as *SOX21* 5-6, was found to strongly enhance reporter expression, with up-regulation occurring in the developing ears of 75% of embryos (Woolfe *et al.,* 2005). *SOX21* is known to be expressed in several sense organs, including the sensory epithelia of the developing inner ear (Hosoya *et al.,* 2011). Of the CNEs associated with *SOX21* tested, up-regulation of expression in the developing ear was only seen in a small number of elements, this suggests that the development of the sense organs is a tightly regulated intricate system (Woolfe *et al.,* 2005). A total of five *PAX6*-associated elements were found to affect gene expression in the developing eye, as well as two associated with *SOX21* (Woolfe *et al.,* 2005).

Several experiments have shown that even a single base substitution in a single CNE or enhancer element can have a significant effect on an organism's morphology. For example, a single base change in a limb-specific enhancer of the *Sonic hedgehog* (*Shh*) gene causes pre-axial polydactyly in mice by directing *Shh* expression ectopically in the anterior limb bud during development (Maas and Fallon 2005). This has also been empirically tested in the mouse, *Mus musculus*, using sequence data from the short-tailed fruit bat, *Carollia perspicillata* (Cretekos et al., 2008). In this experiment the limb-specific transcriptional enhancer of the mouse *Prx1* locus was replaced with the orthologous sequence from the bat. This resulted in elevated *Prx1* expression in the mouse developing forelimb bones, as well as forelimbs that were significantly longer than controls (Cretekos *et al.,* 2008). Given that CNEs play such an important role in the early development of organisms, it is perhaps unsurprising that point mutations in CNEs have recently been shown to be associated with certain pathologies. For example, a heterozygous point mutation in a CNEs associated with *SOX9* appears to be associated with Pierre Robin Sequence (PRS), in which carriers suffer from facial deformities such as cleft palates (Benko *et al.,* 2009).

Purifying selection or accelerated evolution?

Despite being referred to as highly conserved non-coding elements, these elements have been shown to display a surprising amount of variation, both across and even within species. The amount of intra-specific variation in CNEs has been most greatly studied in humans (Drake *et al.,* 2006) and house mice (Halligan *et al.,* 2011; Kousathanas *et al.,* 2011). A study of CNEs associated with several genes, including the human gene *FOXP2,* attempted to link sequence variation with autism, however, similar levels of

sequence polymorphism were found in the healthy controls compared to sufferers (Richler 2006). Therefore, no direct link could be made between the disease and sequence variants, which suggest that despite being ultra-conserved and under strong purifying selection, healthy populations contain a certain amount of variation (Richler 2006). Therefore, in-depth genome and population level studies are necessary to fully understand the evolution and function of CNEs, however, given the expense and time data is mainly only available for humans (e.g. Rosenbloom *et al.,* 2010; The International HapMap Consortium 2010).

One study investigated the effects of large scale CNE deletion on morphology, reproductive fitness, longevity and other parameters in mice (Nobrega *et al.,* 2004). Following the creation of mouse lines in which two gene desert regions (i.e. containing only non-coding DNA) were knocked-out, detailed assessments of their phenotype, gene expression and fitness was conducted. However, no significant differences could be found between the mutant and wild type strains (Nobrega *et al.,* 2004). Therefore, no obvious deleterious effects on the animals could be attributed to this deletion of over 1,000 CNEs. Similarly, no effect on forelimb development or *Prx1* expression was shown following deletion of a *Prx1* limb enhancer in mice (Cretekos *et al.,* 2008). However, in these cases it remains possible that either phenotypic screening was inadequate or deleterious effects were manifested at a later time. Alternatively, these experiments could also prove that there is genuine redundancy in the function of CNEs.

Genetic control of mammalian ear development

The mammalian ear is formed from three parts, the outer, middle and inner ears. Through a combination of paleontological and developmental studies much is known about the timing, origin and genetic control of the auditory system (Cantos *et al.,* 2000; Luo *et al.,* 2011). Within mammals such as the mouse *Mus musculus*, the cochlea is evident from around 10 days into embryonic development (Cantos *et al.,* 2000), and the ear develops from tissue from the three germ layers and neural crest cells (for detailed review see Fekete 1999). The outer ear also contains tissues from the first and second branchial arches, while the middle ear is formed from cells from the neural crest or paraxial mesoderm, as well as the endoderm. The inner ear is formed mainly from placodal ectoderm, with a small part coming from the neural crest (Fekete 1999). A huge number of genes are currently implemented in the control and regulation of vertebrate ear development (for examples see Hadrys *et al.,* 1998; Fekete 1999;

Barrionuevo *et al.,* 2008). Many of which belong to either the PAX or SOX gene families of tissue specific transcription factors which are highly conserved across vertebrates. Experimental evidence has shown, mainly based on gene knock-out mouse models, that many of these genes are involved in controlling correct cochlear coiling and also the development of semicircular canals (e.g. Hadrys *et al.,* 1998; Cox *et al.,* 2000; Burton *et al.,* 2004; Kiernan *et al.,* 2005).

Aims and objectives of this study

Auditory processing in laryngeal echolocating bats is thought to be especially complex with the related structures having undergone functional modifications to cope with the demands of echolocation. In order to gain a greater understanding of the evolutionary processes that have taken place throughout its acquisition, several previous studies have documented the molecular evolution of protein-coding genes with putative roles in mammalian hearing (Li *et al.,* 2008; Li *et al.,* 2010). However, an equally important set of genes are involved in regulating the development of mammalian auditory systems (Fekete 1999). Many of these regulatory genes have been found to be under very strict evolutionary constraint and, therefore, amino acid sequence variation alone cannot account for the diversity in vertebrate auditory systems (e.g. *Pax6* see Puschel *et al.,* 1992). This is particularly likely given that many of these candidate genes are themselves transcription factors, that are known to affect the expression of a number of other genes (Chen and Rajewsky 2007). Furthermore, differential gene expression has been shown to play important roles in patterning the mammalian ear (Kiernan *et al.,* 2005). This means that to fully understand the genetic changes that have taken place throughout the evolution of the mammalian auditory systems, the molecular evolution of non-coding regulatory regions should also be investigated. Particularly, given that many CNEs are either known (or hypothesised) to regulate gene expression; they become suitable candidate markers with which to study the genetic mutations that may be associated with morphological variation in mammalian auditory systems.

Despite being highly conserved regions across all vertebrates, it is hypothesised that CNEs located in the same genomic region as genes, known to be involved in ear development, will show increased rates of substitution in echolocating bat species compared to other mammals that have less derived auditory systems. In particular, comparisons will be made between members of the Old World fruit bats, which are not capable of laryngeal echolocation and display a less modified auditory system, to

species from the two main clades of laryngeal echolocating bats which have highly modified auditory systems, particularly in the inner ear (see Chapters 4 and 5). Literature surveys will be used to identify genes of interest involved in ear development, and henceforth the CNEs located in the same genomic region as these genes will be referred to as 'Ear Development CNEs'. This title is used for simplicity and does not necessarily refer to a proven function of the CNE in question.

Hypothesis 1: It is predicted that the two main clades of echolocating bats will display divergent substitution rates in particular ear development CNEs. If one of the two main clades of echolocating bat displays increased substitution rates in particular ear development CNEs, which are not seen in the other clade, then this might provide evidence of different molecular pathways acting in certain bat lineages. This could then suggest a later acquisition of laryngeal echolocation after the two bat clades diverged, and would therefore, provide support for multiple origins.

Conversely, if all bat species are found to have similar rates of substitution and sequence identity in ear development CNEs, this may suggest that modified auditory systems were ancestral to all bats and thus support a single origin of echolocation. Alternatively, the latter case could also suggest that these particular CNEs were only involved in rudimentary ear development, and not the specialisations seen in the ears of echolocating bats.

MATERIALS AND METHODS

Identification of mammalian CNEs

The CNE database COnserved Non-coDing Orthologous Regions (CONDOR) (Woolfe *et al.,* 2007) was used to create a list of target CNEs for use in this study. The CNEs catalogued by the CONDOR database were originally identified by multiple alignments of orthologous DNA sequences from the fugu, *Takifugu rubripes,* genome with several mammal species, such as the mouse, *Mus musculus*, rat, *Rattus norvegicus*, and human, *Homo sapiens*. However, CONDOR is not an exhaustive list of all CNEs and is limited to those conserved in all vertebrate genomes that are associated almost exclusively with genes that regulate early vertebrate development.

Initially CNE sequences were downloaded for human, mouse, rat, dog and fugu that met the following criteria: they were conserved with at least 60% identity and had a minimum sequence length of 100 base pairs (bp). This resulted in a total of 3,110 CNEs. Species coverage varied considerably; human: 3,110, fugu: 3,086, mouse: 3,047, rat: 2,599, dog: 439, which most likely reflects the quality of the assembly projects and not genomic content. The 3,110 human sequences were used as reference sequences to perform cross-species BLASTN searches on all currently publically available mammalian genomes as well as assembled short read Solexa datasets from the bats *Eidolon helvum, Pteronotus parnellii* and *Rhinolophus ferrumequinum*. In each case only the top hit was retained, with minimum expected value thresholds of 10^{-6} and a minimum of 60% sequence identity. In several cases the top hit was not continuous along the subject sequence; in these instances the longer portion was retained for further analysis. Again, coverage varied considerably across CNEs; 161 CNEs were identified in all 44 mammalian species and 6 CNEs were identified in only 10 or fewer species (see Fig. 3.1). A Perl script was used to calculate the percentage of missing data in each dataset. The seven species with the least missing data were: *Ailuropoda melanoleuca, Callithrix jacchus, Homo sapiens, Macaca mulatta, Pan troglodytes, Papio hamadryas* and *Pongo abelii.* The *Felis catus* dataset had the most missing data with approximately one quarter missing (Fig. 3.1c).

Figure 3.1 Taxonomic and sequence coverage of CNEs used in this study.
a) Number of CNEs downloaded from CONDOR for human (*Homo sapiens*), Fugu (*Takifugu rubripes*), Mouse (*Mus musculus*), Rat (*Rattus norvegicus*) and dog (*Canis familiaris*) with at least 100 base pairs in length and 60% conservation. The similar number identified for human, fugu and mouse highlight the high levels of conservation across divergent taxa, whereas, the lower number for dog and rat most likely reflects low coverage genome assemblies in these species.

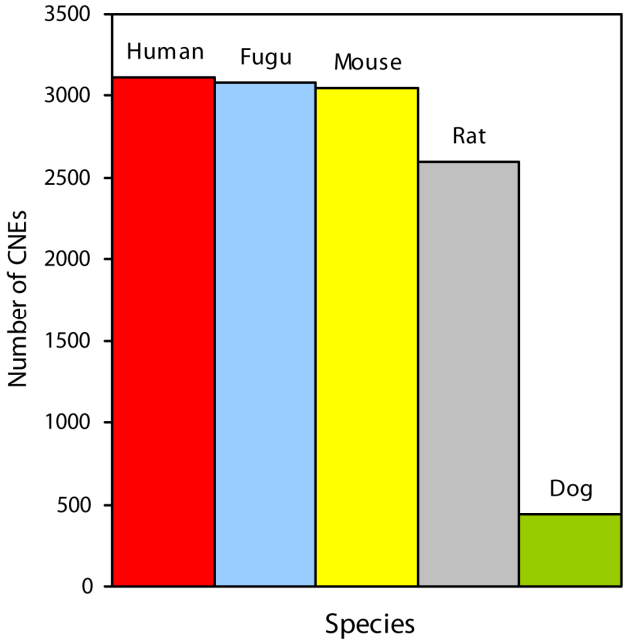

b) Number of CNEs identified by cross-species BLASTN from 40 currently published mammalian genomes plus three Solexa datasets for three bats using human CNEs as a reference. Also included is CNEs coverage for fugu downloaded from CONDOR.

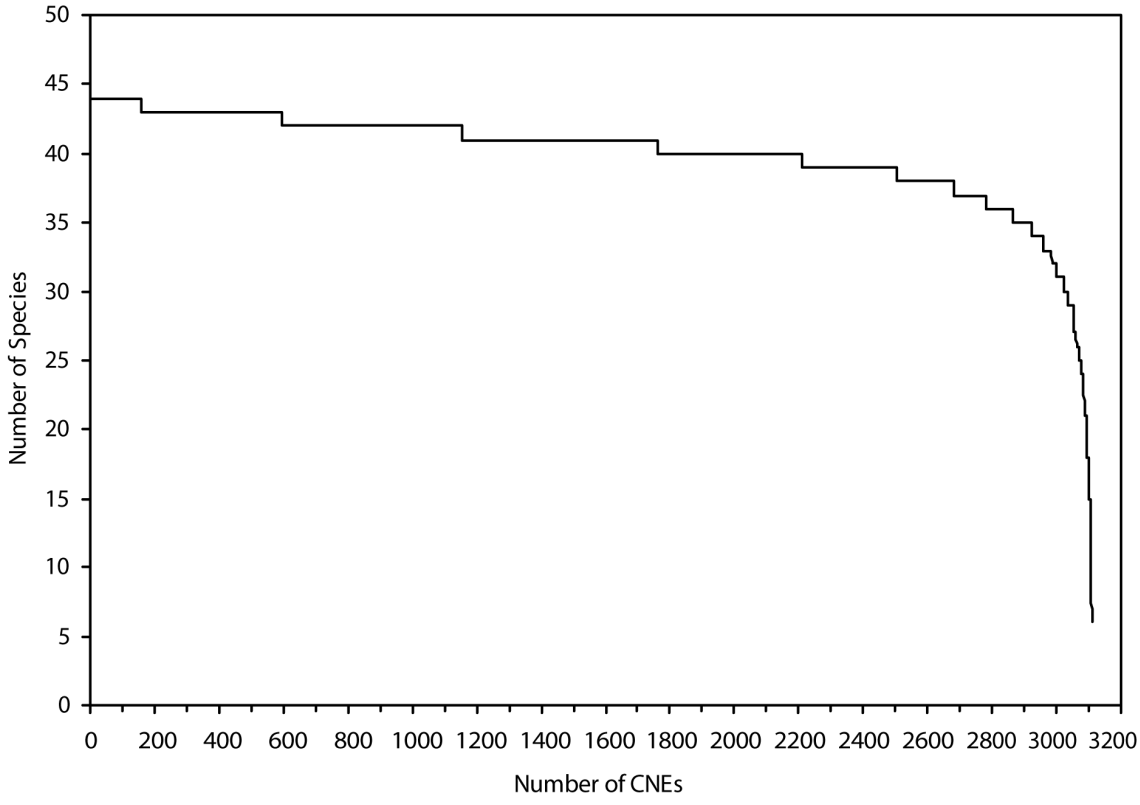

c) Percentage of missing data contained in all datasets. A cut-off of 10% (dashed line) was used to identify the reduced dataset.

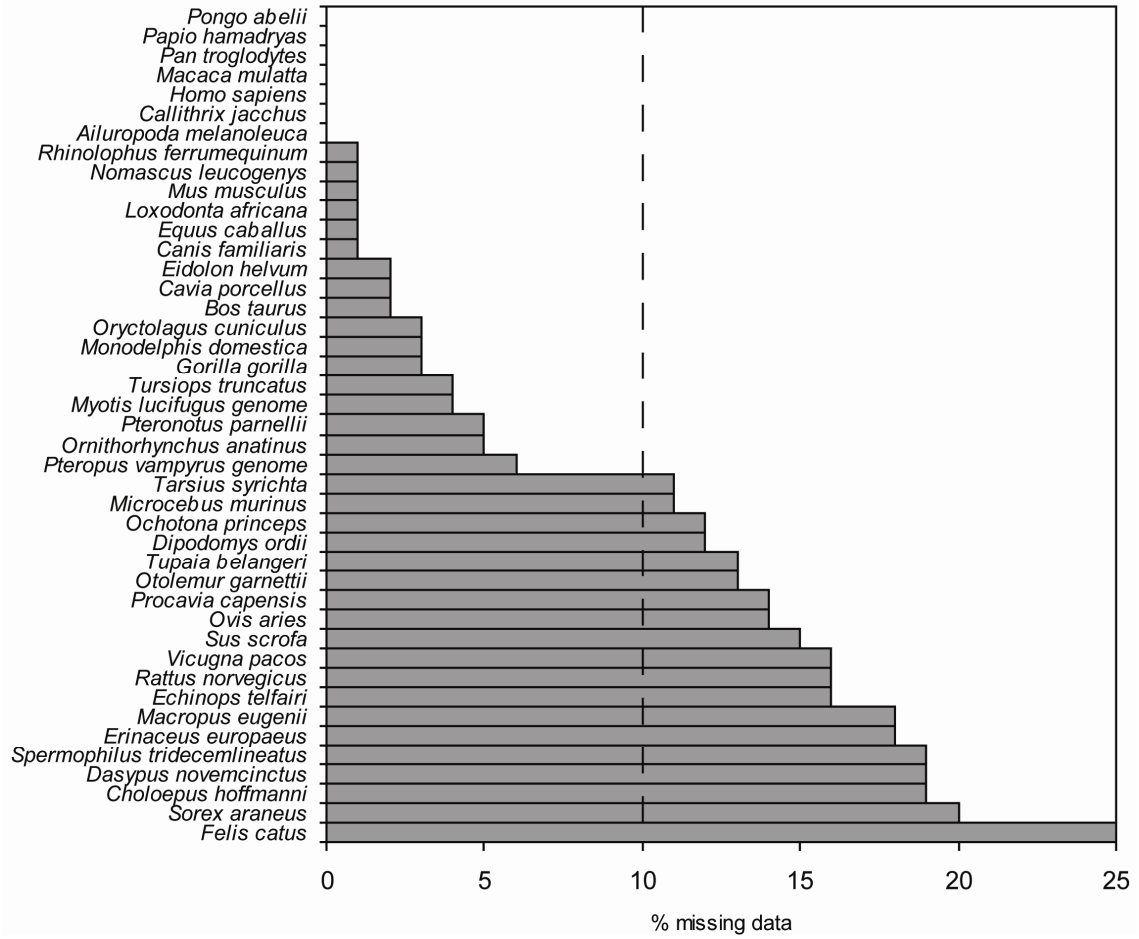

Analyses of mammalian CNEs

To investigate the overall phylogenetic signal of the dataset, and also the lineage specific nucleotide substitution rates, two phylogenetic trees were constructed. The first utilising a concatenated dataset of all CNEs and all taxa (612,850 bp and 44 taxa), and the second with a pruned dataset that excluded species with more than 10% missing data (612,850 bp and 24 taxa). Neighbour-joining trees with the Kimura 2-parameter substitution model and uniform rates among sites with 1,000 bootstraps were constructed in MEGA5 (Tamura *et al.,* 2011). Sites containing either gaps or missing data were excluded from analyses. Tajima's Relative Rates Test (Tajima 1993) was used to explore the substitution rates of the concatenated 3,110 CNE alignment. In this analysis the substitution rates of two sequences are compared to each other, with reference to a third outgroup sequence. It was then determined statistically if the two selected sequences showed different rates of substitution. These analyses were performed in MEGA5 (Tamura *et al.,* 2011). For each analysis, each bat (*Pteropus vampyrus, Eidolon helvum, Rhinolophus ferrumequinum, Myotis lucifugus* and *Pteronotus parnellii*), the dolphin (*Tursiops truncatus*) or the cow (*Bos taurus*) was

compared to the horse (*Equus caballus*), with the human (*Homo sapiens)* sequence used as the outgroup.

CNEs proximally located to ear development genes

All CNEs downloaded from CONDOR were associated with reference genomic regions. These genomic regions are named arbitrarily after one of the transcriptional-regulation and/or development genes they contain. Although this annotation does not necessarily imply direct functional association between CNEs and the particular gene, for this initial screen this is taken to be the case. A literature survey was used to identify all available genes from this list known to be associated with ear development. For each gene associated with ear development, the type of protein, where it is expressed and the putative function and/or mutant or knockout phenotype was documented. In total, 28 genes were identified with roles in ear development (Table 3.1). For each of these genes, concatenated alignments of their respective associated CNEs were constructed based on the 43 mammalian genomes.

Taxa with sequences with >10% missing data were excluded from analysis, giving a final dataset of 24 mammal species with concatenated sequences of 132,493 bp (67,675 bp excluding gaps and ambiguities). For concatenated ear development CNEs, BASEML in the PAML4.4 package (Yang 2007) was used to provide an estimate of lineage-specific nucleotide substitution rates. The Felsenstein 84 model of substitution, no clock, with alpha and kappa parameters estimated from the data were used, together with the constrained species tree with the topology based on the currently accepted phylogeny (Teeling *et al.,* 2002; Nishihara *et al.,* 2006; Murphy *et al.,* 2007).

Two approaches were used to quantify rates of substitution of specific CNEs putatively associated with genes which regulate the development of the auditory system. Firstly, the genomic location of the 28 ear development genes (Table 3.1) was designated into 25 gene regions using information from CONDOR. Concatenated ear development CNE alignments were made for each of these 25 gene regions, using SeaView4 (Gouy *et al.,* 2010), and Tajima's Relative Rates Test (Tajima 1993) was used to explore the substitution rates of these using the same method as described above.

Table 3.1 List of genes associated with ear development – the associated CNEs, of which, are available to download from CONDOR. Gene names, type of protein, broad region of expression and mutant phenotype – typically in the mouse (*Mus musculus*) - unless otherwise stated, are documented. (TF – Transcription Factor)

Gene:	Type of protein	Expressed in:	Mutant phenotype / putative role	Reference:
Bhlhb5	Basic loop helix TFs	Cochlear epithelial		(Brunelli *et al.,* 2003)
Dach1	Dachshund	Overlaps *Pax2 & Eya1*	No obvious ear defects	(Heanue *et al.,* 2002)
Dlx1 and *Dlx2*	Homeobox gene	1st pharyngeal arch	Defective malleus and incus	(Merlo *et al.,* 2000)
Emx2	Homeobox gene	Otic vesicle, branchial arches and skeletogenic neural crest cells	Middle ear ossicles malformed, anomalous hair cell number	(Rhodes *et al.,* 2003)
Esrrb	Estrogen-related receptor gene	Developing inner ear	Humans - autosomal-recessive nonsyndromic hearing impairment (DFNB35)	(Collin *et al.,* 2008)
Eya1	Eyes absent family	Craniofacial mesenchyme	Homozygotes lack ears	(Xu *et al.,* 1999)
Evi1	TF	Middle ear basal epithelial cells, fibroblasts and neutrophil leukocytes	Inflammation of middle ear	(Parkinson *et al.,* 2006)
Gbx2	Homeobox gene	Inner ear	Absence of endolymphatic duct, swelling of membranous labyrinth. Semicircular canals absent	(Lin *et al.,* 2005)
Fign	AAA protein	Expressed widely	Reduced or absent semicircular canals	(Cox *et al.,* 2000)
Gli3	C2H2-type zinc finger protein	Medial-ventral and lateral of otocyst, and surrounding mesenchyme	Vestibular defects - loss of lateral semicircular canal, truncation or absence of anterior semicircular canal. Narrower posterior semicircular canal diameter. Smaller inner ears, with widened endolymphatic ducts, common cruses and cochlear ducts.	(Bok *et al.,* 2007)
Lhx1	LIM domain	Saccule		(Sajan *et al.,* 2007)
Meis1 and *Meis2*	TALE homeobox TF	*Meis1* - cochlear duct *Meis2* - developing acoustic-vestibular ganglion	Assigning regional identity in morphogenesis, patterning, and specification of developing inner ear	(Oscar Sanchez-Guardado *et al.,* 2011)
Hmx2 and *Hmx3*	Homeobox genes	Early – dorso-lateral otic vesicle face Later - entire dorsal otic vesicle	*Hmx2* - lack semicircular ducts, loss of cristae and macula utriculus, fused utriculosaccular chamber. Hmx3 – not severely affected. *Hmx2:Hmx3* – significant anatomical and neurosensory defects in vestibular system	(Rinkwitzbrandt *et al.,* 1995; Hadrys *et al.,* 1998; Wang and Lufkin 2005)

Pax2	Paired-box TF	Medial wall of otic vesicle; endolymphatic duct and sac; cochlea	Rudimentary cochlea but severely malformed	(Burton *et al.,* 2004)
Pax3	Paired-box TF	Neural tube, developing brain, neural crest and derivatives	Humans - Type 1 and 3 Waardenburg syndrome	(Bondurand *et al.,* 2000; Baldwin *et al.,* 2005)
Pax5	Paired-box TF	Overlaps *Pax2*		(Bouchard *et al.,* 2000)
Sox2	Sox family TF	Neural tube and otocyst	Absence - deafness, cochlea under-coiled and hair cells do not differentiate. Missing ampullae and rudimentary development of semicircular canals, extremely small saccule and utricle. Reduced expression - severely hearing impaired, sensory epithelium abnormal, fewer hair cells. 2 ampullae missing, truncated semicircular canals. Cochlea slightly under-coiled.	(Kiernan *et al.,* 2005)
Sox21	Sox family TF	Sensory epithelium, supporting cells	Mild hearing impairment, malformed hair cells	(Hosoya *et al.,* 2011)
Shh	Hedgehog	Ventral midline structures, floor plate, and notochord	Deformed inner ear and surrounding capsule. Regulation of chondrogenesis.	(Liu *et al.,* 2002; Bok *et al.,* 2007)
Tshz1	Zinc fingers TF	Branchial arches	Middle ear malformations (malleus and tympanic ring)	(Coré *et al.,* 2007)
Zic1 and *Zic2*	ZIC family	Developing inner ear, hindbrain, neural crest, and periotic mesenchyme (chick)		(Warner *et al.,* 2003)

Secondly, rates of substitution were estimated for all CNEs classified by gene region for the 24 species with <10% missing sequence data, methods were the same as above. Branch lengths were summed from root to tip for all placental mammals for each CNE genomic region. A Principal Component Analysis (PCA) was performed on the summed branch lengths in PASTv2.09 (Hammer *et al.,* 2001), using the covariation matrix. PCA was used to visualise the variance of the sample so that it could be determined which genomic regions account for most of the variation within the sample. A PCA was also performed on a reduced dataset, using only those CNEs identified as being in the same genomic region as a gene involved in the development of the auditory system.

Bat specific study of CNEs in the *Hmx2/3* gene region

It was then decided to look more closely at sequence variance in CNEs located in the *Hmx2/3* gene region in a wider rage of bat species. CNEs located in this region were downloaded from CONDOR, and the flanking genomic regions from *Myotis lucifugus*, *Equus caballus*, *Felis catus*, *Canis familiaris*, *Bos taurus*, *Homo sapiens*, *Oryctolagus cuniculus* and *Mus musculus* were downloaded from GenBank. Multispecies alignments were constructed by eye in BioEdit v.7.0.9 (Hall 1999) and default settings of 'Primer3' (Rozen and Skaletsky 2000) were used to design suitable primers to amplify a total of four CNEs (see Table 3.2 and Fig. 3.2). Several bases of each primer were adjusted using ambiguity bases based on the multi-species alignment to create degenerate primers.

Table 3.2 Primer sequences used to amplify CNEs from the HMX2/3 gene region.

Name	Sequence	Tm	Predicted Product (bp)
*Hmx*2_9707_F	TGGCAGTTGCTAACCATTACA	59.24	284
*Hmx*2_9707_R	GATTCYGGTCATGAGTGARG	60.47	
*Hmx*2_9711_F	TGACGAATCTTAAAACGGATTG	59.12	496
*Hmx*2_9711_R	GCCTGGAAAATGGAGGAGAT	60.41	
*Hmx*2_9741_F	CCANGAGCAGTTGGAAASTT	57.8	472
*Hmx*2_9741_R	TAAGTGTRCYTTCRACACRTTG	58.89	
*Hmx*2_9716_F	TRCAMGCATCAGATTTTCAT	60.23	432
*Hmx*2_9716_R	CAAATGACATCTCRCAATRG	60.07	

DNA was extracted using Qiagen DNeasy kits, following recommended manufacturer's protocol. The desired fragments of gDNA were amplified using touch-down polymerase chain reaction (PCR) with the following steps; 95°C for 5 minutes activation of *Taq*, 95°C for 30 seconds, 60-50°C for 30 seconds, 72°C for 1 minute for 45 cycles run on a

MJ Research PTC225 Peltier thermocycler. Total volume of each reaction mix was 15 µL, which included approximately 25ng of gDNA, 1.5 µL 10x PCR buffer, 1.2-1.5 µL (25mM) $MgCl_2$, 0.5 µL (10µM) dNTPs, 1 µL (10µM) each forward and reverse primers, 0.1 µL (FastStart Taq DNA polymerase (Roche) and 4.4-4.7 ddH_20. PCR products were run on a 2% agarose gel and visualized using SYBR Safe DNA gel stain (Invitrogen). Successfully amplified products were then purified using ExoSap and sequenced using Sanger sequencing by the Genome Centre of Barts and The London, Queen Mary's School of Medicine and Dentistry. Products were sequenced with the same primers, using BigDye v3.1 and visualized on an ABI 3700 automated DNA sequencer. Directly sequenced samples were added to the multiple alignments downloaded from GenBank, together with all additional placental mammals for which complete sequences were available. Lineage-specific rates of substitution were then calculated with BASEML, with the same model settings as previously described, using an unrooted tree with the constrained species topology (Csorba *et al.,* 2003; Giannini and Simmons 2003; Khan *et al.,* 2010).

Figure 3.2 Schematic reconstruction of the human *HMX2* genomic region. The location of the four CNEs CRCNE00009707, 11, 16 and 41 that were sequenced for this study are indicated by red squares (left to right). Remaining CNEs downloaded from CONDOR are indicated by blue squares, and the four known protein-coding genes in this region (*HMX2, HMX3, BUB3* and *Q6ZR74_Human*) are indicated with black arrows. All positions are approximate and are taken from CONDOR.

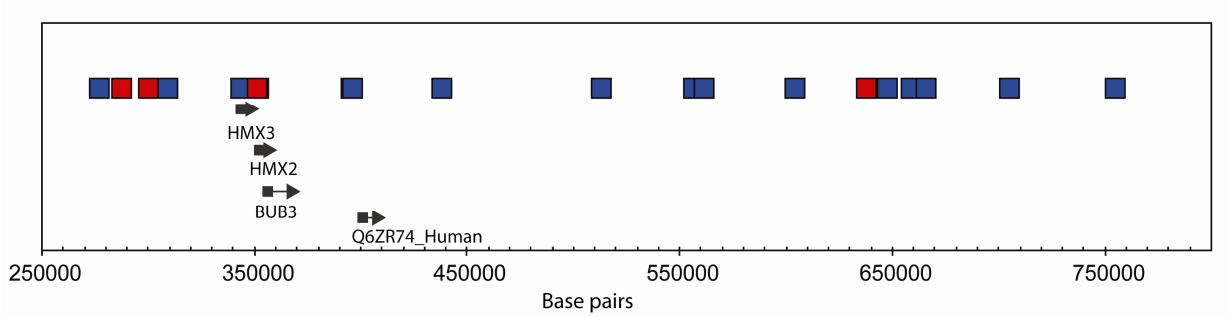

RESULTS

Phylogenetic analyses of mammalian CNEs

Phylogenetic trees were constructed to summarise overall phylogenetic signal and lineage specific nucleotide substitution rates of the complete CNE dataset. The first tree was constructed from a concatenated dataset of all CNEs and all taxa (612,850 bp and 44 species) and the second from a pruned dataset in which species with sequences >10% missing data removed (612,850 and 24 species) (Fig. 3.3). Despite the high levels of sequence conservation there was a considerable degree of phylogenetic signal in the mammalian CNE dataset. Marsupials and placental mammals were both recovered as monophyletic with 100% bootstrap support in both datasets. Xenarthra was the only superorder to be recovered as monophyletic by the larger dataset (Fig. 3.3a). Although all bats were recovered as monophyletic (86% bootstrap support), the correct division of Yinpterochiroptera and Yangochiroptera suborders was not recovered by the larger dataset. Pegasoferae, the proposed superorder containing Chiroptera, Carnivora, Pholidota and Perissodactyla (Nishihara *et al.,* 2006), was recovered by the complete dataset but with weak support (26% bootstrap support).

The smaller dataset recovered Laurasiatheria and Euarchontoglires with 100% bootstrap support (Fig. 3.3b). Furthermore, the correct species topology was supported within Euarchontoglires (Murphy *et al.,* 2007). Within Laurasiatheria, bats were recovered as monophyletic, with Yinpterochiroptera and Yangochiroptera, all recovered with 100% bootstrap support. However, the cow and dolphin were grouped with the horse and carnivores, which together formed the sister group to the bats.

Examination of branch lengths, which are proportional to the rate of substitution, revealed that the mouse (*M. musculus*) and rat (*R. norvegicus*) had by far the longest branches and, therefore, the greatest substitution rates. The lesser hedgehog tenrec (*Echinops telfairi*) and the rock hyrax (*Procavia capensis*) were also seen to be characterised by relatively long branch lengths. Across other species, most had approximately similar branch lengths; with the exception of apes and monkeys, which had relatively short branch lengths.

Within bats, all Yinpterochiroptera studied (*R. ferrumequinum, E. Helvum* and *P. vampyrus*) had approximately equal branch lengths, while of the two Yangochiroptera

species *M. lucifugus* had particularly long branches. Results of Tajima's Rate Test for concatenated sequences of 3,110 mammalian CNEs, downloaded for this study, revealed that rates of substitution were significantly different for all comparisons made (Table 3.3).

Figure 3.3 Neighbour-joining trees constructed under the Kimura 2-parameter substitution model, with uniform rates among sites, support for nodes based on 1,000 bootstrap samples. Gaps and missing data were excluded from analysis, and tree topologies are rooted with the platypus, *Ornithorhynchus anatinus*. a) Tree based on sequence information for all CNEs and all taxa (612,850 bp and 44 species).

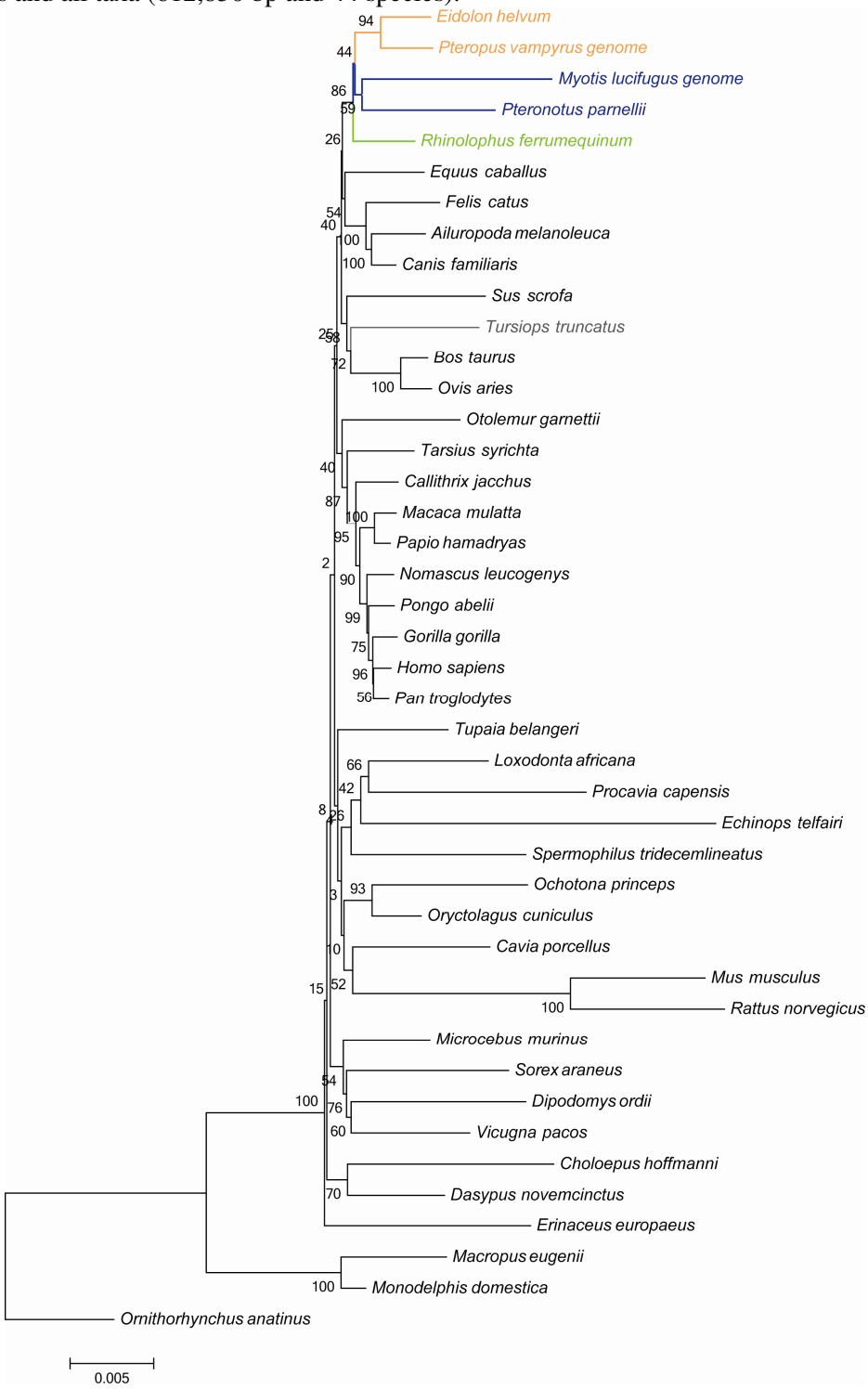

b) Tree based on sequence information for all CNEs and reduced taxonomic coverage (612,850 bp and 24 species).

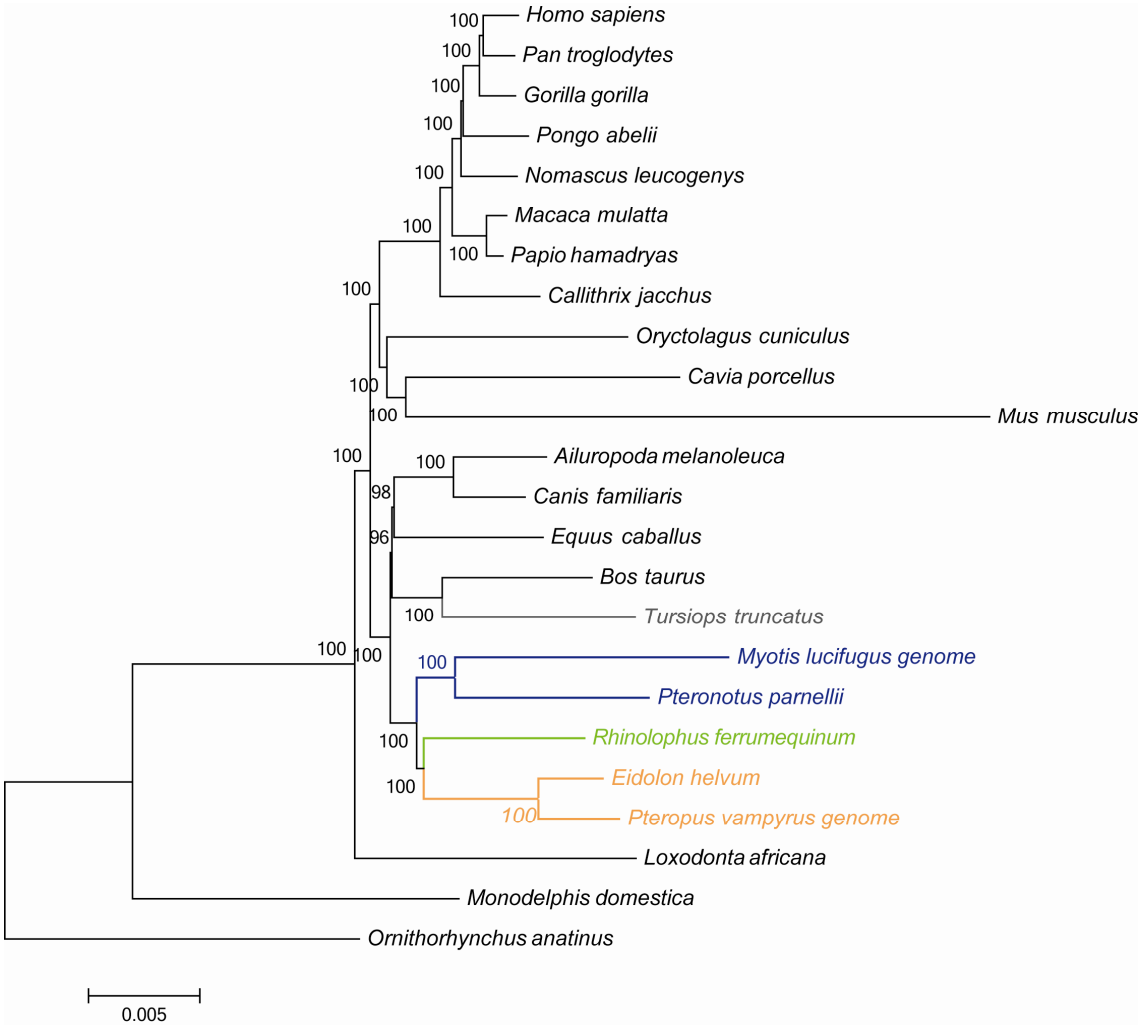

Table 3.3 Results of Tajima's Rate Test for concatenated sequences of all 3,110 mammalian CNEs downloaded for this study. Rates of substitution in focal species compared to *E. caballus,* with *H. sapiens* used as the outgroup.

	Sites in sequences:		Unique differences:				
Focal species:	Identical	Divergent	*Equus caballus*	Focal species	*Homo sapiens*	X^2 (1 df.)	*P*-value
B. taurus	524,411	365	4,705	6,265	5,587	221.84	<0.0001
T. truncatus	502,349	370	4,587	7,063	5,475	526.23	<0.0001
E. helvum	514,716	337	4,522	6,844	5,257	474.37	<0.0001
P. vampyrus	485,417	305	4,314	6,758	4,982	539.48	<0.0001
R. ferrumequinum	530,747	400	4,768	6,571	5,742	286.69	<0.0001
M. lucifugus	502,652	441	4,325	9,546	5,203	1965.17	<0.0001
P. parnellii	498,420	385	4,406	7,547	5,078	825.39	<0.0001

CNEs proximally located to ear development genes

In total, CNEs physically located in the same genomic region as 28 genes with roles in ear development were studied. For these 28 genes, lineage-specific rates of substitution were calculated for a concatenated alignment of their respective CNEs (Fig. 3.4). Rates of substitution calculated for this subset of ear development CNEs were similar to those observed above for the complete dataset. The mouse had the fastest substitution rate and primates had the slowest. Of the bats, all three Yinpterochiroptera species had approximately similar rates of substitution and *M. lucifugus* had the fastest rate of both focal species of Yangochiroptera.

Concatenated CNE alignments were made for each of 25 genomic regions that contained at least one ear development gene and its corresponding CNEs, and Tajima's Relative Rates Test (Tajima 1993) was used to test lineage specific substitution rates (see Table 3.4 and Table B1). For each analysis the substitution rates of one echolocating or non-echolocating Laurasiatheria species sequences was compared to the substitution rate of the horse, with reference to the human sequence.

Following Bonferroni correction of the significance level for the multiple comparisons made per gene, substitution rates between the cow and horse were significantly different for sets of CNEs from three gene regions, *Bhlhb5, Dach1*, and *Zic2*. The cow had the most unique differences in all cases, and, therefore, the faster substitution rate. All bats were found to have significantly higher substitution rates compared to the horse for CNEs from two gene regions, *Shh* and *Tshz1*. Again the bat species had considerably more unique differences for both gene regions. No ear development CNEs were found to have significantly different rates of substitution in all three species of Yinpterochiroptera. Conversely, all three laryngeally echolocating bat species (i.e. excluding the Old World fruit bats), had significantly higher substitution rates compared to the horse for CNEs in the *Hmx2/3* region. Both species of Yangochiroptera, *Myotis lucifugus* and *Pteronotus parnellii*, had significantly higher substitution rates compared to the horse for CNEs from the *Bhlhb5, Emx2, Meis2, Sox21* and *Zic2* gene regions. CNEs found in the *Fign, Lhx1, Meis1* and *Pax2* gene regions were found to have significantly higher substitution rates only in the dolphin (*Tursiops truncatus*). CNEs located in the *Hmx2/3* gene region were also found to have different substitution rate in the dolphin. Therefore, CNEs from the *Hmx2/3* gene region were found to have significantly higher substitution rates in all echolocating taxa and none of the non-

echolocating taxa (*Bos taurus*, *Pteropus vampyrus* and *Eidolon helvum*). Interestingly, whereas *Tshz1* CNE substitution rates were higher in the dolphin - as in all bats - the CNEs located near *Shh* did not have different substitution rates in the dolphin compared to the horse.

Figure 3.4 Estimate of lineage-specific nucleotide substitution rates across concatenated ear development CNE sequence alignments. Calculated with BASEML using the GTR model of substitution, no clock and alpha and kappa estimated from the data.

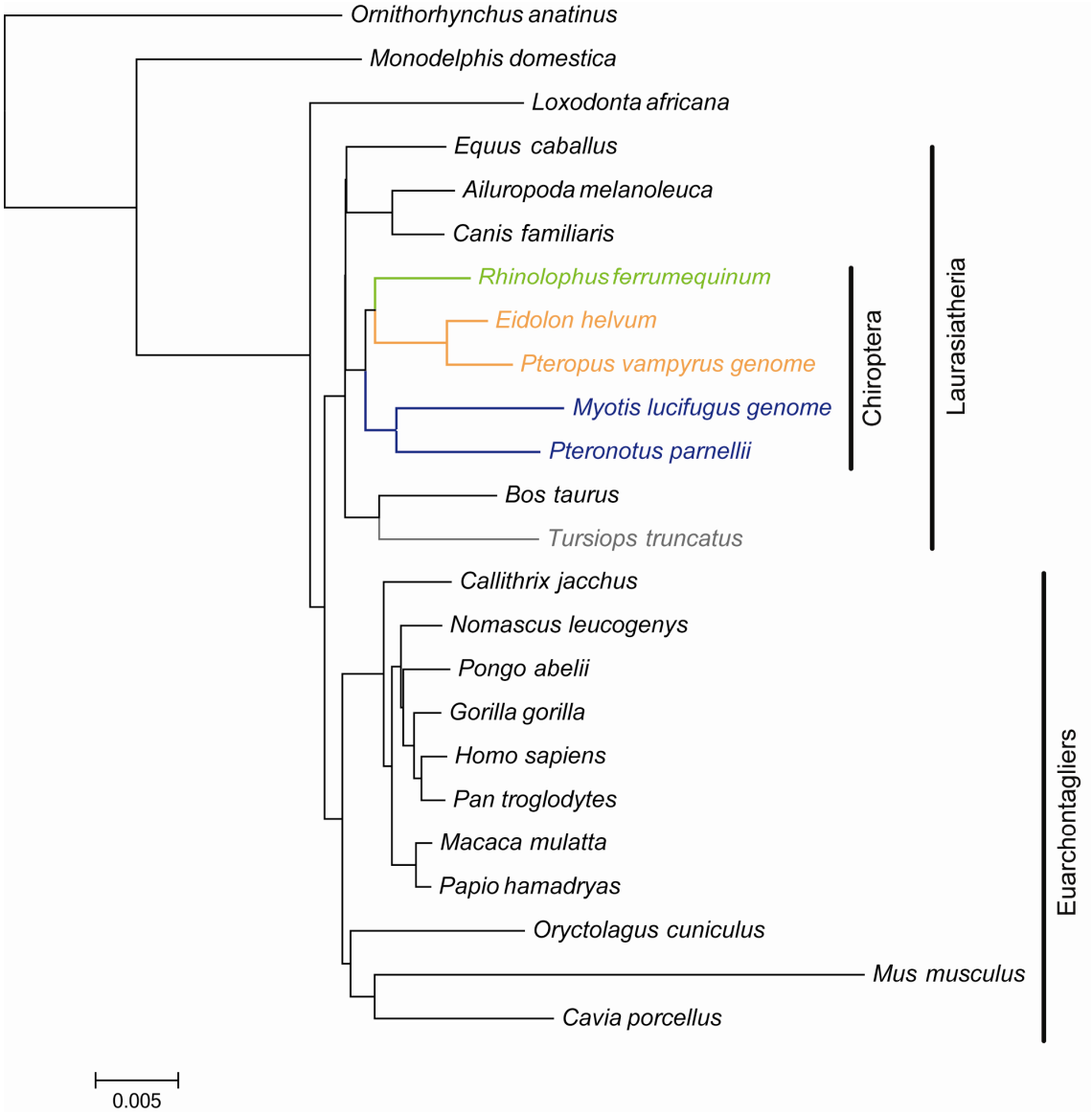

Table 3.4 Results of Tajima's Rate Test for concatenated ear development CNEs. In all tests, species were compared to *Equus caballus* with the *Homo sapiens* sequence used as the out-group. The X^2 test statistic is give with *P*-values at 1 degree of freedom. All tests that are significant at p<0.007 (following Bonferroni corrections for multiple comparisons) are highlighted in bold text.

Gene	*B. taurus*	*T. truncatus*	*E. helvum*	*P. vampyrus*	*R.. ferrumequinum*	*M. lucifugus*	*P. parnellii*
Shh	5.64 (*P* = 0.018)	4.36 (*P* = 0.037)	**41.79 (*P* < 0.001)**	**28.05 (*P*< 0.001)**	**11.92 (*P* = 0.001)**	**23.06 (*P*< 0.001)**	**35.31 (*P*< 0.001)**
Tshz1	5.68 (*P* = 0.017)	**44.08 (*P* < 0.001)**	**16.28 (*P* < 0.001)**	**46.87 (*P* < 0.001)**	**9.71 (*P* = 0.002)**	**23.27 (*P* < 0.001)**	**69.87 (< 0.001)**
Hmx2/3	6.13 (*P* = 0.013)	**25.14 (*P* < 0.001)**	4.15 (*P* = 0.042)	6.70 (*P* = 0.010)	**8.05 (*P* = 0.005)**	**106.88 (*P*< 0.001)**	**16.20 (*P* < 0.001)**
Dlx1	0.29 (*P* = 0.593)	0.36 (*P* = 0.547)	4.31 (*P* = 0.038)	**10.05 (*P* = 0.002)**	5.07 (*P* = 0.024)	**21.93 (*P* < 0.001)**	3.27 (*P* = 0.071)
Meis2	0.21 (*P* = 0.649)	**7.28 (*P* = 0.007)**	0.00 (*P* = 0.948)	1.52 (*P* = 0.217)	1.20 (*P* = 0.273)	**35.68 (*P* < 0.001)**	**12.75 (*P* < 0.001)**
Bhlhb5	**22.53 (P < 0.001)**	**15.69 (*P* < 0.001)**	2.39 (*P* = 0.122)	3.26 (*P* = 0.071)	6.40 (P = 0.011)	**8.82 (*P* = 0.003)**	**10.56 (*P* = 0.001)**
Emx2	0.76 (*P* = 0.384)	0.65 (*P* = 0.421)	0.28 (*P* = 0.598)	0.03 (*P* = 0.857)	0.12 (*P* = 0.728)	**30.15 (*P* < 0.001)**	**9.45 (*P* = 0.002)**
Zic2	**15.02 (*P* < 0.001)**	3.84 (*P* = 0.050)	0.07 (*P* = 0.785)	2.23 (*P* = 0.136)	0.31 (*P* = 0.577)	**7.41 (*P* = 0.006)**	**13.88 (*P* < 0.001)**
Sox21	0.38 (*P* = 0.540)	**9.07 (*P* = 0.003)**	2.18 (*P* = 0.140)	0.63 (*P* = 0.428)	0.15 (*P* = 0.695)	**7.34 (*P* = 0.007)**	**16.49 (*P* < 0.001)**
Dach1	**9.45 (*P* = 0.002)**	**23.52 (*P* < 0.001)**	2.33 (*P* = 0.127)	3.18 (*P* = 0.075)	6.76 (*P* = 0.009)	5.54 (*P* = 0.019)	**10.24 (*P* = 0.001)**
Gli3	0.05 (*P* = 0.816)	0.20 (*P* = 0.659)	**7.52 (*P* = 0.006)**	**9.04 (*P* = 0.003)**	4.57 (*P* = 0.033)	1.46 (*P* = 0.227)	**7.35 (*P* = 0.007)**
Esrrb	0.45 (*P* = 0.500)	3.27 (*P* = 0.071)	2.18 (*P* = 0.140)	0.32 (*P* = 0.572)	2.68 (*P* = 0.101)	6.21 (*P* = 0.013)	**7.25 (*P* = 0.007)**
Sox2	0.53 (*P* = 0.467)	3.20 (*P* = 0.074)	1.47 (*P* = 0.225)	1.80 (*P* = 0.180)	0.29 (*P* = 0.593)	5.45 (*P* = 0.020)	**11.76 (*P* = 0.001)**
Zic1	1.44 (*P* = 0.230)	4.90 (*P* = 0.027)	2.67 (*P* = 0.102)	0.99 (*P* = 0.321)	0.00 (*P* = 1.000)	**58.76 (*P* < 0.001)**	1.01 (*P* = 0.314)
Eya1	0.72 (*P* = 0.395)	0.07 (*P* = 0.790)	5.58 (*P* = 0.018)	3.34 (*P* = 0.068)	0.47 (*P* = 0.494)	2.53 (*P* = 0.112)	3.95 (*P* = 0.047)
Evi1	0.44 (*P* = 0.505)	1.20 (*P* = 0.274)	0.57 (*P* = 0.450)	0.29 (*P* = 0.590)	0.03 (*P* = 0.862)	0.64 (*P* = 0.423)	1.68 (*P* = 0.194)
Fign	2.67 (*P* = 0.102)	**19.21 (*P* < 0.001)**	0.04 (*P* = 0.851)	2.06 (*P* = 0.151)	0.04 (*P* = 0.847)	4.10 (*P* = 0.043)	1.83 (*P* = 0.176)
Gbx2	0.18 (*P* = 0.670)	4.45 (*P* = 0.035)	5.49 (*P* = 0.019)	4.57 (*P* = 0.033)	1.58 (*P* = 0.209)	0.57 (*P* = 0.450)	0.36 (*P* = 0.549)
Lhx1	2.63 (*P* = 0.105)	**10.80 (*P* = 0.001)**	0.13 (*P* = 0.715)	0.67 (*P* = 0.414)	0.04 (*P* = 0.847)	0.67 (*P* = 0.414)	0.03 (*P* = 0.857)
Meis1	0.51 (*P* = 0.473)	**12.84 (*P* < 0.001)**	0.35 (*P* = 0.553)	0.01 (*P* = 0.904)	0.05 (*P* = 0.816)	6.72 (*P* = 0.010)	4.26 (*P* = 0.039)
Pax2	1.72 (*P* = 0.189)	**36.96 (*P* < 0.001)**	2.12 (*P* = 0.145)	0.91 (*P* = 0.339)	4.41 (*P* = 0.036)	0.71 (*P* = 0.399)	1.88 (*P* = 0.170)
Pax3	1.09 (*P* = 0.297)	0.47 (*P* = 0.491)	0.04 (*P* = 0.841)	0.22 (*P* = 0.637)	1.00 (*P* = 0.317)	0.17 (*P* = 0.683)	0.39 (*P* = 0.532)
Pax5	2.00 (*P* = 0.157)	0.00 (*P* = 1.000)	0.33 (*P* = 0.564)	1.00 (*P* = 0.317)	1.00 (*P* = 0.317)	1.00 (*P* = 0.317)	0.00 (*P* = 1.000)

Figure 3.5 PCA of substitution rates of placental mammal CNEs.
a) Analysis of all CNEs from 83 genomic regions, PC1 - 59.58%, and PC2 - 10.38% sample variance.

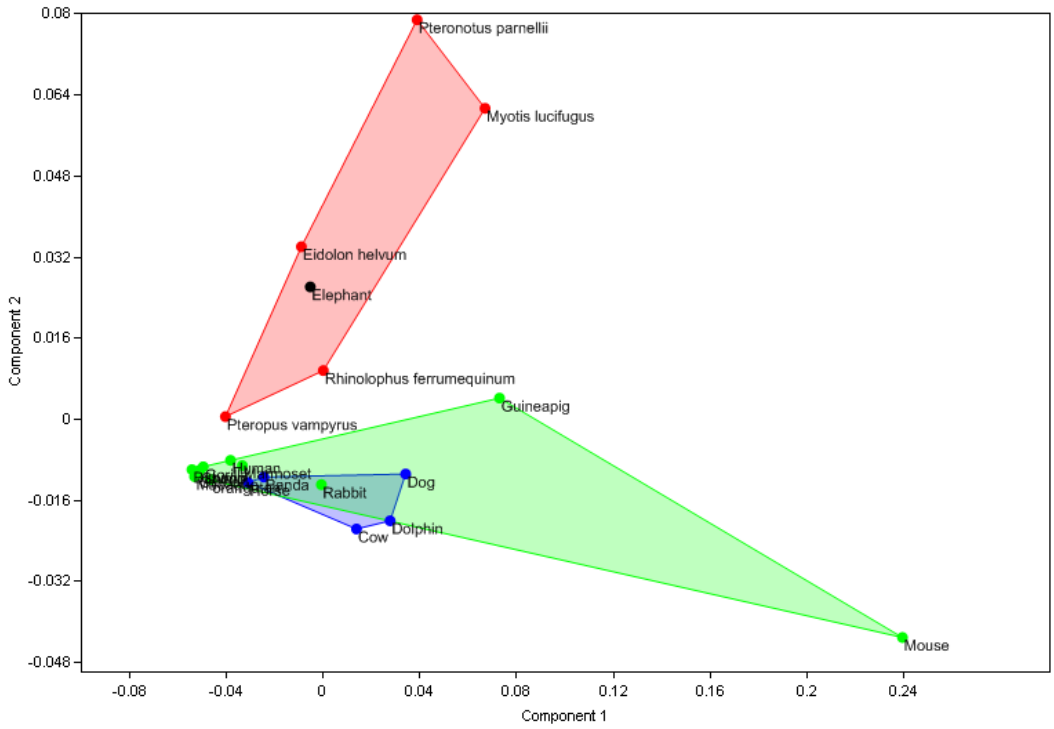

b) Analysis of CNEs associated with ear development, from 23 genomic regions, PC1 - 64.19%, and PC2 - 13.75% sample variance.

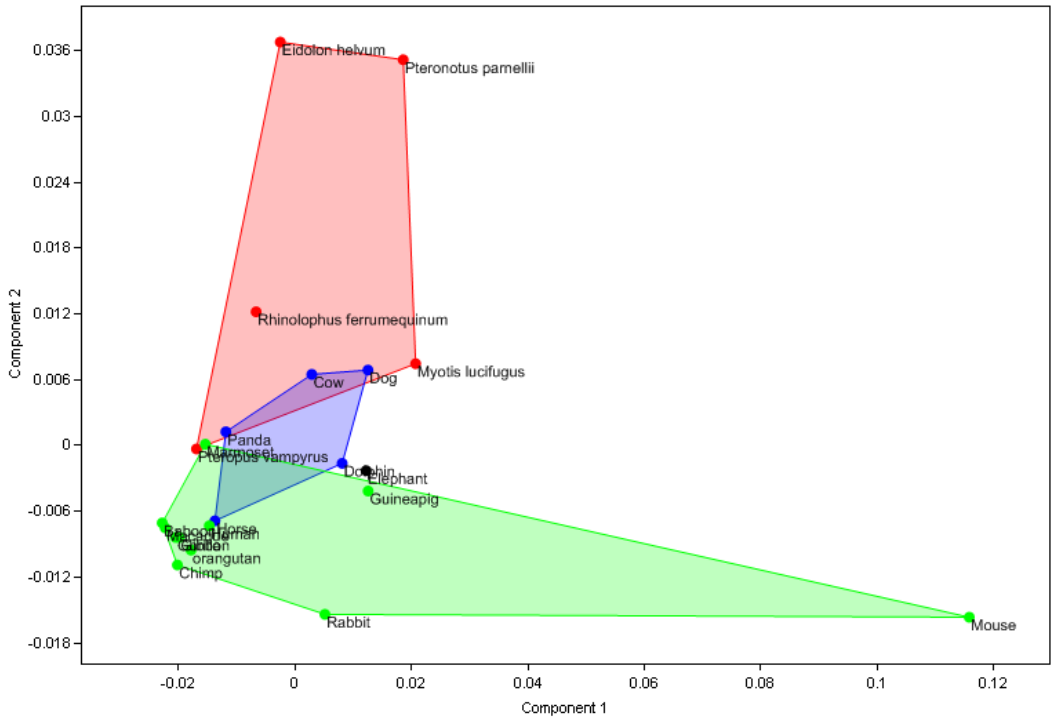

Results of the PCA based on all CNEs (Fig. 3.5a) showed good separation of all bats and Laurasiatheria and Euarchontoglires, however, the elephant was located in the middle of the bat distribution. Loadings and correlations along PC1 suggest that this axis represents a general increase in substitution rate across virtually all CNEs analysed (Table B2). From the distribution of taxa along this axis, this mainly leads to the separation of rodents, and in particular the mouse, from the remaining species and with primates clustering together at the low end of this axis. PC2 leads to separation of bats from Laurasiatheria and Euarchontoglires species, and within bats, Yinpterochiroptera from Yangochiroptera. CNE clusters with the highest loadings for PC2 are *Hlx1*, *Mab21l1*, *Nr2f2* and *Shh*, those with the lowest are *Bcl11b* and *Maf*.

Results of the second analysis (Fig. 3.5b), based only on rates of substitution of CNEs putatively associated with ear development, had a very similar distribution to the whole dataset, except now Laurasiatheria are intermediate to bats and Euarchontoglires. Again, PC1 referred to a general increase in substitution rates across all CNEs (Appendix B). High loadings along PC2 are seen in *Shh*, *Gli3*, *Gbx2* and *Tshz*, whereas, low loadings are seen in *Sox21*, *Sox2*, *Zic2* and *Esrrb*. It is interesting to note that Yangochiroptera are now separated from Yinpterochiroptera only along PC1, which suggests that they generally have faster rates of substitution in the CNEs examined.

Branch-specific substitution rates were plotted for all bat branches for each CNE genomic region (Fig. 3.6). From this it can be seen that substitution rates are highly variable across both species and genomic regions. For virtually every genomic region, the branch with the lowest rates of substitution was the ancestral Yinpterochiroptera branch; followed by the common bat ancestor branch. All tips showed higher substitution rates; generally rates among Yinpterochiroptera are comparable, and typically the two Yangochiroptera had higher rates than the Yinpterochiroptera. Across all genomic regions, CNEs located near *Mab21l1*, *Nr2f2* and *Shh* were seen to have some of the highest rates of substitution.

Figure 3.6 Branch-specific rates of substitution. Old World fruit bat (*E. helvum* and *P. vampyrus*) branches are summed to the node shared with *R. ferrumequinum* to make them comparable.

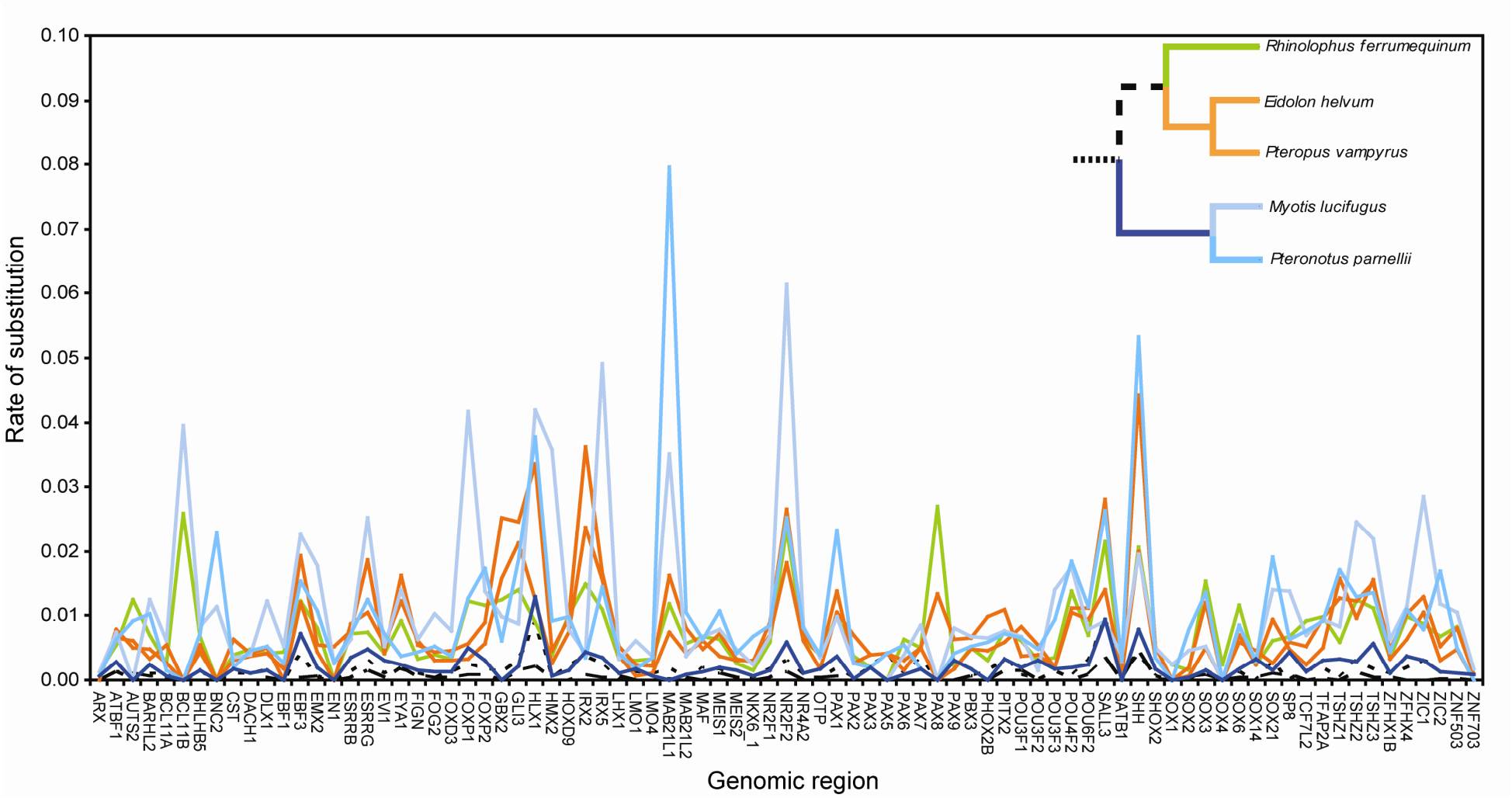

Bat specific study of CNEs in the *Hmx2/3* gene region

Following the above finding that rates of substitution varied in echolocating bats and the dolphin in the *Hmx2/3* gene region, I decided to look more closely at sequence variance in this gene region in a wider rage of bat species. In total four CNE sequences were collected from nine bat families: Rhinolophidae, Hipposideridae, Megadermatidae, Rhinopomatidae, Pteropodidae, Phyllostomidae, Mormoopidae, Vespertilionidae and Nycteridae.

Estimated branch lengths for trees based on all four CNEs showed broadly similar patterns (Fig. 3.7). For these four CNEs, certain members of the bat family Vespertilionidae had the longest branch lengths of all species, which were even longer than the included rodents. Interestingly, these high substitution rates were not seen among all species. In particular, *Myotis lucifugus*, *Kerivoula spp.* and *Murina spp.* displayed long branches, whereas, *Plecotus auritus* did not. For the majority of the four CNE datasets, all Yinpterochiroptera species showed similarly low substitution rates, with the exception of the CNE CRCNE00009716, in which the Old World CF bats (Rhinolophidae and Hipposideridae) had longer branch lengths. According to the genomic alignment of human, mouse, rat and fugu, CRCNE00009716 is the CNE that is most proximally located to both *Hmx2* and *Hmx3*. In CRCNE00009741, which is most distally located to either *Hmx2* or *Hmx3*, the Old World fruit bats, *Cynopterus brachyotis* and *C. sphinx,* had considerably longer branch lengths than the remaining Yinpterochiroptera species.

Visual inspection of the four alignments revealed that in two cases (CRCNE00009707 and CRCNE00009711) the majority of substitutions within the Vespertilionidae studied were located in the first and last 100 bps of the alignment. Furthermore, many of the observed nucleotides at the divergent sites were either ‘G’ or ‘C’ in the Vespertilionidae as opposed to typically ‘A’ or ‘T’ in many of the remaining mammal species.

Figure 3.7 Estimates of lineage-specific nucleotide substitution rates across four CNE sequence alignments from the *Hmx2/3* gene region calculated with BASEML using the GTR model of substitution, no clock and alpha and kappa estimated from the data. a) CRCNE00009707; b) CRCNE00009711; c) CRCNE00009716; d) CRCNE00009741.

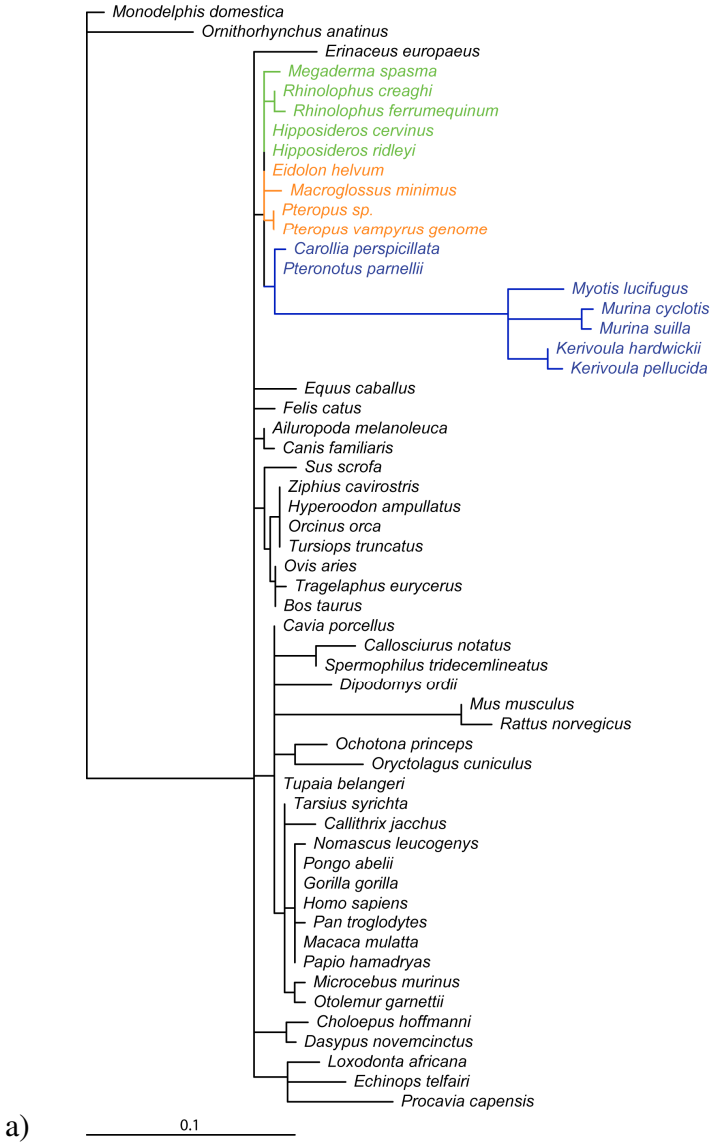
Monodelphis domestica
Ornithorhynchus anatinus
Erinaceus europaeus
Megaderma spasma
Rhinolophus creaghi
Rhinolophus ferrumequinum
Hipposideros cervinus
Hipposideros ridleyi
Eidolon helvum
Macroglossus minimus
Pteropus sp.
Pteropus vampyrus genome
Carollia perspicillata
Pteronotus parnellii
Myotis lucifugus
Murina cyclotis
Murina suilla
Kerivoula hardwickii
Kerivoula pellucida
Equus caballus
Felis catus
Ailuropoda melanoleuca
Canis familiaris
Sus scrofa
Ziphius cavirostris
Hyperoodon ampullatus
Orcinus orca
Tursiops truncatus
Ovis aries
Tragelaphus eurycerus
Bos taurus
Cavia porcellus
Callosciurus notatus
Spermophilus tridecemlineatus
Dipodomys ordii
Mus musculus
Rattus norvegicus
Ochotona princeps
Oryctolagus cuniculus
Tupaia belangeri
Tarsius syrichta
Callithrix jacchus
Nomascus leucogenys
Pongo abelii
Gorilla gorilla
Homo sapiens
Pan troglodytes
Macaca mulatta
Papio hamadryas
Microcebus murinus
Otolemur garnettii
Choloepus hoffmanni
Dasypus novemcinctus
Loxodonta africana
Echinops telfairi
Procavia capensis
0.1

a)

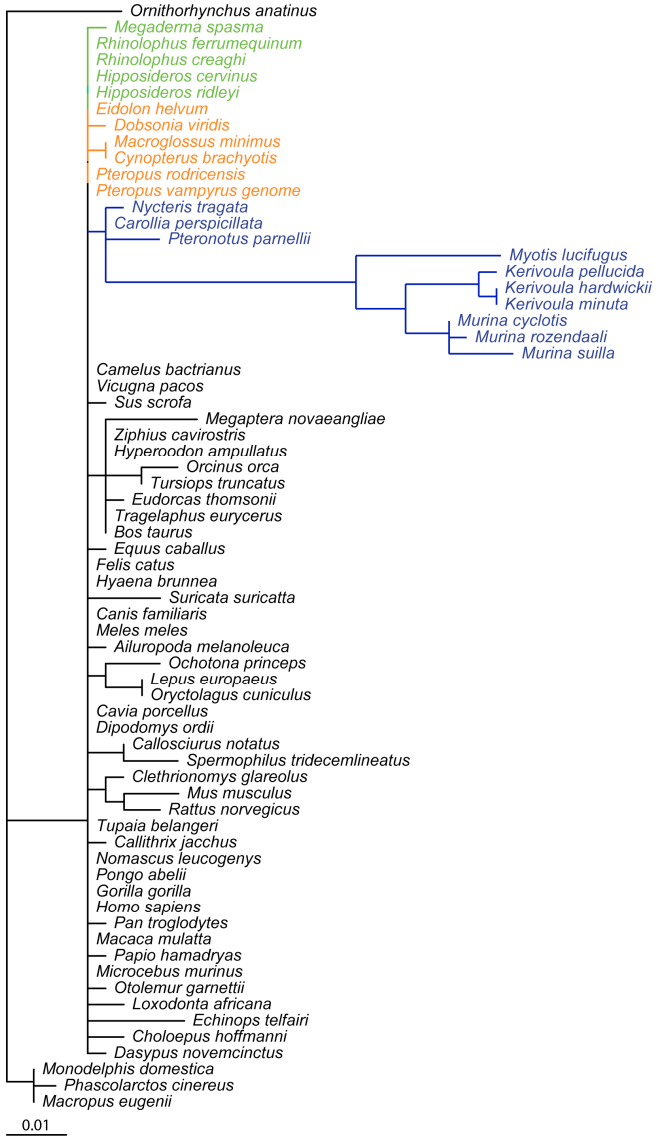
Ornithorhynchus anatinus
Megaderma spasma
Rhinolophus ferrumequinum
Rhinolophus creaghi
Hipposideros cervinus
Hipposideros ridleyi
Eidolon helvum
Dobsonia viridis
Macroglossus minimus
Cynopterus brachyotis
Pteropus rodricensis
Pteropus vampyrus genome
Nycteris tragata
Carollia perspicillata
Pteronotus parnellii
Myotis lucifugus
Kerivoula pellucida
Kerivoula hardwickii
Kerivoula minuta
Murina cyclotis
Murina rozendaali
Murina suilla
Camelus bactrianus
Vicugna pacos
Sus scrofa
Megaptera novaeangliae
Ziphius cavirostris
Hyperoodon ampullatus
Orcinus orca
Tursiops truncatus
Eudorcas thomsonii
Tragelaphus eurycerus
Bos taurus
Equus caballus
Felis catus
Hyaena brunnea
Suricata suricatta
Canis familiaris
Meles meles
Ailuropoda melanoleuca
Ochotona princeps
Lepus europaeus
Oryctolagus cuniculus
Cavia porcellus
Dipodomys ordii
Callosciurus notatus
Spermophilus tridecemlineatus
Clethrionomys glareolus
Mus musculus
Rattus norvegicus
Tupaia belangeri
Callithrix jacchus
Nomascus leucogenys
Pongo abelii
Gorilla gorilla
Homo sapiens
Pan troglodytes
Macaca mulatta
Papio hamadryas
Microcebus murinus
Otolemur garnettii
Loxodonta africana
Echinops telfairi
Choloepus hoffmanni
Dasypus novemcinctus
Monodelphis domestica
Phascolarctos cinereus
Macropus eugenii
0.01

b)

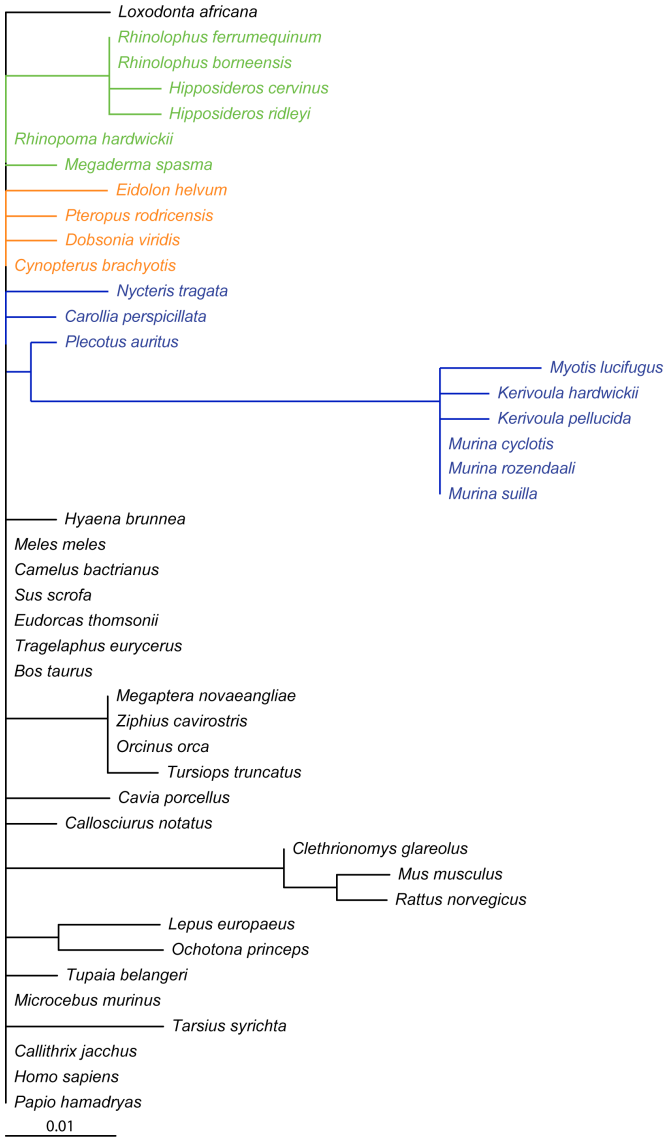
Loxodonta africana
Rhinolophus ferrumequinum
Rhinolophus borneensis
Hipposideros cervinus
Hipposideros ridleyi
Rhinopoma hardwickii
Megaderma spasma
Eidolon helvum
Pteropus rodricensis
Dobsonia viridis
Cynopterus brachyotis
Nycteris tragata
Carollia perspicillata
Plecotus auritus
Myotis lucifugus
Kerivoula hardwickii
Kerivoula pellucida
Murina cyclotis
Murina rozendaali
Murina suilla
Hyaena brunnea
Meles meles
Camelus bactrianus
Sus scrofa
Eudorcas thomsonii
Tragelaphus eurycerus
Bos taurus
Megaptera novaeangliae
Ziphius cavirostris
Orcinus orca
Tursiops truncatus
Cavia porcellus
Callosciurus notatus
Clethrionomys glareolus
Mus musculus
Rattus norvegicus
Lepus europaeus
Ochotona princeps
Tupaia belangeri
Microcebus murinus
Tarsius syrichta
Callithrix jacchus
Homo sapiens
Papio hamadryas
0.01

c)

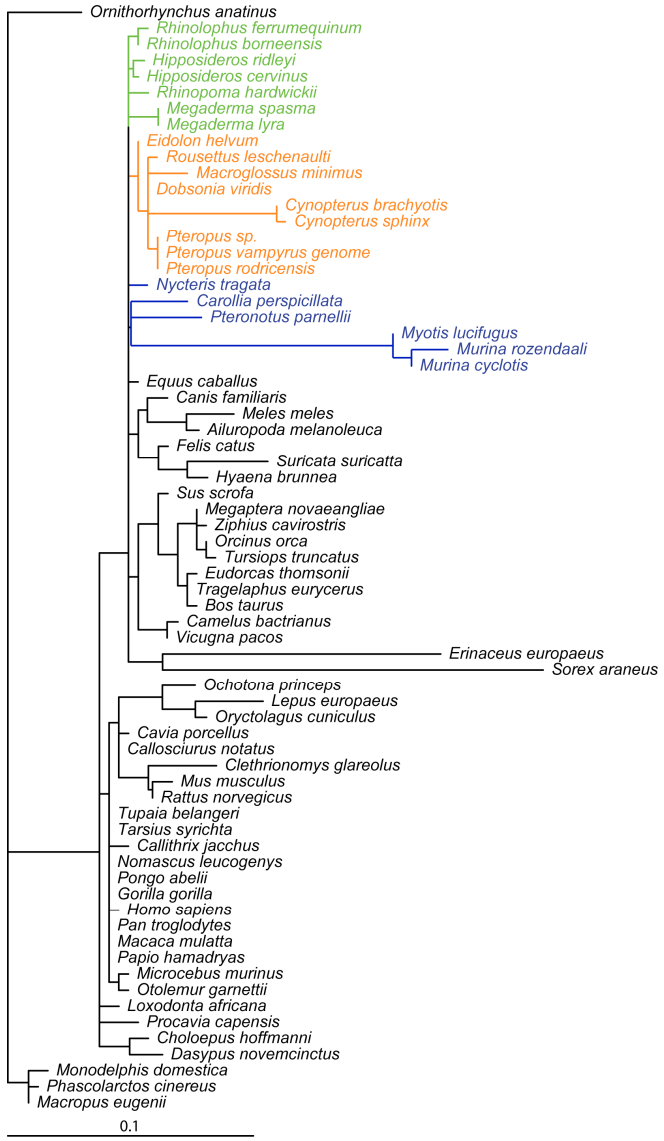
Ornithorhynchus anatinus
Rhinolophus ferrumequinum
Rhinolophus borneensis
Hipposideros ridleyi
Hipposideros cervinus
Rhinopoma hardwickii
Megaderma spasma
Megaderma lyra
Eidolon helvum
Rousettus leschenaulti
Macroglossus minimus
Dobsonia viridis
Cynopterus brachyotis
Cynopterus sphinx
Pteropus sp.
Pteropus vampyrus genome
Pteropus rodricensis
Nycteris tragata
Carollia perspicillata
Pteronotus parnellii
Myotis lucifugus
Murina rozendaali
Murina cyclotis
Equus caballus
Canis familiaris
Meles meles
Ailuropoda melanoleuca
Felis catus
Suricata suricatta
Hyaena brunnea
Sus scrofa
Megaptera novaeangliae
Ziphius cavirostris
Orcinus orca
Tursiops truncatus
Eudorcas thomsonii
Tragelaphus eurycerus
Bos taurus
Camelus bactrianus
Vicugna pacos
Erinaceus europaeus
Sorex araneus
Ochotona princeps
Lepus europaeus
Oryctolagus cuniculus
Cavia porcellus
Callosciurus notatus
Clethrionomys glareolus
Mus musculus
Rattus norvegicus
Tupaia belangeri
Tarsius syrichta
Callithrix jacchus
Nomascus leucogenys
Pongo abelii
Gorilla gorilla
Homo sapiens
Pan troglodytes
Macaca mulatta
Papio hamadryas
Microcebus murinus
Otolemur garnettii
Loxodonta africana
Procavia capensis
Choloepus hoffmanni
Dasypus novemcinctus
Monodelphis domestica
Phascolarctos cinereus
Macropus eugenii
0.1

d)

DISCUSSION

Phylogenetic analysis of mammalian CNEs

Neighbour-joining trees constructed from concatenated CNEs recovered the major sub-divisions within mammals, and, in many cases, the correct familial placements. This suggests that, although CNEs are highly conserved, enough lineage-specific substitutions have accumulated for them to contain considerable phylogenetic signal when sufficient numbers are considered. Bats were recovered as monophyletic, and support was found for the Yinpterochiroptera and Yangochiroptera suborders. No evidence was found for accelerated evolution of CNEs in *Rhinolophus ferrumequinum* compared to the two Old World fruit bats, *Eidolon helvum* and *Pteropus vampyrus.* There was ambiguity as to the sister-group of bats; Pegasoferae was weakly supported, while Cetartiodactyla, *Equus caballus*, and carnivores, received higher support.

The rodents, *Mus musculus* and *Rattus norvegicus*, consistently had the longest branch lengths, while apes and monkeys, had consistently relatively shorter branches. Causes for lineage-specific differences in rates of nucleotide substitution have been studied previously (as reviewed in Galtier and Duret 2007; Bromham 2011). In rodents, the higher substitution rates have previously been attributed to the larger effective population size (N_e) and shorter generation time, and not simply adaptive evolution (Janes *et al.,* 2011).

The total number of CNEs examined here, 3,110, represents only a small fraction of the total number of CNEs contained within a typical mammalian genome. For example, previous studies have identified ~100,000 CNEs between human, chimpanzee, mouse, rat and dog (Prabhakar *et al.,* 2006; Kim and Pritchard 2007). Therefore, this study will have only picked up some of the large scale evolutionary signals that are contained within the non-coding component of bat genomes. Undoubtedly, many more interesting patterns and features will be revealed by broader studies in the future.

CNEs associated with ear development genes

Rates of substitution calculated for ear development CNEs were similar to those estimated for the complete dataset. Rodents, and other small bodied taxa, had the fastest substitution rate and primates the slowest rates. In summary, in bats, all three

Yinpterochiroptera had approximately similar rates of substitution, and *M. lucifugus* had the highest rate of the two Yangochiroptera species.

When sorted into individual gene regions, with rates of substitution re-calculated for all species, several interesting taxonomic patterns emerged. All five bat species had significantly greater substitution rates for CNEs in two gene regions. No ear development CNEs were found to have elevated substitution rates in only the three Yinpterochiroptera. Both Yangochiroptera had significantly greater substitution rates in CNEs from five gene regions. CNEs from four genomic regions were found to have significantly greater substitution rates in only the dolphin. When the taxa are grouped by echolocation ability, an even more interesting pattern emerges. All echolocating taxa (i.e. all three laryngeally echolocating bat species and the dolphin), had significantly greater substitution rates, compared to the horse, in the *Hmx2/3* region. Whereas, none of the non-echolocating taxa (two Old World fruit bats and the cows) had significantly different rates compared to the horse.

Interpreting the above greater substitution rates in echolocating taxa is not straightforward, and there are several important considerations that need to be taken into account. Firstly, it is presently not known how the CNEs studied here are functionally related to the developmental genes used to name the genomic region in which they were located (Woolfe *et al.,* 2007). Secondly, it remains empirically untested what effect, if any, the different substitutions have with regards to regulation of gene expression. Thirdly, increased substitution rate does not necessarily imply adaptive evolution, but could also feasibly represent relaxed constraint on these elements in the focal taxa. Finally, as a point of reference, the cow was found to have significantly greater substitution rates for three genes, and, therefore, it seems likely that lineage-specific rates of substitution are common. Previously, the Tajima Rate Test was used to examine relative rates of substitution in teleost fishes and coelacanths (Lang *et al.,* 2010; Lee *et al.,* 2011). These studies confirm that lineage-specific differences in CNE rates of substitution are common in vertebrates. Mutation rates are affected by effective population size (N_e) and generation time in mammals (Charlesworth 2009). Therefore, differences in N_e may have a confounding effect on the results of the relative rates tests performed in this study. I decided to compare bat and dolphin sequences to the horse, using the human sequences as the outgroup for several reasons. Firstly, sequences were compared to the horse, as out of the nine currently available Laurasiatheria species

(excluding the two bats and dolphin) only genomes for the horse and the dog have good coverage. However, it could be argues that neither of these genomes are ideal, due to the problems associated with domestication, such as population bottlenecks and artificial selection. The horse was chosen because its coverage is high, whereas, the common shrew or hedgehog might have been a preferred choice given their similar body sizes and N_e to bats. However, both of these genomes are only available with low-coverage. Previously published simulations suggest that choice of outgroup should not affect the result of relative rates tests significantly, as long as the outgroup is valid and that the distance between the ingroup taxa and the outgroup are minimized (Robinson *et al.,* 1998). Therefore, members of the Euarchontoglires were considered. Rodents were discounted due to the documented high rates of substitution (Kim and Pritchard 2007). Of the remaining species, the human genome was chosen as this has the best coverage genome, however, given that primates were shown to have short branch lengths this might not be ideal.

Alternatively, if it can be assumed that proximity to the reference gene might imply a functional link with the CNE, what interpretations of the above pattern can be made? CNEs from the *Hmx2/*3 gene region were found to have significantly greater substitution rates in all echolocating taxa but not in non-echolocating taxa. Interestingly, dolphin CNEs in the *Tshz1* gene region have greater substitution rates, as in all bats, dolphin CNEs associated with *Shh* did not have different substitution rates compared to the horse. When limited to the auditory system, *Tshz1* is required for middle ear development (Coré *et al.,* 2007), while *Shh* has been implicated in regulation of chondrogenesis of the outer ear (Liu *et al.,* 2002). The mammalian middle ear ossicles are frequently cited as one of the most important auditory system components for high-frequency hearing (Manley 2010). While bats are known to display morphologically diverse pinnae, cetaceans do not posses any outer ears. However, *Shh* also have a critical roles in limb patterning (Welscher *et al.,* 2002), and, therefore, it is possible that the bat specific changes detected may relate to some of the many other functions of this gene, particularly given their modified limbs. CNEs located in three gene regions, *Emx2, Sox21* and *Meis2*, were found to have higher substitution rates in the two Yangochiroptera species, as well as the dolphin in the latter two cases. This could suggest that different genes are involved in the development of the auditory system specialisations seen in echolocating Yinpterochiroptera and Yangochiroptera.

The dolphin alone was found to have increased substitution rates in the CNEs located in the *Fign, Lhx1, Meis1* and *Pax2* gene regions. Mutations in several of these genes are known to affect the semicircular canals and vestibular systems (e.g. Cox *et al.,* 2000; Burton *et al.,* 2004). Interestingly, the semicircular canals of cetaceans have previously been shown to be considerably reduced in size (Ketten 2000; Spoor *et al.,* 2002). Therefore, this warrants detailed investigation in a wider range of cetaceans.

Several analyses suggested that, among bat branches, substitution rates were the lowest along the common bat ancestor branch and also, the ancestral Yinpterochiroptera branch. On the other hand among tips, rate comparisons across species were relatively consistent, with the exception of the Yangochiroptera, which tended to have higher substitution rates compared to Yinpterochiroptera.

Bat specific study of CNEs in the *Hmx2/3* gene region

Examination of estimated rates of substitution in nine bat families and other mammals, of CNEs located in the *Hmx2/3* gene region, revealed that, for the four elements examined, certain members of the bat family Vespertilionidae had the longest branch lengths. Increased substitution rates were particularly high in *Myotis lucifugus*, *Kerivoula spp*. and *Murina spp*., but not *Plecotus auritus.* This is particularly interesting when their corresponding echolocation calls are considered. Whereas, Kerivoulinae and Murininae, have some of the highest frequency calls documented with high repetition rate, *P. auritus* is known as a 'whispering' bat due to its low-intensity calls (Waters and Jones 1995; Schmieder *et al.,* 2010). The Old World CF bats (Rhinolophidae and Hipposideridae) had longer branch lengths compared to the remaining Yinpterochiroptera, only for CRCNE00009716. According to the genomic alignment of human, mouse, rat and fugu, CRCNE00009716 is the CNE most proximally located to *Hmx2* and *Hmx3*.

Although members of Vespertilionidae were shown to have high substitution rates in a number of CNEs putatively associated with *Hmx*2 and *Hmx3*, the substitutions were not always equally distributed throughout the length of the CNE but instead in some cases were clustered at one end. Therefore, it remains uncertain if this is genuine sequence variation in the CNE itself, or the CNE may be truncated. Furthermore, many of the substitutions in these species involved either 'G' or 'C', where the corresponding bases in other species were typically 'A' or 'T'. Biased gene-conversion has previously been

cited as a cause of non-adaptive increased rate of substitution in non-coding regions (Galtier and Duret 2007). Furthermore, in analyses such as these, where putative homologs are identified based purely on sequence similarity, there is always the possibility that paralogs will be aligned. Therefore, the functional significance of these substitutions, if any, remains undetermined.

Further Work:

The approach adopted here was an *a priori* test of rates of substitution in CNEs that could be linked to the development of the auditory system. However, an alternative approach could involve screening all CNEs for differences in rates of evolution and then looking for functional association between those that display the greatest rates. This could involve a significance test to determine which lineages are evolving at significantly different rates, such as the ‘‘Shared Rates Test’’ (Kim and Pritchard 2007). However, this method is more applicable for comparing CNEs across a small number of taxa rather than gaining a broad view of CNE evolution across many divergent species. In order to rule out relaxed constraint to account for the increased rates of substitution, and also to assess the levels of positive selection acting on bat CNEs associated with the developing auditory system, it would be interesting to study population level variation.

As mentioned above, sometimes the gene regions used to define the CNE datasets may contain more than one gene; therefore, it is necessary to confirm functional associations between the CNE and the gene in question. Presently, each CNE region is named after one of the transcriptional-regulation or development genes they contain (Woolfe *et al.,* 2007). However, this gene is chosen at random, and does not imply a functional association. In many of the cases, such as *Dach1*, this was the only annotated gene in the region, however, in other cases, such as *Shh*, many other genes are located close by. Future annotations and functional assays might help document the true association between CNEs and developmental genes.

Several web-based tools exist for predicting transcription factor binding sites; e.g. ConSite (Sandelin *et al.,* 2004), rVista (Loots and Ovcharenko 2004) and TESS (Schug and Overton 1997). This is one future approach that could be used to explore how the specific observed sequence variation could have a functional effect on gene expression.

As many vertebrate CNEs are less than 100 base pairs long they were filtered out by the initial screen. However, these CNEs are also likely to be functionally relevant. Furthermore, all CNE sequences were not recovered for all bat species by BLASTN. Whether this is due to lack genome coverage, extreme sequences divergence or deletion of the CNE in the particular species is unknown at present. For at least the three Solexa datasets, coverage is known to be good at approximately 22x, therefore, poor coverage is unlikely to be the cause of the missing data in the three bat species. Equally, studying patterns of lineage-specific CNE loss or gain may be just as informative as studying the CNEs that are present.

Conclusions

CNEs located in the genomic region of the Homeobox genes *Hmx2* and *Hmx3* were found to have increased rates of substitution in echolocating taxa (laryngeal echolocating bats and one toothed whale), but not in either the cow or Pteropodidae, when compared to the horse. Additional evidence from four CNEs located proximally to *Hmx2/3* suggests that these elements are under different evolutionary constraints in Yinpterochiroptera and Yangochiroptera. CNEs located in the genomic region of different genes associated with the development of the auditory system, show variation in substitution rate in each bat suborders. In summary these findings could suggest that different selective constraints have acted on the developmental pathways of the auditory systems in each of the two bat suborders.

CHAPTER FOUR

Correlates of High-Frequency Hearing and Cochlear Morphology

SUMMARY

Mammalian hearing ranges extend from below 1,000 Hz to over 150 kHz; and many clades have evolved specialised hearing in response to ecological divergence. Bats are one such group; with the inner ears of many echolocating species having undergone substantial structural modifications in order to process the high frequency sounds produced during laryngeal echolocation. Subsequently, upper hearing limits of many laryngeally echolocating bat species are >100 kHz (five times those of humans). Traditionally, studying the minute features of inner ears proved problematic; to overcome these problems high-resolution micro-computed tomography (μCT) scans were taken of inner ears of 16 bat families representing a cross-section of bat diversity. By studying the morphological adaptations of bat cochleae inferences may be drawn regarding the associated adaptations of major echolocation call types, as well as the evolutionary origins of echolocation.

Cochlear gross morphology i.e. overall size and number of turns, was compared between echolocating and non-echolocating bats, as well as with a number of non-bat mammals. The length of the basilar membrane – the structure supporting the hair cells – was estimated and correlated with hearing ranges and echolocation call parameters. Results revealed highly variable cochlear morphologies, within and across bat clades. In agreement with previous studies, the cochleae of echolocating bats were found to be hypertrophic and structurally complex, and, therefore, supported previous assertions of morphological convergence between echolocating clades. No clear evidence of relaxation or 'loss of function' was found in Old World fruit bats, which therefore, does not support a loss of sophisticated echolocation in this lineage.

INTRODUCTION

The auditory system and how sound is heard

An animal's survival depends on its ability to interact with its environment; in particular it must be able to orientate itself, detect and successfully avoid predators and efficiently find food. Whereas diurnal animals mainly rely on visual cues for this, many nocturnal animals, or those living in low light levels, have highly adapted auditory and olfactory systems for these roles (e.g. Barton *et al.,* 1995). Adaptations of the auditory system may be passive, such as increased listening ability to either allow prey detection e.g. the barn owl, *Tyto alba* (Payne 1971) and the bottlenose dolphin, *Tursiops truncatus* (Gannon *et al.,* 2005) or, conversely, alert prey to the presence of predators e.g. the silver Y moth, *Autographa gamma* (Skals *et al.,* 2003). Alternatively, they may involve active processes, such as echolocation, e.g. cave swiftlets, *Collocalia spodiopygius* (Griffin and Thompson 1982) and certain bats species (for examples see Fenton 1984).

The mammalian hearing system consists of three principal parts; the outer, middle and inner ear. The outer ear is most conspicuously represented by the pinnae, but also includes the funnel-like concha which leads to the ear canal (Rosowski 1996). Although pinnae are functionally very important for initial sound acquisition and localisation in most terrestrial mammals, they can be greatly reduced and have been entirely secondarily lost in some marine and fossorial mammals (Nevo 1979; Wartzok and Ketten 1999). The outer ear initially receives the external sound stimuli, or acoustic waves (Manley *et al.,* 2004). From here acoustic waves travel to the middle ear; represented by the tympanic membrane, the middle ear air spaces, the three ossicles and the Eustachian tube (Rosowski 1996). As the acoustic waves reach the tympanic membrane (the eardrum), they cause vibrations which leads to sequential movement of the three ossicles (malleus, incus and finally stapes). The sound information is transferred to the fluid-filled inner ear, which houses the ear's sensory structures, when the stapes apply pressure to the oval window, which is a membrane covered opening into the central part of the cochlea (Rosowski 1996). The cochlea acts as a resonating chamber to the waves passing through, and it is only once the waves have passed through that the information is finally transferred to the brain in the form of nerve impulses, where it is interpreted as the sound we perceive (Fig. 4.1). This process is a cascade of interdependent processes, as the output of one stage acts as the input to the next (Rosowski 1996).

Figure 4.1 Overview of the path taken by sound-waves as they travel from outer ear pinnae to the brain via the middle and inner ears.

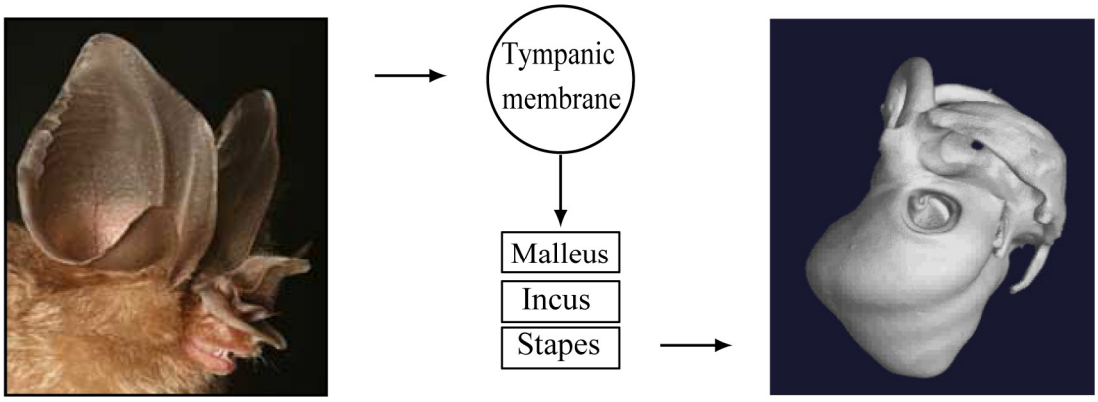

1. Outer-ear - initial reception of external sound stimuli.

2. Middle-ear - sequential transfer of vibrations.

3. Inner-ear - amplification of sound followed by transfer to the brain.

The evolution of high-frequency hearing

Within amniotes, turtles and tuataras are representative taxa of unspecialized hearing capabilities; they have the least specialized hearing organs and possess hair cells that respond only to low frequencies of less than 1 kilohertz (kHz) (Manley 2000). Since splitting from other basal amniotes, approximately 300 Ma ago, the lineage that gave rise to mammals has evolved hearing organs which utilize frequencies greatly above that of 'primitive' low frequency hearing. High-frequency hearing is particularly well developed in certain species of echolocating mammals. For example, the upper hearing limits, as suggested by the highest call frequency, of the short-eared trident bat, *Cleotis percivali,* is 212 kHz (Fenton and Bell 1981), and that of the clear-winged woolly bat, *Kerivoula pellucida,* is 250 kHz (Schmieder *et al.,* 2010). At the other extreme, some mammal species have acquired increased sensitivity to low-frequency sound; examples include subterranean mammals, African and Asian elephants, and baleen whales (Heffner and Heffner 1980; Ketten 1997; see references within Mason and Narins 2001).

Considerable effort has been placed in pinpointing the morphological adaptations that allow high-frequency hearing in mammals. The first key innovation, cited as a prerequisite, is the transition from one- to three-ossicle middle ears, with fossil evidence proving the presence of this in the early mammaliaformes, such as Morganucodonta (Rosowski and Graybeal 1991; Vater *et al.,* 2004; Manley 2010). Later changes to the inner ear, such as elongation of the basilar membrane, and specialisation of hair cells, are all thought to be crucial for the ongoing extension of the upper hearing limit of

higher mammals (Meng and Fox 1995; Ruggero and Temchin 2002). The cochlea is the primary hearing organ, and within modern amniotes its morphology has become considerably diverse (Manley 2000). Cochleae consist of coiled cavities within the temporal bone, one located on either side of the head, containing the structures that separate the components of a complex sound by frequency and intensity (Ashmore and Gale 2000). The generalized form of the mammalian cochlea is a bony spiral canal, very similar in shape to a snail shell; this coiled form is regarded as the definitive mammalian cochlea. The cochlea turns counter-clockwise on the left-hand side and clockwise on the right. Coiling evolved after the division between monotremes and the marsupial-placental lineage, and is thought to have evolved as a mechanism to accommodate the elongated sensory structures of the inner ear (Manley 2000; Luo *et al.,* 2011). Despite overall similarities of gross shape, the number of turns varies considerably across mammals (for examples see Manoussaki *et al.,* 2008). Consistent relationships have not been found between number of turns with either hearing capabilities or phylogenetic relationship. For example, in echolocating bottlenose dolphins, *Tursiops truncatus,* the hearing range is 150 Hz – 152 KHz and they have 2.25 cochlear turns (Ketten 2000; Manoussaki *et al.,* 2008), which is the same number of turns as the Asian elephant, *Elephas maximus,* in which the hearing range is entirely limited to 'low' frequency sounds (17 Hz – 10.5 kHz) (Heffner and Heffner 1980). While within Rodentia, mice, *Mus musculus,* have 1.5 turns, rats, *Rattus norvegicus,* 2.5 and guinea pigs, *Cavia porcellus*, 4 (Jero *et al.,* 2001; Manoussaki *et al.,* 2008; Albuquerque *et al.,* 2009).

The cochlear spiral is formed around a central hollow core of bone, known as the modiolus, which contains the cochlear nerve (Bruns *et al.,* 1989; Meng and Fox 1995). Projecting into the spiral canal, from the centre, is an osseous shelf, known as the spiral lamina, which partially bisects the lumen, the partition is completed by the basilar membrane (Bruns *et al.,* 1989). This allows the fluid filled space inside the cochlea to be functionally divided into two compartments: the scala vestibule and the scala tympani (Fig. 4.2). However, the two scala are continuous at the apex of the cochlea, termed the helicotrema (Delmaghani *et al.,* 2006). There is also a third compartment, the scala media, which lies between the other two scala, which is formed between the basilar membrane and Reissner's membrane.

Figure 4.2 Mid-section through the cochlea of the frog-eating bat *Trachops cirrhosus.* This cochlea is made up of six half turns, starting from the cochlear aqueduct at the base and ending at the helicotrema, which are formed around the auditory nerve. The fluid spaces making up each turn are divided into three compartments; cross-sections of the scala tympani (T1-6), those of the scala media (e.g. M1) and finally the scala vestibuli (e.g. V1). These sections are separated by three membranes; RM, Reissner's membrane; TM, tectorial membrane; BM, basilar membrane, which are supported by bony projections and ligaments; PSL, primary spiral lamina; SSL, secondary spiral lamina; SG, spiral ganglion; SV, stria vascularis. Taken from (Bruns *et al.,* 1989).

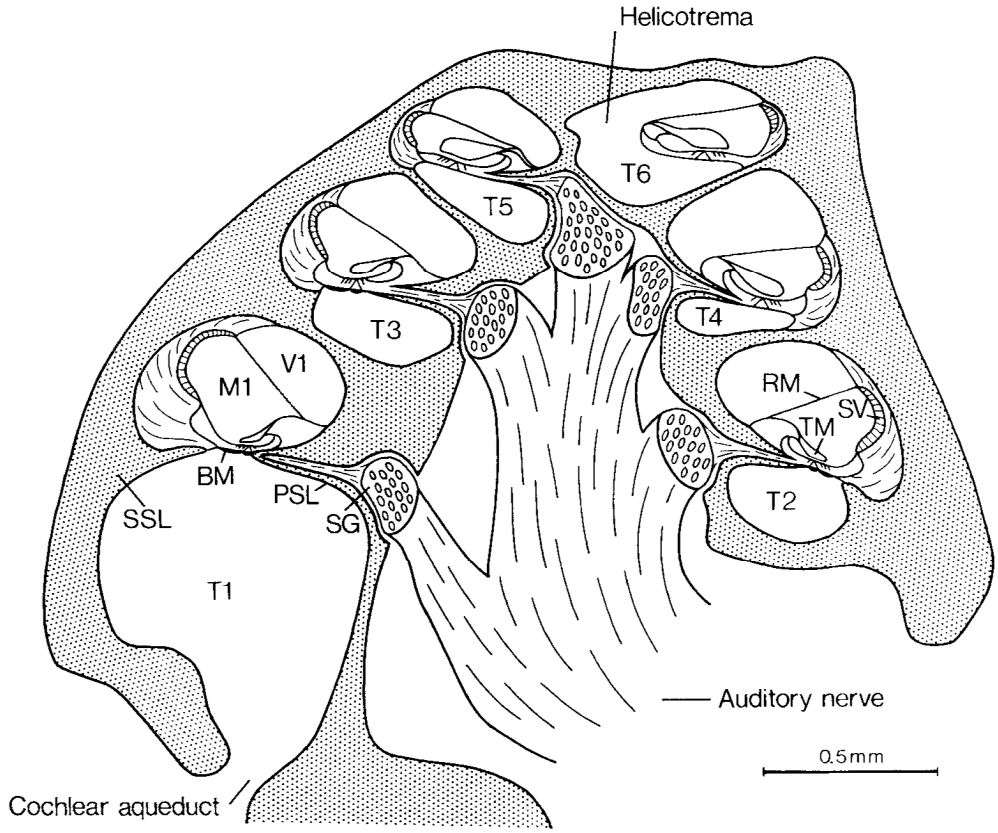

One of the key features of the cochlea is the tonotopical organisation of the distribution of the range of sound frequencies perceived along the spiral (Robles and Ruggero 2001). Here, high frequency sounds are determined by the basal turns and lower frequencies towards the apex, as modelled by a number of studies (e.g. Inselberg 1978; Richter *et al.,* 1998; Rhode and Recio 2003), and is partly achieved by a decrease in stiffness of the basilar membrane from base to apex. The precise movements of the membrane are controlled by its specific elastic property, thought to involve the extracellular protein Emilin-2, and are crucial for the transduction of sound by the hair cells (Amma *et al.,* 2003).

The sensitivity and frequency selectivity of mammalian hearing is due to local mechanical feedback processes within the cochlea, which is controlled by hair cells (Jia and He 2005). Hair cells are specialised epithelial cells, and are named after the sensory projections, cilia and stereocilia, that project from the apical end (Coffin *et al.,* 2004).

Mammalian hair cells, housed together with supporting cells, make up the Organ of Corti (Ulfendahl and Flock 1998). Each inner ear is thought to contain between 15,000 to 30,000 neurosensory hair cells (Frolenkov *et al.,* 2004). Within these cells there is a division of labour with each mammalian cochlea containing two distinct hair cell types (Coffin *et al.,* 2004). Outer hair cells (OHC) amplify low-intensity sounds and play a role in the sharpening of frequency tuning curves and inner hair cells (IHC) are the primary auditory receptors (Ulfendahl and Flock 1998). OHCs are unique in mammals, and, therefore, so is the finely tuned hearing they provide, and also have a unique property of electromotility (for more details see Dallos and Fakler 2002). Electromotility allows the OHC to rapidly change length controlled by changes to its membrane potential, and is thought to be mediated by the motor-protein Prestin (Zheng *et al.,* 2000; Jia and He 2005). The *Prestin* gene has been found to be under positive selection on the phylogenetic branches leading to all mammals and certain echolocating mammals (Franchini and Elgoyhen 2006; Li *et al.,* 2008; Li *et al.,* 2010; Liu *et al.,* 2010a).

Morphological correlates of hearing

Within mammals there is considerable variation in hearing capabilities (Heffner and Heffner 2008) and inner ear morphology (Gray 1951; Manoussaki *et al.,* 2008). However, to date, very few consistent relationships have been found linking the two. It has been stated that the length of the uncoiled cochlea, or more precisely the length of basilar membrane, can be used to predict the range and precision of a species' hearing capability (Gray 1951). This has been theoretically demonstrated (Gray 1951; West 1985; Rosowski and Graybeal 1991), and it has been concluded that generally, as basilar membrane length increases so does the overall hearing range. Additionally, there is a negative correlation between absolute basilar membrane length and high- and low-frequency hearing limits (West 1985). The situation is complicated by the fact that basilar membrane length is positively correlated with body mass (Rosowski and Graybeal 1991; Kirk and Gosselin-Ildari 2009).

The coiled mammalian cochlea accommodates the elongated basilar membrane within the confined space of a skull, and in the past it has been doubted as to whether the coiling itself has a functional effect (Meng and Fox 1995; Manley 2000). Interestingly however, given its putative role in accommodating the basilar membrane, little relation has been found between the number of turns and basilar membrane length (West 1985).

This is because the diameter of turns is high variable, for example, guinea pigs have a high number of turns (Gray 1951), yet their basilar membrane length is comparable to other rodents. The number of cochlear turns, among ground dwelling mammals, has been shown to correlate strongly with octave hearing range (West 1985). Furthermore, more recently it has been suggested that the coiled structure has important mechanical constraints particularly on the low-frequency limit of hearing (Cai *et al.,* 2005; Manoussaki *et al.,* 2006; Manoussaki *et al.,* 2008).

It is perhaps unsurprising that it is often stated that high-frequency hearing and sound emission are governed by an animal's size (Ketten 2000). This relationship may be artifactual however, as in fact hearing capabilities directly correlate with inter-aural distance (Heffner and Heffner 1980). Across 32 genera, including several auditory specialists, such as echolocators and marine mammals, a strong relationship was found between maximum inter-aural distance divided by speed of sound (maximum Δt) and the high-frequency hearing limit (Heffner and Heffner 1982). However, when this relationship was reviewed including more taxa, echolocating bats and cetaceans were found to have higher than expected highest audible frequencies for their 'functional head' sizes (maximum Δt) (Heffner and Heffner 2008). Conversely, subterranean mole rats have much lower audible frequency ranges; in fact their highest audible frequencies are comparable to those of the elephant (Heffner and Heffner 2008).

Environmental correlates of hearing

A large amount of evidence supports the view that the niche and environment have fundamental effects on the specializations of hearing ability. For example, species that occupy terrestrial, subterranean or aquatic habitats have all evolved contrasting hearing capabilities (Heffner *et al.,* 1994; Wartzok and Ketten 1999). One study investigated associated morphological adaptations of the ears within the Rodentia family Heteromyidae, that are found in a range of habitats from extremely dry to relatively moist (Webster and Webster 1980). The middle ears of the most xeric species were highly inflated, with inner ear modifications that may relate to specialised low-frequency hearing (Webster and Webster 1980). Interestingly, chinchillas, *Chinchilla laniger*, that live in arid, barren areas of relatively high elevation (Spotorno *et al.,* 2004), also display hypertrophy of middle ear cavities (Nummela 1995), although the functional significance of this is unknown.

Of the two mammalian orders that have convergently evolved aquatic lifestyles, Sirenia and Cetacea, members of both have lost external auditory features. Furthermore, some species of Sirenia show degraded auditory canals (Ketten *et al.,* 1992). Studies of the West Indian manatee, *Trichechus manatus,* suggest that the cochlear ducts are particularly poorly developed basally, and, therefore, this species is unlikely to be able to hear frequencies above 20 kHz and is probably poor at sound localization (Ketten *et al.,* 1992). In stark contrast to this are the auditory systems of cetaceans, which have become highly evolved. Extant cetaceans can be divided into two sub-orders, baleen and toothed whales. Toothed whales are capable of sophisticated echolocation and produce high frequency clicks and whistles of up to 150 kHz (Ketten 1994). Meanwhile, baleen whales do not echolocate, but instead employ low-frequency calls, 12 Hz-3 kHz (Ketten 1994). Anatomical studies have shown three forms of cetacean cochleae; one within baleen whales and two within toothed whales. One form occurs in species such as the Amazonian dolphin, *Inia geoffrensis,* and the harbour porpoise, *Phocoena phocoena*, which are mainly solitary, found inshore and produce the highest frequency sounds, whereas the other form is seen in the remaining species, such as the common dolphin, *Delphinus delphis*, that generally form pods (Ketten 1994). Another interesting feature of the cetacean labyrinth is that there is a dramatic difference in the scaling factors of the conjoined auditory and vestibular systems (Ketten 1997; Spoor *et al.,* 2002).

Pinnipeds pose an interesting situation; they spend a large proportion of time hunting underwater but breed and nurse young on land and, therefore, their hearing capabilities must be suited to both environments. A detailed behavioural study examined seals and sea lions, and found that all animals tested had more sensitive underwater hearing (Schusterman 1981). Interestingly, true seals, which lack external pinnae, were found to be able to hear higher frequency sounds underwater compared to eared-seals, which in turn could hear higher frequency airborne sounds (Schusterman 1981). Furthermore, the bones of middle ears of true seals were found to be ten times heavier compared to those of similarly sized terrestrial mammals (Nummela *et al.,* 1999).

Intra-specific variation and cochlear plasticity

The mammalian cochlea spiral represents a continuous organic structure, and as such it is difficult to adequately describe and document its form using quantitative means. As such, literature searches can provide a range of values for cochlear turns per species,

e.g. published values for the guinea pig range from 3.5 – 4.25 turns (West 1985; Albuquerque *et al.,* 2009). Whether this is a function of physical or procedural variation is unclear. One of the best studied auditory systems is that of humans, and medical researchers have so far documented cases of patients with cochlear turns varying from none to three (Scott and Carey 2006; Tian *et al.,* 2006). It is normally assumed that in a healthy person the number is two and a half turns (Tian *et al.,* 2006), although a recent study that examined a number of human temporal bones found that 65% of those examined had more than two and a half and 11% had more than two and three quarter turns (Biedron *et al.,* 2009). In humans it appears that sexual dimorphism is negligible (Miller 2007).

Extracting functional information from the labyrinth

Several factors govern the morphology of species' auditory systems; phylogeny, environment, physical and mechanical constraints all play a role (Webster and Webster 1980; Nummela 1995; Cai *et al.,* 2005; Vater and Kossl 2011). Nevertheless, several studies have explored the possibility of extracting functional information either directly from bony labyrinths or using x-ray imagery to infer hearing capabilities. The close anatomical relationship between the dimensions of the intact bony labyrinth preserved in osteological specimens to that of the membranous cochlea of living animals makes these inferences possible (Meng and Fox 1995; Kirk and Gosselin-Ildari 2009). This approach has been used to reconstruct hearing capabilities of one of the earliest known mammaliaformes, *Morganucodon* (Graybeal *et al.,* 1989; Rosowski and Graybeal 1991), early marsupials and placentals (Meng and Fox 1995), fossil primates (Kirk and Gosselin-Ildari 2009; Coleman *et al.,* 2010), extinct reptiles (Walsh *et al.,* 2009) and also the putative hearing and vocalisations of fossilised bats (Habersetzer and Storch 1992). Due to the basal position of these fossil taxa in relation to modern species, approaches like this raise exciting possibilities to answering long standing questions regarding the evolution of hearing.

Bat hearing, echolocation and ears

Echolocating bats have arguably the most specialised auditory systems of any mammalian group. Virtually all aspects of echolocating bats' ears are modified: from the size, shape and structure of the external pinnae to the gross morphology of the cochlea. As the primary means by which sound is detected, the pinnae of echolocating

bats play an important role, and morphologically bat pinnae are diverse across species (for example Ma and Muller 2011) (Fig. 4.3). Several hypotheses have been put forward to explain the array of structural modifications of pinnae, including improved target localisation (Mogdans *et al.,* 1988), increased passive listening capabilities, (Fiedler 1979; Bruns *et al.,* 1989) and some studies suggest a direct relationship between pinnae size and echolocation call frequency (Obrist *et al.,* 1993). Some species, such as the horseshoe bats, have ridges along the lateral edge thought to help focus high frequencies into narrow beams (Kuc 2009).

As is the typical mammalian case, bats possess three middle ear ossicles (Fig. 4.4). It has been suggested that bat middle ears display certain features necessary for transmission of ultrasonic frequencies (references within Vater and Kossl 2004). However, previously no difference in scale was found between the middle ear bones of four bat species compared to those of equally sized mammals (Nummela *et al.,* 1999).

Arguably of the three parts of the auditory system the inner ears of echolocating bats show the most adaptations for the high-frequency hearing associated with laryngeal echolocation. The cochlea is hypertrophic and has 2.5 to 3.5 complete turns, compared to only 1.75 in non-echolocating Old World fruit bats (Altringham 1996). Therefore, the variation displayed within bats encompasses nearly the entire range shown by other mammals. The different requirements posed by each mode of echolocation have produced a series of different, although sometimes convergent inner ear adaptations (Kossl *et al.,* 1999; Kossl *et al.,* 2004). For example, the auditory foveae found in horseshoe and mustached bats (Schuller and Pollak 1979; Russell *et al.,* 2003), are directly associated with the long CF component of their echolocation call, in order to accommodate this feature the basal turn of the cochlea in these species is greatly enlarged. Previous studies suggest specific adaptations of the anchoring system of the basilar membrane in echolocating bats, and also the thickness of the basal section of the basilar membrane (Kucuk and Abe 1992). One of the earliest comprehensive studies of variation of cochlear morphologies in bats was that of Ade Pye [the series of studies covered the Emballonuridae and Rhinolophidae (Pye 1966b), the Phyllostomidae and Mormoopidae (Pye 1967) including Pteronotus parnellii (Pye 1980), the Megachiroptera (containing the Pteropodidae) and also Vespertilionidae (Pye 1966a)].

Figure 4.3 Surface mesh representations of bat pinnae, collected using computed tomography of ethanol preserved specimens. Taken from Ma and Muller (2011).

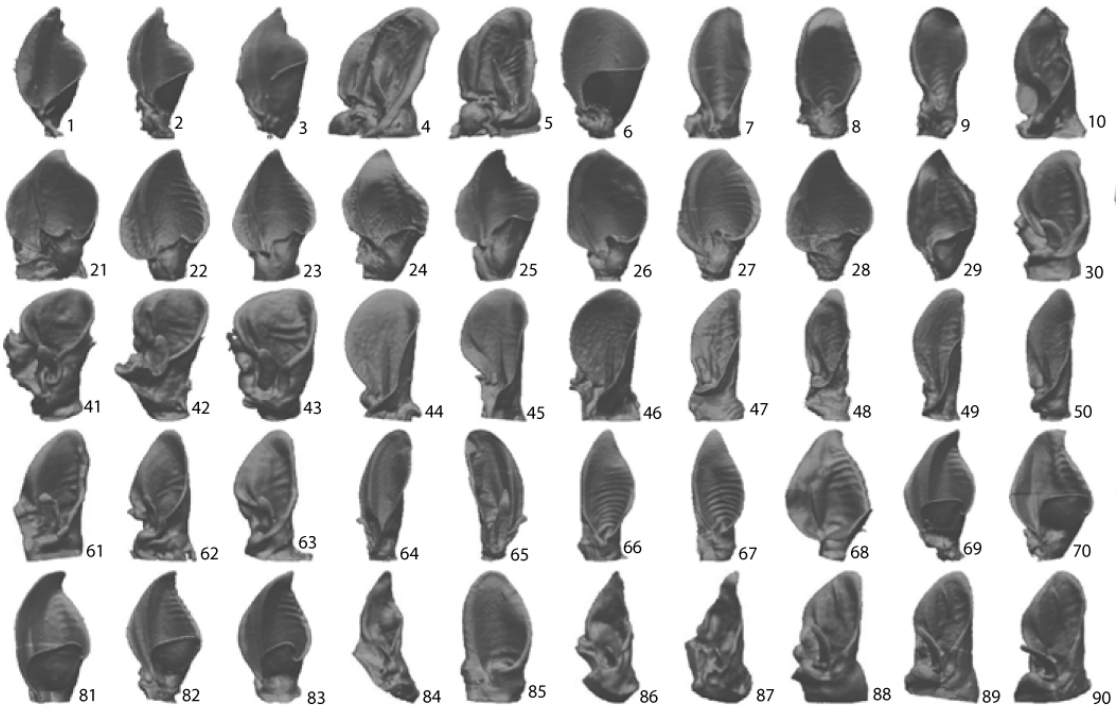

Figure 4.4 The three middle ear bones of *Trachops cirrhosus* in dorsal view. A: Malleus. B: Incus. C: Stapes. Taken from Bruns *et al.* (1989).

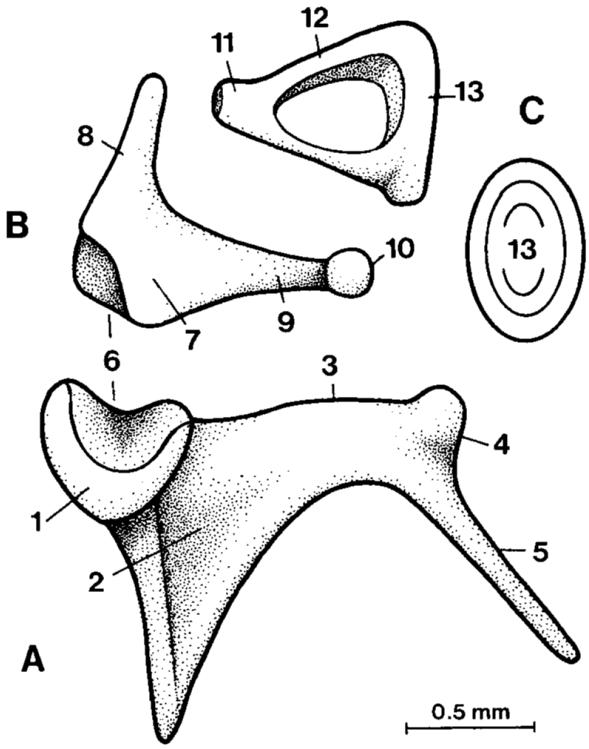

Aims and objectives of this study

This study created three-dimensional bat inner ear volumes, representing a cross-section of bat species and ecology. They were used to study the morphology of bat inner ears in relation to echolocation call type and hunting strategy of the species in question. Correlations were investigated between call parameters, e.g. minimum, maximum and peak-energy frequency, and morphological characteristics of the cochlea, and species that have evolved convergent echolocation call-types e.g. horseshoe bats and *Pteronotus parnellii.* This should allow us to understand the functional constraints acting on the two clades of echolocating bats and, therefore, might suggest how many times sophisticated echolocation has evolved. This could also be determined by evidence of relaxation in the inner ears of non-echolocating Old World fruit bats that may be consistent with a loss. Alternatively, it may be possible to find evidence of convergence between the two main clades of echolocating bats and, therefore, evidence of multiple origins.

Hypothesis 1: Echolocation places great sensory demands on the auditory system. Therefore, I predicted that echolocating animals will show high levels of morphological adaptation in the gross structure of the cochlea, compared to non-echolocating animals. This will be examined in terms of number of cochlea turns, overall size and basilar membrane length.

Hypothesis 2: I predicted that echolocating bats, which posses the most sophisticated echolocation abilities, will show higher levels of cochlear adaptation compared to other echolocating mammals i.e. toothed whales.

Hypothesis 3: Given that echolocating bats display significant adaptations for echolocation, and given the alternative evolutionary scenarios of echolocation, then either Old World fruit bat cochleae should provide evidence of degeneration, or there will be no sign of degeneration coupled with clear functional adaptation in the two groups of echolocating bats. For example, evidence of degeneration of the inner ears of Old World fruit bats might be provided by increased inter- and intraspecific morphological variation in size and shape.

Hypothesis 4: I predicted that the morphological parameters representing the cochlea will be correlated with both auditory and echolocation thresholds in bats.

MATERIALS AND METHODS

Study sample

A total of 68 specimens, representing 56 bat species from 16 families, were obtained for this study from museums and private collections (Appendix C Table C1). Species were prioritised based on maximising taxonomic and geographic coverage, ecological diversity, behavioural differences and echolocation call type. As this evolutionary study aimed to document as much bat morphological diversity as possible, a shallow but wide approach was taken, with the majority of species represented by a single specimen. In five cases, *Plecotus auritus, Pipistrellus pipistrellus, Miniopterus schreibersii, Noctilio leporinus* and *Rhinolophus pearsonii,* multiple individuals were used to allow quantification of intra-specific variation. Additionally, three specimens of *Rhinolophus philippinensis* representing documented size-morphs were included. Preservation state and method of preparation varied considerably between specimens; seven were complete specimens preserved in ethanol, the remaining specimens being prepared skulls. Adult specimens were used, apart from *Hypsignathus monstrous* where the only available specimen was a female sub-adult. Due to lack of choice, and in some cases, documentation, it was impossible to control for gender, and, therefore it must be assumed that sexual dimorphism is minimal.

Acquisition of µCT-scans

Each specimen was scanned in the frontal plane using the Metris X-Tek HMX ST 225 Computed Tomography (CT) System at the Department of Mineralogy, EMMA Division, The Natural History Museum, London. The complete basal part of the skull was scanned so as to include both inner ears (see Fig. 4.5a), with the exception of specimen NHM.65.3990, where the single remaining bony labyrinth was dislodged from the skull and was thus scanned directly. Following calculation of the centre of rotation and cropping the region to reconstruct to the desired region of interest, volumes were constructed using CT PRO (Metris X-Tek, UK). Reconstructed volumes were then visualized using VG Studio Max 2.0 (Volume Graphics, Heidelberg, Germany). Each scan consists of voxels (the 3D equivalent of pixels), each of which is assigned a CT (grey) value based on the density of the material. Denser material, such as bone, appears as white areas and the internal voids of the labyrinth appear black due to its low density (Fig. 4.5b). The voxel size of each specimen is listed in Table C1. The ‘region grower’

tool in VG Studio Max was used to digitally dissect the internal voids of the bony labyrinth, i.e. the cochlea and semicircular canals, to produce a digital endocast (Fig. 4.5c). In most cases only left labyrinth voids were extracted. However, prior to extraction labyrinths were examined to decide which was best preserved, as some specimens had considerable damage. In a number of specimens both labyrinths were extracted to examine intra-individual variation; though previous studies suggested that in healthy individuals there is little variation (Schmelzle *et al.,* 2007). From these solid 3D regions of interest, StereoLithography (STL) files, which describe the surface geometry, were produced.

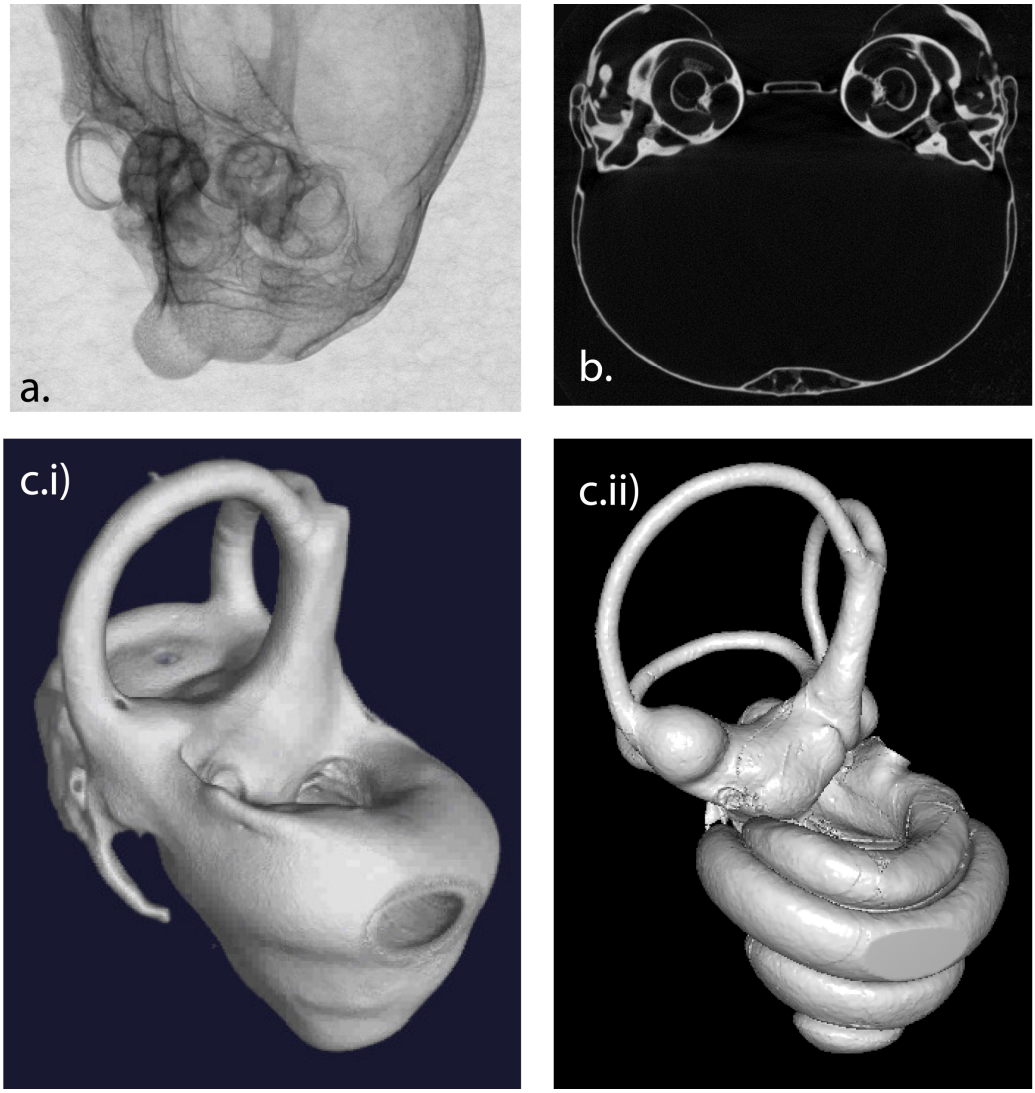

Figure 4.5 Acquisition of x-rays, digital dissection and three-dimensional reconstruction of the internal void of bat inner ears. a) Single x-ray projection of the skull from *Hypsignathus monstrosus* (Pteropodidae); in total 1352 x-rays were taken of each specimen, with it rotated a fraction of a degree between each. b) The centre of rotation is determined and all 1352 x-rays are aligned to produce a 3D representation of external and internal features of the skull, in this case the echolocating bat *Myotis lucifugus*; the two cochleae are clearly visible on the upper lateral part of the skull. c) Digital image of the external surface of the inner ear of *Pteronotus macleayi grisea* (i), and the corresponding digitally dissected internal void (ii).

Estimating basilar membrane length

STL files were imported into MeshLab v1.2.2 (MeshLab Visual Computing Lab – ISTI – CNR) and converted into Stanford polygon file format (.ply). The .ply files were imported into individual projects of Landmark v3.6 (Wiley 2007). The 'single point' feature was used to place a series of landmarks along the length of the depression between the scala media and the scala tympani, corresponding to the outer edge of the basilar membrane (Fig. 4.6a). These points estimated the approximate position of the basilar membrane, as soft tissues were not preserved in the majority of the specimens, and furthermore CT scanning is not a suitable method to image these structures. In total, a series of 86 approximately equidistantly placed landmarks were positioned along the length of the spiral turns, beginning at the base of the basilar membrane just below the round window (where the depression between the two scala is first visible), and ending at the apex of the cochlea (Fig. 4.6b and c). This number of landmarks more than adequately describes the path of the membrane and represents a compromise between efficiency and accuracy. The 3D coordinates were exported into Microsoft Excel, where the total Euclidean distance was calculated by summing the distance between each set of consecutive points. Where the distance (x) between points (p_1, p_2, p_3) and (q_1, q_2, q_3) is calculated using the formula:

$$x = \sqrt{(p_1 - q_1)^2 + (p_2 - q_2)^2 + (p_3 - q_3)^2}$$

This method should produce reliable results, but may overestimate lengths as values are taken from the outer edge, however, this is consistent with estimates calculated by previous studies (e.g. Meng and Fox 1995). As straight lines between points represent the minimum distances, the estimates of basilar membrane length could be affected if too few points are used. However, as suggested by Fig. 4.7, there is little deviation between the straight line and curved line representations of the 86 points. This method is less applicable in particular species, for example, in horseshoe bats the inflation of the basal turn makes the path of the basilar membrane difficult to follow, and this could lead to considerable over- or underestimation at different points along the cochlea. Due to damage in a small number of specimens it was only possible to estimate basilar membrane length from 65, out of the maximum 68, specimens (Table C1). These measurements were then combined with those from previous studies (Table C2). Log_{10} basilar membrane lengths were calculated and plotted against log body mass$^{0.33}$. Phylogenetic correction was undertaken to investigate the effects of log body mass$^{0.33}$ after controlling for shared ancestry (for details see the section below).

Figure 4.6 Representations of the path of the basilar membrane (dashed line) measured for this study. Arrows correspond to start and end points.

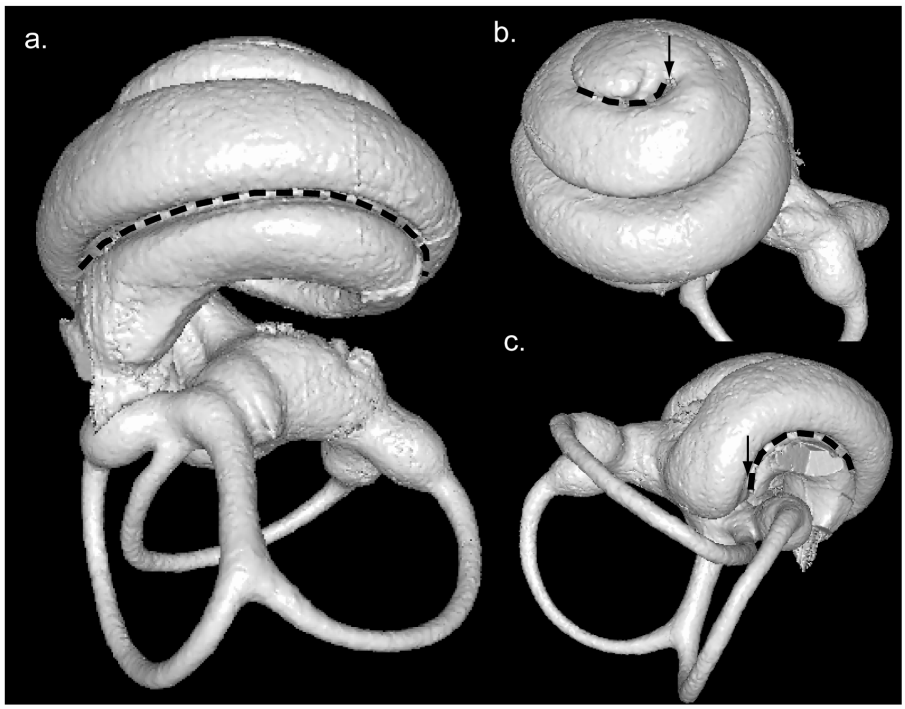

Figure 4.7 Deviation in estimated basilar membrane lengths. The 86 landmarks collected are represented by circles; curved black line represents the curved path between points; thin dotted lines represent the length of straight lines between points used to estimate basilar membrane length; white points represent half the number of points, and the dashed line the straight line distance between them. The difference between the total lengths estimated for 86 or 42 points is 0.170 mm, which suggests that this method is fairly robust.

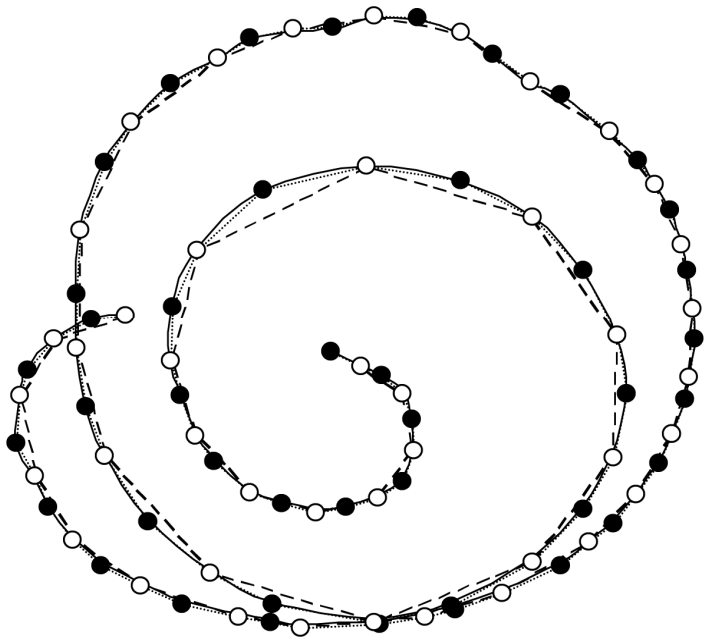

Recording the number of spiral turns

The number of cochlear turns was measured in each bat species, following the methods of West (1985). The cochlea is viewed apically and a line drawn from the point of the round window, where the cochlear duct initially begins to curl, to the apex. The number of times the line is crossed by the path of the duct is then recorded. This allows measurements to be taken to the nearest one quarter of a complete turn, and therefore, values are not continuous. It was possible to measure the number of turns from 67 specimens from this study, values were then supplemented with those from literature sources (Table C1 and 3), including additional bat species and also non-bat mammals (West 1985; Ketten *et al.,* 1992; Ketten 1994; Vater and Siefer 1995; Altringham 1996; Manoussaki *et al.,* 2008).

Auditory thresholds, inner ear morphology and ecology

Principal component analysis (PCA) was used to explore the relationship between species ecology, auditory thresholds and morphology. Hearing parameters (i.e. min., max. and optimum frequency audible) were collated for 56 mammalian species (Fig. C1), with values typically taken from behavioural audiograms, and where possible, the maximum and minimum threshold frequencies calculated at 60 dB SPL were used. Three morphological parameters, basilar membrane length, number of cochlea turns and log body mass were used. Separate PCA were preformed on the three hearing and three morphological variables then axes summarising the explanatory variable were plotted against one another. PCAs were performed in PASTv.2.09 (Hammer *et al.,* 2001), with a covariation matrix for hearing parameters, and correlation for morphological parameters. Species ecologies were broadly classified as volant, terrestrial and aquatic.

To explore interactions between bat auditory systems and echolocation performance, a comparative ecomorphological dataset was collected. In addition, to the morphological values described above, several call parameters were collated. Due to different call types, for example constant-frequency (CF) and frequency-modulated (FM) sweeps, it is difficult to meaningfully parameterise all calls with a comparable method. For this reason several categories were used, which include: type of call, mean frequency at maximum intensity, minimum frequency, maximum frequency and oral-nasal emitter. Echolocation call parameters were collected from as many sources as possible. If two values were available averages were calculated, if more than two were available extreme values were removed prior to averages being calculated. Further to the

echolocation call information, body mass, forearm length (FA) and dietary preferences were also collected. Auditory thresholds, i.e. optimum, maximum and minimum frequencies, were taken from literature sources for as many bats and other mammals as possible.

Old and New World constant-frequency bats

Two families of Old World bats are typified by CF calls: Rhinolophidae and Hipposideridae, and also the single species of the New World family Mormoopidae, *Pteronotus parnellii*. It is theoretically predicted that there is a strong relationship between basilar membrane length and call frequency. In addition to this, body size, as measured by forearm length and body mass, should be related with basilar membrane length and call frequency. This was examined using echolocation and morphological values for a total of 46 Rhinolophidae, 6 Hipposideridae and *P. parnellii*. Three specimens represented that documented size morphs of *R. philippinensis* (Small morph: location = Buton, male, FA = 47.4mm, wt = 6.5g; Large morph, location = Buton, male, FA = 55.3mm, wt = 12.0g; Intermediate morph, location = Kabaena, female, FA = 48.4mm, wt = 7.0g). In particular the position of these three individuals will be studied in relation to the others, to identify deviations in either physical features or call-frequency that may be related to harmonic hopping that has been reported in this species (Kingston and Rossiter 2004). All echolocation and morphological variables were logged transformed to equalise variances and normalise data.

Echolocation calls and inner ear morphology

The above analysis was repeated for 63 bat species for which echolocation variables were available (minimum, maximum and peak energy frequency), these values were analysed with multiple regression analysis including body mass, basilar membrane length and the number of cochlear turns included as a factor.

Phylogenetic correction

Closely related taxa might be expected to be phenotypically more similar than chance, therefore, to control for shared ancestry of characters, and thus ensure independence of data-points, phylogenetic correction is necessary. A number of methods have been previously developed for this (for examples see Garland *et al.,* 2005). The majority of methods are suitable for instances when the characters of interest follow a simple linear

relationship, typically modelled with least squares regression (through the origin). For this current study, to determine if after correcting for the phylogenetic relationships, the differences in bat cochleae and body mass were maintained, Bayesian phylogenetic mixed models (BPMMs) were used in 'MCMCglmm' (Hadfield 2010) in R v.2.11.1 (http://www.r-project.org). This phylogenetic correction is based on an 'animal model' approach. The animal model is a linear mixed effects model – a type of model that contains both fixed and random effects – in which the genetic merit of an individual is treated as a random effect to be estimated. Within the model, an individual's 'genetic merit' is included as an explanatory variable for the phenotypic trait of interest. This value is the additive effect of an individual's genotype on the trait expressed relative to the population mean phenotype. A simple example of the single trait (y) in individual (i) has been given as follows (Wilson *et al.,* 2009):

$y_i = \mu + a_i + e_i$

In this case μ is the population mean, a_i are the effects of i's genotype relative to μ, and e_i is a residual term.

Although, typically this method has previously been used to estimate heritability of traits within populations (for example in sheep, Reale *et al.,* 1999; Wilson *et al.,* 2006). More recently it has also increasingly been used across species (Cornwallis *et al.,* 2010; Horvathova *et al.,* 2011; Longdon *et al.,* 2011). The advantage of using this method is that it allows sophisticated models to be fitted, that not only allow genetic parameters to be estimated but also known, or hypothesised, non-genetic factor's influence on the phenotype under study (Hadfield 2010). This method also supports a range of distributions and variance structure for the random effects, for example interactions with categorical or continuous variables (Hadfield 2010). Practically, this method is robust to small amounts of missing data, and has been developed to reduce the computing time that is necessary to adequately sample the posterior distribution.

Molecular clocks and fossil calibration points

In order to perform a phylogenetic correction, a calibrated species phylogeny must be obtained i.e. with branch lengths in a unit that corresponds to species divergence. In this study the phylogeny was topologically constrained based on the findings of previous large scale molecular datasets. Branch lengths were calculated using fossil calibration points of key nodes combined with sequence divergence of a molecular marker, in this case the mitochondrial gene *Cytochrome b*; this is essentially a 'molecular clock'

approach (Zuckerkandl and Pauling 1962). The utility of *Cytochrome b* as a marker for estimating divergence times along a broad scale of taxonomic resolution has been previously demonstrated by a wide range of studies (for examples see Martin *et al.,* 2000; Farias *et al.,* 2001). More recently, an analysis of over 200 mammal species suggests that *Cytochrome b* can accurately reconstruct relationships at Superorder, Order, Family and also genus levels (Tobe *et al.,* 2010). However, one potential drawback is that *Cytochrome b* has been shown to be under positive selection in bats (Shen et al 2010), and this may affect divergence times estimates.

The use of fossil calibration points have received some criticism, (e.g. Bininda-Emonds *et al.,* 2007 and references within). One of the most frequently cited is the relative incompleteness of the fossil record; on average the bat fossil record is estimated to be 88% incomplete (Eiting and Gunnell 2009). Also, a species presence in the fossil record proves its existence from that particular time-point onwards; as absence does not prove absence of the species in evolutionary history. Therefore, the utility of the fossil record is limited to inferring the 'latest' first presence. Accurate dating from the fossil record also depends heavily on correct species assignment, which can often based on a single tooth or bone fragment, or involves 'matching up' extinct taxa with modern extant taxa.

Constructing the phylogeny and estimating branch lengths

Cytochrome b sequences were obtained for as many species as possible; preference was given to complete sequences. In a limited number of cases, congeneric substitutes were used if actual species were not available. In the cases of multiple haplotypes, a representative sequence was chosen at random. The majority of sequences were obtained from GenBank, therefore, all species identifications are assumed to be correct. Nucleotide sequences were aligned using ClustalW2 (Larkin *et al.,* 2007) and checked by eye. The alignment was imported into BEAUti v. 1.5.4 (Drummond and Rambaut 2007), this utility was used to produce the correctly formatted input file (xml-file) for BEAST v.1.5.4 The topology was constrained by enforcing monophyly of major clades, together with a total of 16 fossil calibration points collected from literature sources (Table C4). It was attempted to have a wide range of calibration points that were distributed across the tree. Despite recent molecular taxonomic advances, the exact placement of Chiroptera within Laurasiatheria remains unclear. Previously, bats were placed as sister group to Cetartiodactyla, Carnivora and Perissodactyla (for review see Springer *et al.,* 2004), however, more recently Chiroptera were placed in a clade with

Carnivora and Perissodactyla (Nishihara *et al.,* 2006; Murphy *et al.,* 2007). Therefore, two phylogenies were constructed, each with one of these topological constraints (Fig.4.8). Analyses were run in BEAST v.1.5.4 using an uncorrelated log-normal relaxed molecular clock (Drummond *et al.,* 2006), a Yule speciation prior and a GTR+I+Γ model, for 10,000,000 generations, with every 1000 parameters logged. Calibration points were set with a normal prior distribution with ± 0.5 standard deviation. Tracer v.1.5 was used to check for appropriate burn-in length and run convergence. The maximum clade credibility tree was produced using TreeAnnotator v.1.5.4, with a sample burn-in of 200 and node heights set to mean-heights.

Figure 4.8 The two phylogenetic trees constructed.
Tree A. Bats as the sister group to Cetartiodactyla, Carnivora and Perissodactyla (for review see Springer *et al.,* 2004).

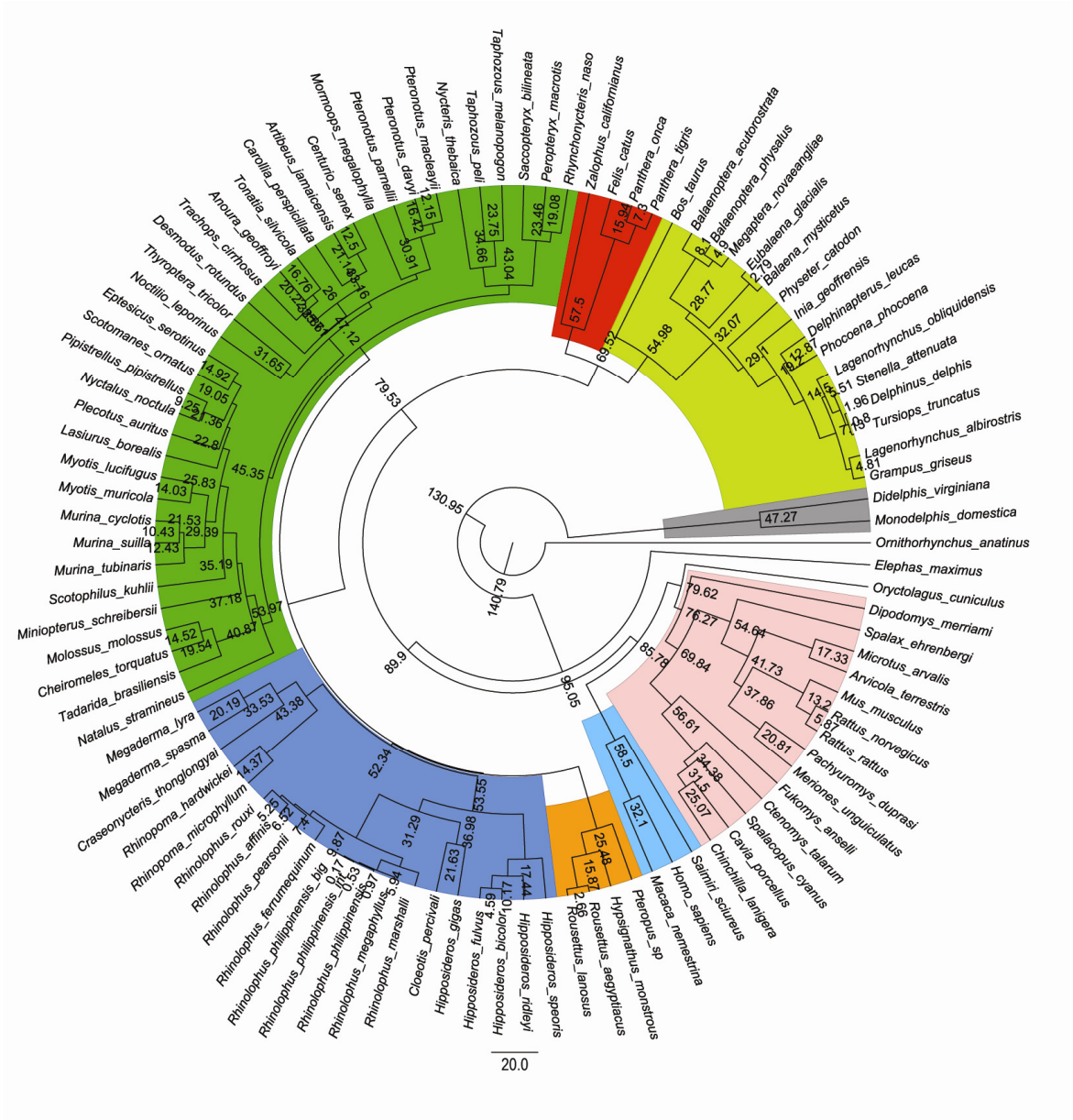

Tree B follows the more recent placement of bats in a clade with Carnivora and Perissodactyla (Nishihara *et al.,* 2006; Murphy *et al.,* 2007).

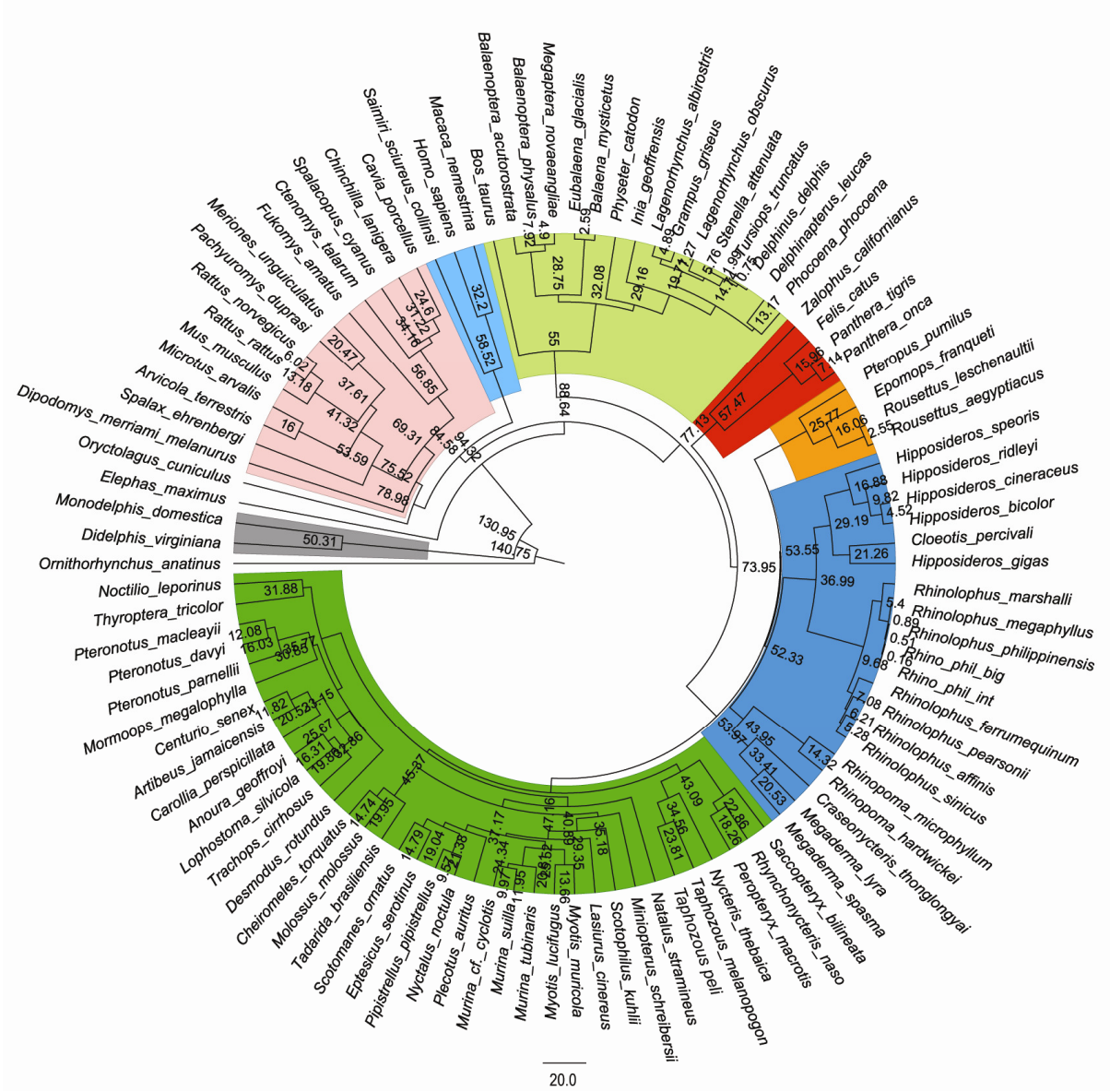

MCMCglmm

For each relationship a corresponding character matrix was constructed that was taxonomically consistent with the above phylogenies. The character matrices consisted of log basilar membrane, log spiral number, log body mass$^{0.33}$, and log hearing and echolocation call frequencies and clade variables.

Defining and testing effect of priors

Although it may be desirable to avoid using priors, thus maximizing the information from the data, default settings in MCMCglmm use improper priors which are known to cause numerical problems (Wilson *et al.,* 2009). Therefore, in all analyses proper priors

were specified. To determine what effect, if any, different priors had on the results, model variants were tested and the run results compared. Firstly, with a low degree of belief (n=1), observed phenotypic variation, e.g. log basilar membrane length was divided equally between the phylogenetic and residuals effect, and then a greater proportion (i.e. 95%) was attributed to the phylogenetic effect (Table C5). Secondly, observed phenotypic variation was divided equally between phylogenetic and residual effects, but with respective degrees of belief of n=1 and n=10. In large informative datasets the prior should have little impact on parameter estimates, but it is still necessary to compare results from different runs to ensure the analysis is robust to prior specification (Wilson *et al.,* 2009). Since initial tests of priors suggested that estimated parameters were approximately equal, it was decided to use a prior with n=1, with phenotypic variance divided equally for all runs.

Running analysis

All analyses were run with the same basic settings: animal as a random effect and pedigree information from the dated phylogeny, with proper priors with a low degree of belief and phenotypic trait variance divided equally between genetic and residual effects. All models were run with 150,000 iterations, with 15,000 burn in and a thinning interval of 50.

Multivariate shape analysis of bat cochlea

The mammalian cochlea is a highly complex 3D structure that contains far more structural variation than can be studied using 2D methods alone. However, how to best study a 3D coiled structure, such as the cochlea, remains uncertain. Surprisingly this shape is not an isolated case, and similar problems have been explored in palaeontology (Raup 1961; Ward 1980; Johnston *et al.,* 1991) and also mathematics (Illert and Pickover 1992; Lucca 2003). Although in some cases these methods are applicable for describing irregular oscillations of the spiral (Illert and Pickover 1992; Lucca 2003), they are generally only suitable for describing structures with a consistent whorl cross-section. Furthermore, these methods are only useful for describing physical, and not functional, features. Mammalian cochleae have previously been characterised as ratios, corresponding to change of radii along each turn, and this is significant correlated with hearing range (Manoussaki *et al.,* 2008).

Collecting three dimensional surface information

The extracted inner ear volumes represent complex solid objects from which it is difficult to determine biologically homologous points for species comparisons. Therefore, the following analyses of the basilar membrane spiral path used semi-landmarks; which are a series of coordinates used to represent a curve (Bookstein 1997). The morphological variation was then analysed with Eigenshape Analysis (ESA) (Lohmann 1983), utilising a program written by Prof. Norman MacLeod, NHM. The three principal analytical stages are: 1 Sample interpolation, 2 Procrustes (GLS) alignment and 3 Principal Component Analysis (PCA).

Homologous reference points are necessary so that structures can be maximally aligned; the most basal part of the spiral turn was chosen for this (see Fig.4.6c). From this point, 85 additional 3D landmarks were collected, which were equivalent to those used to estimate basilar membrane length in the previous section. Sampled points were then converted into 100 equally spaced points along the cochlea outline. Step lengths were equal between the first 99 points and the final step length was slightly longer; this minimises error across all points, but leads to slightly artificial coordinates for the final point. Procrustes alignment was then carried out; this method typically involves three steps, alignment of position, size and orientation of shapes. Following alignment, visual inspection of the superimposed dataset was carried out and the sample mean shape was calculated (Fig. 4.9). Finally, a PCA of the superimposed 3D coordinates was performed using a covariance matrix to express inter-variable relationships. Canonical Variates Analysis (CVA) was performed on PC axes accounting for 95% of sample variance in order to view maximum separation between groups.

Figure 4.9 Plots of cochlear (x,y) landmarks; sample mean-shape (left), and superimposed landmarks for the entire sample (right).

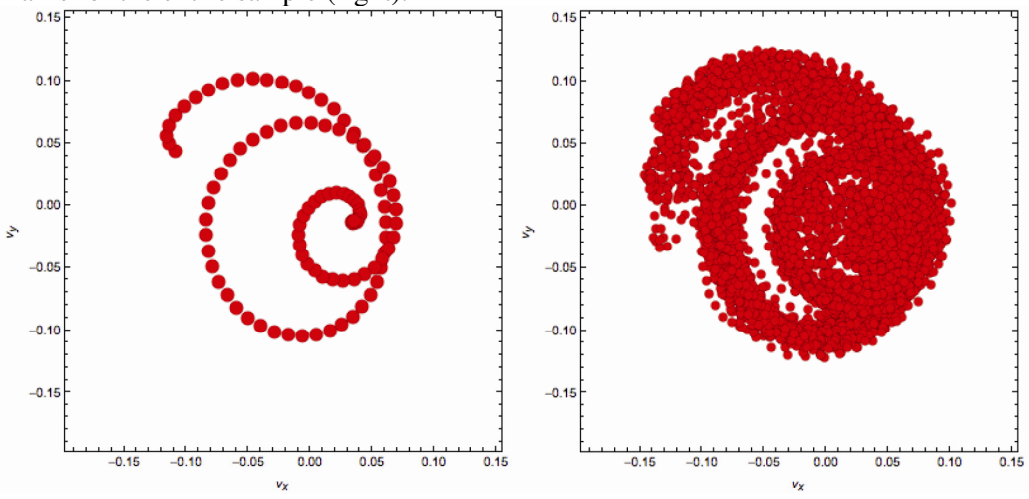

RESULTS

In total, 76 inner ears were extracted from 68 specimens representing 56 bat species. Following reconstruction, some inner ears were found to be damaged and, therefore, it was not possible to record all measurements from all specimens. Initial inspection of the gross morphology revealed high levels of morphological variation. Within certain families (e.g. Rhinolophidae, Pteropodidae) inter-specific variation was low, whereas, within other families (e.g. Hipposideridae, and Mormoopidae) it was higher, apparently as a consequence of species-specific echolocation call types (Fig. 4.10).

Basilar membrane length

Basilar membrane lengths were estimated directly from the surface of 65 'extracted' inner ear volumes using the distance between the series of three dimensional points that traced its path. A comparison of species values measured by this study and those from previous studies revealed similar values (Table C2), however, values estimated by this study were typically larger, this might suggest systematic bias in the method, but could also be due to genuine individual variation. To distinguish between these possibilities it would be necessary to directly compare measurements from the same specimen using both CT scans and serial sections.

Regression analysis of log basilar membrane length (mm) versus log body mass$^{0.33}$, for all available non-echolocating mammals (i.e. with baleen whales and Old World fruit bats omitted) resulted in the following OLS regression: log basilar membrane = 0.53 log body mass$^{0.33}$ + 0.66, (n = 27, R^2 = 0.80, F = 100.32 , P = 3.19 x 10 $^{-10}$). When restricted to placental mammals alone results were similar: OLS regression: log basilar membrane = 0.50 log body mass$^{0.33}$ + 0.72, (n = 24, R^2 = 0.90, F = 193.16, P = 2.26 x 10 $^{-12}$). Prediction Intervals (PI) were calculated based on the placental mammal sub-sample. The progression of basilar membrane length from monotremes to marsupials to placental mammals was evident. The single extant platypus species, *Ornithorhynchus anatinus,* represents the most primitive mammalian state, and as such has the shortest basilar membrane; the two marsupial species have longer basilar membranes and the remaining placental mammals longer still.

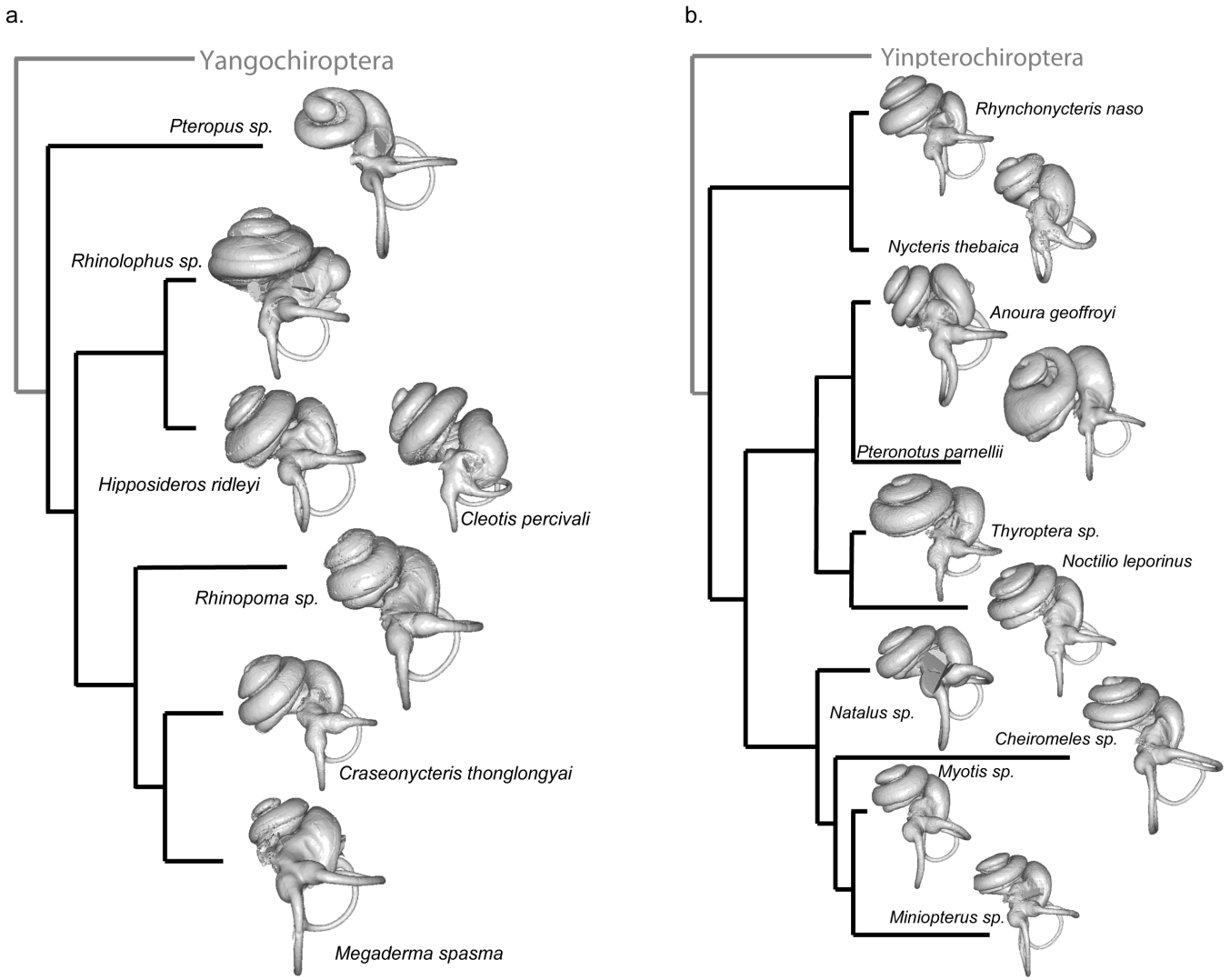

Figure 4.10 Phylogenetic relationships between (a) Yinpterochiroptera and (b) Yangochiroptera, with representative inner ear volumes for each family studied.

The majority of laryngeal echolocating bats were seen to fall above the placental mammal regression line and within the 95% PI (Fig. 4.11). Of the remaining species that fell outside and above the 95% PI, nearly all were the Old World CF bats, with the exceptions of *Taphozous peli* and *Cheiromeles torquatus.* A single laryngeal echolocating bat fell below the regression line, *Macroderma gigas,* however, none fell below the 95% PI. Therefore, the majority of echolocating bats have longer basilar membranes, given their body mass, compared to non-echolocating mammals. In contrast, non-echolocating Old World fruit bats fell very close to the placental mammal regression line, suggesting similarly proportioned basilar membranes to other non-echolocating mammals. In contrast, all cetacean species, whether toothed or baleen, fell below the regression line but within the PI. Only two non-echolocating mammals fell outside the PIs; the platypus, *O. anatinus,* which fell below and the Californian sea lion, *Zalophus californianus*, which fell above.

It was then tested to see if echolocating bats had significantly longer basilar membranes, compared to non-echolocating taxa after correcting for phylogenetic relatedness. Baleen and toothed cetaceans were omitted due to their specialised low- and high-frequency hearing respectively, and also due to their much larger body mass. Across the remaining taxa there was no evidence to suggest differential scaling (see Table 4.1 and C6). Laryngeal echolocation was a significant factor when added to the regression of basilar membrane versus body mass, however, there was only small improvement in model fit (ΔDIC = 0.492 and 1.087, depending on the tree used). The addition of CF echolocation also did not improve model fit, either when added in combination with laryngeal echolocation, or alone. The significance of these factors were determined by comparisons of DIC values of models, with these echolocation abilities coded as factors, typically a significant improvement in DIC value is taken as an difference equal to 2 or more.

Table 4.1 Difference in DIC value between models of basilar membrane length versus body mass including echolocation as a factor, and correcting for phylogenetic relatedness.

Model comparison		ΔDIC ($DIC_0 - DIC_1$) Tree A	Tree B
1 vs. 2	Different size categories	-0.346	-0.497
1 vs. 3	Laryngeal echolocation	1.087	0.492
1 vs. 4	Laryngeal echolocation + CF	0.311	-0.634
1 vs. 5	CF bats	-0.081	-0.877

Figure 4.11 Log body mass$^{0.33}$ vs. log basilar membrane length for a range of echolocating and non-echolocating mammals. Species are categorised by echolocation ability and sub-order; laryngeal echolocating bats are represented by dark blue circles; CF bats by green circles; Old World fruit bats by orange circles; echolocating toothed whales by blue diamonds; non-echolocating baleen whales by black diamonds; the remaining non-echolocating placental mammals by grey triangles, marsupials by black triangles and the platypus by the asterisk.

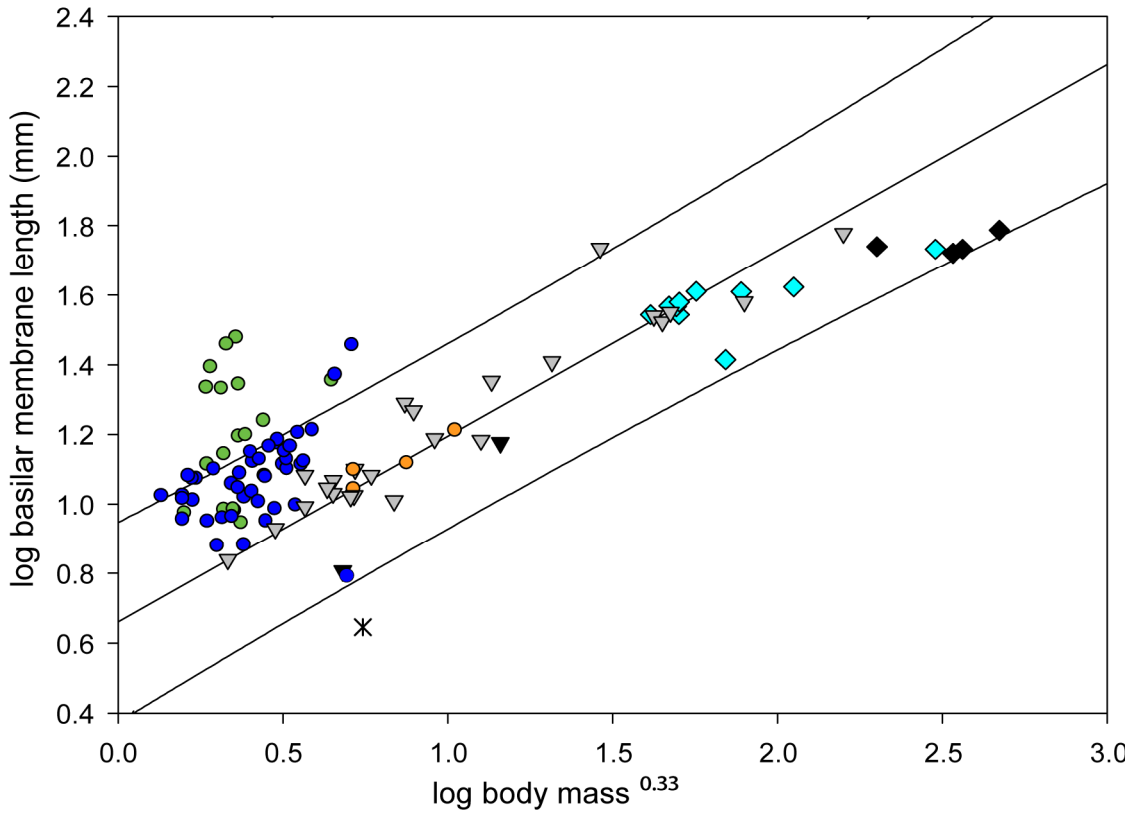

Number of spiral turns

The measured numbers of cochlear turns were combined with published values, to give a total of 109 placental mammal values, representing a range of 'typical' and specialist hearing systems. Typically, turn number was measured to the nearest one quarter turn, however, some values were more precise and so approximate a continuous distribution and, therefore, sample averages were calculated and compared using pair-wise *t*-tests. Spiral number was highly variable across mammals, as well as between bat families (Fig. 4.12). Echolocating bats had the highest mean number of turns, which was significantly higher than Old World fruit bats ($p<0.0001$), but not non-echolocating placental mammals ($p>0.5$, after correcting for multiple tests Table 4.2b). This is likely due to the inclusion of the guinea pig in the latter sample. Old World fruit bats had significantly lower numbers of turns compared to non-echolocating placental mammals ($p<0.001$) and also baleen whales ($p<0.05$).

Figure 4.12 Average spiral number, ± SD for groups of mammals: 1 Pteropodidae (n=6); 2 Rhinolophidae (n=7); 3 Hipposideridae (n=6); 4 Rhinopomatidae (n=2); 5 Megadermatidae (n=4); 6 Craseonycteridae (n=1); 7 Vespertilionidae and Miniopteridae (n=12); 8 Mormoopidae (n=5); 9 Phyllostomidae (n=20); 10 Molossidae (n=6); 11 Nycteridae (n=1); 12 Natalidae (n=2); 13 Emballonuridae (n=5); 14 Thyropteridae and Noctilionidae (n =2); 15 Primates (n=3); 16 Carnivores (n=5); 17 Equidae and Bovidae (n=3); 18 Glires (n=7); 19 Elephant (n=1); 20 Manatee (n=1); 21 Toothed whales (n=7); 22 Baleen whales (n=3).

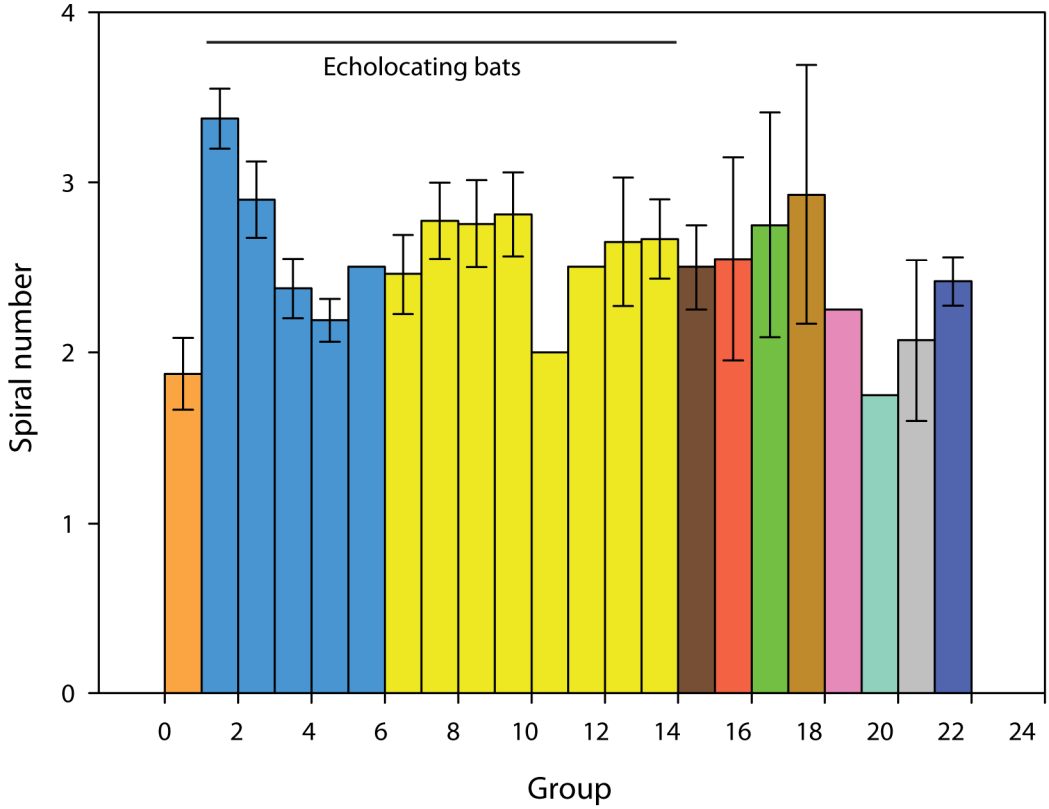

Table 4.2 a) Estimated mean spiral number for echolocating and non-echolocating taxa.

Group	n	Mean ± SD	Max.	Min.
Echolocating bat	73	2.72 ± 0.4	3.75	2.0
Old World fruit bat	6	1.88 ± 0.2	2.25	1.75
Baleen whales	3	2.42 ± 0.1	2.25	2.25
Toothed whales	7	2.07 ± 0.5	2.5	1.5
Non-echolocating placental mammals	20	2.65 ± 0.6	4.25	1.75

b) *P*-values for pair-wise comparisons using *t*-tests with non-pooled SD. Uncorrected *P*-values are shown below the diagonal. *P*-values with Bonferroni correction are shown in bold-font and *P*-values with Holm correction are shown in italic-font, both above the diagonal.

	Echo. bats	Fruit Bats	Baleen whale	Toothed whale	Placental mammals
Echolocating bats	-	**$2.3x10^{-4}$** *$2.3x10^{-4}$*	**0.439** *0.219*	**0.103** *0.072*	**1.000** *0.697*
Old World Fruit bats	$2.3x10^{-5}$	-	**0.042** *0.034*	**1.000** *0.697*	**0.001** *0.001*
Baleen whale	0.044	0.004	-	**1.000** *0.476*	**1.000** *0.521*
Toothed whale	0.010	0.348	0.119	-	**0.233** *0.141*
Placental mammals	0.647	$9.3x10^{-5}$	0.173	0.023	-

Cochlear turns, basilar membrane length and body mass

Spiral number, basilar membrane length (mm) and body mass (g) were collected for 95 mammalian species. For visualisation purposes, taxa are grouped by number of cochlear turns, and additionally, echolocating bat species are distinguished (Fig. 4.13). Model comparisons based on AIC scores of multiple regression analyses, suggest that adding either factor, i.e. number of spiral turns or laryngeal echolocation, resulted in improved model-fit in the relationship between basilar membrane length and body mass (Table 4.3 and C7). Step-wise multiple regression suggested that in addition to these single factors, there was also a significant interaction between the two factors (i.e. number of turns and laryngeal echolocation) and that adding this term resulted in a highly improved model (AIC = -161.088). However, after phylogenetic correction (Table 4.3b and C7), neither laryngeal echolocation nor number of turns had a significant effect.

Figure 4.13 Plot of log basilar membrane length versus log body mass$^{0.33}$. Bat species (circles) and non-bat mammals (diamonds) are grouped by number of cochlear half turns (colours).

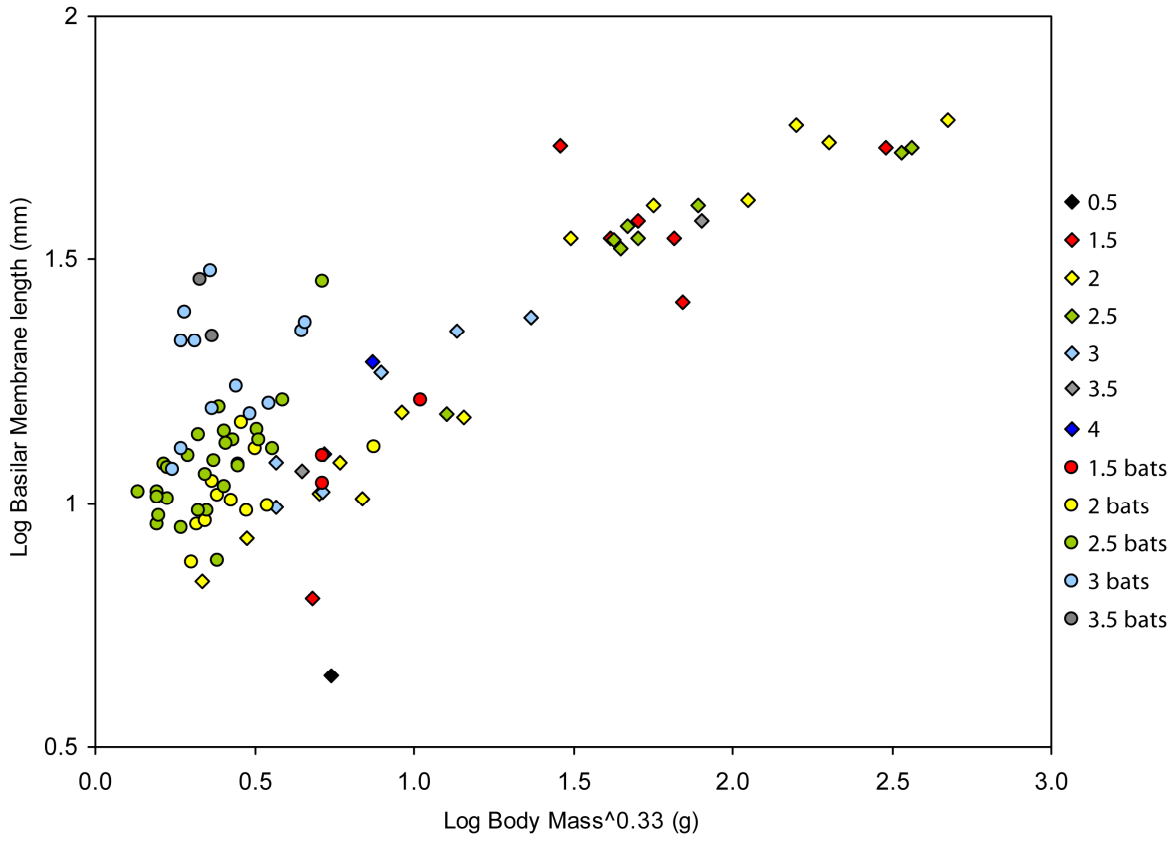

Table 4.3 Multiple regression model comparison: basilar membrane length vs. body mass
a) AIC values for OLS multiple regression analysis.

Model comparison	Effect	ΔAIC
1 vs. 2	Number of turns	27.887
1 vs. 3	Laryngeal echolocation	22.291
1 vs. 4	Number of turns and laryngeal echolocation	53.85

b) DIC values, for phylogenetic correction.

Model comparison	Effect	Tree A ΔDIC	Tree B ΔDIC
1 vs. 2	Number of turns	-0.904	-1.563
1 vs. 3	Laryngeal echolocation	0.564	0.048
1 vs. 4	Number of turns and laryngeal echolocation	-1.479	-2.158

Cochlear morphology, hearing and ecology

Principal components analysis of species' auditory thresholds and morphology revealed several patterns. The three hearing parameters were summarized by PC1, which accounted for 91.8% of the sample variance, and as expected, high loadings confirmed that maximum and optimum hearing parameters had the greatest influence on this axis (Table 4.4a). The PCA of the morphological variables, using a covariance matrix, resulted in PC1 and PC2 that explained 66.2 and 31.3% of the total variance, respectively. High loadings of PC1-Morphology suggest that variation in basilar membrane mainly account for the variation along this axis. The number of cochlear turns had the highest positive loading of PC2-Morphology, and body mass had the most negative loading (Table 4.4b). Using plots of PC1-Hearing vs. PC1-Morphology and PC2-Morphology it was possible to broadly recover three ecological categories; namely 'volant', 'terrestrial', and 'aquatic' groups (Fig. 4.14).

The distribution of species, in the plot of PC1-Hearing vs. PC1-Morphology, suggest that points for Old World fruit bats overlap with the distribution of terrestrial mammals in terms of hearing parameters and basilar membrane length. Conversely, despite a small overlap between some echolocating bat species and terrestrial mammals, the majority of echolocating bats have comparable basilar membrane length, to the terrestrial and subterranean species, but much higher optimum and maximum hearing parameters.

Table 4.4 PCA Eigenvalues, variance and loadings for (a) Hearing and (b) Morphology

A				Loadings	
	Eigenvalue	% variance	Min.	Min.	Opt.
PC1	2743	91.8	0.05	0.90	0.43
PC2	231	7.7	0.06	-0.43	0.90
PC3	15	0.5	1.00	-0.02	-0.08

B				Loadings	
	Eigenvalue	% variance	N° turns	Membrane	Body mass
PC1	1.99	66.2	-0.25	0.96	0.09
PC2	0.94	31.3	0.68	0.24	-0.70
PC3	0.07	2.4	0.69	0.11	0.71

Figure 4.14 PCA of mammalian auditory thresholds, ecotype and inner ear morphology

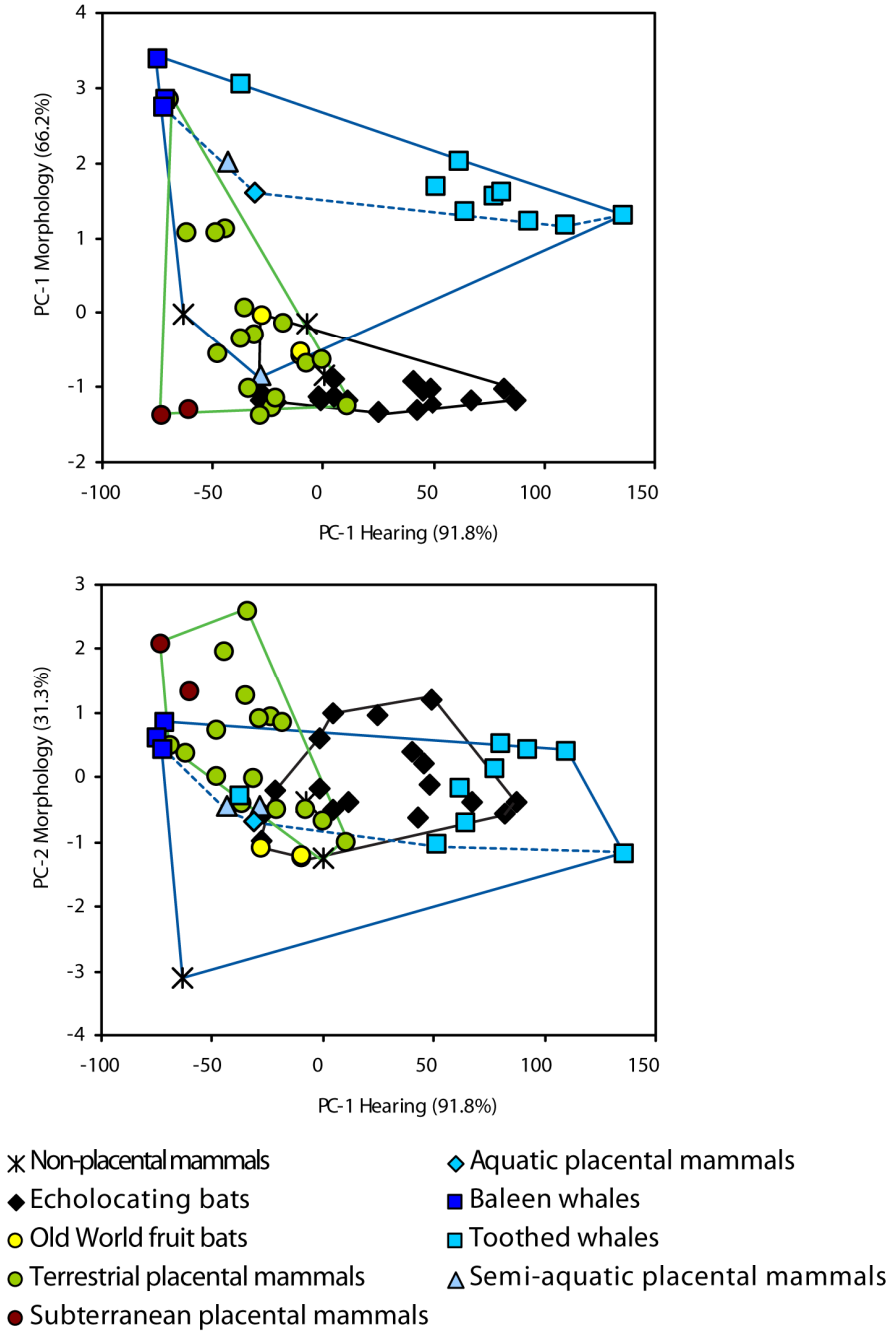

Within Cetacean species, there is a clear division between baleen and toothed whales. There also appears to be a pattern between hearing and basilar membrane length; with toothed whales having shorter basilar membranes and higher hearing parameters. A similar pattern is seen within bats, with echolocating bats having shorter basilar membrane lengths and higher hearing parameters compared to Old World fruit bats. The plot PC1-Morphology and PC2-Morphology suggests there may be some relationship between the number of cochlea turns, body mass and hearing range within certain groups e.g. bats. However, within other groups such as cetaceans there does not seem to be a relationship.

Most species broadly fit their ecological assignments. Notable exceptions are the Indian elephant, *Elephas maximus,* and the European water vole *Arvicola terrestris.* The sperm whale, *Physeter catodon,* lay closer to the baleen whales than the toothed whales, based on hearing and morphological parameters. Within bats, non-echolocating Old World fruit bats were found at the extremes of the laryngeal echolocating bats. Rodents and the short-tailed opossum, *Monodelphis domestica,* were distributed closer to the laryngeal echolocating bats than were the Old World fruit bats. The two included subterranean mammals appear to be separated from terrestrial placental mammals. This analysis attempted to explore general relationships between hearing parameters and morphological features of the inner ear across a broad taxonomic sample of species with different ecologies. Results suggest that different patterns may be present in each taxonomic group, therefore, this analysis would benefit from increased sampling and also correcting for phylogenetic relatedness of the sample.

Constant-frequency bats

To relate inner ear morphology and constant frequency (CF) echolocation calls, data from Rhinolophidae, Hipposideridae and *P. parnellii* were used. For all species, basilar membrane length was strongly negatively correlated with echolocation call frequency (log CF = -1.08 log basilar membrane + 3.18, R^2 = 0.67, F = 28.82, P < 0.0001). Therefore, echolocating bats with higher CF calls had shorter basilar membrane lengths (Fig. 4.15a). Overall species trends suggest a negative association between body size (either body mass or forearm) and echolocation call frequency, with *Rhinolophus* spp consistently showing lower calls, than *Hipposideros* spp, of similar body mass (Fig. 4.15b).

Figure 4.15 Plots of echolocation call frequency and basilar membrane length versus body size (body mass and forearm) for CF echolocating bats. Hipposideridae (blue squares); Rhinolophidae (dark blue triangles) (circled points correspond to the three size morphs of *R. philippinensis*), and *P. parnellii* (yellow circle).
a) Log basilar membrane length vs. log echolocation frequency.

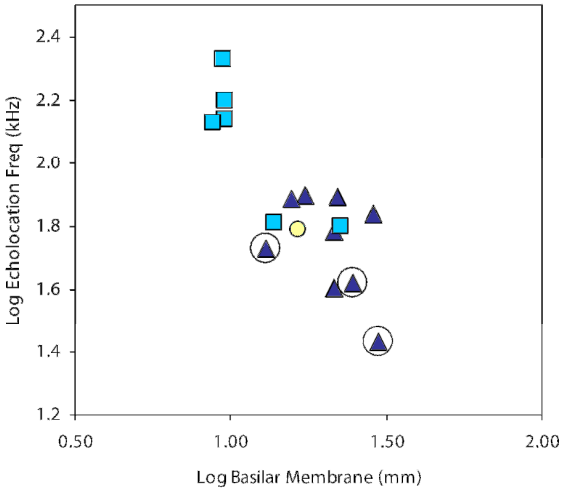

b) Log forearm and body mass vs. log echolocation frequency – top row; vs. log basilar membrane length – lower row.

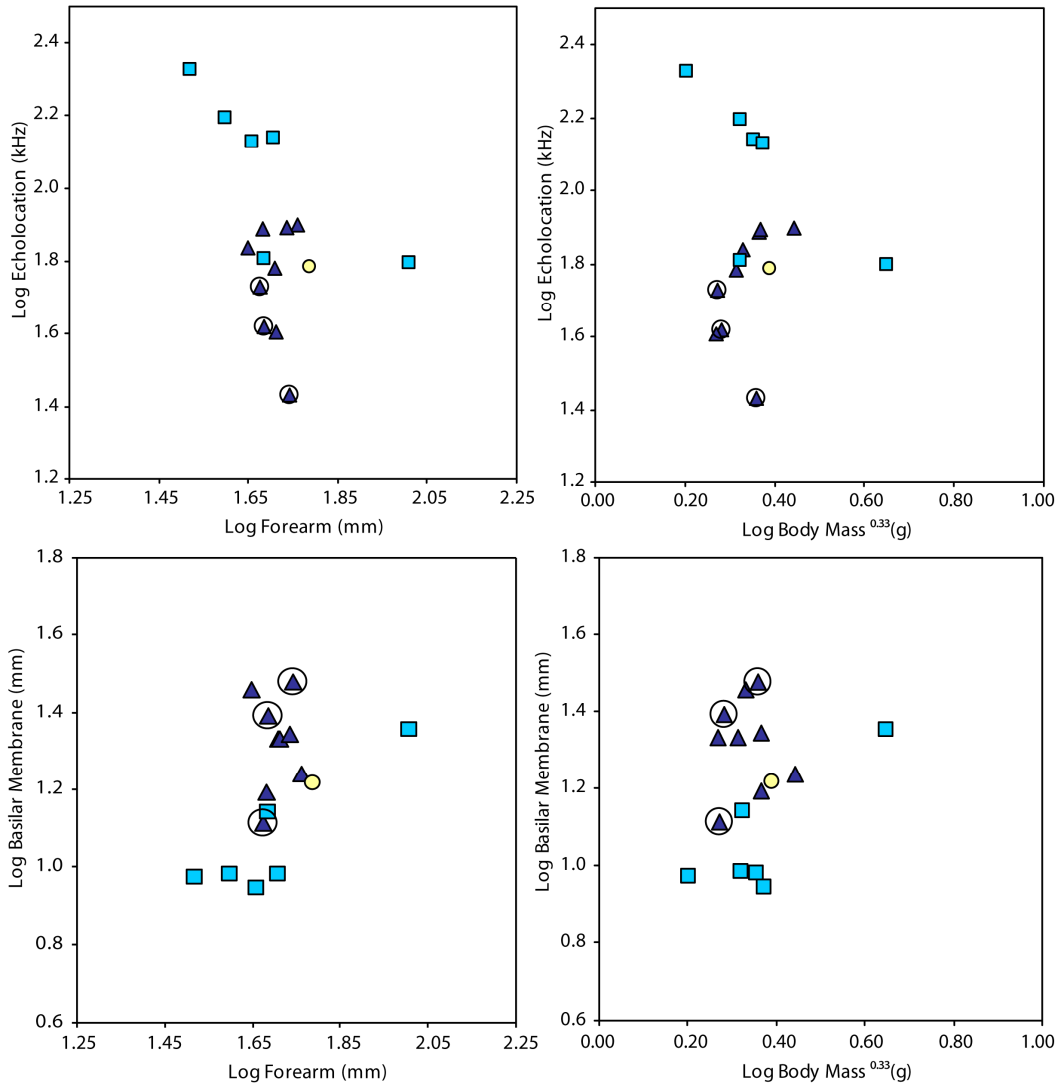

However, the overall trend was not significant, probably reflecting the small sample sizes (Forearm – $R^2 = 0.21$, $F = 3.67$, $P > 0.05$; Body mass - $R^2 = 0.01$, $F = 0.19$, $P > 0.05$). Therefore, at least for this subsample, neither body size measure accounted for much of the echolocation call frequency variance. Previous studies found strong positive relationships between basilar membrane length and body mass in mammals, however this was not detected in bats (Forearm – $R^2 = 0.22$, $F = 3.89$, $P > 0.05$; Body mass - $R^2 = 0.06$, $F = 0.83$, $P > 0.05$).

Rhinolophus philippinensis morphs

To assess whether putatively recently evolved size-morphs of *Rhinolophus philippinensis* fit the overall pattern for their genus, I calculated the average forearm length and echolocation call frequency for 46 *Rhinolophus spp*. from values obtained from literature sources. I found a significant negative relationship between call frequency and both forearm length (log CF = 1.76 log forearm + 4.81; $R^2 = 0.501$, F = 44.23, $P = 3.78 \times 10^{-8}$) and basilar membrane length (log CF = -0.974 log basilar membrane + 3.09; $R^2 = 0.682$, F = 23.63, $P < 0.0001$). Echolocation call frequencies for *R. philippinensis* small and medium morphs fell within the 95% PI for forearm length. The call frequencies of the medium and large morph fell within the 95% PI for basilar membrane length, though the small morph was on this line (Fig. 4.16). Both regressions suggest lower frequencies in the *R. philippinensis* morphs than expected for either their respective forearm or basilar membrane length.

Figure 4.16 Morphology vs. peak energy echolocation call for Rhinolophidae. Log forearm vs. echolocation frequency (left), and log basilar membrane vs. echolocation call (right). Values for *Rhinolophus spp*. taken mainly from literature sources are represented by black circles; the small, medium and large *R. philippinensis* morphs are represented by red, orange and yellow circles. OLS regression and 95% prediction intervals are shown based on black points only.

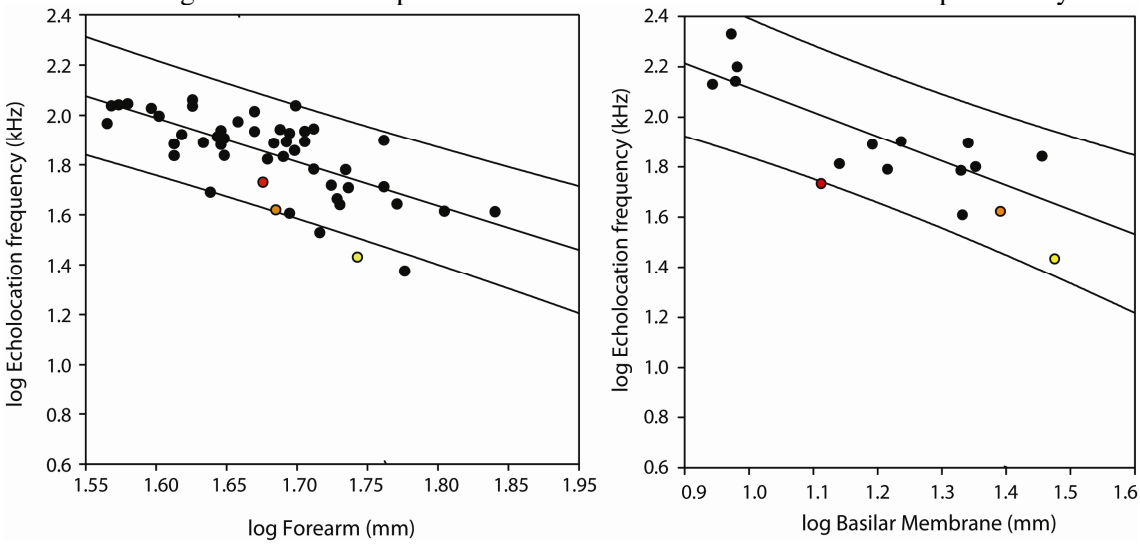

Echolocation call analysis

To assess whether call parameters relate to cochlea morphology and body mass across 63 echolocating bat species (including two *Rousettus spp.*), I undertook multiple regression analyses for published minimum, maximum and peak-energy frequency components. For each model, I fitted body mass and basilar membrane length, including number of turns as a factor. Step-wise multiple regression suggested that full models for all three call parameters were significant, (Min. $P = 2.85 \times 10^{-6}$, Max. $P = 5.00 \times 10^{-4}$, Peak $P = 4.37 \times 10^{-5}$) and resulted in the best AIC values (Table 4.5). There was a negative relationship between all three call parameters with body mass and basilar membrane length, and the effect of number of cochlear turns was highly significant for minimum call frequency. These results remained significant after correcting for phylogenetic relatedness (Table C9).

Table 4.5 Multiple regression analysis of minimum, maximum and peak-energy call parameters versus body mass, basilar membrane length and the number of cochlear turns.

a) Without correcting for phylogeny

	Min. frequency	Max. frequency	Peak frequency
AIC	-19.16	-25.46	-13.11
RSE	0.19 (56 DF)	0.19 (56 DF)	0.20 (56 DF)
Mult. R^2	0.46	0.34	0.40
Adj. R^2	0.41	0.27	0.34
F	8.03 (6, 56 DF)	4.84 (6, 56 DF)	6.27 (6, 56 DF)
Overall *P*	2.85×10^{-6}	5.00×10^{-4}	4.37×10^{-5}
Coefficients (*P*)			
Intercept	2.47 (6.49×10^{-13})	2.84 (6.04×10^{-16})	2.60 (5.33×10^{-13})
log body mass$^{0.33}$	-0.70 (0.0001)	-0.30 (0.11)	-0.64 (0.003)
log basilar memb.	-0.68 (0.01)	-0.80 (0.002)	-0.57 (0.04)
Number of turns	0.06 (0.52), 0.29 (0.01), 0.34 (0.01), 0.58 (0.02)	-0.11 (0.24), 0.09 (0.37), 0.09 (0.46), 0.28 (0.24)	-0.12 (0.24), 0.15 (0.18), 0.09 (0.50), 0.28 (0.29)

b) Model comparisons, correcting for phylogeny, of minimum, maximum and peak-energy call parameters versus body mass, basilar membrane length and the number of cochlear turns.

Comp.	Model	Peak	Min.	Max.
1 vs. 2	log body mass$^{0.33}$ vs. basilar membrane	-2.44	1.44	-4.26
1 vs. 3	log body mass$^{0.33}$ vs. log body mass$^{0.33}$ + basilar membrane	2.85	2.44	0.04
3 vs. 4	log body mass$^{0.33}$ + basilar membrane vs. log body mass$^{0.33}$ + basilar membrane + N^{o} turns	16.94	13.59	22.53

Multivariate shape analysis

As seen earlier in this chapter, echolocating bat cochleae show striking morphological diversity. Many species vary greatly in the number of turns and the level of expansion along the spiral whorl. As a preliminary study of this complex structure, a three-dimensional landmark analysis was conducted on the path taken by the outer edge of the basilar membrane as it progressed from the base of the cochlea to the apex in 61 specimens. Eigenshapes (ES) 1 and 2 together accounted for 81.8% of the sample variance, however, species points were distributed in a horseshoe artefact, which suggests that the variance expressed by ES1 and ES2 covary (Fig. 4.17). This suggests the PCA was only partially successful, and also that there are integral issues with the dataset being analysed. Aside from this, there is a high degree of phylogenetic signal in the data with family members clustering together. However, Old World fruit bats were located at one extreme of the morphospace, while the majority of laryngeal echolocating bats were grouped together. Both ES1 and ES2 were important in separating Old World fruit bats from the laryngeal echolocating species. A CVA of ES1 – ES7 (accounting for >96% sample variance), in which Pteropodidae, echolocating Yinpterochiroptera and Yangochiroptera were defined, revealed significant groupings (Wilks' λ = 0.155; 14, 104 DF; F = 11.45; P = 1.879 x 10^{-15}). The non-echolocating Old World fruit bats (Pteropodidae) were cleanly separated from all echolocating bats, whereas, there was overlap between certain echolocating Yinpterochiroptera and Yangochiroptera (Fig. 4.18).

Figure 4.17 Results of 3D Eigenshape analysis of bat gross cochlea morphology.

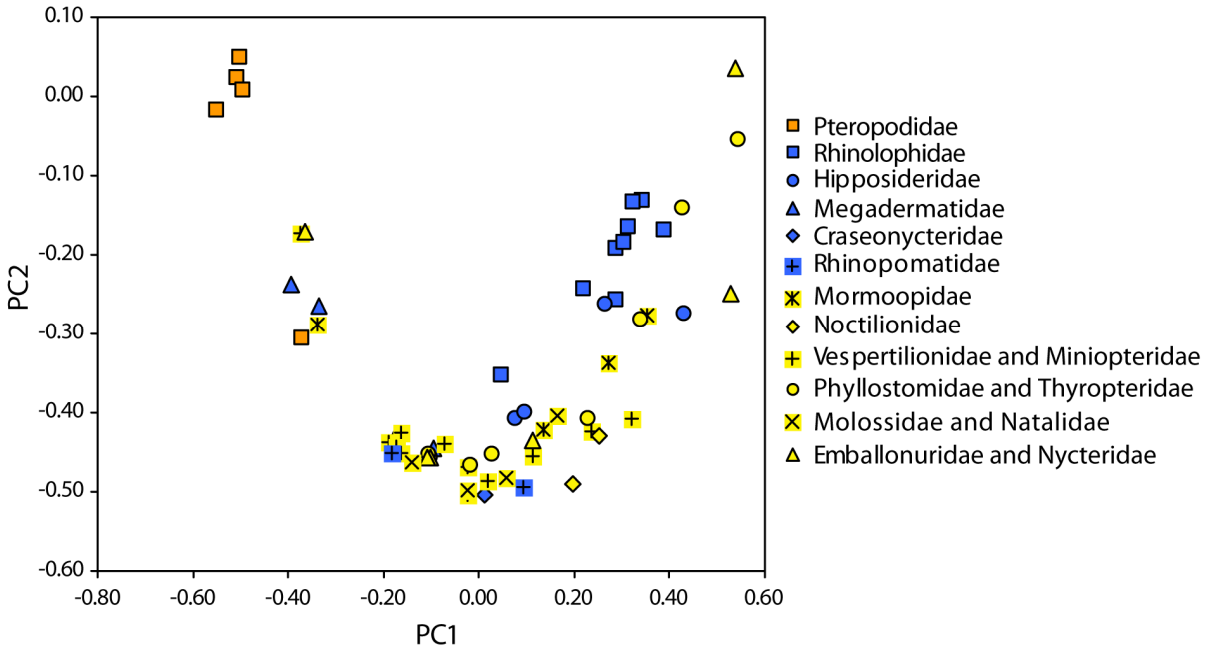

Figure 4.18 CVA of ES-1 to ES-7 of the shape variation expressed by bat cochleae. Old World fruit bats (red); echolocating Yinpterochiroptera (blue) and Yangochiroptera (yellow) are grouped with convex hulls to highlight the morphospace occupied. Bat families are indicated by text.

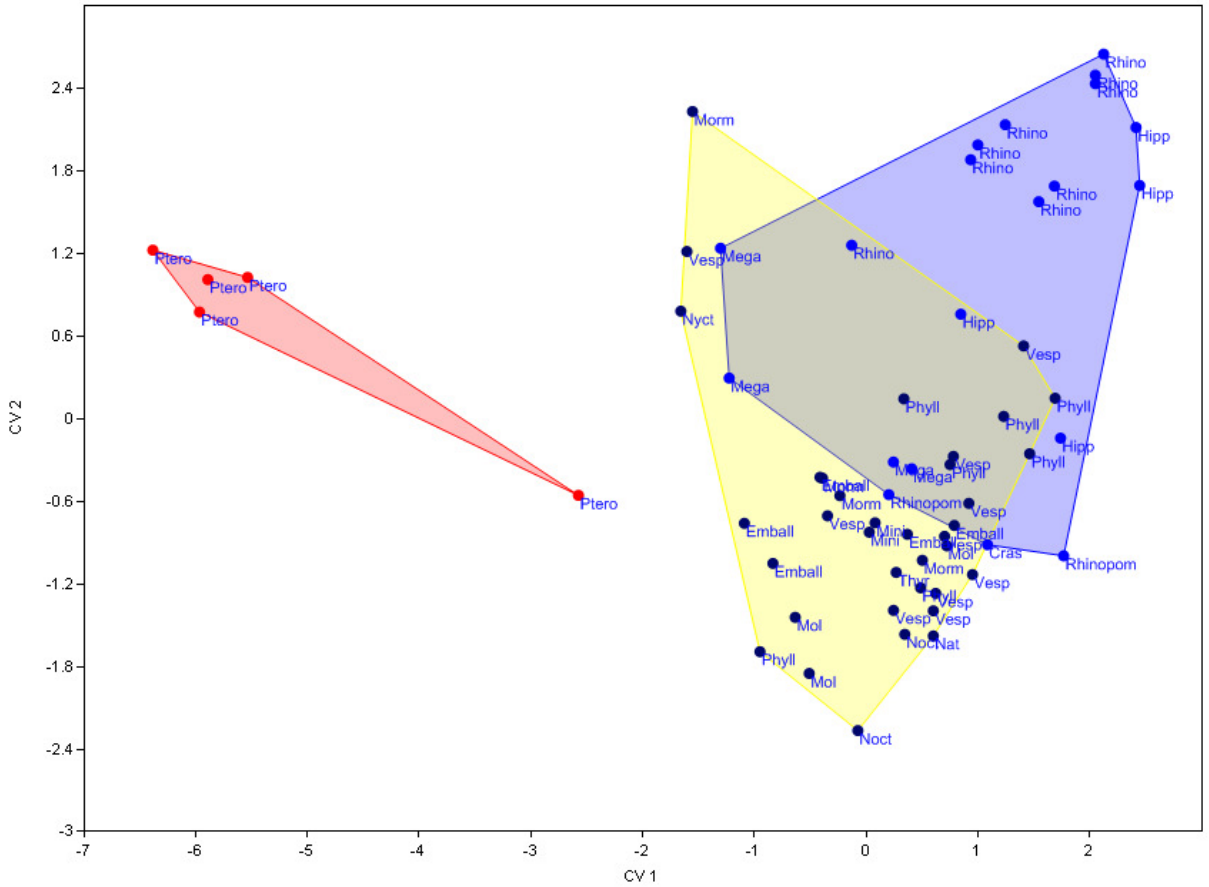

DISCUSSION

The mammalian snail-shell shaped cochlea houses membrane bound fluid compartments, supporting membranes and the inner- and outer- hair cells; features that all provide mammals with their characteristic high-frequency hearing. Through a combination of palaeontology, developmental biology and mathematical studies, much has been determined about the early transitionary period during the evolution of the coiled cochlea as well as its functional role in the acquisition of high-frequency hearing (Cantos *et al.,* 2000; Manoussaki *et al.,* 2008; Luo *et al.,* 2011). This study undertook a morphological analysis of the gross structure of the cochleae of ~50 laryngeal echolocating bat species and compared these to the cochleae of non-echolocating bats and mammals. Morphological variation of the inner ears was documented in relation to echolocation abilities to determine the functional changes that have occurred in relation to the high frequency sounds of echolocation. Across the bat order, cochleae were found to have highly variable morphologies, with evidence of both phylogenetic and functional signatures relating to echolocation ability.

Previous studies concerning the secondary loss of morphological traits in vertebrates have documented increased intra- and interspecific morphological variation in the body components under question (for example: Lande 1978; Adriaens *et al.,* 2002). Following this, it could be hypothesised that in Old World fruits evidence of a secondary loss of laryngeal echolocation could be provided by increased inter- and intraspecific morphological variation in inner ear size and shape. Due to time constraints it was not possible to extract and examine both labyrinths from the Old World fruit bat species included in this current study. However, visual inspection of the external labyrinth morphology did not reveal obvious deviation between the two sides within an individual. As mentioned earlier, published studies suggest that within species some variation in cochlea morphology, for example number of turns (West 1985; Tian *et al.,* 2006; Albuquerque *et al.,* 2009; Biedron *et al.,* 2009), is to be expected. Therefore, it would be necessary to study a large number of specimens per species in order to fully quantify 'typical' levels of morphological variation.

Basilar membrane, cochlear turns and hearing

Basilar membrane lengths were highly variable across the bat species studied. Typically, echolocating bats had elongated basilar membrane, however, this was not

found to be true after phylogenetic correction. All Old World fruit bats were found to have basilar membrane lengths consistent with non-echolocating mammals. Therefore, values were not consistently higher across all laryngeally echolocating bat species compared to non-echolocating taxa; for example, *Macroderma gigas* had a similarly proportioned basilar membrane to a marsupial. This is in agreement with previous studies that found certain species of the Megadermatidae have surprisingly small cochleae for their body mass (Habersetzer and Storch 1992), and suggest not all echolocating bats have hypertrophic cochleae.

The subset of echolocating bats examined here had a significantly higher number of turns compared to Old World fruit bats, but not compared to a sample of published values for non-echolocating mammals. Interestingly, Old World fruit bats were shown to have a lower number of cochlear turns than other non-echolocating mammals, which highlights the variation between taxonomic groups. A positive association between basilar membrane length and the number of cochlear turns, accounting for body mass, was found across mammals, although this was not significant after phylogenetic correction. Surprisingly, there was also no significant effect of laryngeal echolocation on basilar membrane length. A negative allometrical relationship was found between body mass and basilar membrane length, indicating small mammals have proportionally longer basilar membranes than large mammals. This means that cochlea coiling, to accommodate the basilar membrane, may be more important in small-bodied species. For example, certain members of the echolocating Yinpterochiroptera, such as horseshoe bats, have low body weights and long basilar membranes, which might partly explain the high number of cochlea turns observed. Furthermore, body size, basilar membrane, number of turns and selection for optimal hearing all interplay, as was seen in the PCA of hearing parameters, morphological variables and ecology. Moreover, body mass is likely more constrained in subterranean and volant mammals compared to aquatic taxa.

The method used to estimate basilar membrane lengths may result in slight overestimation, since it is not always clear precisely where membranes begin or end, and also estimates are based on the outer edge of the membrane. However, by using μCT imaging it is possible to reconstruct the internal space of intact inner ears to within a few micrometers of the actual volume in living specimens (see references within Walsh *et al.,* 2009), and also alleviate the shrinkage problems of soft tissues and serial

sections (Spoor and Zonneveld 1995). It is also important to consider cochlea width together with basilar membrane length and number of turns (Meng and Fox 1995), as a very tightly coiled cochlea could have a high number of turns but also a short basilar membrane. This might partly explain why the echolocating bats included in this study had much more developed cochleae compared to those of echolocating whales, in terms of basilar membrane length and number of turns (Ketten 1997; Spoor *et al.,* 2002). Furthermore, echolocating cetaceans do not have increased number of cochlear turns but instead have a greatly expanded basal turn (Ketten 1997). Due to the tonotopic organisation of the cochlear it is not necessarily essential for an animal with high-frequency hearing to have either many turns or long basilar membranes.

Echolocation and cochlea morphology

For CF echolocating bats a significant negative relationship between peak-energy echolocation frequency and basilar membrane length was found. This was extended to all laryngeal echolocating bats, and again significant negative relationships were found between minimum, maximum and peak-energy echolocation call frequency and basilar membrane length and body mass. There was typically a positive association with call parameters and the number of cochlea turns. This relationship was clearest in CF bats, as non-CF bats typically use calls that include FM components, and so frequency varies considerably from start to end making parameters difficult to estimate. Although, theory predicts that as mammalian basilar membrane length increases the range of audible frequencies should decrease (West 1985), this is only true in species with non-specialist hearing, and not in echolocating bats.

The hipposiderid, *Cleotis percivali* has one of the highest known echolocation calls, CF ~212 kHz (Fenton and Bell 1981), which is considerably higher than the other *Hipposideros* species included in this study (64-157 kHz). Inspection of its cochlea suggests that basal turn has been extremely modified compared to the other species studied. These modifications are consistent with the tonotopic organisation of the cochlea, as the basal cochlear area is involved in amplifying the highest frequencies. This is thought to be at least partly achieved by a decrease in stiffness of the basilar membrane from base to apex (Robles and Ruggero 2001). *Pteronotus parnellii* represents an unusual case of convergent evolution in call type; it is the only New World species to use CF echolocation, a trait otherwise only seen in *Rhinolophus* and *Hipposideros spp*. As in the Old World species, *P. parnellii* has both a well-developed

auditory fovea (Kossl *et al.,* 2003), and considerable expansion of the cochlea throughout the basal turn.

Typically echolocation peak-frequency in members of the Rhinolophidae is inversely related to body size and correlated with cochlear width (e.g. Francis and Habersetzer 1998). However, several species, such as *R. philippinensis* and *R. capensis*, have echolocation call frequencies that have become decoupled from body size and, in the latter case cochlear morphology (Kingston and Rossiter 2004; Odendaal and Jacobs 2011). In this current study only a small sample of *R. philippinensis* was available (n = 3), therefore, data from many more individuals is necessary to determine the pattern between echolocation call frequency and basilar membrane length. However, for individuals measured here, echolocation frequency does seem lower than expected given forearm, body mass, or basilar membrane length. The above findings, combined with previous studies, suggest there may be a fairly plastic relationship between cochlear size and CF echolocation in Rhinolophidae, which may relate to their unique auditory foveae (Francis and Habersetzer 1998; Odendaal and Jacobs 2011). Features related to echolocation call emission in *R. capensis* show evidence of independent evolution to body and cochlea size, suggesting selection can act on individual components of the echolocation pathway (Odendaal and Jacobs 2011). In summary, there may be many more selection pressures, including physical, environmental, morphological and ecological factors, driving echolocation call evolution than are currently understood.

Three-dimensional analyses of shape

Morphometric analysis of shape representations of the path taken by the basilar membrane along the cochlea, suggested it is possible to separate non-echolocating taxa from laryngeal echolocating bats species, and that both clades of echolocating bats display certain similar characteristics. This analysis picked up a degree of phylogenetic signal, as is particularly evident in the horseshoe bats; this suggests that structural modification to bat inner ears occurred after the families divided. Since this analysis represents a preliminary 3D analysis of a highly complex structure, it would benefit from considerable development and the inclusion of more species of bats and non-bats.

CT has become increasingly applied to a wide range of developmental and evolutionary studies (for examples see Spoor *et al.,* 2007b; Walsh *et al.,* 2009; Veselka *et al.,* 2010a).

However, arguably computational and analytical techniques have not kept pace (Rowe and Frank 2011), although methods for analysis of 3D surfaces do exist (e.g. Polly and MacLeod 2008). The spiral shape of the mammalian cochlea represents a considerable problem for morphometric analysis for several reasons. Firstly, transitions between numbers of turns cause particular problems. This limits applicability of the approach, as it is arguable whether a spiral with three complete turns is an elongation of two complete turns, or an addition of one turn. In the latter case, it then becomes problematic to allocate homologous points; the former case is also a problem, but one which semi-landmarks might overcome. Secondly, as the cochlea duct projects into the middle of the internal void the surface is discontinuous and, therefore, creates problems involving surface analysis.

Further work

It would be interesting to study bat specific adaptations of the anchoring mechanism of the basilar membrane, as well as observing the ontogeny of the inner ear, to see if cochleae develop similarly to those of other species. For example, the upper cochlear turn of the Mongolian gerbil, *Meriones unguiculatus,* continues to grow up to 10 days after birth, thus contributing more to the elongation process than the basal turn (Harris *et al.,* 1990). Observing the ontogeny of the growing cochlea could also allow homologous features to be found. It is also possible to use middle ear values to reconstruct hearing capabilities (Lange *et al.,* 2004); therefore, it would be interesting to see if adaptations of each stage of the auditory process (i.e. outer, middle and inner ear) of bat species are correlated to produce similar predicted auditory thresholds.

Currently, some open source databases of bat CT scans, such as Digimorph (http://www.digimorph.org/index.phtml) exist; however this study represents the first multi-species reconstructions of bat inner ears. As time progresses it should be possible to combine these two sources, as well as comparative measurements taken directly from fossil bat inner ears to reconstruct the sensory perception of extinct early bats. Using CT technology it should be possible to reconstruct 3D volumes from 2D fossils and, therefore, accurately map the progressive evolution of the inner ears, therefore, tracing the exact evolutionary time point that the cochlea expanded in size and complexity.

Conclusions

Many laryngeally echolocating bats were shown to have cochleae with longer basilar membranes and a high number of turns. However, these traits were not universal across all echolocating species, and, furthermore, many were not robust to phylogenetic correction. The inner ears of Old World non-echolocating fruit did not deviate significantly from other non-echolocating mammals in terms of basilar membrane length, although they did have a lower number of turns. Correlations with echolocation call parameters suggest that inner ear morphology is adapted for call structure in echolocating species.

CHAPTER FIVE

The Morphology of Bat Vestibular Systems in Relation to Wing Morphology, Echolocation and Flight

SUMMARY

Bats possess several traits that may place unusual selection pressures on their vestibular systems. Firstly, they are unique among mammals in being capable of powered flight. Secondly, many species spend much of their lives hanging upside down. Thirdly, echolocating bats possess hypertrophic cochleae, which are likely to place physical constraints on the size and shape of the vestibular system due to the confined space of the petrosal bone. Studying the vestibular system of bats could thus reveal how semicircular canals size and shape have become adapted for specialised locomotion and ecology, as well as reveal important insights into how selection can circumvent evolutionary constraints. It follows that changes in semicircular canal structure could also shed light on the evolution of echolocation in bats. Yet despite these factors, few studies have previously examined the structure of bat vestibular systems.

Here I constructed high-resolution three dimensional volumes of the vestibular system of over 50 bat species, and, combined with existing data, compared the size and shape of the mammalian vestibular systems with special reference to flight and echolocation. In proportion to body mass, Old World fruit bats were found to have semicircular canals similar in size to those of other mammals. Conversely, semicircular canal size in echolocating bats was found to be highly variable with no clear relationship with body mass. Additionally, it appears that the enlarged cochleae of echolocating bats have led to changes in canal shape. Such changes may relate either to spatial constraints or semicircular canal sensitivity. Differential selection pressures may have acted on the semicircular canals of echolocating Yinpterochiroptera and Yangochiroptera, which could support disparate evolutionary pathways during the acquisition of echolocation in each clade.

INTRODUCTION

Mammalian semicircular canals and locomotion

Throughout their ~200 million years of evolution, mammals have adapted to a wide range of ecological niches. Members of this class can be found in the air, on and under the ground and also in semi- or fully aquatic environments. Such contrasting environments have placed disparate selection pressures on animals' anatomical, physiological and ecological traits, particularly in relation to locomotion, orientation and sensory stimulus. Therefore, it is to be expected that the results of these pressures would be manifested by adaptations of the sensory organs, such as the vestibular system.

It is a necessity of all higher organisms, capable of movement, to have a system by which to regulate body and eye orientation with respect to gravity, during both locomotion and at rest. In vertebrates, this role is undertaken by the vestibular end-organs, and, in fishes, also the lateral line system. All mammals except monotremes possess five main vestibular end-organs: three semicircular canals, and two otolith organs (Kornhuber 1974). Each semicircular canal is a semicircular osseous duct enclosing an internal membranous duct that contains a flow of endolymph which responds to angular head movements (Fig 5.1). Despite some similarities in function and location of the semicircular canals and otoliths, the sensory inputs of each can be described as being of a 'different modality' since linear and angular accelerations are independent of each other (Ivanenko *et al.,* 1997).

The vestibular system maintains the body's equilibrioception (sense of balance) by monitoring angular acceleration together with additional sensory inputs. Therefore, the semicircular canals interact with organs and systems to maintain balance in a kinetic system affected by both internal and external stimuli. Additionally, the semicircular canals maintain a sense of balance by stabilisation of gaze, by means of the vestibulo-ocular reflex (VOR). This system mainly involves compensatory eye movements i.e. to counteract head movements and maintain the angle of vision (Cohen 1974). Stimulation of each individual semicircular canal has distinct effects on particular eye muscles (Cohen 1974; Cox and Jeffery 2008); for example a forward head tilt stimulates the anterior semicircular canals which leads to contraction of the inferior obliquus muscle, resulting in an upwards eye roll (Lowenstein 1974). Furthermore, stimulation of the

semicircular canals results in body and limb movements to support the consequent head movements (Cohen 1974). It has been suggested that the semicircular canal system's role in stabilisation of vision should be especially important in rapidly moving gliding and arboreal animals (Spoor *et al.,* 2007). However, the functional importance of the semicircular canals in stabilisation of vision has since been questioned; with the conclusion that its morphology is arranged 'secondarily, if at all, for diminishing the burden of transforming vestibulo-ocular reflex signals in the most agile species' (Jeffery and Cox 2010).

It has been known for approximately 200 years that the vestibular organs play an important role in monitoring body movement (see references cited within Kornhuber 1974); since then many attempts to relate locomotor ability and vestibular morphology have been made. Some of the earliest, and perhaps best known, observations of this nature were those by Gray (1906) of the bony labyrinth of the three-toed sloth, *Bradypus tridactylus.* He noted that the canals were smaller than those seen in other species, that they were not semicircular but instead quadrilateral, and that they deviated from the normal orthogonal planes and appeared 'somewhat pressed together' (Gray 1906). These features were attributed to the sloth's slow movements and 'inverted' lifestyle.

More recently, a growing body of research has shown significant correlations between semicircular canal parameters and both agility and body mass. Typically overall size (expressed in terms of the average radius – see below) of semicircular canals increase with body mass and heightened agility (for examples see: Schmelzle *et al.,* 2007; Spoor *et al.,* 2007; Cox and Jeffery 2010). A strong negative allometric relationship has been found between semicircular canal size and body mass in vertebrates, in which the former does not increase proportionally with the latter but instead increases at a smaller rate. Fewer consistent results have been found concerning the otolith organs of higher vertebrates; generally mammalian otoliths have been found to be small albeit with some notable exceptions, such as, seals, porpoises and kangaroos (Gray 1905; Gray 1906). As well as the variation in relative size of the semicircular canal complex across taxa, the three canals also differ relative to each other, with the anterior semicircular canal often larger than the other two (Graf and Vidal 1996). One emerging pattern, particularly in terrestrial animals, is that the lateral semicircular canal is most functionally linked to

agility, and is most powerful in characterising species that mainly transverse two versus three dimensional environments (Cox and Jeffery 2010).

Figure 5.1 Computer generated image, from this study, showing the bony labyrinth of *Pteronotus (Chilonycteris) macleayi grisea* (NHM.65.3990). The figure on the left is a dynamic cutaway showing the internal duct of the anterior semicircular canal (1), and also the widening of the base of this canal corresponding to the ampulla (2). The figure on the right shows all three semicircular canals intact, as can be seen all three (anterior, lateral and posterior) canals are positioned approximately orthogonally to each other.

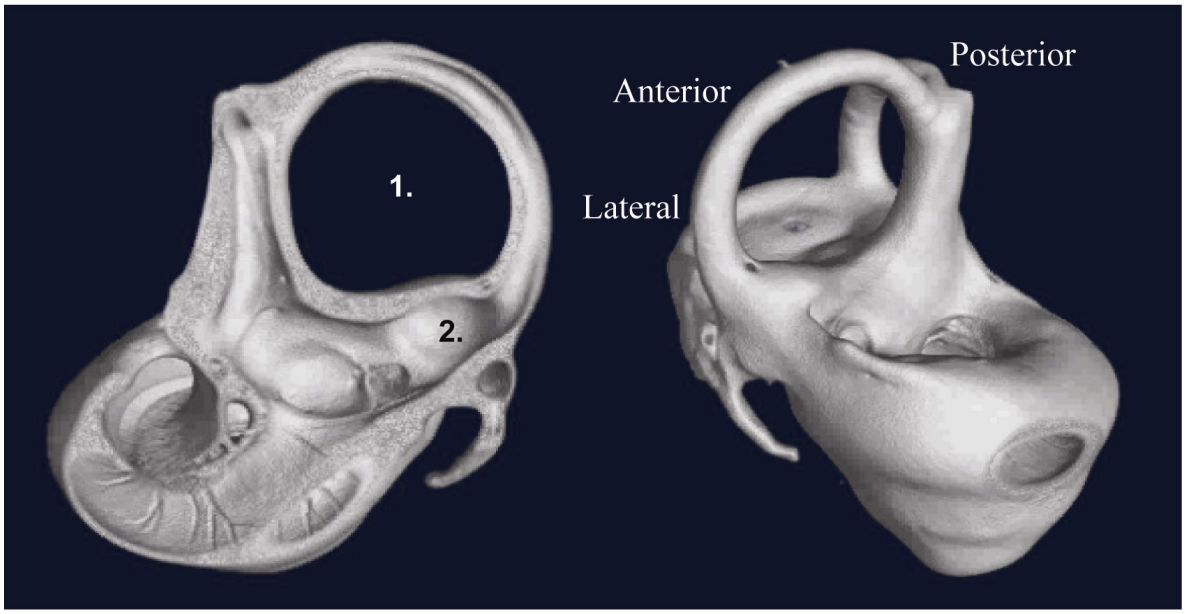

Terrestrial mammals

Terrestrial life, as seen in most ground-dwelling or arboreal mammals, is highly variable. Most mammals are quadrupeds; however, forms of bipedalism have evolved independently in three extant groups (Primates, Rodents and Macropods). In this respect Primates are exemplars of variability, with members displaying diverse locomotory techniques from obligate bipedalism to brachiation. Humans are uniquely habitually bipedal, and attempts have been made to relate this to their enlarged anterior and posterior semicircular canals (Spoor *et al.,* 1994). Arboreal animals also show interesting features that have been linked to increased locomotory demands; for example, arboreal marsupials have longer lateral semicircular canal compared to their terrestrial counterparts (Schmelzle *et al.,* 2007). Therefore, it seems possible to relate changes in locomotory mode, ecological factors and semicircular canal morphology.

Subterranean mammals

Four mammalian orders, (Rodentia, Notoryctemorphia, Afrosoricida and Soricomorpha) have completely subterranean representatives, which either very occasionally or never

return to the surface during their lives (Nevo 1979). Many of these species display convergent morphological adaptations such as reduction of organs, e.g. limbs and eyes, with an associated increase in other senses, e.g. olfaction and tactile senses, for use in navigation in confined dark spaces (Nevo 1979). The subterranean lifestyle is also thought to affect the vestibular system, with the semicircular canals of two mole rat species found to be significantly larger, and calculated to be more mechanically sensitive. These differences appear most pronounced in the lateral semicircular canal, when compared to those of the common rat, *Rattus norvegicus* (Lindenlaub *et al.,* 1995). Similarly a study examining the mechanical sensitivity of the semicircular canals of the European mole, *Talpa europaea*, in terms of the duct length, cross-section area of the lumen and also the plane area, found that the area of the lumen was significantly larger in moles compared to *R. norvegicus* (McVean 1999).

Aquatic and semi-aquatic mammals

Cetaceans are secondarily aquatic animals that evolved from smaller terrestrial mammals, during the Eocene (Van Valen 1968; Thewissen *et al.,* 2001; Spoor *et al.,* 2002). The vestibular systems of all extant cetaceans show massive reductions (Gray 1905; Ketten 1997; Spoor *et al.,* 2002). It is argued that this condition relates to their fully aquatic lifestyle and results from diminished vision coupled with fused cervical vertebrae that has led to reduced head movements and a subsequent loss of function (Ketten 1997). Other interpretations suggest the size reduction results from adaptive modifications that occurred shortly after they became marine animals (Spoor *et al.,* 2002). In either scenario, it is suggested that their fused necks render them incapable of refined compensatory head movements in response to overstimulation of the semicircular canals in the aquatic environment and, therefore, without the size reduction they would be in a constant state of vertigo (Ketten 1997; Spoor *et al.,* 2002). However, not all cetaceans have fused cervical vertebrae, and the degree of fusion varies considerably across species (Buchholtz 2001). Although, a recent study determined that bottlenose dolphins, *Tursiops truncatus*, displayed less accentuated head movements compared to a cow, *Bos taurus* (Kandel and Hullar 2010), little is known about neck movements in other species. Interestingly, other marine mammals, such as pinnipeds, have well developed semicircular canals, possibly due to their semi-aquatic lifestyle (Gray 1905). Therefore, further research is necessary to determine the precise functional role of reduced size semicircular canals in cetacean.

Aerial, gliding and highly mobile animals

Ever since the proportionally small semicircular canals of the sloth were attributed, in part, to its slow movement, semicircular canal size has been considered an important predictor of agility. Lowenstein (1974) predicted that given the variety in length, diameter and shape of canals across vertebrates, species that are free-swimming, flying or highly active would have longer canals with smaller diameters than terrestrial taxa. In the little brown bat, *Myotis lucifugus*, the anterior semicircular canal was found to be 30% larger than the posterior canal. Interestingly, despite the larger overall size this canal had the narrowest duct diameter (Ramprashad *et al.,* 1980). Yet there is little empirical evidence for a dramatic increase of semicircular canal size in what would be considered highly agile animals. For example, gliding animals show no significant deviations (Schmelzle *et al.,* 2007; Spoor *et al.,* 2007b), while a study comparing the vestibular nerve fibres between gliding and ground squirrel species found no significant differences (Snell and Rylander 2001). Early work on the semicircular canals of birds also found little relationship between relative 'size' and either flying ability (including terrestrial versus arboreal birds) or taxonomic relationship (Hopkins 1906). Recent analyses, however, found that birds have larger semicircular canals than mammals or dinosaurs, and that volant birds have larger semicircular canals than flightless forms (Sipla 2007).

Reconstructing past locomotor ability

Several studies have used morphological measurements, either from the inner ears of extant species or taken directly from fossil remains, to reconstruct locomotor ability in a number of extinct groups, including early mammals (Luo *et al.,* 2011), primates (Kirk and Gosselin-Ildari 2009; Ni *et al.,* 2010), early cetaceans (Spoor *et al.,* 2002), notoungulates (Macrini *et al.,* 2010), reptiles (Witmer *et al.,* 2003; Walsh *et al.,* 2009) and birds (Sipla 2007; David *et al.,* 2010). These studies have been able to shed light on questions such as: what was the mode of flight of *Archaeopteryx* (Sipla 2007)? When did early hominins become bipedal (Spoor 2003)? And, at which point did proto-cetaceans adopt a fully aquatic lifestyle (Spoor *et al.,* 2002)?

The vestibular systems of bats

For several reasons, studying the vestibular system of bats could provide important insight and understanding into the relationship between semicircular canal structure,

motion and ecology. Firstly, within mammals, the unique ability of bats to undertake powered (and often highly manoeuvrable) flight is likely to place extreme demands on their vestibular system to maintain balance. Secondly, many bat species spend much of their lives roosting in an upside-down position. Thirdly, echolocating bats possess enlarged cochleae, potentially conferring constraints in the confined space of the petrosal bone on the size and shape of the semicircular canals. Yet despite these factors, few studies have examined the structure of bat vestibular systems, and previous work has concentrated on single species (Ramprashad *et al.,* 1980; Fejtek *et al.,* 1995; Kirkegaard and Jorgensen 2001) precluding comparative evolutionary analyses.

If semicircular canal size was found to be related to hypertrophy of the cochlea in echolocating taxa, then studying semicircular canal morphology could also shed light on the evolution of echolocation in bats. Bat monophyly confirms powered flight evolved once; since then species radiated to display a wide range of flight and behavioural specialisations. Crucially, bats also subsequently evolved echolocation, at least once and possibly on multiple occasions. Undoubtedly due to its role in orientation and prey location, this key innovation would have had significant implications on the function of the vestibular system.

Aims and objectives of this study

This study aimed to detail the morphological variation of bat vestibular systems, encompassing ecologically diverse species. I undertook this in two parts: firstly, using high-resolution μ-computed tomography (μCT) scans of bat vestibular labyrinths. From the resultant volumes, linear and multivariate measurements were taken, including traditional (e.g. radius of curvature) and novel approaches (e.g. semi-landmark outlines). Secondly, an in-depth ecomorphological dataset was compiled, containing anatomical, morphological and behavioural measurements for the study species. By combining these two parts, I then characterised adaptations of the bat vestibular system in relation to the functional constraints of their aerial lifestyles. Further to this, adaptations of the vestibular system were compared to the acquisition of echolocation, to see if any direct correlations of the vestibular system can be related to echolocation ability, and conversely if adaptations of echolocating bat vestibular systems can reveal insights into their evolutionary past.

Specifically the following hypotheses were tested:

Hypothesis 1: Bats are the only group of truly volant mammal. I predicted that given their high agility they would have larger semicircular canals, relative to their body mass, compared to non-volant mammals.

Hypothesis 2: I predicted that within bats, wing-shape and hunting strategy would correlate with the size and shape of semicircular canals. Specifically, bats using highly manoeuvrable hunting strategies should have larger and, therefore, more sensitive semicircular canals.

Hypothesis 3: I predicted that the two groups of laryngeal echolocating bats would possess modified semicircular canals compared to non-echolocating fruit bats, due to the constraints on canal shape and size imposed by expansion of the cochlea. Furthermore, within echolocating bats, I predicted that there would be an association between semicircular canal morphology and the particular mode of echolocation employed i.e. FM or CF. I also predicted that there would be a positive association between semicircular canal size and use of vision by bats (either for orientation or prey location).

MATERIALS AND METHODS

Gross structure and measurements of the vestibular system

All mammals possess three semicircular canals (anterior, posterior and lateral) which lie approximately orthogonally to each other, and each is responsible for monitoring head movements in one of the three dimensions. For this reason they are collectively known as the kinetic labyrinth (Swartz *et al.,* 1996). One end of each canal is dilated, which is known as the ampulla, and contains hair cells involved in the transmission of vestibular nerve fibres (Swartz *et al.,* 1996). The two otolith organs, the utricle and saccule, are formed from calcium salts secured to, and partially embedded in, the otolith membrane which sits above a layer of sensory and supporting cells (Lowenstein 1974). The utricle and saccule sense linear acceleration of the head (Jaeger *et al.,* 2008). Unfortunately, these two structures are not preserved in most specimens and, therefore, it was not possible to include them in the current study.

Comparative anatomical semicircular canal studies have progressed significantly over the last one hundred years in terms of techniques, measurements taken, and functional inferences made (e.g. Hopkins 1906; Witmer *et al.,* 2003). There are a number of consistent measures taken in most studies, which are regarded as the most informative (see Fig. 5.2). The radius of curvature, R, is the most commonly used estimate of canal size; however, it cannot provide information of canal shape. R is most commonly calculated as the average radius of canal height and width. Over the years it has been measured using a variety of methods (including indirect and direct measures, and estimated by best-fitting circles) (Lindenlaub and Oelschlager 1999; Cox and Jeffery 2010) from a variety of media (e.g. photographs, CT-scans, specimens and casts) (Spoor and Zonneveld 1995; Sipla 2007). When comparing absolute values across datasets some caution is necessary as measurements can be taken from lumen centres (Spoor and Zonneveld 1995) and at other times from the canal edge (Schmelzle *et al.,* 2007). Streamline length, termed L, is usually measured across the middle of the duct lumen (Lindenlaub and Oelschlager 1999), and is basically the length the fluid flows through. L can also be used to calculate the plane area, termed P. Canal area has been shown to be closely related to canal sensitivity, and is involved in the calculation of cupula mechanical sensitivity, which contains the sensory hair cells (Oman *et al.,* 1987). The average radius, (2P/L) can be used as an estimate of shape (Cox and Jeffery 2010), a perfectly circular semicircular canal has a value of 2P/L that is equal to R. The plane of

torsion measures how much the canal arc is twisted out of its principal plane, leading to out-of-plane deviations (Cox and Jeffery 2010). This is thought to be more likely in smaller animals, due to spatial constraints of the petrosal bone, and also to affect the anterior semicircular canal more (Blanks *et al.,* 1985).

Figure 5.2 Three commonly measured values of semicircular canals size. Radius of curvature, termed R, is the average radius of canal height and width. Streamline length, termed L, is indicated by the dashed grey line, which encloses the yellow area known as the plane area, termed P.

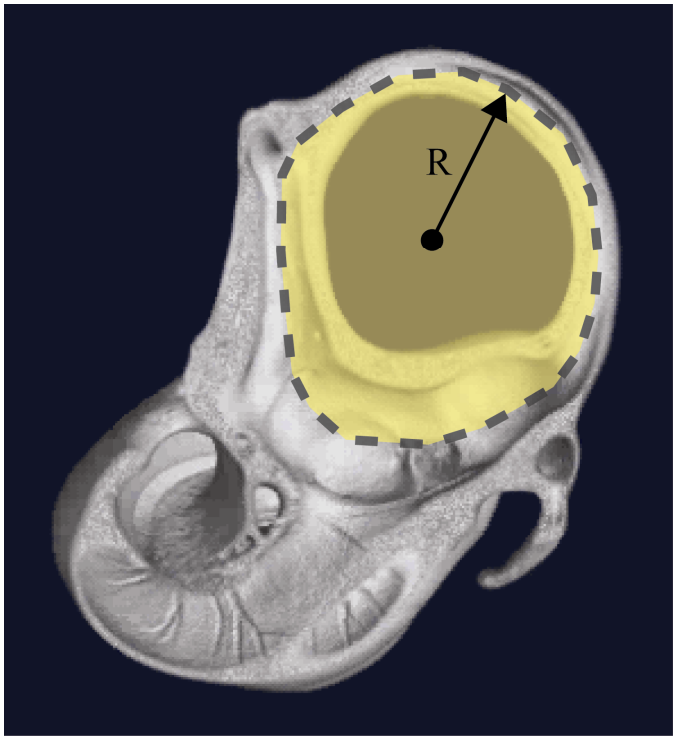

Study sample and acquisition of µCT-scan data

I examined the vestibular system of 68 bat specimens, representing 56 different species from 16 families, chosen to maximise taxonomic and geographic coverage, ecological diversity and echolocation call type. For full technical details of specimens, µCT scan acquisition and digital dissection, see methods section (Chapter 4).

Radius of curvature and linear measurements

Stereolithography (.STL) files, representing inner ear volumes, were imported into MeshLab v1.2.2 (MeshLab Visual Computing Lab – ISTI – CNR) and converted into Stanford polygon files (.ply). Each .ply file was imported into an individual project of Landmark v3.0, and the dimension tool was used to measure linear distances directly from the three dimensional volumes. Linear measurements of height and width of each semicircular canal were taken (Fig. 5.3); measurements were taken between mid-points

of each lumen duct. The radius of curvature was calculated as half the average length (l) and width (w) of each canal, $R = 0.5 \times \left(\frac{h + w}{2} \right)$ (Spoor and Zonneveld 1998).

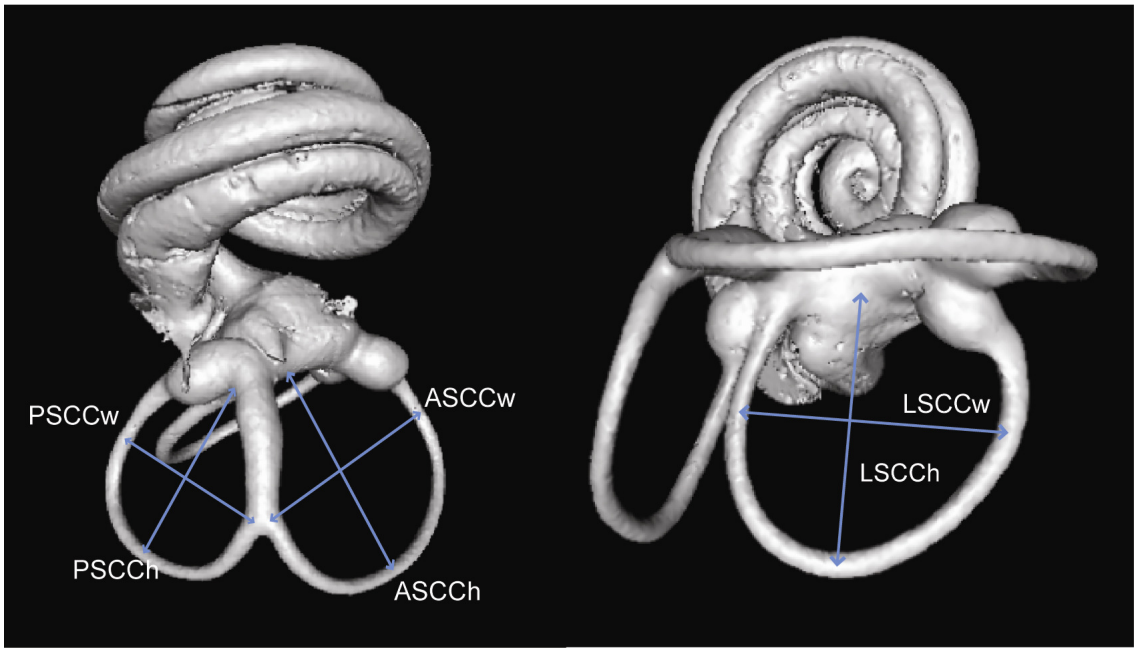

Figure 5.3. Digital endocast of the right inner ear of *Cheiromeles torquatus* (BMNH. 1844.10.17.7) - showing how the three Rs (anterior semicircular canal - ASCC, posterior semicircular canal - PSCC and lateral semicircular canal - LSCC) were measured. Heights (h) and widths (w) were measured to the lumen mid-point as described in Spoor and Zonneveld (1995).

In several cases, one or more of the three semicircular canals were damaged, thus making it impossible to accurately measure canal height or width. Therefore, across the taxonomic sample, coverage for each canal varies. For the anterior canal, measurements were taken twice and averaged for all samples, so allowing the error of measurements to be calculated and thus giving a measure of the accuracy and reliability of the method. In order to make functional interpretations based on representative species individuals, it is assumed that inter-specific variation is greater then intra-specific variation. In a subset of specimens, both labyrinths were extracted, so that both sets of semicircular canals could be measured and, therefore, inter-individual differences quantified. However, it has been demonstrated previously that - at least in the short-tailed shrew, *Blarina brevicauda* - individual asymmetry and also sexual dimorphism is negligible (Welker *et al.,* 2009).

Relative semicircular canal size

To determine how the size of three semicircular canals differs with respect to each other, both within and between species, values taken by this study were combined with

published radius of curvature values for 11 bat species (Spoor et al., 2007; Cox and Jeffery 2010). Species averages were not calculated across studies or for the size morphs of *Rhinolophus philippinensis*, therefore, the final dataset consisted of 60 species represented by 64 sets of points, not including damaged specimens (see Appendix D, Table D1). Relative semicircular canal size was calculated by dividing R by the cube root of body mass. Unfortunately, due to the nature of the specimens, few actual body mass or gender classifications were available. Therefore, body mass was taken from literature sources, as discussed in Chapter 4. Wherever possible, gender and geographic location was taken into consideration and in a small number of cases where species values were not available, values of congeneric taxa with comparable forearm values were used.

Relationship between cochlea and semicircular canal size

To test whether cochlear expansion in echolocating bats has affected the size of each semicircular canal, relative cochlea size was plotted against relative semicircular canal size. Measurements were taken to allow comparison with published cochleae and semicircular canal data from a total of 40 non-bat species (Spoor *et al.,* 2002). Cochlear size is calculated as the average value of the slant height, and the widths of the first and second cochlear turns (Fig. 5.4).

Figure 5.4 Digital endocast of *Cheiromeles torquatus* inner ear (BMNH. 1844.10.17.7). The three measurements used to calculate average cochlea size, according to Spoor (2002): slant height (a), width of the first (b) and second (c) cochlear turns.

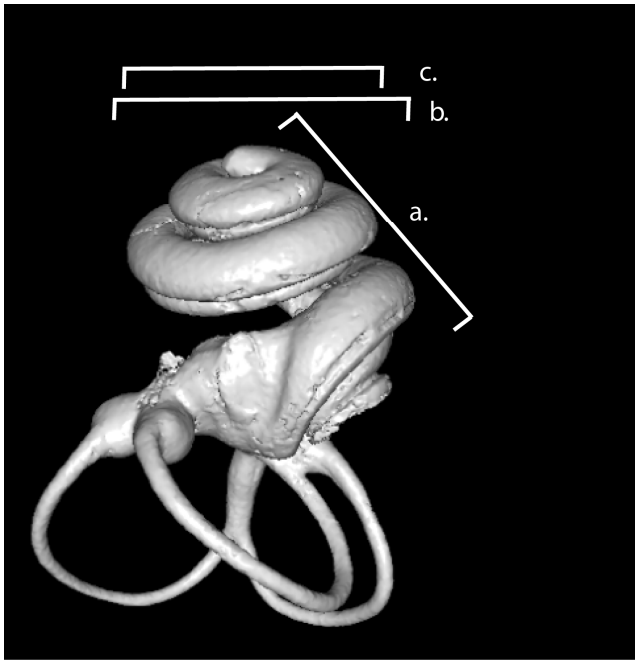

Relative cochlea and semicircular canal size are calculated as average size divided by cube root body mass; these values were then $\log_{10}$ transformed to normalise the variance. Values were measured for 55, 55 and 57 bat specimens for the anterior, posterior and lateral canals respectively.

Examining allometry

To test whether bats have proportionally larger semicircular canals compared to non-volant mammals, the bat dataset (i.e. 65 lateral, 63 posterior and 63 anterior R values) was combined with published R values for 156 non-bat species (Spoor *et al.,* 2002; Spoor *et al.,* 2007b; Cox and Jeffery 2010). In order to compare inter-individual variation and investigate the allometric relationship, semicircular canal size was compared to overall body mass of the animal. If values were unobtainable for particular species, those of suitable congeneric taxa were used. Semicircular canal and body mass values were $\log_{10}$ transformed to normalise the variance, and canal radius was then plotted against body mass$^{0.33}$ (to allow comparison between a linear value with a volume metric). The relationship between these variables was explored in the R statistical package version 2.11.1 (R Development Core R Development Core Team 2011) using a modified protocol as outlined in Knell (2009), as follows:-

1. Log–log scatterplots of the data were plotted. These were then determined to be either: (a) a clear discontinuous relationship, (b) a clear continuous relationship (but not a straight line), (c) a straight line relationship, or (d) not possible to determine the nature of the relationship by visual inspection.
2. For 1(d), if a simple linear regression was fitted and examination of standard diagnostic plots indicated no systematic deviation from a straight line, this was considered sufficient.
3. For 1(b), a range of appropriate models were fitted and compared on the basis of AIC. Once the best model was identified, normal model-checking procedures were followed.
4. For 1(a), the overlap in the X-variable is an important factor that needs to be taken into account as well as the position of the break-point. Relative frequency density plots were used to verify the discontinuous relationship and, where clear, appropriate models were fitted to the data and compared using AIC.

Once the appropriate models were chosen, the parameters of these were examined to define the allometric relationships; for example, if a linear model best describes the data

a regression with a slope of one would signify isometry. Bat values, as described above, were added to the dataset and the relationship re-examined.

Wing morphology and flight behaviour

To study how the vestibular system in bats varies in relation to flight performance, a dataset of comparative ecomorphological values was assembled. Quantitatively, several morphological measures of bat wings have been used to infer flying 'style'. Three of the most commonly used measures are wing aspect ratio (WAR), wing loading (WL) and wing tip shape indices (WTS) (Norberg 1987; Arita and Fenton 1997). WAR is an approximation of wing shape, and it is calculated by dividing the squared wing span (distance between the tips of the two extended wings) by wing area (Norberg 1981). Low WARs are associated with shorter wingspans and larger wing areas, and typically with larger wing loadings. Bats with wings of this type are predicted to have slow and manoeuvrable flight patterns within vegetation (Norberg 1981). WL measures the force per unit area of the wings that must be supported during flight and is calculated by dividing body weight by the wing area. WTS describes the shape of the wings, higher values means a blunt-rounded ended wing whereas low values imply a more pointed wing (Arita and Fenton 1997). Where possible values were obtained directly from either wing traces or photographs of the subject species, or where available from published sources (Norberg 1981; Norberg 1987; Norberg and Rayner 1987; Kingston *et al.,* 2000; Mancina 2005) (Table D2). Relationships between ecomorphological variables and canal size, for 63 bat species, were explored with step-wise multiple regression analysis, preformed in the R statistical package version 2.11.1. To investigate if separate evolutionary pressures had acted on Yangochiroptera and Yinpterochiroptera, the data were divided appropriately into the two groups and the above multiple regressions were repeated.

Phylogenetic correction

Closely related taxa might be expected to be phenotypically more similar than chance; therefore, to control for shared ancestry of characters, and thus ensure independence of data-points, phylogenetic correction was necessary. The same procedure as described in Chapter Four was used (See Chapter Four Methods, and Table D3 for fossil constraints). For subsequent analyses two hypothetical dated phylogenies containing all taxa, and the chiropteran sub-tree were used, these are shown by Fig.5.5.

Figure 5.5 The two dated phylogenies used to carry out phylogenetic correction.

a) Tree A - bats were placed as sister group to Cetartiodactyla, Carnivora and Perissodactyla (for review see Springer et al., 2004).

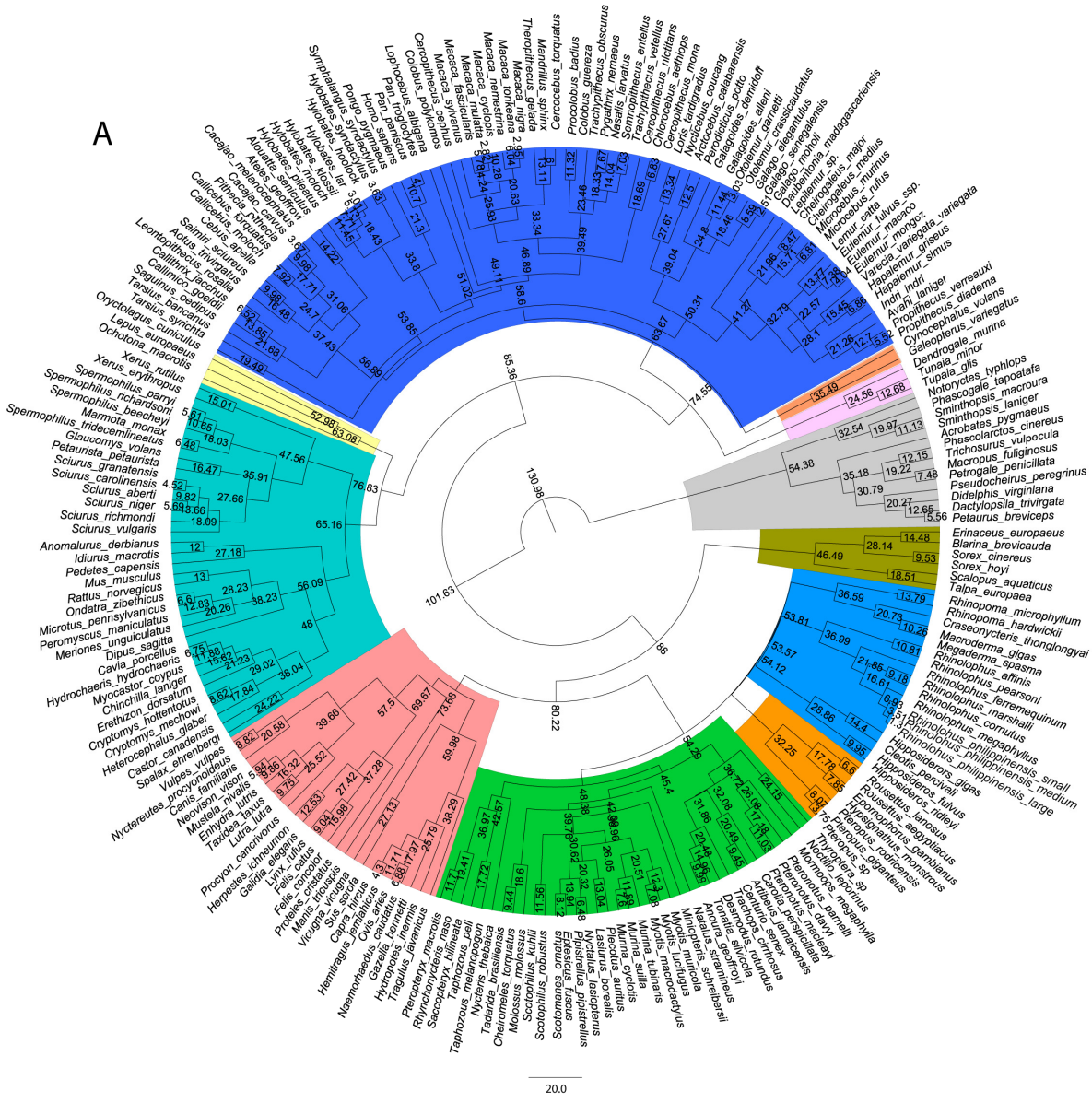

b) Tree B - follows the more recent placement of Chiroptera forming a clade with Carnivora and Perissodactyla (Nishihara *et al.*, 2006; Murphy *et al.*, 2007).

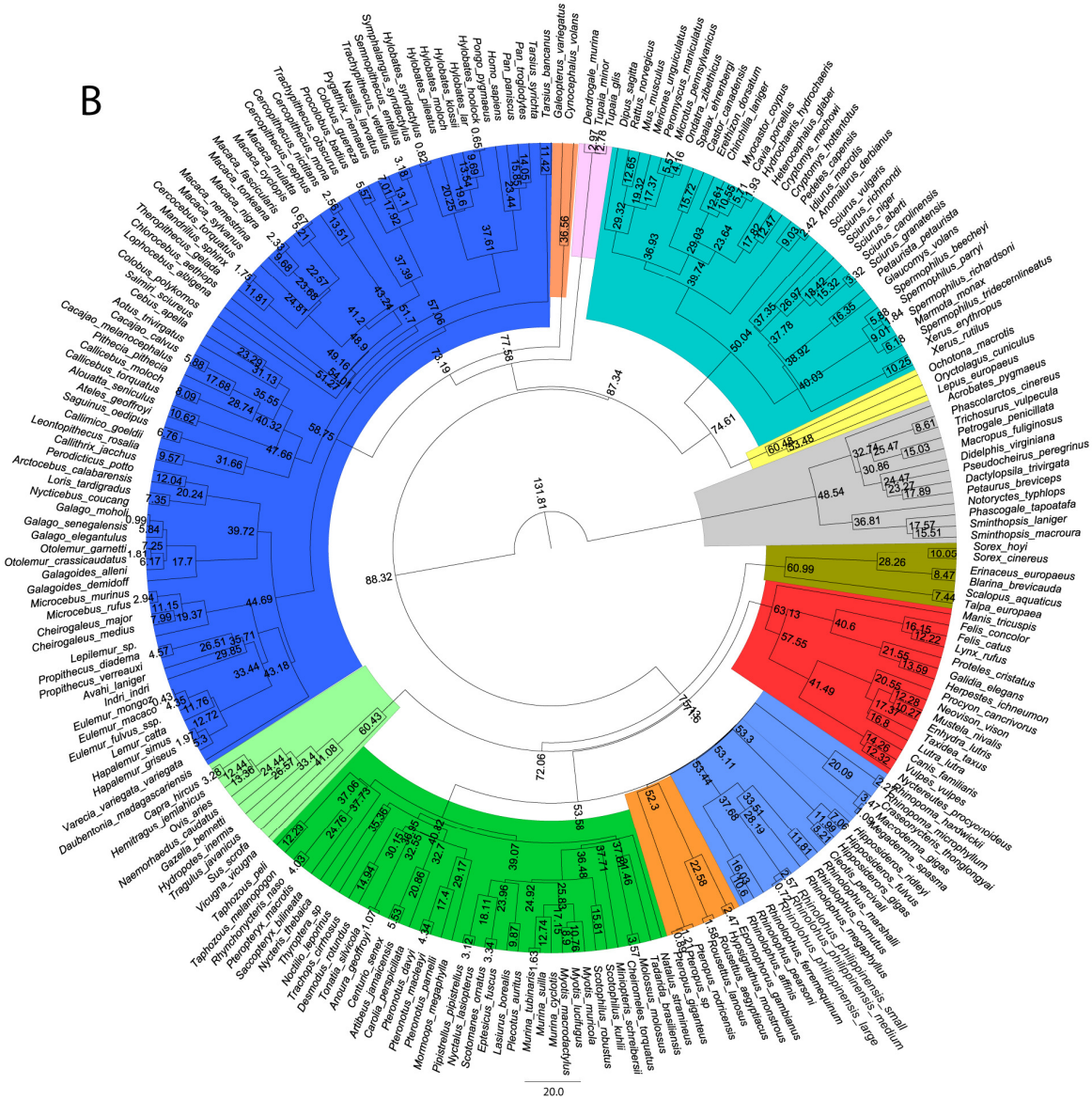

c) Tree C - The bat sub-tree.

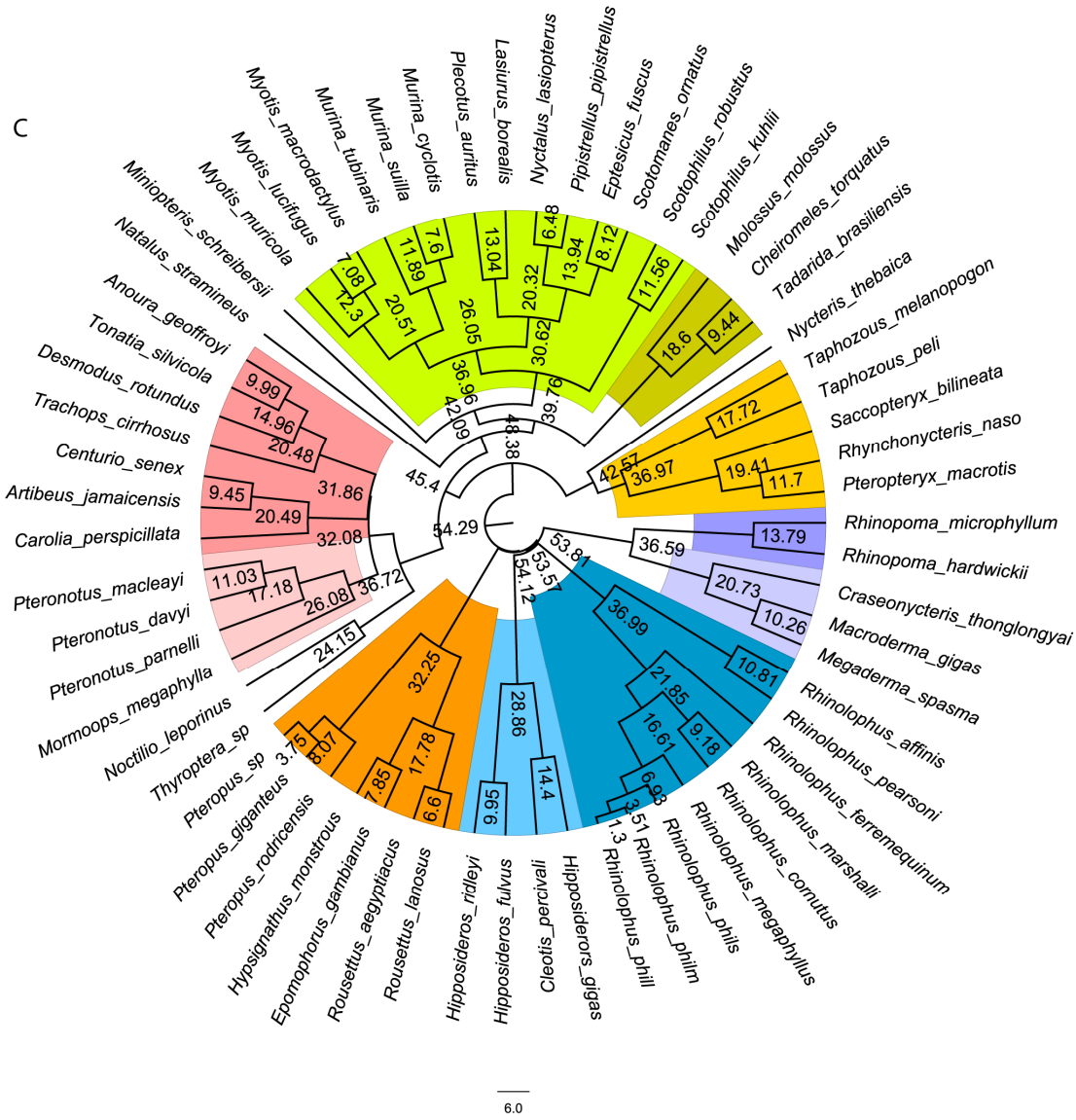

MCMCglmm

The first stage of the analysis was to construct a corresponding character matrix for the 228 species in the study that is taxonomically consistent with the above phylogeny. This character matrix consisted of log radius semicircular canals, log body mass$^{0.33}$, two different size classes and finally the clade variables.

Defining and testing effect of priors

For reasons discussed in Chapter Four, in all analyses proper priors were specified with a low degree of belief (n = 1). To determine what effect, if any, priors might have on the results, four alternative priors were tested (as detailed in Chapter Four). These initial tests of priors, based on an analysis of log radius lateral semicircular canal and log body mass$^{0.33}$, suggested little effect of priors on the results i.e. parameters were

approximately equal (Table D4). It was thus decided to use a prior where variance in semicircular canal radius was divided equally for all future runs.

Running analysis

All analyses were run with the same basic settings, with animal as the random effect and pedigree information from the dated phylogeny, proper priors with a low degree of belief and phenotypic trait variance divided equally between genetic and residual effects. All models were run with 150,000 iterations with 15,000 burn in and thinning interval of 50.

1. To test whether powered flight (and gliding), correlates with modified semicircular canal size, all bats (and gliding mammals) were designated as volant and all other mammals as non-volant.
2. To determine whether laryngeal echolocation capabilities have affected semicircular canal size, taxa were classified as echolocating or non-echolocating. The latter group was composed of Old World fruit bats and all non-echolocating mammals.
3. To test whether there is an association between semicircular canal morphology and the modes of echolocation employed, as the lineages that have evolved CF echolocation posses the most expanded cochleae, taxa were classed as CF or non-CF, with only Old World CF bats and *Pteronotus parnellii* included in the former group.
4. To test whether powered flight and different hunting strategies correlate with semicircular canal size, given that echolocating bats use more highly manoeuvrable hunting strategies than Old World fruit bats, this was used to assign different agility levels to taxa. For non-bat mammals agility scores were taken from previous studies (Spoor et al., 2007; Cox and Jeffery 2010), Old World fruit bats were assigned an agility level higher then terrestrial taxa and all echolocating bats a higher level again.

Examination of semicircular canal shape

Semicircular canal mechanics depend heavily on the size of the duct, and also the canal, the flow of fluid through the lumen is also likely to be affected by the overall shape of the canal. Therefore, semicircular canal shape was examined across all bat species. This analysis compares measurements that are independent of size and, therefore, problems associated with correcting for overall body size are negated.

Bi-variate shape analysis

Initially, to obtain a simple measure of semicircular canal shape, I calculated the ratio of canal height to canal width, using the values measured previously to calculate radius of curvature. The more circular the semicircular canal, the closer the value will be to one, whereas a more elliptical canal will yield values above or below one depending on the direction of the distortion.

Geometric morphometric analysis

To obtain more detailed shape information, I applied a geometric morphometric technique called Eigenshape Analysis (Lohmann 1983; MacLeod 1999). This technique standardises for the overall 'raw' size of an object and then maximally aligns the outline shapes so that only differences in shape are assessed. In this instance, due to the homogenous features of the semicircular canals, a standard Eigenshape analysis is sufficient to analyse the variation in shape between species.

Each semicircular canal is approximately planar, so it was possible to capture most of the shape variation by tracing a two dimensional (2D) outline along the internal edge of the canal. The 3D volumes of each specimen were rotated until the plane was maximally aligned parallel to the field of vision and then a 2D projection of this was captured and exported. The 2D images were then imported into Media Cybernetics *Image-Pro Plus* (v.5.1). Continuous outlines were captured manually, using the *capture outline* function, along the canal outline between homologous start and end points, to allow subsequent maximal alignment (Fig. 5.6). Outlines were converted into a series of 200 equally-spaced semi-landmark data points, the *x,y* coordinates of which were then exported into a text file.

Figure 5.6 Tracing semicircular canal outlines. Starting points for each canal were as follows (left to right): Anterior - point of inflection of the ampullae; Posterior - maximum point of curvature at apex of canal; Lateral - where canal projects freely from the base.

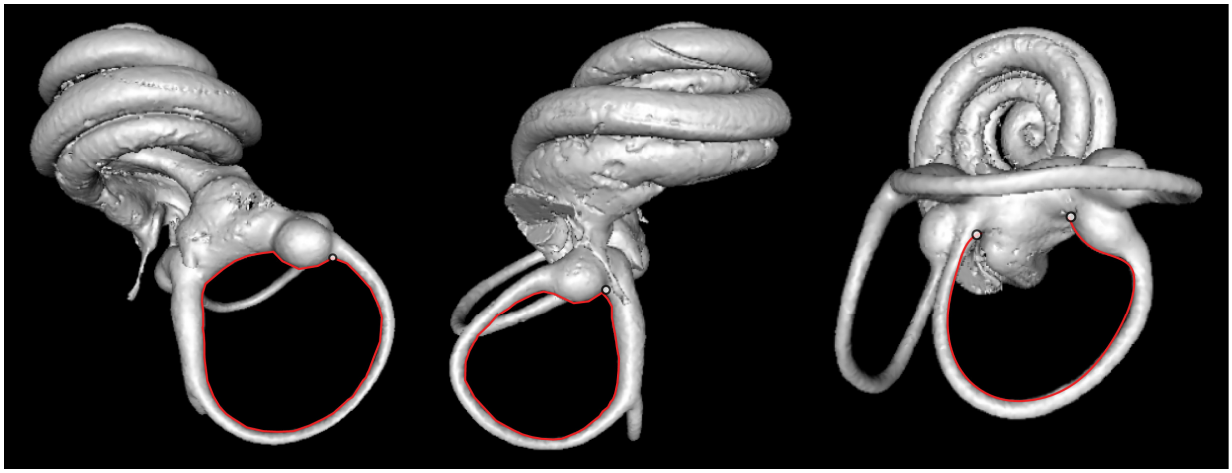

The canal shape was captured as a closed outline in the case of the anterior and posterior canals, and an open outline for the lateral canal for 55, 54 and 58 specimens respectively. The 200 coordinates used to capture the outline were higher than needed to sufficiently capture the relatively simple outline of each canal; therefore, a FORTRAN program (xy-Phi.exe, written by Prof. Norman MacLeod) was used to reduce this number to 100 points. These points were then transformed into the ϕ format (= net angular change between adjacent points around the outline, see MacLeod (1999) to remove size and increase the efficiency of the analysis. The analysis of the curve set was then carried out using the Eigenshape2.1.exe program, which implements a singular value decomposition of the pair-wise covariance matrix of ϕ shape functions. The procedure summarizes the shape variation present in the sample as a series of orthogonal multivariate vectors (Eigenshapes) expressing the set of variance-maximized shape trends. The lengths of these vectors (given as Eigenvalues) reflect the degree to which each represents the sample variance, and the projections of the original ϕ shape functions onto these vectors (given as sets of Eigenshape scores) represent a shape-similarity-ordination of the outlines. The first Eigenshape axis (ES1) represents the shape trend all outlines have in common. Subsequent Eigenshapes (ES2, ES3, ESn) represent shape-distinction trends (MacLeod 2002). Models were constructed using ESModels1(2.1).exe, which allow modes of shape change to be visualised along each axis.

A canonical variates analysis (CVA) was performed on the Eigenscores that explained 95% of the sample shape variance. Three groups were predefined – corresponding to

Old World Fruit bats, the remaining echolocating Yinpterochiroptera and the Yangochiroptera. The CVA constructs new variables that describe the relative positions of these groups within the sample, and is used to visualise the maximum extent of separation. The CVA was performed using PAST v.2.09 (Hammer *et al.,* 2001).

Relative arrangement of semicircular canals

Previous research has investigated the effect of mode of echolocation call emission (i.e. oral versus nasal) on the orientation of inner ears in relation to the palate (Pedersen 1993; Pedersen 1995; Pedersen 2007). This was studies in 57 specimens, representing 56 bat species including two size morphs of *Rhinolophus philippinensis*, by measuring the approximate angle between the anterior semicircular canal and the lateral semicircular canal (see Fig. 5.7). This was achieved by manipulating the 3D inner ear volume until the lateral semicircular canal was at the maximal horizontal position and then a two dimensional image was captured and angles measured in *Image-Pro Plus* (v.5.1). Families were coded as nasal (Rhinolophidae, Hipposideridae, Megadermatidae, Rhinopomatidae, Nycteridae and Phyllostomidae) oral (all remaining laryngeal echolocating species, including Craseonycteridae) or none (Pteropodidae) following Pedersen (1993 and 1995).

Figure 5.7 Digital endocast of the inner ear of *Cheiromeles torquatus*, x º represents the measured angle between lateral and anterior semicircular canals. Both semicircular canals are not truly planar and, therefore, this is an approximate measurement of their orientation.

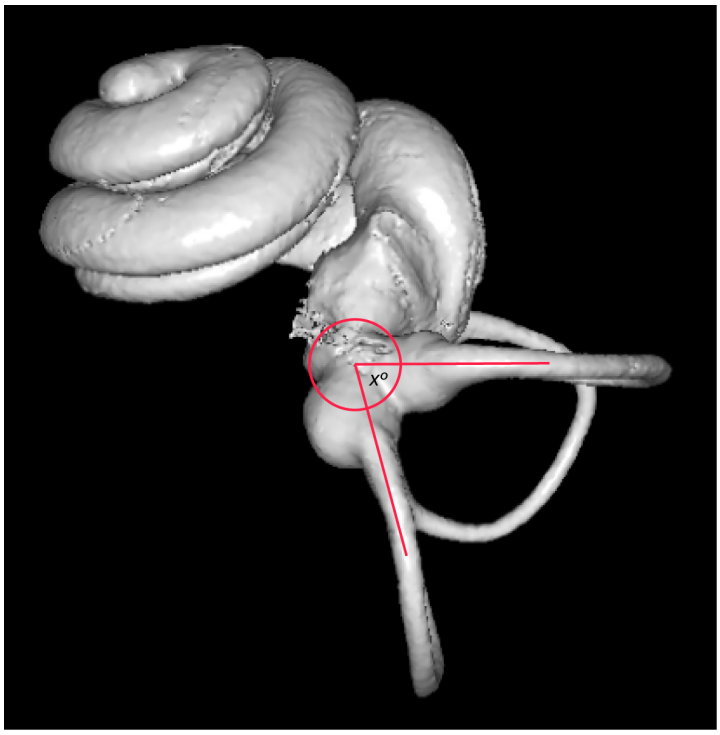

RESULTS

To study the effects that powered flight and laryngeal echolocation have had on the bat vestibular system, I compared the size and shape of the three semicircular canals across a number of echolocating bat species, the Old World fruit bats and also a phylogenetically diverse range of mammals.

Intra-individual and specific variation

Linear measurements of the anterior semicircular canal were repeated twice, for 63 specimens, and suggested that the values obtained were repeatable. Measured intra-individual variation was lower than intra-specific variation for three individuals (*Rhinolophus pearsonii, Pteronotus parnellii* and *Carollia perspicillata*) for which bilateral semicircular canals were extracted (Table D5). Therefore, in the remaining individuals only the left semicircular canal was 'extracted', or when damaged, the right. Intra-specific variation was low; therefore the use of a single species representative was justified. When multiple specimens per species were available, however, linear measurements were averaged prior to analysis, similarly where both sides of the semicircular canals were available for the same individual average values were used to avoid pseudo-replication. For Eigenshape analysis, when multiple specimens were available, one outline per species was chosen at random.

Relative semicircular canal size

The distribution of the relative size of all three canals, across 60 species, showed that the anterior semicircular canal is the largest in all Yangochiroptera and Pteropodidae studied (Fig. 5.8). Furthermore, in virtually all of these species the lateral and posterior canals were similarly sized. The principal exception to this is the vampire bat, *Desmodus rotundus,* in which the posterior was larger than the lateral semicircular canal. Within the echolocating Yinpterochiroptera, the situation was somewhat different, with all semicircular canals being similarly sized. However, in members of the horseshoe bat family, Rhinolophidae, the lateral semicircular canal was the largest, and the posterior semicircular canal the smallest. It is possible that this is linked to cochlear expansion; it is therefore interesting to note that this is not shown by *Pteronotus parnellii*, a New World species with similar cochlear expansion.

Figure 5.8 Relative size of the three semicircular canals across members of the two bat clades. (Arrow indicates *P. parnellii*).

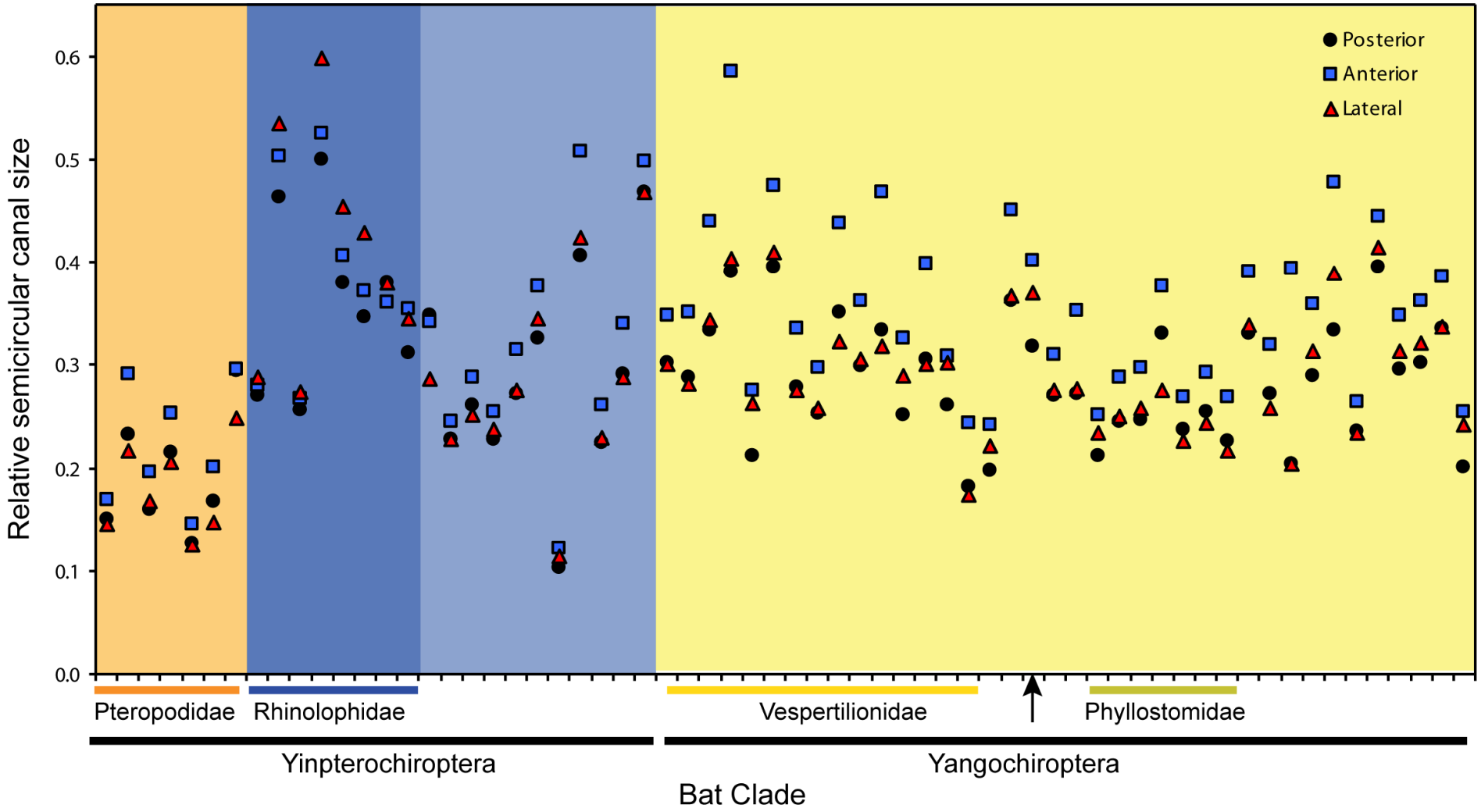

Model fitting and allometry

Published log radius of curvature (R) values, for each semicircular canal, was plotted against log body mass$^{0.33}$ (g) for 156 non-bat mammals. From initial inspection of the distribution it was not possible to determine if a continuous or discontinuous relationship best described the data. Simple linear and non-linear models were fitted to the data and Akaike information criterion (AIC) values compared; this revealed that the simple linear relationships had a significantly worse score, and more importantly, overestimated semicircular canal size at low and high body masses (Table D6). Examination of standard diagnostic plots revealed that the data were left-skewed and not strictly unimodal, and, therefore, simple linear models were rejected (Fig. D1). Although non-linear models were favoured over simple linear models based on AIC values, they poorly fitted at the two extremes of the dataset (see Fig. D2). Furthermore, there is no physiological basis to assume the relationship between semicircular canal size and body mass is non-linear.

The suitability of two discontinuous models were subsequently assessed: firstly, one with a body mass cut-off of 130g, and secondly, one that follows the natural grouping particularly evident in the lateral semicircular canal data (see Fig. D3). The body mass cut-off value (130g) was chosen arbitrarily after examination of the density plots and histograms (Fig. D1); these plots indicate a break in the data when log semicircular canal R / log body mass$^{0.33}$ is approximately zero, corresponding to a body mass of ~130 g. Following this, groups were divided, with a body mass of 130 g, being the approximate upper limit along the x-axis across all three semicircular canals, and this value also corresponds to the upper limit of the grouping along the y-axis particularly evident in the lateral semicircular canal dataset. Both discontinuous models appeared to fit the data well; however, the model following the observed grouping within the dataset had a significantly better AIC score than the one with the 130g cut-off and, therefore, was used for subsequent analyses.

Bat semicircular canal size compared to other mammals

Log semicircular canal size versus log body mass$^{0.33}$ values for echolocating and non-echolocating bat species were combined with the non-bat mammals mentioned above (Fig. 5.9). The distribution of points revealed considerable variation in semicircular canal size vs. body mass within the bat order.

Figure 5.9 Allometry of the anterior, lateral and posterior semicircular canals. 95% prediction intervals (yellow shaded regions) and 95% confidence intervals (orange shaded regions) are shown for the mammal regression lines. Old world fruit bats (yellow points); echolocating bats (blue points); mammals with body masses > 130g (grey points) and < 130g (black points).

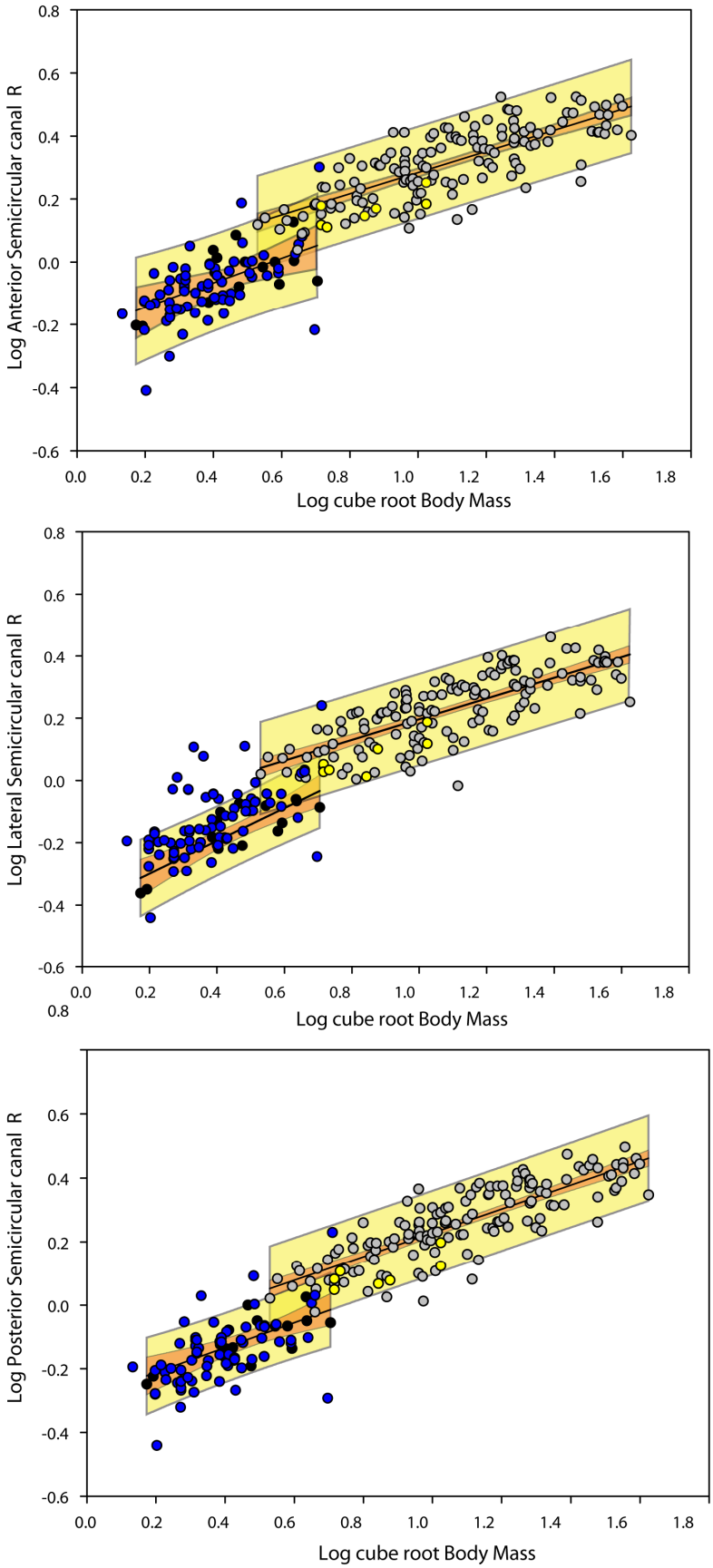

All seven Old World fruit bat species fell within the 95% prediction intervals (PI) for all three semicircular canals, and so were within the expected distribution given their weight (140g – 1.175kg). In fact all non-echolocating Old World fruit bat data points fell below the regression line for this size class, and thus it could be argued that they have slightly smaller semicircular canals than might be expected. The distribution of the points for Old World fruit bats was similar to those of the three gliding marsupials and two flying lemurs, in the dataset.

The echolocating bats superficially fitted the distribution that would be expected for their size range (2.56g – 135.5g), with most falling within the 95% PI of the anterior and posterior semicircular canals. For the anterior semicircular canal, one species fell above the 95% PI (the false vampire bat - *Cardioderma cor*) and several species fell below the 95% PI (*Cleotis percivali,* the small morph *Rhinolophus philippinensis* and the false vampire bat *Macroderma gigas*). For the posterior semicircular canal, species that fell above the 95% PI were *C. cor* and *R. megaphyllus*, and those below were *C. percivali,* the small morph *R. philippinensis, M. gigas* and also *Thyroptera sp*. The published body mass of *Cheiromeles torquatus* (135.5g.) places it at the break-point in the dataset. If this species is pooled with the other echolocating bats, then the anterior and posterior semicircular canals are much larger than expected for its size, whereas in the larger size class it falls within the 95% PI for the anterior and posterior canals, however both canals are still much larger compared to those of the similarly sized Pteropodidae.

The lateral semicircular canal radii of echolocating bats showed the most widely distributed points of all three canals. Two species, *C. percivali* and *M. gigas,* fell below the 95% PI suggesting smaller than expected lateral canals. More strikingly, a large number of echolocating bat species fell greatly above the 95% PI, suggesting much larger semicircular canals than expected given their body mass; these species included six *Rhinolophus spp*., *Rhinopoma hardwickii*, *C. cor* and *P. parnellii.*

Phylogenetic correction of eco-morphological determinants:

For each semicircular canal, I investigated the allometric scaling of the radius of curvature versus body mass after correcting for the potentially confounding effect of phylogeny. These corrections were first applied to the simple linear and the discontinuous models described previously. See Electronic Appendix D for full

equations and significance levels, with ΔDIC > 2 taken as the significance level of model improvement.

All model comparisons suggested that linear relationships with two size classes (model 1b) resulted in improved DIC values (Table 5.1) and, therefore, this model was used for all further analyses. None of the models that included either flight or laryngeal echolocation resulted in improved model fit; therefore, we can conclude that after correcting for phylogeny there was no significant effect of either trait on semicircular canal size. However, a marginally significant effect was found for the lateral semicircular canal when animals were classified as CF echolocators, other bats and other mammals (ΔDIC = 1.312 & 3.01 depending on the phylogeny used). The only semicircular canal to exhibit a significant effect of agility was also the lateral canal.

Table 5.1 Hypotheses testing with phylogenetic correction.

Model comparison:	ΔDIC ($DIC_0 - DIC_1$)					
	Anterior		Posterior		Lateral	
	Tree A	Tree B	Tree A	Tree B	Tree A	Tree B
1a Simple linear vs. 1b Size category	7.25	6.51	3.42	4.75	12.67	11.19
1b Simple linear vs. 1c Size category with interaction	-0.63	1.54	-0.77	-1.61	3.98	1.18
1b Two size categories vs. 2 Size category and flight	-1.01	-0.65	-1.04	0.66	-1.17	-1.47
1b Two size category vs. 3a Size category and echolocation	-0.98	-1.26	-0.79	-1.41	-0.35	-0.34
1b Two size category vs. 3b Size category and CF echolocation	-1.29	-1.01	-0.45	-0.43	1.31	3.01
1b Two size category vs. 4 Size category and agility	-5.39	-3.35	-2.63	-0.07	3.28	4.33

Multiple regression analyses of flight parameters

To explore the relationship between semicircular canal R, body mass and wing parameters, step-wise multiple regressions were undertaken for each canal. In each of these regressions, log semicircular canal R was fitted as the response variable, and the potential explanatory variables were log body $mass^{0.33}$, wing parameters [log wing aspect ratio (WAR), log wing loading (WL) and log wing tip shape (WTS)], and a cofactor to specify the two size classes. Body mass was included in the model as correlates with WAR and WL. In all of the above analyses, only log body $mass^{0.33}$ was found to have a significant effect (see Table 5.2a) thus, no significant relationship was found between wing parameters and semicircular canal size across all bat species. Since

the two main clades of echolocating bats (Yangochiroptera and Yinpterochiroptera) vary in the morphology and size of their vestibular systems (see Fig. 5.8), separate regressions were also fitted for these groups. Note, Old World fruit bats were excluded from Yinpterochiroptera due to differences in body mass and also their small sample size (n = 7). Regression results for Yangochiroptera revealed that both body mass and wing loading have a significant relationship with posterior semicircular canal size, and only body mass with the remaining two canals (Table 5.2). No significant relationship with wing parameters reflecting shape, i.e. aspect ratio and tip index were found. Following phylogenetic correction (using tree B), this relationship between posterior semicircular canal size, body mass and wing loading was no longer significant ($p > 0.05$). For the echolocating Yinpterochiroptera stepwise multiple regression results suggested that factors with consistent relationships with semicircular canal size were those reflecting wing-shape (WTS and WAR) (Table 5.2). After phylogenetic correction however, many of these terms become non-significant (Table 5.2b). However, visual inspection of a plot of log lateral canal size vs. log WTS (Fig. 5.10), suggest *R. philippinensis* (small morph) to be an outlier. Excluding this individual, and repeating the above analyses results in much greater support for the relationship between semicircular canal size and measures of wing-shape (Table 5.2a). After accounting for phylogenetic relatedness, analyses excluding *R. philippinensis* (small morph) were now highly significant for all three canals and both WTS and WAR (Table 5.2b). This is likely due to the small sample size being sensitive to outliers.

Figure 5.10 Relationship between log lateral semicircular canal radius vs. log WTS for echolocating Yinpterochiroptera. The potential outlier, *Rhinolophus philippinensis* small morph (grey point), falls outside the 95% prediction interval, calculated from the remaining species (black points).

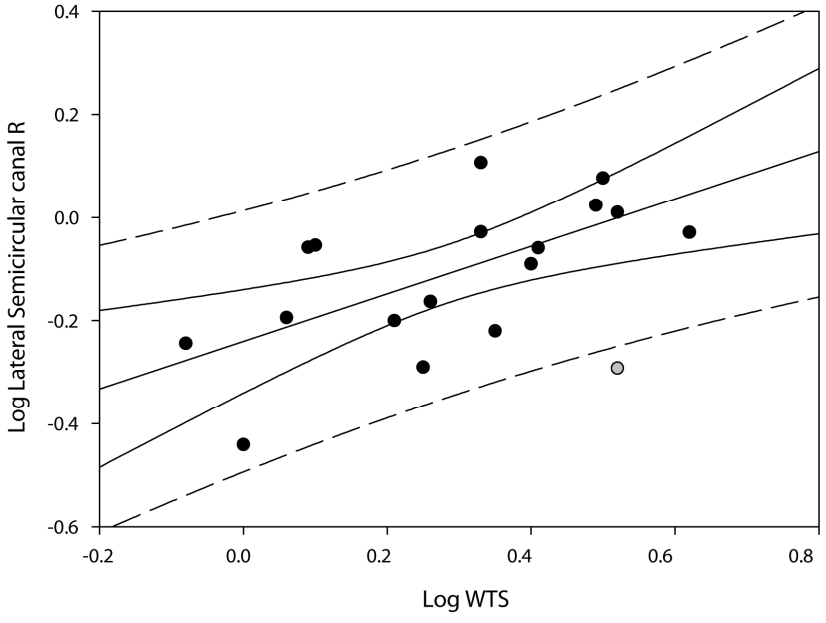

Table 5.2 Bat semicircular canal size vs. wing parameters

a) Multiple regression analysis for semicircular canal shape vs. bat wing morphology

All bats:	Mult. R^2	Adj. R^2	F (DF)	*P*
log Anterior R = 0.49 log body mass$^{0.33}$ - 0.27	0.60	0.60	89.1 (1, 59)	2.14 x 10^{-13}
log Lateral R = 0.44 log body mass$^{0.33}$ - 0.33	0.48	0.46	22.48 (2, 49)	1.19 x 10^{-7}
log Posterior R = 0.50 log body mass$^{0.33}$ - 0.34	0.59	0.59	85.85 (1, 59)	4.13 x 10^{-13}
Yangochiroptera only:	Mult. R^2	Adj. R^2	F (DF)	*P*
log Anterior R = 0.51 log body mass$^{0.33}$ - 0.27	0.55	0.53	41.94 (1, 35)	1.83 x 10^{-7})
log Lateral R = 0.57 log body mass$^{0.33}$ - 0.37	0.62	0.61	57.81 (1, 36)	5.40 x 10^{-9}
log Posterior R = 0.26 log body mass$^{0.33}$ + 0.18 log WL - 0.45	0.68	0.66	36.64 (2, 34)	3.29 x 10^{-9}, logbm$^{0.33}$ = 0.05, logWL =0.01
Echolocating Yinpterochiroptera only:	Mult. R^2	Adj. R^2	F (DF)	*P*
log Anterior R = 0.28 log WTS + 0.52 log WAR- 0.61	0.33	0.23	3.43 (2, 14)	0.06, logWTS = 0.06, logWAR= 0.08
log Lateral R = 0.37 log WTS - 0.23	0.26	0.21	5.61 (1, 16)	0.03,
log Posterior R = 0.30 log WTS + 0.59 log WAR - 0.71	0.40	0.31	4.65 (2, 14)	0.03, logWTS = 0.04, logWAR= 0.04
Echolocating Yinpterochiroptera excl. *R .philippinensis*:	Mult. R^2	Adj. R^2	F (DF)	*P*
log Anterior R = 0.38 log WTS + 0.55 log WAR - 0.65	0.554	0.486	8.08 (2, 13)	0.01, logWTS = <0.01, logWAR = 0.03
log Lateral R = 0.50 log WTS + 0.56 log WAR - 0.71	0.567	0.506	9.18 (2, 14)	0.003, logWTS = <0.01, logWAR = 0.04
log Posterior R = 0.41 log WTS + 0.62 log WAR - 0.75	0.615	0.556	10.4 (2, 13)	0.002, logWTS = <0.01, logWAR = 0.01

b) Models parameters with phylogenetic correction using Tree C, *P*-values are based on MCMC results.

Clade	Model	*P*	*P*	DIC
Yangochiroptera:	log Posterior R = 0.35 log BM$^{0.33}$ + 0.15 log WL - 0.45	*p*(log BM$^{0.33}$) 0.03	*p*(log WL) 0.06	-107.84
Yinpterochiroptera incl. *R .philippinensis*:	log Anterior R = 0.30 log WTS + 0.51 log WAR - 0.62	*p*(log WTS) 0.06	*p*(log WAR) 0.08	-21.49
	log Lateral R = 0.38 log WTS + 0.51 log WAR - 0.65	” 0.04	” 0.14	-19.48
	log Posterior R = 0.30 log WTS + 0.60 log WAR - 0.72	” 0.06	” 0.05	-22.45
Yinpterochiroptera excl. *R .philippinensis*:	log Anterior R = 0.40 log WTS + 0.55 log WAR - 0.66	*p*(log WTS) <0.01	*p*(log WAR) 0.02	-33.58
	log Lateral R = 0.44 log WTS + 0.55 log WAR - 0.69	” <0.01	” 0.04	-33.91
	log Posterior R = 0.39 log WTS + 0.62 log WAR - 0.75	” <0.01	” 0.01	-33.14

Relative cochlea and semicircular canal size

Log relative semicircular canal size (i.e. radius of curvature) was plotted against log relative cochlea size for each bat together with 40 non-bat mammals (data from Spoor *et al.,* 2002). Ordinary Least Squares (OLS) regression lines with 95% confidence and prediction intervals were fitted to the non-bat data and the bat values were then superimposed (Fig. 5.11, see Appendix D for values from this study). OLS and reduced major axis (RMA) regression of the 40 non-bat placental and marsupial mammal species revealed slopes of the relationship between log relative cochlea size and log relative semicircular canal size are all approximately one (Table 5.3a). Figure 5.11 shows that, for all three semicircular canals, Old World fruit bats fall very close to the regression lines and are within the PI. Similarly, species from Megadermatidae are also close to the line of best fit for the non-bat mammals, especially in the case of the lateral semicircular canal. By comparison, for the remaining echolocating bats, points for all three canals fell below the line of best fit, but generally within the PI. The exceptions to this are the Old World CF bats and *Pteronotus parnellii,* as points for their anterior and posterior canals fell below the PIs. These results suggest that echolocating bats have relatively large semicircular canals and cochleae. Whereas in most mammals there is an isometric relationship between the two inner ear components, this is not the case in CF bats, which have relatively larger cochleae compared to semicircular canals. After correcting for phylogenetic relatedness, the effects of Old World CF bats are significant across all three canals. However, when *P. parnellii* was included together with the CF bats, models were only significant for anterior and posterior canals (Table 5.3b).

Table 5.3 Log relative semicircular canal size and log relative cochlea size.

a) Results of OLS and RMA regression for 40 non-bat placental and marsupial mammal species.

Regression	Model parameters	R^2	Significance
OLS	log Rel. Lateral = 1.03 log Rel. cochlea - 0.33	0.89	F = 322.08, $P = 3.48 \times 10^{-20}$
RMA	log Rel. Lateral = 1.09 log Rel. cochlea - 0.29	0.90	T = 17.95, $P = 3.47 \times 10^{-20}$
OLS	log Rel. Anterior = 1.07 log Rel. cochlea -0.21	0.91	F= 383.11, $P = 1.91 \times 10^{-21}$
RMA	log Rel. Anterior = 1.12 log Rel. cochlea -0.17	0.91	T= 19.54, $P = 2.02 \times 10^{-21}$
OLS	log Rel. Posterior = 1.00 log Rel. cochlea -0.30	0.90	F= 354.51, $P = 7.29 \times 10^{-21}$
RMA	log Rel. Posterior = 1.06 log Rel. cochlea -0.26	0.90	T= 18.80, $P = 7.69 \times 10^{-21}$

b) Model comparisons following phylogenetic correction.

Comparison	ΔDIC ($DIC_0 - DIC_1$)					
	Anterior		Posterior		Lateral	
	Tree A	Tree B	Tree A	Tree B	Tree A	Tree B
Effect of Old World CF bats	4.16	4.14	2.28	2.45	2.49	2.45
Effect of all CF bats	2.25	2.28	2.78	3.18	0.53	0.57

Figure 5.11 Relative semicircular canal size vs. relative cochlea size across a range of mammals. OLS regression (bold line) of non-bat mammals is shown with 95% confidence (solid line) and prediction (dashed line) intervals. Non-bat placental mammals (grey circles) and marsupial mammals (grey triangles) from Spoor *et al*. (2002). Pteropodidae (orange circles), Megadermatidae (light blue circles), Yangochiroptera (green circles), *Pteronotus parnellii* (yellow circle), Rhinolophidae (dark blue circles), and remaining echolocating Yinpterochiroptera (medium blue circles) represent the bat species included by this study.

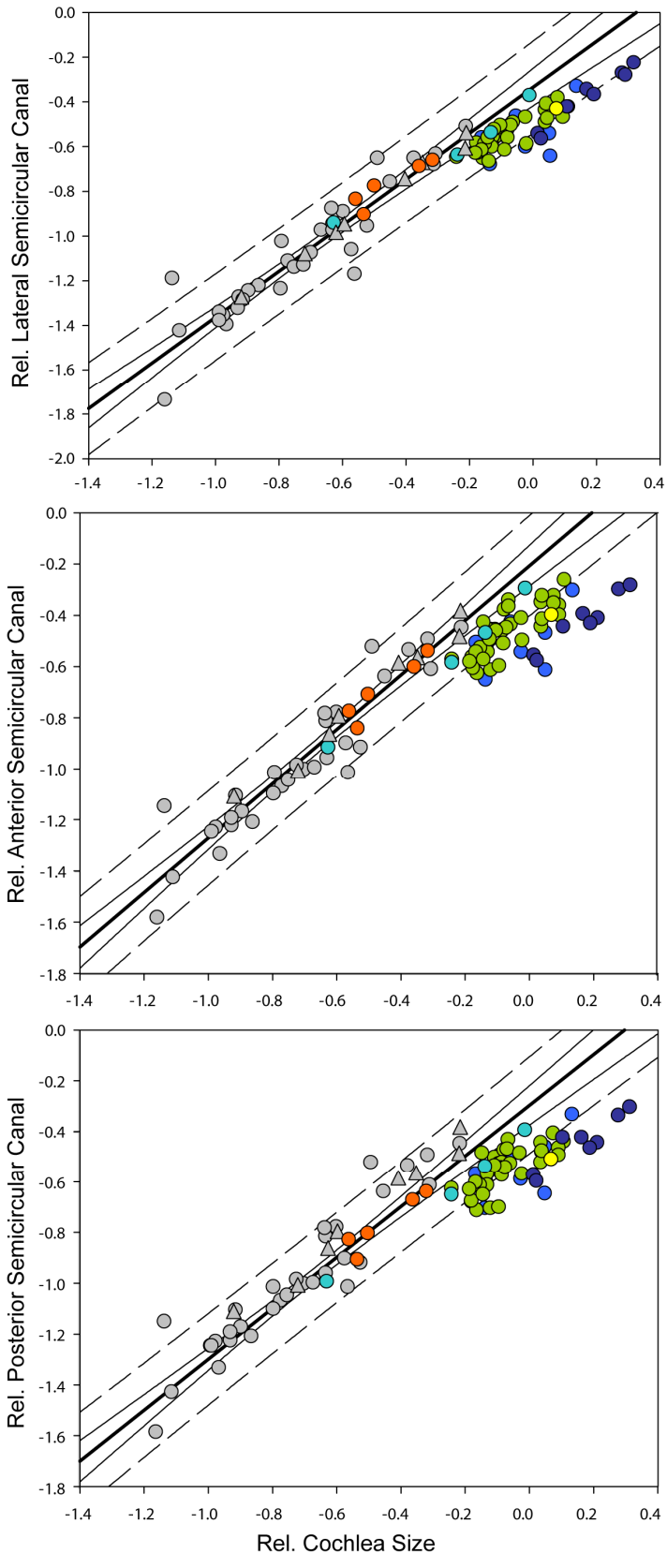

Bi-variate shape analysis

To initially assess variation in semicircular canal shape, ratios between canal height and width were calculated. Box-plots of these ratios show considerable differences between species and also between the three canals (Fig. 5.12). Group mean ratios suggested that the posterior semicircular canal is the most circular across all clades, and that the anterior and lateral semicircular canals are more elliptical (Table 5.4a). Following Bonferroni corrections for multiple tests, anterior semicircular canal shape differs significantly between Old World fruit bats and echolocating Yinpterochiroptera ($P = 8.3 \times 10^{-5}$), but not between Old World fruit bats and Yangochiroptera ($P = 0.44$) (Table 5.4b). Furthermore, there was also a significant difference between the shape of anterior canals between echolocating Yinpterochiroptera and Yangochiroptera ($P = 0.01$). Examination of the mean ratios suggested that echolocating Yinpterochiroptera had more elliptical anterior semicircular canals than either of the other two groups. The mean ratio of lateral semicircular canals of echolocating Yinpterochiroptera and Yangochiroptera were found to be similar, however, both clades of echolocating bats had significantly different shaped lateral semicircular canals compared to Old World fruit bats ($P = 0.029$ and $P = 0.023$), again suggesting that echolocating bats have more elliptical canals. No significant difference in the mean posterior semicircular canal ratio was found between any of the three groups.

Figure 5.12 Box and whisker plots of mean semicircular canal ratios shape, for Old World fruit bats (orange), echolocating Yinpterochiroptera (blue) and Yangochiroptera (yellow). The median ratio (solid lines) and the mean ratio (dashed lines), 25th and 75th percentiles (boxes) and 10th and 90th percentiles (whiskers) with all outliers shown.

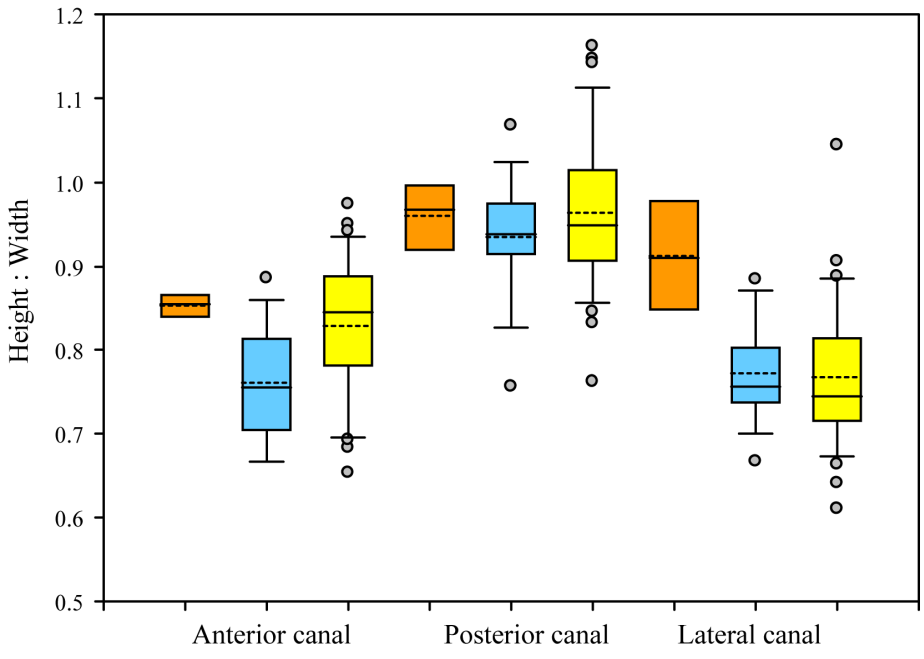

Table 5.4 Mean semicircular canal shape for Old World fruit bats, echolocating Yinpterochiroptera and Yangochiroptera.

a) Values correspond to group mean ± standard deviation, minimum and maximum value (sample size).

	Anterior semicircular canal	Lateral semicircular canal	Posterior semicircular canal
Old World	0.854 ± 0.016	0.913 ± 0.075	0.960 ± 0.042
Fruit bats	0.831 - 0.875 (5)	0.818 - 1.020 (5)	0.936 - 1.013 (5)
Echolocating	0.760 ± 0.068	0.772 ± 0.058	0.935 ± 0.071
Yinpterochiroptera	0.667 - 0.886 (18)	0.700 - 0.885 (19)	0.756 - 1.068 (18)
Yangochiroptera	0.830 ± 0.083	0.767 ± 0.089	0.964 ± 0.090
	0.693 - 0.974 (33)	0.610 - 1.044 (34)	0.762 - 1.162 (33)

b) Significance tests of mean semicircular canal shape across Old World fruit bats, echolocating Yinpterochiroptera and Yangochiroptera. *P*-values following Bonferroni correction for multiple tests, are given in order for anterior, lateral and posterior semicircular canal comparisons.

Comparison (A, L, P)	Old World Fruit bat	Echolocating Yinpterochiroptera	Yangochiroptera
Old World Fruit bat	-	8.3×10^{-5}, 0.03, 1.00	0.44, 0.02, 1.00
Echolocating Yinpterochiroptera	2.8×10^{-5}, 0.01, 0.34	-	0.01, 1.00, 0.63
Yangochiroptera	0.15, 0.01, 0.87	0.003, 0.82, 0.21	-

Eigenshape analysis

Eigenshape analysis was used to quantify the shape variation shown by the outline of each semicircular canal. Species values for Eigenshapes 1 to 3 (ES1-3) for anterior, lateral and posterior semicircular canals were plotted, models calculated to represent shape change along each axis (Figures 5.13a-b). Canonical variates analysis of the three semicircular canals utilised the shape variation represented by Eigen-axes 1-20, corresponding to 95% of the total sample variance (Fig. 5.14).

Beginning with the anterior semicircular canal, ES1-3 together corresponded to over half of the sample variance (Total variance = 56.6%). Models suggest ES1 represents a transition from a rounded to a more compressed canal. Along ES2 the majority of shape change appears to occur around the ampullae of the canal, with a transition from a prominent ampulla and narrow-pointed apex to one with a flattened ampulla and a wider canal apex. ES3 represents a narrowing of the top and bottom of the canal with corresponding expansion of the side opposite the ampulla. Plots of CV1-2 for the anterior semicircular canal sample showed clear and significant separation between Old World fruit bats and echolocating bats (Wilks' $\lambda = 0.139$, DF = 42 & 66, $P = 0.0002$), with some overlap between the two groups of echolocating bats (Fig. 5.14).

Figure 5.13 Results of Eigenshape analysis of the three semicircular canals.

a) Models representing shape change along the first three Eigenshape axes. Shaded lines indicate low to high values along each axis (black – light grey). Anterior models: ES1 (-0.2, -0.1, 0, 0.1, 0.2); ES2 (-0.2, -0.1, 0, 0.1, 0.2); ES3 (-0.2, -0.1, 0, 0.1, 0.2); Lateral models: ES1 (-0.4, -0.2, 0, 0.2, 0.4); ES2 (-0.3, -0.15, 0, 0.15, 0.3); ES3 (-0.15, -0.1, 0, 0.1, 0.15); Posterior models: ES1 (-0.25, -0.1, 0, 0.1, 0.25); ES2 (-0.25, -0.1, 0, 0.1, 0.25); ES3 (-0.15, -0.1, 0, 0.1, 0.15);

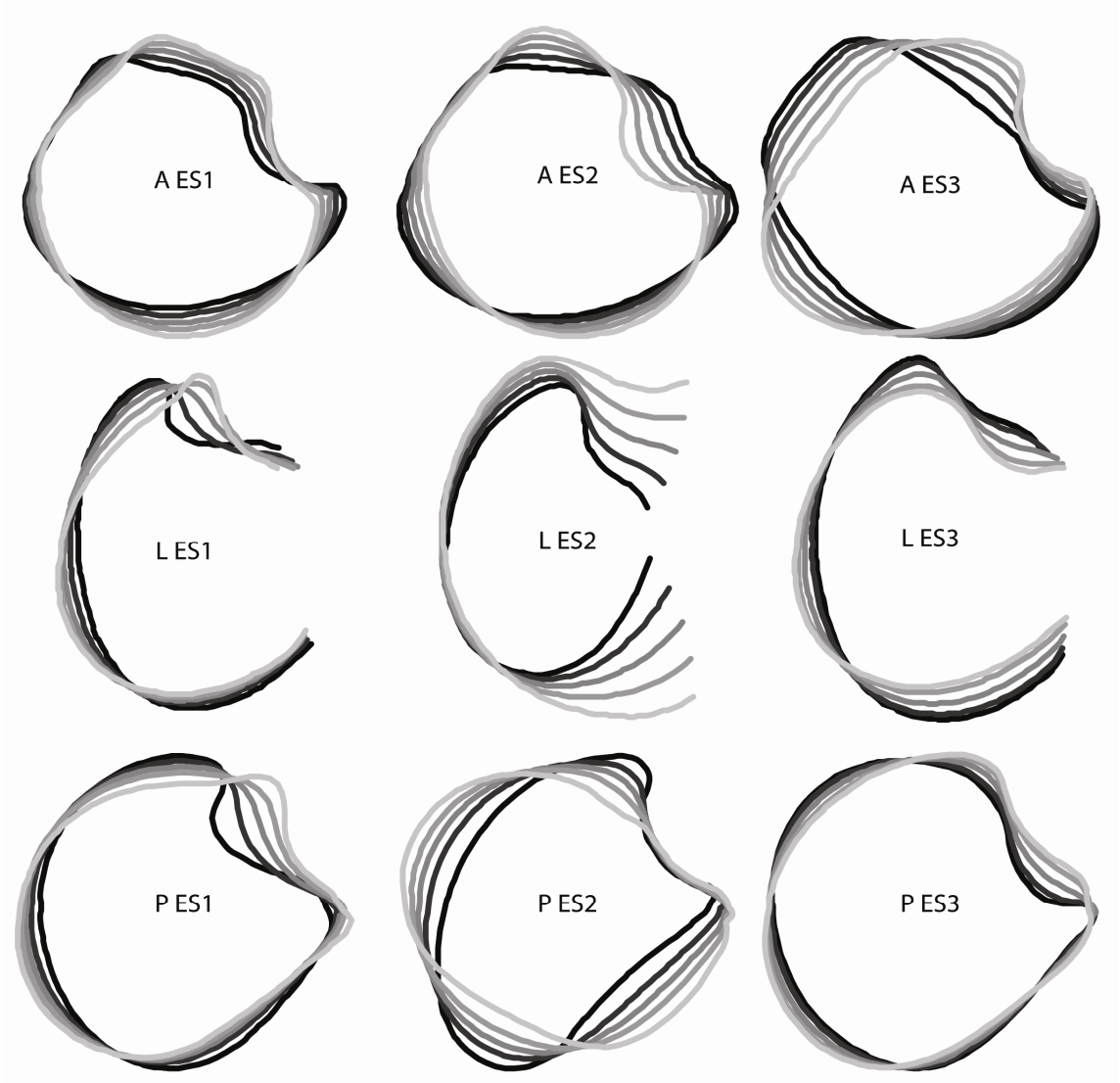

b) ES1-3 plots for the three semicircular canals (anterior, lateral and posterior). Bat species are colour coded as follows: Old World fruit bats (orange squares), echolocating Yinpterochiroptera (blue diamonds), horseshoe bats (dark blue diamonds) and Yangochiroptera (yellow circles) species.

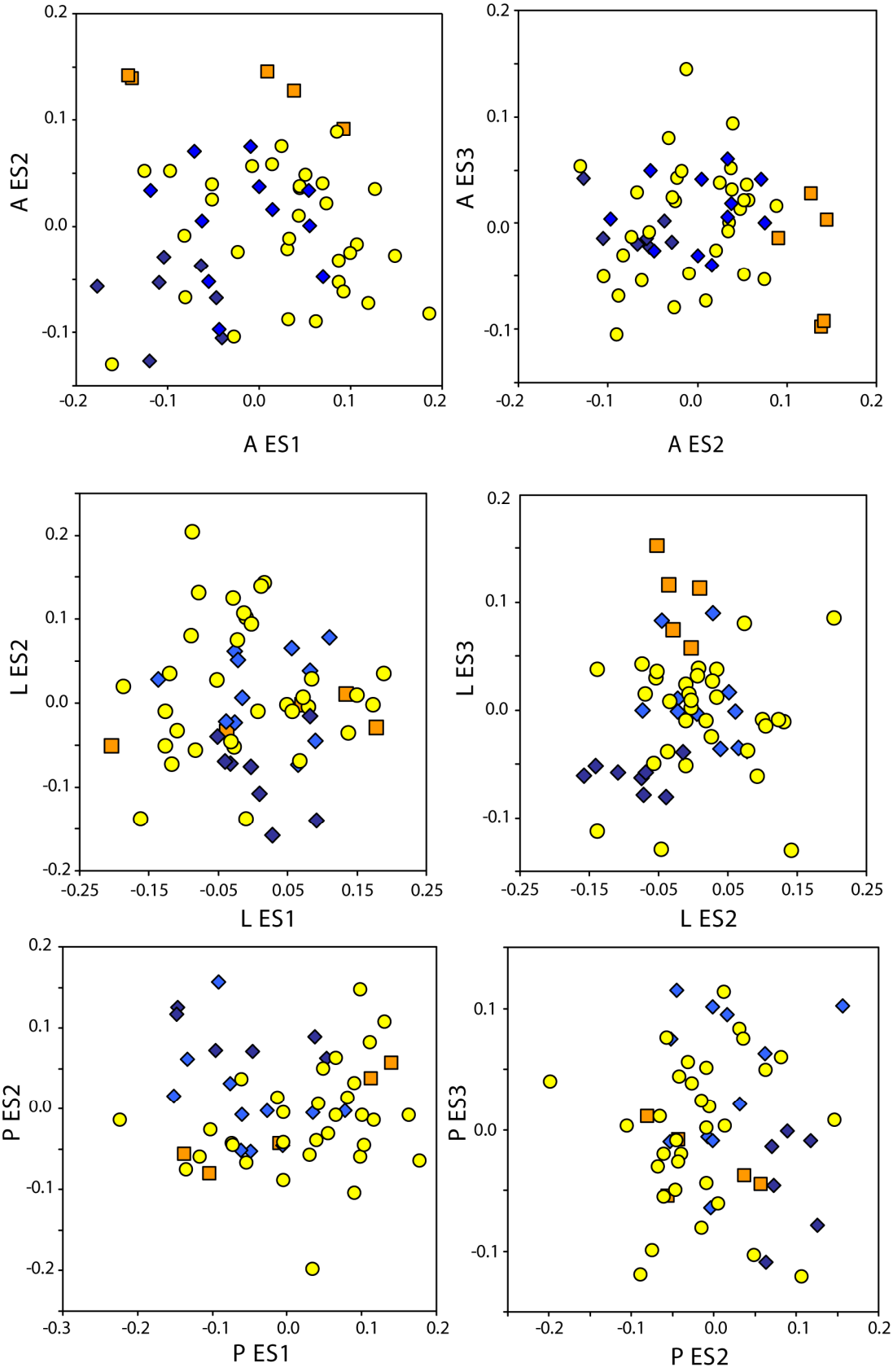

Figure 5.14 Canonical variates analysis of Eigenshape 1-20 for the three semicircular canals. Bat species are colour coded as follows: Old World fruit bats (orange squares), echolocating Yinpterochiroptera (blue diamonds), horseshoe bats (dark blue diamonds) and Yangochiroptera (yellow circles) species.

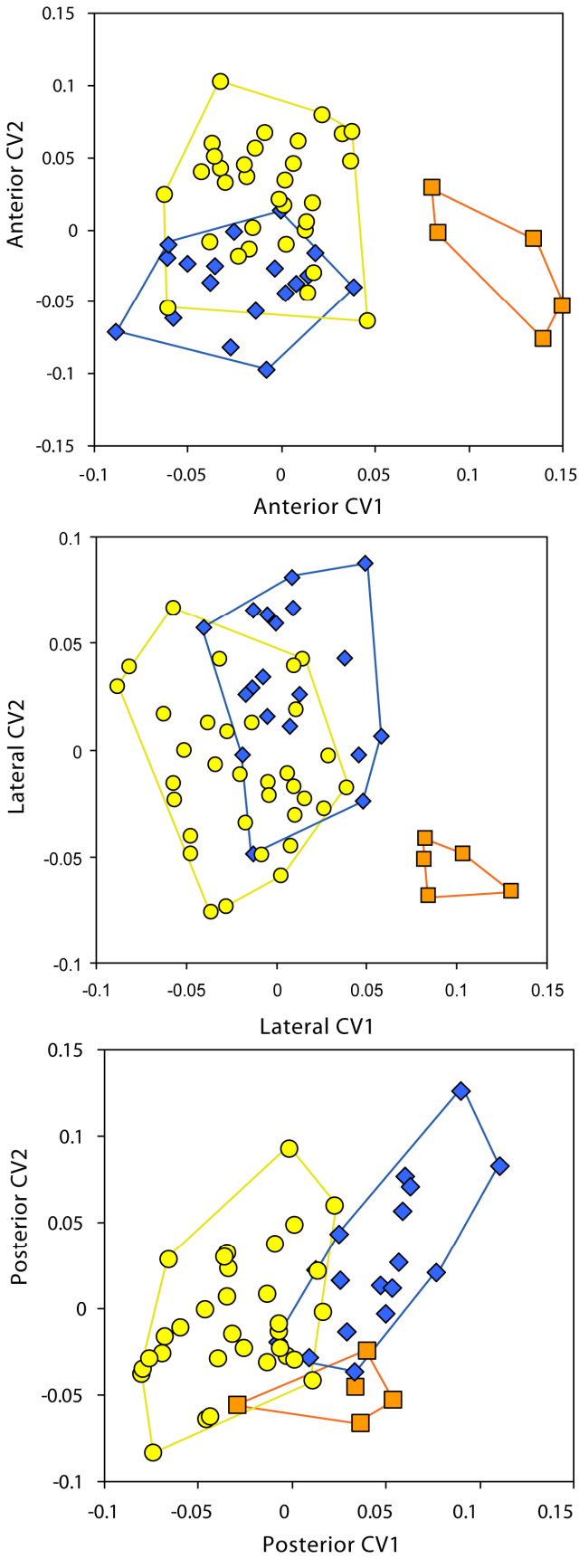

Plots and corresponding models for lateral canals revealed considerable variation in canal shape (Fig. 5.13a). Alone, ES1 accounted for 48.0% of total variance. Horseshoe bats were located at the high end of ES1 and the low end of ES2; models suggest this corresponds to flattened ampullae with a narrow gap between the canals. ES3 appeared to be most informative in separating Old World fruit bats from echolocating species. Models suggest this axis corresponds to a transition from smoother rounder canals to those that are wider and more elliptical. The CVA of lateral semicircular canals showed a clear separation of the Old World fruit bats from the remaining bats, but with a larger overlap between echolocating species. Again, this separation was significant (Wilks' $\lambda = 0.214$, DF = 40 & 70, $P = 0.005$).

Together ES1-3 corresponded to over half the total sample variance of the posterior canals (Total variance = 60.9%). Models along ES1 and ES2 suggested high levels of shape variation along these axes. ES2 concerned a shift from a long narrow canal to one that is rounder i.e. shorter and wider. The shape variation expressed by ES1 and ES3 seemed to be focused on similar regions of the canal – most change occurred around the ampullae. The posterior semicircular canal CVA showed minimal sample overlap of all three groups, however, the grouping was significant (Wilks' $\lambda = 0.209$, DF = 40 & 64, $P = 0.011$).

Semicircular canal shape versus body and cochlea size

To investigate whether the observed shape changes relate to functional changes in sensitivity or structural constraint, the above measures of semicircular canal shape were regressed against values of bat body mass and relative cochlea size (see Table 5.5). Only lateral semicircular canal shape was found to show a significant relationship with body mass [log lateral semicircular canal shape = 0.16 log body mass$^{0.33}$ - 0.18]. This positive trend suggests that as bat body size increases then the ratio of canal height to width also increases, and eventually exceeds one. Both anterior and lateral canal shape had a significant negative relationship with relative cochlea size (Table 5.5) [log anterior semicircular canal shape = -0.09 log relative cochlea - 0.10] and the lateral canal [log lateral semicircular canal shape = -0.11 log relative cochlea - 0.12]. These negative trends suggest that as the relative cochlea size increases the ratio of these two canals decreases and, therefore, tend to a more elliptical shape.

Table 5.5 Significance levels of the relationship between semicircular canal shape (h/w) with body mass and cochlea size.

Shape vs.		Mult.R^2	Adj. R^2	F-statistic (DF)	*P*-value
Body mass	Anterior	0.027	-0.002	0.91 (1, 53)	0.345
	Lateral	0.374	0.363	32.84 (1, 55)	4.362×10^{-7}
	Posterior	0.065	0.047	3.67 (1, 53)	0.061
Relative cochlea size	Anterior	0.123	0.106	7.41 (1, 53)	0.009
	Lateral	0.192	0.177	13.07 (1, 55)	0.001
	Posterior	0.006	-0.013	0.32 (1, 53)	0.572

Relationships between canal shape and measures of cochlea and body size were further explored using species values for ES1-3 (Table 5.8). For the anterior canal, ES2 and body mass had a significant positive relationship [Anterior ES2 = 0.16 log body mass$^{0.33}$ - 0.07] and a negative relationship with relative cochlea size [Anterior ES2 = -0.23 log relative cochlea - 0.02]. Examination of the models along this axis, suggest that the largest animals or those with the smallest relative cochlea have the most circular canals (see Fig. 5.15).

For the lateral canal, values for Eigenshape 2 and 3 had a significant negative relationship with body mass [Lateral ES1 = 0.23 log body mass$^{0.33}$ - 0.09, Lateral ES3 = -0.16 log body mass$^{0.33}$ + 0.07] and Eigenshape 3 had a positive relationship with relative cochlea size [Lateral ES3 = 0.19 log relative cochlea + 0.02]. Examination of the models along this axis, suggest that as either body mass increases or relative cochlea size decreases, there seems to be lateral expansion of the semicircular canal (see Fig. 5.15).

None of the first three Eigenshape axes for the posterior canal had a significant relationship with body mass. Only Eigenshape 1 had a marginally significant negative relationship with relative cochlea size [Posterior ES1 = -0.16 log relative cochlea - 0.01]. Examination of models suggests that as relative cochlea size increases then there is lateral constriction of the canal (see Fig. 5.13). The above significant models were then re-run, this time correcting for the phylogenetic relatedness of species (Table 5.7). After phylogenetic correction only lateral semicircular canal relationships involving ES3 remained significant, as did the relationship between anterior ES2 and relative cochlea size.

Table 5.6 Semicircular canal shape vs. animal size

a) Significance levels of the relationship between semicircular canal shape and body mass.

ES vs. Body mass	Multiple R^2	Adjusted R^2	F-statistic	*P*-value
Anterior ES1	0.010	-0.009	0.511 (1, 53)	0.478
Anterior ES2	0.197	0.182	12.99 (1, 53)	0.001
Anterior ES3	0.027	0.008	1.46 (1, 53)	0.233
Lateral ES1	0.225	0.211	15.99 (1, 55)	1.92×10^{-4}
Lateral ES2	0.024	0.006	1.36 (1, 55)	0.249
Lateral ES3	0.261	0.248	19.45 (1, 55)	4.84×10^{-5}
Posterior ES1	0.018	-0.001	0.95 (1, 51)	0.334
Posterior ES2	0.032	0.013	1.70 (1, 51)	0.198
Posterior ES3	0.059	0.040	3.19 (1, 51)	0.080

b) Significance levels of the relationship between semicircular canal shape and relative cochlea size.

ES vs. Cochlea	Multiple R^2	Adjusted R^2	F-statistic	*P*-value
Anterior ES1	0.032	0.014	1.74 (1, 53)	0.193
Anterior ES2	0.377	0.365	32.09 (1, 53)	6.16×10^{-7}
Anterior ES3	0.009	0.009	0.49 (1, 53)	0.486
Lateral ES1	0.061	0.044	3.60 (1, 55)	0.063
Lateral ES2	0.001	-0.017	0.078 (1, 55)	0.781
Lateral ES3	0.366	0.354	31.72 (1, 55)	6.28×10^{-7}
Posterior ES1	0.089	0.071	5.00 (1, 51)	0.030
Posterior ES2	0.021	0.002	1.11 (1, 51)	0.297
Posterior ES3	0.007	-0.012	0.38 (1, 51)	0.541

Table 5.7 Linear regressions between semicircular canal shape with body mass and relative cochlea size following phylogenetic correction.

ES vs. Body mass	*p*(log body mass$^{0.33}$)	DIC
Anterior ES2 = 0.11 log body mass$^{0.33}$ - 0.05	0.039	-183.74
Lateral ES1 = 0.15 log body mass$^{0.33}$ - 0.04	0.061	-143.51
Lateral ES3 = -0.19 log body mass$^{0.33}$ + 0.09	< 4e-04	-192.63
ES vs. relative cochlea size	*p*(log rel. cochlea)	DIC
Anterior ES2 = -0.20 log rel. cochlea - 0.02	< 4e-04	-184.87
Lateral ES3 = 0.18 log rel. cochlea + 0.02	<4e-04	-172.91
Posterior ES1 = -0.14 log rel. cochlea - 0.02	0.106	-116.09

Figure 5.15 Plots of semicircular canal shape versus two measures of size – body mass and relative cochlea size. Shape vs. relative cochlea size (yellow points) and shape vs. body mass (grey points). AES, PES and LES refer to the corresponding Eigenshape of the anterior, posterior and lateral canals. Solid lines represent the OLS regression, and dashed lines the 95% confidence interval. Models represent shape change along the axis.

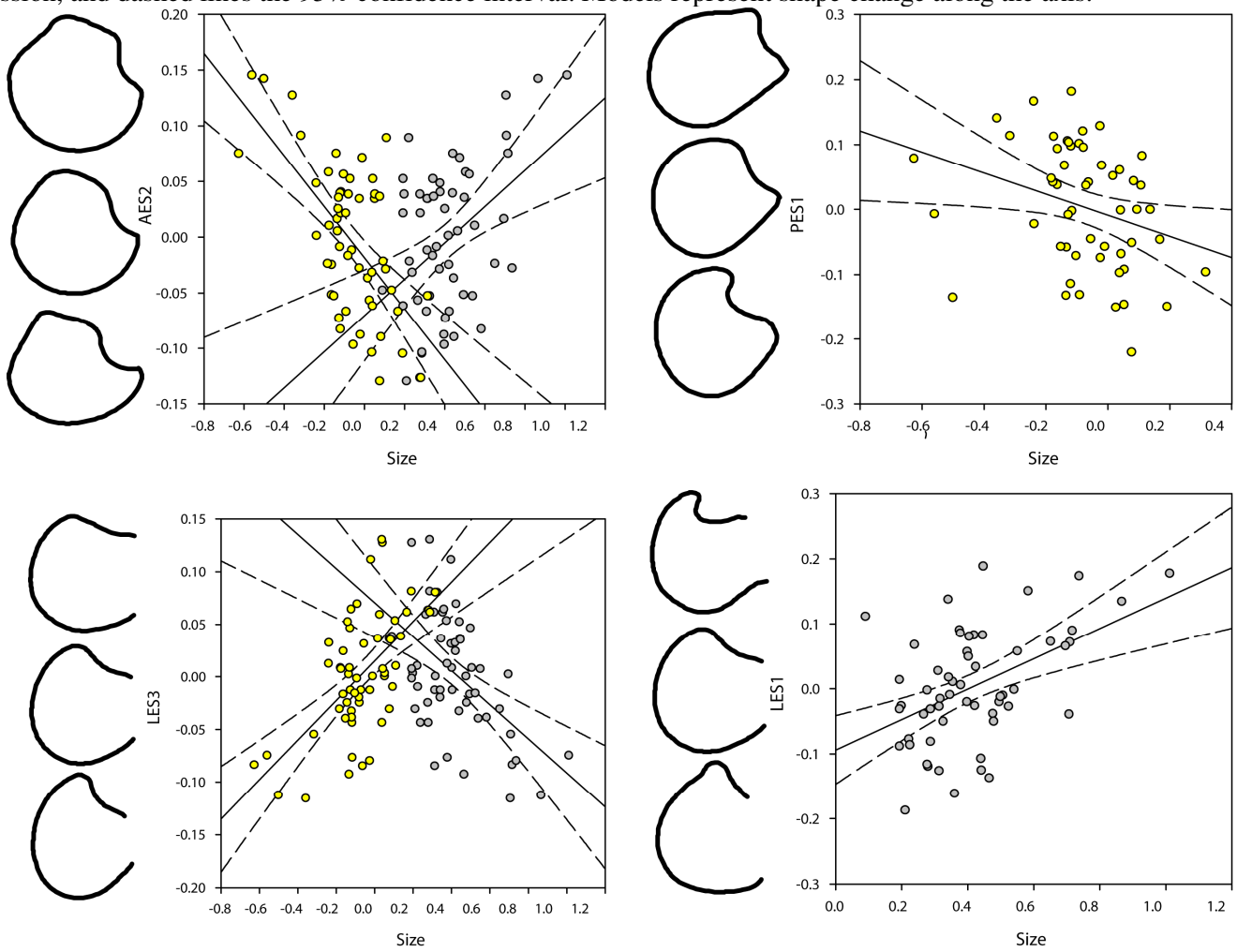

Relative arrangement of semicircular canals

Box and whisker plots of the angle between lateral and anterior semicircular canals are shown for each bat clade (Yinpterochiroptera and Yangochiroptera), with groups defined by call emission (none, oral and nasal) (see Fig. 5.16 and Appendix D). These plots suggest that Old World fruit bats are the group with the largest angle between canals which most closely approximates 90º and, therefore, an orthogonal relationship between canals. Non-echolocating Old World fruit bats (n = 5) have a significantly wider mean angle between canals compared to echolocating bats (n = 52) ($\bar{x}_1 = 86.53$, $\bar{x}_2 = 73.05$, t = 2.61, DF = 4, $P = 0.030$). Generally, oral emitters (n = 26) were seen to have a greater angle between canals than nasal emitters (n = 26) ($\bar{x}_1 = 75.23$, $\bar{x}_2 = 70.87$, t = 2.16, DF = 47, $P = 0.018$). Anecdotally, *Craseonycteris thonglongyai* - the sole oral emitting Yinpterochiroptera species - has a larger angle than its nasal emitting relatives (n = 18). Within Yangochiroptera, although the oral emitters have a larger angle between canals ($\bar{x}_1 = 74.76$, n = 25) it is not significantly wider than that of the nasal emitters ($\bar{x}_1 = 70.03$, n = 8) (t = 1.69, DF = 10, $P = 0.062$).

Figure 5.16 Box and whisker plots of the measured angle between the lateral and anterior semicircular canals for oral and nasal emitting echolocating bats. The median angle (solid lines) and the mean angle (dashed lines), 25th and 75th percentiles (boxes), 10th and 90th percentiles (whiskers) and all outliers are shown for the different groups which are represented by different colours.

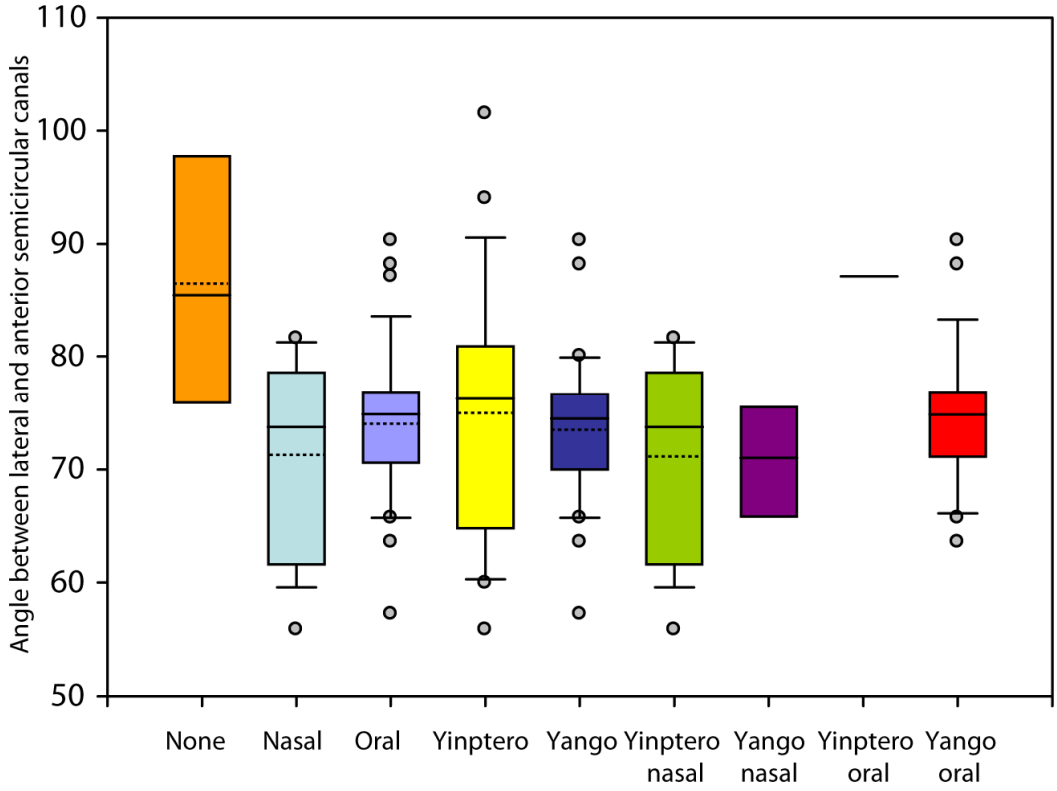

DISCUSSION

Phylogenetic comparative studies (Harvey and Pagel 1991) are frequently employed to reveal functionally relevant morphological adaptations, often by examining the adaptive significance of phenotypic variation within a phylogenetic context. However, such methods are prone to complications by inconsistent scaling parameters across taxa, which can arise from divergent selection pressures or physical constraints acting on particular groups of species. For example, these issues are likely to be especially true of mammals, which range in body mass from approximately 2g to over 80,000kg (Hill 1974; Tershy 1992; Jurgens 2002). Earlier studies have adopted different approaches to take into account this extreme variation; for example, by calculating separate allometric relationships for different size classes (e.g. Nummela 1995), by grouping all taxa into a single class (e.g. Spoor *et al.,* 2007), or by limiting the sample to terrestrial placental mammals thus omitting fully volant and aquatic species (e.g. Silva and Downing 1995).

In this study, I applied new methods in comparative phylogenetics to a wide spectrum of mammal species to test whether the acquisition of echolocation and flight has been associated with modifications in the vestibular system of bats. Values for as many species as possible were collected, taxa were grouped by body mass, and separate class allometries calculated. A previous study found similar scaling differences in middle ear bones across animals with different skull sizes (Nummela 1995), while a lack of correlation between semi-circular canal size and body mass in short-tailed shrews, *Blarina brevicauda,* has also led to suggestions of differential scaling properties in species of different size (Welker *et al.,* 2009). In this study, I found support for a difference in scale between large and small non-flying taxa that was robust to phylogenetic correction. At the same time, however, I found no strong evidence for models with different allometries (i.e. slope gradients) within each group following phylogenetic correction, suggesting that although there might be changes in overall magnitude, the negative allometrical relationship is of the same order. This suggests there are different constraints acting on species; and thus the size categories adopted here, although perhaps imperfect, are justified. Although there was some overlap of size range between classes, this could be due to taxonomic constraints, and body mass data taken from published sources will always contain a certain amount of error.

Bat semicircular canal size and shape

Compared to non-flying mammals, bats showed greater variation in semicircular canal size relative to their body mass. In particular the horseshoe bats (Rhinolophidae) were found to have proportionally large lateral canals for their body mass. At the same time, however, these bats, as well as other echolocating bats to a lesser extent, were found to possess small canals relative to the size of their expanded cochleae. Furthermore, horseshoe bats that possess very large relative cochleae were characterised by more elliptical canals. I found additional evidence of modified canal shape in relation to body mass, again suggesting more elliptical canals in smaller species. This pattern was found to be most clear in the anterior and lateral semicircular canals, which tend to be the largest in most mammals. Therefore, in the case of the bats studied here, it seems there is evidence of spatial competition between the semicircular canals and the expanded cochlea in echolocating bats. It has previously been hypothesised that low body mass correlates with structural constraints of the semicircular canals. For example, it was predicted that smaller animals would have increased out-of-plane torsion i.e. deviation from planar and circular form in order to fit inside the petrous part of the temporal bone; so far however, little supporting evidence has been found (Schmelzle *et al.,* 2007; Cox and Jeffery 2010). This suggests that the additional complication of the hypertrophic cochleae combined with small body size seen in echolocating bats presents more extreme spatial constraints that are not seen in other similarly sized mammals.

Exactly what effect shape has on semicircular canal sensitivity is currently unclear. It has been suggested that a move away from circularity towards a more elliptical shape leads to a decrease in sensitivity, however, it is predicted that very extreme deviations from circularity are needed to significantly reduce sensitivity (McVean 1999; Cox and Jeffery 2010). It also seems that deviations from circularity can be counteracted with an increase in internal lumen radius (McVean 1999). Therefore, it might be expected that very small animals may have proportionally wider semicircular ducts.

Bat semicircular canal size and flight

Across all bat species no significant signature of flight was found. However, lateral semicircular canals were shown to correlate with agility when echolocating bats were assigned heightened agility over Old World fruit bats. This supports previous findings that the lateral canal is most strongly correlated with locomotor ability in mammals (e.g. Cox and Jeffery 2010). Separate analyses of the two clades of echolocating bats, found strong evidence that semicircular canal size of echolocating Yinpterochiroptera

correlates with wing shape and not body mass. This could reflect the fact that the vestibular systems of the Rhinolophidae and Hipposideridae have become adapted to slow manoeuvrable flight in cluttered environments. Alternatively, the correlation between wing shape and semicircular canals could in a sense be spurious and be an artefact of the enlarged cochleae of Rhinolophidae and Hipposideridae, whereas, the semicircular canal size of Yangochiroptera strongly correlates with body mass, and thus this could be the major constraint in this clade. Additionally a positive correlation was found between posterior semicircular canal size and wing loading, with smaller canals associated with species with lower wing loading, though, this relationship was not significant after phylogenetic correction. The posterior semicircular canals are responsible for monitoring rotation of the head in the sagittal plane i.e. the vertical plane which divides the body into left and right sections and so could be involved in monitoring movement during flight. Bat species with high wing loading are able to fly faster and so may require more sensitive canals.

A large body of work has mathematically characterised wing morphology in bats and birds, and correlated this with flight performance (Norberg 1981; Norberg and Rayner 1987; Norberg *et al.,* 2000). Correlates have been found between wing morphology, resource partitioning, echolocation call, habitat use and population structures (Aldridge and Rautenbach 1987; Kingston *et al.,* 2000; Miller-Butterworth *et al.,* 2003; Hodgkison *et al.,* 2004). Such wing measurements originate from the field of aerodynamics, and while can be applied with some success to rigid bird and insect wings, may not be suitable for bat flight membranes that show unique flexibility and elastic properties (Swartz *et al.,* 2003). Furthermore measurements taken directly from outstretched wings of stationary bats may not reflect the true surface-area during flight (Swartz *et al.,* 2003), while measurements taken from fluid-preserved specimens may be affected by shrinkage. Values used in this study were from several sources and so may suffer from the associated errors, for example, different methods utilised for recording ‘wing area’, such as inclusion of the back or tail membrane (see examples within Norberg 1981). Wing loading depends on body mass, therefore, some within-species variation due to gender and seasonal fluctuations should be expected, which introduces error. These are all potential reasons for the limited correlation between semicircular canal size and wing parameters, particularly in Yangochiroptera, aside from the possibility that there genuinely is little correlation.

Speculation that large canals are associated with heightened agility were recently supported by experimental evidence that larger canals confer increased vestibular-nerve afferent sensitivity (Yang and Hullar 2007). It is apparent, however, that when attempting to explain evolutionary patterns of vestibular system morphology and locomotion, contradictions emerge, for example, cetaceans are agile yet have reduced canals, and moles show restricted movements yet have enlarged semicircular canals. Therefore, it is not true to say universally that more agile animals have larger semicircular canals. Previous studies that found strong correlations between semicircular canal radius and agility (Spoor et al., 2007; Cox and Jeffery 2010) tested the hypothesis by assigning each taxon to one of six agility categories (extra slow – fast) based on field observations, literature and video footage. However, such categories are somewhat subjective, and define the pace of movement more than agility itself. 'Agility', in a true sense should measure all components of movement, and, therefore, combines aspects of balance, coordination, reflexes and ease of movement, which might result in oversimplification. For example in Cox and Jeffery (2010) echolocating bats, grey squirrels and gibbons have the same agility score. It could also be argued that flying or aquatic mammals are considerably more agile then any terrestrial mammal. At the other extreme, sloths are the slowest, and are grouped with certain primates and dugongs (Spoor et al., 2007; Cox and Jeffery 2010).

Given that previous studies found birds to have larger semicircular canals than mammals or dinosaurs, and volant birds to have larger semicircular canals than non-volant forms (Sipla 2007), it is perhaps surprising that within mammals there is no clear indication that all bats have larger semicircular canals compared to non-volant mammals. This was also true of previously sampled gliding mammals (Spoor *et al.,* 2007). This apparent inconsistency could arise for many reasons, including differential physiological constraints acting on the phylogenetically disparate groups and that birds have generally undergone more dramatic modifications for flight. Furthermore, birds like pterosaurs, which also had enlarged semicircular canals (Witmer *et al.,* 2003) are aerial predators and, therefore, principally rely on visual cues for orientation. Evidence also suggests that birds can isolate their visual and vestibular systems from some movements of the body, i.e. accelerations due to linear and angular displacement, during locomotion (Warrick *et al.,* 2002). Birds also have much simpler and smaller cochleae (Walsh *et al.,* 2009) and, therefore, there may not be the same spatial constraints hypothesised to exist within the skulls of mammals.

The vestibular system, echolocation and vision

Measurements found that the mean angle between the anterior and lateral semicircular canals in nasal echolocation call emitters was lower than that in oral emitters. The mean angle between the anterior and lateral canals in Old World fruit bats was the most similar to 90º; which is the assumed condition in most mammals. Therefore, my findings are in agreement with previous studies that concluded that the different emission modes require different optimal head orientations (Pedersen 1993). Furthermore, the different emission modes are likely to affect the orientation of the lateral semicircular canal; because typically a horizontal orientation is desired (Pedersen 1993; Witmer *et al.,* 2003). Observations of bats in flight and terrestrial locomotion suggest that individuals actively maintain their heads in a horizontal position (for examples see Horowitz *et al.,* 2004; Riskin *et al.,* 2006). In the majority of analyses, all aspects of semicircular canal morphology were shown to be more similar between the two clades of echolocating bats, typically to the exclusion of the Old World fruit bats. Compensatory cervical reflexes are crucial for stabilisation of gaze (Warrick *et al.,* 2002), and morphological convergence in the cervical vertebrae and roosting behaviour of the two clades of echolocating bats (to the exclusion of Old World fruit bats) has previously been shown (Fenton and Crerar 1984). These features likely account for some of the similarities found between the semicircular canals of the two clades of echolocating bats. It is difficult to directly compare echolocation ability with semicircular canal morphology, particularly given the evidence suggesting the size and shape of the semicircular canal may be affected by hypertrophic cochleae of echolocating bats. It therefore becomes difficult to determine which modifications are adaptive and which represent structural constraints. However, research involving *Eptesicus fuscus* suggested that echolocation can provide additional input information to the vestibular system (Horowitz *et al.,* 2004), therefore, there may indeed be some sensory association between the two systems.

Given the putative variation in reliance of vision during orientation and prey location in bats, coupled with function constraints on the neck, it should be possible to determine a functional association with semicircular canal size and vision in bats. However, as quantitative values of visual acuity in bats are currently unavailable, only a qualitative assessment is possible. The four false vampire bats (Megadermatidae) show unusual patterns in all bi-plots of semicircular canal morphology compared to the other laryngeal echolocating bats, especially *Cardioderma cor,* which has large semicircular

canals for its body mass. The African species of Megadermatidae (including *C. cor* and *Lavia frons*) possess exceptionally large eyes and pinnae compared with other insectivorous bats (Csada 1996). Furthermore, it is postulated that this family use visual cues for hunting and prey detection (references cited within Fiedler 1979; Ratcliffe *et al.,* 2005). Solid empirical evidence supporting the use of vision over passive listening remains scant (Ratcliffe *et al.,* 2005), however, if the Megadermatidae do use visual cues for prey acquisition then this could partly explain the unusual canal sizes. Interestingly, *C. cor* has the largest eyes, followed by *L. frons* and then the remaining species - which follows the pattern of semicircular canal size variation seen. Another consistent anomaly *Cheiromeles torquatus* – the aptly named giant naked bat - is the largest echolocating bat (by mass), lacks typical fur and has relatively large and obvious eyes (Leong *et al.,* 2009). All Molossids are known to fly very quickly, and of these *C. torquatus* has possibly the fastest flight speed and is thought to be a hawker with low manoeuvrability (Hassanloo *et al.,* 1995; Heller and Volleth 1995). The individual studied here has the largest absolute anterior semicircular canals of the bats studied, which may reflect its hunting strategy. Eye size in bats varies widely across species, from being very small in some echolocating species to large in the Old World fruit bats (as summarised in Eklöf 2003). Some bats may use vision for long distance migration (Suthers and Wallis 1970; Orbach and Fenton 2010). Several echolocating bat species use visual inputs for aspects of orientation and prey detection (Bell 1985). Most bats have intact shortwave opsins, tuned to UV light (Zhao *et al.,* 2009a; Shen *et al.,* 2010), while all have functional rhodopsin pigments, enabling vision in dim-light (Zhao *et al.,* 2009b; Shen *et al.,* 2010). Therefore, given the disparity in visual acuity across bat species, coupled with the role of vision stabilization of the semicircular canals it seems likely that this will be another potential source of adaptive variation across species.

Most bats perform daily manoeuvres, such as landing at roost sites, involving complex, rapid movements as well as adopting postures with feet over heads (Riskin *et al.,* 2009). While roosting in up-side-down positions, bats are able to echolocate, feed, groom and sleep. An experiment exposing *Carollia perspicillata* to microgravity environments found that, unlike other species (i.e. rabbits, rats and cats), bats did not display righting behaviour, and instead adopted a highly controlled posture providing stability (Fejtek *et al.,* 1995). This suggests that their behavioural reflexes are very different to terrestrial mammals when exposed to changes in acceleration. At least two bat species, *Desmodus rotundus* and *Mystacina tuberculata,* are capable of terrestrial locomotion (Riskin *et al.,*

2006), with others, such as *C. torquatus,* being capable of quadrupedal locomotion with considerable agility (Leong *et al.,* 2009). Several bat physiological systems show anatomical adaptations for their roosting habit, e.g. the digestive system (Ofusori *et al.,* 2008), various adhesive structures (Thewissen and Etnier 1995), cervical vertebrae (Fenton and Crerar 1984) and feet anatomy (Leong *et al.,* 2009). Therefore, it is highly likely, given the evidence presented here, bats' vestibular systems have undergone similar adaptations (and also structural constraints) to allow behavioural flexibility in the changing environments that they face daily.

Further work:

A possible caveat in the allometric scaling of mammalian semicircular canal size, using body mass, is that in relation to non-volant species, bats, particularly echolocating species, might be under selective constraints for small body mass (Jones 1999; Maurer *et al.,* 2004). However, bat bones are relatively denser compared to terrestrial mammals, and so skeletons contribute disproportionally to the total body mass (Dumont 2010). Furthermore, other potential measures of body size are arguably equally problematic; for example: cranial measures vary with diet (Freeman 1988), brain size with both foraging technique (Hutcheon *et al.,* 2002) and mating system (Pitnick *et al.,* 2006), and forearm length with wing shape and foraging ecology (Norberg and Rayner 1987). Insectivorous bats may also have smaller relative brain size compared to those of frugivorous bats (Eisenberg and Wilson 1978; Armstrong 1983).

Semicircular canal sensitivity is related to overall canal size (Yang and Hullar 2007), however, it remains unclear how other parameters - such as internal radius, the total volume of fluid and the canal shape - may affect sensitivity. Therefore, all these measures are important considerations for future studies. Although canal shape was investigated in this study, out-of-plane torsion was not; therefore, future three-dimensional analysis may more accurately measure shape variation and spatial constraints across species.

Unfortunately, due to the poor availability of specimens this study was not able to document any soft-tissue features. It is technically much more difficult to study the intact soft-tissue features, as they are frequently damaged during dissection and suffer from shrinkage and distortion during fixation. This was the principal reason that

detailed measures of visual acuity were omitted from this study. Currently, there are very few published measures of bat vision available. Previously, orbit size was used as a proxy (e.g. Goudy-Trainor and Freeman 2002). Although this was also attempted here, it had limited success due to the preservation state of spirit specimens. As experimentally and behaviourally derived values of visual acuity become available, it might thus be possible to study this further. Within the vestibular system, further structures that would be ideal subjects for comparative studies are the eminentiae cruciatae (which divide the anterior and posterior cristae into equal parts (Kirkegaard and Jorgensen 2001) and have been postulated as convergent adaptation for flight (Horowitz *et al.,* 2004)). This structure has been described as well developed or present in a limited number of bat species (e.g. Ramprashad *et al.,* 1980; Kirkegaard and Jorgensen 2001), but it is suggested to be lacking or rudimentary in other mammals (Igarashi and Yoshinob 1966) and so warrants further investigation.

Conclusions

The hypothesis that all bats have larger semicircular canals compared to non-volant mammals was not supported. No difference was found between semicircular canal size of non-echolocating Old World fruit bats and other mammals; conversely, the size of semicircular canals of echolocating bats was highly variable. In particular the vestibular systems of the horseshoe bats, Rhinolophidae, seem to be highly modified in both size and shape, and contrary to other mammals, their lateral semicircular canals are the largest. No consistent relationship between wing morphology and semicircular canal size was found across all bat species. However, a phylogenetically robust significant relationship was found between semicircular canal size and wing shape in echolocating Yinpterochiroptera. Whether the modifications seen in the echolocating Yinpterochiroptera vestibular system represent adaptations for highly manoeuvrable flight, or physical constraints due to cochlear expansion, remain unclear and warrant further work.

Collectively, laryngeal echolocating bats were found to have modified semicircular canals compared to non-echolocating Old World fruit bats. This, combined with the similarities between Old World fruit bat semicircular canals and non-echolocating mammals, this could provide additional support to the hypothesis that Old World fruit bats were never capable of sophisticated echolocation.

CHAPTER SIX

GENERAL DISCUSSION

This comparative study examined patterns of molecular and morphological evolution associated with the acquisition of high-frequency hearing in mammals, based on inferences about function drawn from two protein-coding genes, non-coding regulatory regions and the gross structure of the inner ear. As well as documenting species specific adaptations, one of the ultimate aims was to see if the newly generated evidence could be used to infer which of the two competing scenarios regarding the evolution of laryngeal echolocation in bats is more likely. Briefly, these are either at least two independent origins or one gain in the common ancestor of all bats followed by loss in the Old World fruit bats.

i. Functional 'hearing genes'

The molecular evolution of two putative mammalian 'hearing' genes was examined in Chapter Two. Both genes, *Tmc1 and Pjvk*, showed evidence of positive selection on branches of the echolocating Yinpterochiroptera, and, in *Tmc1,* positive selection was also detected in the Yangochiroptera. Furthermore, positive selection was detected in echolocating cetaceans in both genes. Conversely, *Tmc1 and Pjvk*, were both found to be under purifying selection in Old World fruit bats, and furthermore, no evidence of positive selection was found on the bat common ancestor branch. Convergent amino acid substitutions were found between members of the two main clades of echolocating bats, and also between these and the bottlenose dolphin, *Tursiops truncatus*. The strongest evidence of convergent substitutions was between species of *Hipposideros* and *Kerivoula,* two genera containing species with the highest currently known echolocation calls (Francis and Habersetzer 1998; Schmieder *et al.,* 2010). Strong evidence of convergent substitutions was also seen in *Tmc1* between the two bat species that have independently evolved constant frequency echolocation.

This brings the total number of mammalian 'hearing' genes examined across echolocating mammals to four: *Gja1, Prestin*, *Tmc1* and *Pjvk.* With the exception of *Gja1,* which was found to be highly conserved across both echolocating and non-echolocating taxa (Wang *et al.,* 2009), the remaining three showed similar patterns of molecular evolution. The three genes, *Prestin*, *Tmc1* and *Pjvk*, which are either

necessary or essential for normal outer hair cell (OHC) function (Marcotti *et al.,* 2006; Schwander *et al.,* 2007; Dallos *et al.,* 2008) showed strong evidence of many convergent substitutions, with associated positive selection, in echolocating taxa that have independently evolved echolocation.

ii. Conserved Non-coding Elements

Examination of the substitution rates of highly Conserved Non-coding Elements (CNEs) putatively associated with genes, many of which are transcription factors, involved in the regulation of the development of mammalian auditory systems revealed several interesting patterns (Chapter Three). CNEs from two gene regions (*Shh* and *Tshz1*) showed increased substitution rates in all bats examined, while one region (*Hmx2/*3) showed increased rates only in echolocating bats. CNEs from five gene regions (*Bhlhb5, Emx2, Meis2, Sox21* and *Zic2*) showed higher substitution rates only in the Yangochiroptera. While, CNEs from four gene regions (*Fign, Lhx1, Meis1* and *Pax2*) showed higher substitution rates only in the dolphin. Rates of nucleotide substitution in CNEs, associated with *Hmx2/*3, were shown to be particularly high in Vespertilionidae, and in particularly *Kerivoula spp*. and *Murina spp*.

The functional significance of increased substitution rates in CNEs is somewhat unclear, but could suggest that the development of the auditory system in each of the groups, i.e. echolocating Yinpterochiroptera, Yangochiroptera, and toothed whales, involves subtlety different regulatory pathways. In line with previous studies (Kim and Pritchard 2007), however, without corroborating experimental evidence, putative associations between increased substitution rates of CNEs, gene expression and functional effects must be viewed tentatively.

iii. Cochlea morphology

For Chapters Four and Five, 3D internal volumes of bat inner ears were collected and analysed using μ-Computed Tomography. Measurements of basilar membrane length and number of spiral turns revealed that both clades of laryngeal echolocating bats had modified auditory systems compared to both Old World fruit bats and some non-bat mammals. Typically, laryngeal echolocating bats had longer basilar membranes and more turns than Old World fruit bats; however, after correcting for phylogenetic relatedness few relationships remained significant.

Across mammals the gross morphology, as well as the internal cellular components, of the cochlea is highly variable; e.g. guinea pigs, gerbils, kangaroo rats and subterranean rodent species have highly coiled characteristically conical cochleae, while murids have more flattened cochleae with fewer turns (as summarised in Vater and Kossl 2011). It seems that consistent patterns between cochlear morphology and hearing ability cannot be found even between taxonomically closely related species. Therefore, it is unsurprising that among distantly related taxa, such as the two clades of laryngeal echolocating bats or toothed whales, few consistencies in cochlea structure can be found.

The situation is further complicated in echolocating animals, such as bats, as in many cases accurate audiograms are unavailable; in these taxa, it was assumed that their auditory systems are tuned with highest sensitivity at their specific echolocation call frequency. However, previous studies suggest that bat low-frequency hearing is not only correlated with high-frequency hearing sensitivity but also pup isolation calls, and in some species prey vocalisations (Bruns *et al.,* 1989; Bohn *et al.,* 2006). Additionally, it seems that until the interactions between body size, basilar membrane length, cochlear turns and hearing limits are fully understood any correlative approach may be over simplifying a highly complex system.

iv. Semicircular canal morphology

The second component of the inner ear to be examined was the semicircular canals of the vestibular system. Particular families of laryngeal echolocating bats were found to have highly modified semicircular canals; Rhinolophidae were found to have the most modified semicircular canals, possibly as a consequence of their enlarged cochleae, whilst those of Old World fruit bats were equivalent to those of similar sized non-bat mammals. Across all bats, no signal of powered flight was detected in the morphology of their semicircular canals; furthermore, fossil evidence suggests that flight evolved prior to sophisticated echolocation (Simmons *et al.,* 2008). This suggests that the morphological differences seen in the vestibular systems of echolocating bats do in fact relate to the acquisition of echolocation.

Echolocating Yinpterochiroptera and Yangochiroptera could be distinguished from each other by a number of features of their inner ears, which is suggestive of differential

selection pressures. However, their semicircular canals also share some features, to the exclusion of Old World fruit bats, for example, the distributions of size and shape overlap. This could again support independent but parallel evolutionary pathways during the acquisition of echolocation in each clade. Furthermore, morphological variation of the vestibular system of the bat species studied does not provide evidence of relaxation in Old World fruit bats.

Summary of findings - convergent evolution or relaxation?

Bringing together the above sources of evidence, and previously published work, it appears that molecular and morphological evolution putatively linked to the acquisition of laryngeal echolocation in bats continued to occur after the two bat clades diverged (Figure 6.1). For example within Mormoopidae, *Pteronotus parnellii* has evolved CF echolocation, and the associated morphological adaptations of the inner ear, independently to the Old World CF bats. Recent published phylogenies suggest that *P. parnellii* is a basal member of the *Pteronotus* clade and, therefore, these characters evolved following the divergence of the *Pteronotus* and *Mormoops* clades (Smotherman and Guillen-Servent 2008). Similarly, Rhinolophidae display morphologically distinct inner ears from the remaining Yinpterochiroptera. Therefore, this suggests that radical cochlear and auditory processing changes can occur over relatively short time periods.

Using the methods adopted by this study, i.e. ancestral sequence reconstruction, it is possible to determine along which branches in the species phylogeny convergent substitutions took place. I am therefore able to reject the possibility that sequence similarity between the two main echolocating clades, with the exclusion of the Old World fruits, represents retained ancestral states. Analyses of two protein-coding genes found evidence of only one parallel amino acid substitution between the common ancestor of bats and the dolphin; however, phylogenetic analyses of CNEs did recover all bats as monophyletic. Therefore, it is possible that the common ancestor of bats had moderately increased hearing capabilities compared to non-bat mammals. Published Old World fruit bat audiograms suggest relatively sensitive hearing, ~1 Hz - 70 kHz (Neuweiler 1984; Koay *et al.,* 1998), and yet their inner ears and outer hair cell proteins were not found to deviate from typical mammals. Therefore, it seems possible that good auditory acuity evolved early on in the history of bats, however as species radiated, their auditory systems, and echolocation capabilities, continued to evolve into the sophisticated laryngeal echolocation seen today in extant bats.

Figure 6.1 Summary of main findings mapped onto the bat phylogeny. Convergent substitutions in *Tmc1* and/or *Pjvk* are represented by arrows, text boxes denote selection. Branches with significantly modified inner ears are denoted in bold. All bat taxa names in bold font are thought to possess some form of echolocation. The placement of five fossil bat taxa (†) with respect to extant taxa is uncertain therefore, branches are represented with dashed lines, otherwise phylogeny followed (Eick *et al.*, 2005; Teeling *et al.*, 2005; Simmons *et al.*, 2008).

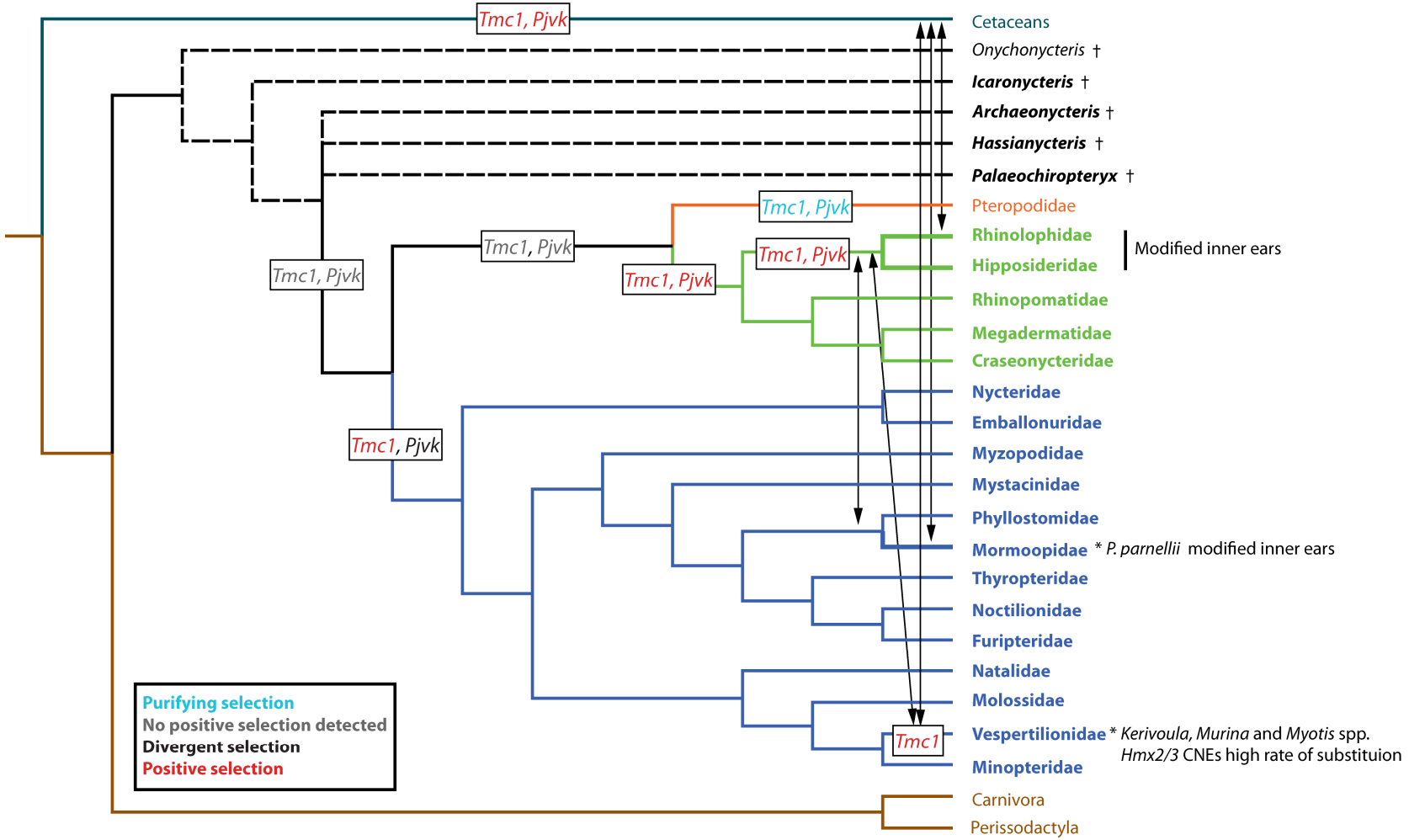

Surprisingly, instead of clarifying the situation, the currently known early Eocene bat fossils continue to provide a source of conflict concerning the origins of echolocation. The main controversy surrounding the Messel bats is not their echolocation capability, as morphological analysis of their inner ears suggests all were capable of some form of 'rudimentary' echolocation (Habersetzer and Storch 1989), but rather their placement with respect to extant taxa. As their placement in the modern phylogeny changes it can radically alter the number of independent gains of echolocation necessary, if loss in Old World fruit bats is not considered (Simmons and Geisler 1998; Springer *et al.,* 2001). However, studies that attempted to address their phylogenetic placement have admitted that the situation remains unresolved (Eick *et al.,* 2005).

As highlighted earlier in this study, phenotypic convergence is not uncommon in nature. Some of the most extreme physical adaptations have repeatedly evolved in independent groups, for example, powered flight has evolved in birds, bats and pterosaurs and a fully aquatic lifestyle in cetaceans and sea cows. It is postulated that forms of echolocation may have independently evolved a minimum of eight times within vertebrates (Gould 1965; Konishi and Knudsen 1979; Griffin and Thompson 1982; Forsman and Malmquist 1988; Gould 1988; Pye and Pye 1988; Thomas *et al.,* 2004; Siemers *et al.,* 2009), and within bats, there are known specific cases of echolocation and ecological convergence (Jones and Holderied 2007; Fenton 2010). Fossil evidence also suggests that as early land vertebrates evolved, certain features of the auditory system developed in parallel in some now extinct lineages (Luo 2007; Manley 2010). As bats evolved flight prior to echolocation, it seems possible that two separate clades were able to evolve echolocation in parallel given the physical and ecological constraints associated with the lifestyle of aerial insectivores.

The natural world also contains evidence of a number of traits and structures that appear to have undergone 'regressive' evolution (e.g. see Nevo 1979; Jeffery 2005; Lahti *et al.,* 2009). Typically a signal of relaxation is vestigiality or intermediate structures between states. For example, secondarily flightless bird species were shown to have predictably smaller semicircular canals compared with volant species, although ranges did overlap (Sipla 2007). A previous study of squamate reptiles found evidence that snake-like bodies had evolved approximately 25 times in different lineages, and was frequently associated with two specific ecotypes (Wiens *et al.,* 2006). For Old World fruit bats to lose echolocation, it would require a number of genetic and morphological

modifications, a scenario for which there is no evidence. However, if Old World fruit bats had lost laryngeal echolocation, we should expect signatures of this, not only in the inner ears, but also in the hyoid apparatus, which is not the case (Veselka *et al.,* 2010a).

FUTURE WORK

A persistent problem of reconstructing the origins of laryngeal echolocation in bats is determining the correct placement of early fossil bats. At present it seems doubtful that morphological evidence alone will provide confident placement of the fossil bat taxa. Furthermore, due to the preservation state of most fossil bats it seems unlikely that ancient DNA will be recovered from early fossils. Currently the oldest ancient DNA to be extracted from bat sub-fossils is only approximately 820 years old (Bogdanowicz *et al.,* 2009). Low confidence in the placement of fossil taxa is exacerbated by a lack of synapomorphies uniting Yinpterochiroptera. Therefore, if morphological characters independent of echolocation are found, this may aid the situation. Furthermore as more complete fossil taxa are found, it may become possible to establish their correct placement with respect to extant taxa.

In the future, it may be possible to combine CT information from fossil bats with extant bats, and non-bat mammals, in order to detail the morphological changes that have taken place in the inner ear. As CT methods are non-destructive even rare specimens can be used, measurements are repeatable and both external and internal structures can be studied (Sipla 2007; Franzen *et al.,* 2009; Walsh *et al.,* 2009; Ashkenazi *et al.,* 2010; Kruta *et al.,* 2010). An addition utility of CT imagery is that it is possible to retro-deform fossils that have become damaged by taphonomic processes during fossilisation (Witmer and Ridgely 2008) Therefore, eventually it may be possible to reconstruct accurate 3D representations of fossils that have been severely compressed, which is the case in many early bat fossils. Thus, avoiding drawing inaccurate inferences from poorly preserved fossils (Simmons *et al.,* 2010).

The geographic origin of bats is currently unclear, the resolution of which could improve our understanding of the origins of echolocation. At present, the earliest known non-echolocating bats are from the New World (Simmons *et al.,* 2008) while the majority of the earliest echolocating taxa are from the Old World (Simmons and Geisler 1998). This suggests a large amount of missing fossil evidence. Therefore, much more evidence regarding the early global radiations of bats is needed.

Aside from features, such as inner ears, directly involved in the perception of echoes, the structures associated with echolocation call emission may be just as informative. Published evidence suggests that the echolocation call emission apparatus in horseshoe bats may be under separate selection to the auditory system (Odendaal and Jacobs 2011). Thus, by widening this study to include a larger number of bats the flexibility and constraints of the system may be better understood.

The occurrence of parallel sequence evolution in multiple proteins expressed in OHCs in echolocating taxa is intriguing (this study and e.g. Liu *et al.,* 2010a). Genome approaches could be used to examine levels of sequence convergence in a wider range of loci between echolocating taxa, in order to determine if convergence is limited to outer hair cell proteins or not. Furthermore, at present the functional significance of these amino acid substitutions is unknown and it remains conjecture that they confer meaningful adaptations. Through structural protein analysis it may be possible to explore at least how the substitutions affect protein folding. Similarly, the functional effect of sequence variation in bat CNEs is unknown, the previously developed GFP reporter assay could be used to test empirically the effects of sequence variation on gene expression in the developing ear (Woolfe *et al.,* 2005).

CONCLUSIONS

My interpretation of the molecular and morphological evidence collected throughout this study supports the hypothesis of multiple origins of laryngeal echolocation in bats. However, based on my results alone it is not possible to entirely reject the hypothesis that the common ancestor of all bats had increased hearing capability compared to other mammals. Nonetheless, in combination with previously published findings, my data suggest that the earliest bats had neither characteristically modified inner ears nor modified OHC proteins, to enable them capable of sophisticated echolocation. Furthermore, neither 'hearing gene' examined was shown to be under relaxed selection in Old World fruit bats. In other words, while the common ancestor of all bats may have had enhanced hearing capabilities compared to non-bat mammals, this appears to have been subsequently modified after the divergence of Yangochiroptera and Yinpterochiroptera. Therefore, no support was found for a loss of laryngeal echolocation within Old World fruit bats.

REFERENCES:

Accetturo M, Creanza TM, Santoro C, Tria G, Giordano A, Battagliero S *et al* (2010). Finding new genes for non-syndromic hearing loss through an *in silico* prioritization study. *PLoS ONE* **5:** e12742.

Adriaens D, Devaere S, Teugels GG, Dekegel B, Verraes W (2002). Intraspecific variation in limblessness in vertebrates: a unique example of microevolution. *Biol. J. Linn. Soc.* **75:** 367-377.

Albuquerque AAS, Rossato M, de Oliveira JAA, Hyppolito MA (2009). Understanding the anatomy of ears from guinea pigs and rats and its use in basic otologic research. *Braz. J. Otorhinolaryngol.* **75:** 43-49.

Altringham JD (1996). *Bats: Biology and Behaviour*. Oxford University Press.

Aminetzach YT, Srouji JR, Kong CY, Hoekstra HE (2009). Convergent evolution of novel protein function in shrew and lizard venom. *Curr. Biol.* **19:** 1925-1931.

Amma LL, Goodyear R, Faris JS, Jones I, Ng L, Richardson G *et al* (2003). An emilin family extracellular matrix protein identified in the cochlear basilar membrane. *Mol. Cell. Neurosci.* **23:** 460-472.

Arita HT, Fenton MB (1997). Flight and echolocation in the ecology and evolution of bats. *Trends Ecol. Evol.* **12:** 53-58.

Armstrong E (1983). Relative brain size and metabolism in mammals. *Science* **220:** 1302-1304.

Ashkenazi S, Klass K, Mienis HK, Spiro B, Abel R (2010). Fossil embryos and adult Viviparidae from the Early-Middle Pleistocene of Gesher Benot Ya'aqov, Israel: ecology, longevity and fecundity. *Lethaia* **43:** 116-127.

Ashmore J, Gale J (2000). The cochlear (Primer). *Curr. Biol.* **10:** 325-327.

Au WWL, Simmons JA (2007). Echolocation in dolphins and bats. *Phys. Today* **60:** 40-45.

Bailey WJ, Slightom JL, Goodman M (1992). Rejection of the "Flying Primate" hypothesis by phylogenetic evidence from the E-globin gene. *Science* **256:** 86-89.

Baker RJ, Bininda-Emonds ORP, Mantilla-Meluk H, Porter CA, Van Den Bussche RA (2011). Molecular timescale of diversification of feeding strategy and morphology in New World leaf-nosed bats (Phyllostomidae): A phylogenetic perspective. In: Gunnell GF and Simmons NA (eds) *Evolutionary History of Bats: Fossils, Molecules and Morphology*. Cambrideg University Press: Cambridge.

Baldwin C, Hoth C, Macina R, Milunsky A (2005). Mutations in *PAX3* that cause Waardenburg syndrome type 1: Ten new mutations and review of the literature. *Am. J. Med. Genet.* **58:** 115-122.

Baron G, Jolicoeur P (1980). Brain structure in Chiroptera - some multivariate trends. *Evolution* **34:** 386-393.

Barton RA, Purvis A, Harvey PH (1995). Evolutionary radiations of visual and olfactory brain systems in primates, bats and insectivores. *Phil. Trans. R. Soc. Lond. B* **348:** 381-392.

Bejder L, Hall BK (2002). Limbs in whales and limblessness in other vertebrates: mechanisms of evolutionary and developmental transformation and loss. *Evol. Dev.* **4:** 445-458.

Bekaert M, Teeling EC (2008). UniPrime: a workflow-based platform for improved universal primer design. *Nucleic Acids Res.* **36**.

Bell GP (1985). The sensory basis of prey location by the California leaf-nosed bat *Macrotus californicaus* (Chiroptera, Phyllostomidae). *Behav. Ecol. Sociobiol.* **16:** 343-347.

Benko S, Fantes JA, Amiel J, Kleinjan DJ, Thomas S, Ramsay J *et al* (2009). Highly conserved non-coding elements on either side of *SOX9* associated with Pierre Robin sequence. *Nat. Genet.* **41:** 359-364.

Biedron S, Westhofen M, Ilgner J (2009). On the number of turns in human cochleae. *Otol. Neurotol.* **30:** 414-417.

Bielawski JP, Yang ZH (2004). A maximum likelihood method for detecting functional divergence at individual codon sites, with application to gene family evolution. *J. Mol. Evol.* **59:** 121-132.

Bininda-Emonds ORP, Cardillo M, Jones KE, MacPhee RDE, Beck RMD, Grenyer R *et al* (2007). The delayed rise of present-day mammals. *Nature* **446:** 507.

Blanks RHI, Curthoys IS, Bennett ML, Markham CH (1985). Planar relationships of the semicircular canals in rhesus and squirrel monkeys. *Brain Res.* **340:** 315-324.

Bogdanowicz W, Csada RD, Fenton MB (1997). Structure of noseleaf, echolocation, and foraging behavior in the Phyllostomidae (Chiroptera). *J. Mammal.* **78:** 942-953.

Bogdanowicz W, Van Den Bussche RA, Gajewska M, Postawa T, Harutyunyan M (2009). Ancient and contemporary DNA sheds light on the history of mouse-eared bats in Europe and the Caucasus. *Acta Chiropt.* **11:** 289 - 305.

Bok J, Dolson DK, Hill P, Ruther U, Epstein DJ, Wu DK (2007). Opposing gradients of Gli repressor and activators mediate Shh signaling along the dorsoventral axis of the inner ear. *Development* **134:** 1713-1722.

Bondurand N, Pingault V, Goerich DE, Lemort N, Sock E, Le Caignec C *et al* (2000). Interaction between *SOX10*, *PAX3* and *MITF*, three genes altered in Waardenburg syndrome. *Am. J. Hum. Genet.* **67:** 1907-1917.

Bookstein FL (1997). Landmark methods for forms without landmarks: morphometrics of group differences in outline shape. *Med. Image Anal.* **1:** 225-243.

Borowsky R (2008). Restoring sight in blind cavefish. *Curr. Biol.* **18:** R23-R24.

Bouchard M, Pfeffer P, Busslinger M (2000). Functional equivalence of the transcription factors Pax2 and Pax5 in mouse development *Development* **127:** 3703-3713.

Bromham L (2011). The genome as a life-history character: why rate of molecular evolution varies between mammal species. *Phil. Trans. R. Soc. Lond. B* **366:** 2503-2513.

Brunelli S, Innocenzi A, Cossu G (2003). *Bhlhb5* is expressed in the CNS and sensory organs during mouse embryonic development. *Gene Expr. Patterns* **3:** 755-759.

Bruns V, Burda H, Ryan MJ (1989). Ear morphology of the frog-eating (*Trachops cirrhosus*, Family, Phyllostomidae) - Apparent specializations for low-frequency hearing. *J. Morphol.* **199:** 103-118.

Buchholtz EA (2001). Vertebral osteology and swimming style in living and fossil whales (Order : Cetacea). *J. Zool.* **253:** 175-190.

Bumrungsri S, Sripaoraya E, Chongsiri T, Sridith K, Racey PA (2009). The pollination ecology of durian (*Durio zibethinus*, Bombacaceae) in southern Thailand. *J. Trop. Ecol.* **25:** 85-92.

Burton Q, Cole LK, Mulheisen M, Chang W, Wu DK (2004). The role of *Pax2* in mouse inner ear development. *Dev. Biol.* **272:** 161-175.

Cai HX, Manoussaki D, Chadwick R (2005). Effects of coiling on the micromechanics of the mammalian cochlea. *J. Royal Soc. Interface* **2:** 341-348.

Cantos R, Cole LK, Acampora D, Simeone A, Wu DK (2000). Patterning of the mammalian cochlea. *Proc. Natl. Acad. Sci. U. S. A.* **97:** 11707-11713.

Castoe TA, de Koning APJ, Kim HM, Gu WJ, Noonan BP, Naylor G *et al* (2009). Evidence for an ancient adaptive episode of convergent molecular evolution. *Proc. Natl. Acad. Sci. U. S. A.* **106:** 8986-8991.

Charlesworth B (2009). Effective population size and patterns of molecular evolution and variation. *Nat. Rev. Genet.* **10:** 195-205.

Chen JJ, Sun M, Lee SG, Zhou GL, Rowley JD, Wang S (2002). Identifying novel transcripts and novel genes in the human genome by using novel SAGE tags. *Proc. Natl. Acad. Sci. U. S. A.* **99:** 12257-12262.

Chen K, Rajewsky N (2007). The evolution of gene regulation by transcription factors and microRNAs. *Nat. Rev. Genet.* **8:** 93-103.

Christin PA, Weinreich DM, Besnard G (2010). Causes and evolutionary significance of genetic convergence. *Trends Genet.* **26:** 400-405.

Cleveland CJ, Betke M, Federico P, Frank JD, Hallam TG, Horn J *et al* (2006). Economic value of the pest control service provided by Brazilian free-tailed bats in south-central Texas. *Front. Ecol. Environ.* **4:** 238-243.

Coffin A, Kelley M, Manley GA, Popper AN (2004). Evolution of sensory hair cell. In: Manley GA, Popper AN and Fay RR (eds) *Evolution of the Vertebrate Auditory System*. Springer-Verlag: New York, pp 55-94.

Cohen B (1974). The vestibulo-ocular reflex arc. In: Kornhuber HH (ed) *Vestibular System Part 1 Basic Mechanisms*. Springer - Verlag: Berlin. Vol. VI/1.

Coleman MN, Kay RF, Colbert MW (2010). Auditory morphology and hearing sensitivity in fossil New World monkeys. *Anat. Rec.* **293:** 1711-1721.

Collin RWJ, Kalay E, Tariq M, Peters T, van der Zwaag B, Venselaar H *et al* (2008). Mutations of *ESRRB* encoding estrogen-related receptor beta cause autosomal-recessive nonsyndromic hearing impairment DFNB35. *Am. J. Hum. Genet.* **82:** 125-138.

Coré N, Caubita X, Metchata A, Bonedb A, Djabalib M, Fasanoa L (2007). *Tshz1* is required for axial skeleton, soft palate and middle ear development in mice *Dev. Biol.* **308:** 407-420.

Cornwallis CK, West SA, Davis KE, Griffin AS (2010). Promiscuity and the evolutionary transition to complex societies. *Nature* **466:** 969-U991.

Corte-Real HBSM, Dixon DR, Holland PWH (1994). Intron-targeted PCR - a new approach to survey neutral DNA polymorphism in bivalve populations. *Mar. Biol.* **120:** 407-413.

Courts SE (1998). Dietary strategies of Old World fruit bats (Megachiroptera, Pteropodidae): how do they obtain sufficient protein? *Mammal. Rev.* **28:** 185-193.

Cox GA, Mahaffey CL, Nystuen A, Letts VA, Frankel WN (2000). The mouse fidgetin gene defines a new role for AAA family proteins in mammalian development. *Nat. Genet.* **26:** 198-202.

Cox PG, Jeffery N (2008). Geometry of the semicircular canals and extraocular muscles in rodents, lagomorphs, felids and modern humans. *J. Anat.* **213:** 583-596.

Cox PG, Jeffery N (2010). Semicircular canals and agility: the influence of size and shape measures. *J. Anat.* **216:** 37-47.

Cretekos CJ, Wang Y, Green ED, Martin JF, Rasweiler JJ, Behringer RR *et al* (2008). Regulatory divergence modifies limb length between mammals. *Genes Dev.* **22:** 141-151.

Csada R (1996). *Cardioderma cor. Mamm. Species* **519:** 1-4.

Csorba G, Ujhelyi P, Thomas N (2003). *Horseshoe bats of the world (Chiroptera: Rhinolophidae)*. Alana Books: Shropshire, United Kingdom.

Cui J, Pan YH, Zhang YJ, Jones G, Zhang SY (2011). Progressive pseudogenization: Vitamin C synthesis and its loss in bats. *Mol. Biol. Evol.* **28:** 1025-1031.

Dallos P, Fakler B (2002). Prestin, a new type of motor protein. *Nat. Rev. Mol. Cell Biol.* **3:** 104-111.

David R, Droulez J, Allain R, Berthoz A, Janvier P, Bennequin D (2010). Motion from the past. A new method to infer vestibular capacities of extinct species. *Comptes Rendus Palevol* **9:** 397-410.

Delmaghani S, del Castillo FJ, Michel V, Leibovici M, Aghaie A, Ron U *et al* (2006). Mutations in the gene encoding pejvakin, a newly identified protein of the afferent auditory pathway, cause DFNB59 auditory neuropathy. *Nat. Genet.* **38:** 770-778.

Drake JA, Bird C, Nemesh J, Thomas DJ, Newton-Cheh C, Reymond A *et al* (2006). Conserved noncoding sequences are selectively constrained and not mutation cold spots. *Nat. Genet.* **38:** 223-227.

Dror AA, Avraham KB (2010). Hearing impairment: a panoply of genes and functions. *Neuron* **68:** 293-308.

Drummond AJ, Ho SYW, Phillips MJ, Rambaut A (2006). Relaxed phylogenetics and dating with confidence. *PLoS Biol.* **4:** 699-710.

Drummond AJ, Rambaut A (2007). BEAST: Bayesian evolutionary analysis by sampling trees. *BMC Evol. Biol.* **7**.

Dumont ER (2010). Bone density and the lightweight skeletons of birds. *Proc. R. Soc. Biol. Sci. B.* **277:** 2193-2198.

Duret L, Dorkeld F, Gautier C (1993). Strong conservation of noncoding sequences during vertebrates evolution - potential involvement in posttranscriptional regulation of gene-expression. *Nucleic Acids Res.* **21:** 2315-2322.

Eick GN, Jacobs DS, Matthee CA (2005). A nuclear DNA phylogenetic perspective on the evolution of echolocation and historical biogeography of extant bats (Chiroptera). *Mol. Biol. Evol.* **22:** 1869-1886.

Eisenberg JF, Wilson DE (1978). Relative brain size and feeding strategies in the Chiroptera. *Evolution* **32:** 740-751.

Eiting TP, Gunnell GF (2009). Global completeness of the bat fossil record. *J. Mamm. Evol.* **16:** 151-173.

Eklöf J (2003). Vision in echolocating bats. Doctoral thesis, Göteborg University.

Enard W, Przeworski M, Fisher SE, Lai CSL, Wiebe V, Kitano T *et al* (2002). Molecular evolution of *FOXP2*, a gene involved in speech and language. *Nature* **418:** 869-872.

Engstrom PG, Fredman D, Lenhard B (2008). Ancora: a web resource for exploring highly conserved noncoding elements and their association with developmental regulatory genes. *Genome Biol.* **9**.

Fejtek M, Delorme M, Wassersug R (1995). Behavioral reactions of the bat *Carollia perspicillata* to abrupt changes in gravity. *Biol. Sci. Space* **9:** 77-81.

Fekete DM (1999). Development of the vertebrate ear: insights from knockouts and mutants. *Trends Neurosci.* **22:** 263-269.

Fenton MB (1974). Role of echolocation in evolution of bats *Am. Nat.* **108:** 386-388.

Fenton MB (1984). Echolocation - implications for ecology and evolution of bats. *Q. Rev. Biol.* **59:** 33-53.

Fenton MB (2010). Convergences in the diversification of bats. *Curr. Zool.* **56:** 454-468.

Fenton MB, Bell GP (1981). Recognition of species of insectivorous bats by their echolocation calls. *J. Mammal.* **62:** 233-243.

Fenton MB, Crerar LM (1984). Cervical-vertebrae in relation to roosting posture in bats. *J. Mammal.* **65:** 395-403.

Fenzl T, Schuller G (2007). Dissimilarities in the vocal control over communication and echolocation calls in bats. *Behav. Brain Res.* **182:** 173-179.

Ficker M, Powles N, Warr N, Pirvola U, Maconochie M (2004). Analysis of genes from inner ear developmental-stage cDNA subtraction reveals molecular regionalization of the otic capsule. *Dev. Biol.* **268:** 7-23.

Fiedler J (1979). Prey catching with and without echolocation in the Indian false vampire (*Megaderma lyra*). *Behav. Ecol. Sociobiol.* **6:** 155-160.

Forsman KA, Malmquist MG (1988). Evidence for echolocation in the common shrew, *Sorex araneus*. *J. Zool.* **216:** 655-662.

Franchini LF, Elgoyhen AB (2006). Adaptive evolution in mammalian proteins involved in cochlear outer hair cell electromotility. *Mol. Phylogenet. Evol.* **41:** 622-635.

Francis CM, Habersetzer J (1998). Interspecific and intraspecific variation in echolocation call frequency and morphology of horseshoe bats, *Rhinolophus* and *Hipposideros*. In: Kunz TH and Racey P (eds) *Bat Biology and Conservation* Smithsonian Institution Press: Washington and London.

Franzen JL, Gingerich PD, Habersetzer J, Hurum JH, von Koenigswald W, Smith BH (2009). Complete primate skeleton from the Middle Eocene of Messel in Germany: morphology and paleobiology. *Plos One* **4**.

Freeman PW (1988). Frugivorous and Animalivorous Bats (Microchiroptera) - Dental and Cranial Adaptations. *Biol. J. Linn. Soc.* **33:** 249-272.

Freeman PW (2000). Macroevolution in Microchiroptera: Recoupling morphology and ecology with phylogeny. *Evol. Ecol. Res.* **2:** 317-335.

Frolenkov GI, Belyantseva IA, Friedman TB, Griffith AJ (2004). Genetic insights into the morphogenesis of inner ear hair cells. *Nat. Rev. Genet.* **5:** 489-498.

Gall LF, Tiffney BH (1983). A fossil Noctuid moth egg from the late Cretaceous of eastern North America. *Science* **219:** 507-509.

Galtier N, Duret L (2007). Adaptation or biased gene conversion? Extending the null hypothesis of molecular evolution. *Trends Genet.* **23:** 273 - 277.

Gannon DP, Barros NB, Nowacek DP, Read AJ, Waples DM, Wells RS (2005). Prey detection by bottlenose dolphins, *Tursiops truncatus*: an experimental test of the passive listening hypothesis. *Anim. Behav.* **69:** 709-720.

Garland T, Bennett AF, Rezende EL (2005). Phylogenetic approaches in comparative physiology. *J. Exp. Biol.* **208:** 3015-3035.

Giannini NP, Simmons NB (2003). A phylogeny of megachiropteran bats (Mammalia: Chiroptera: Pteropodidae) based on direct optimization analysis of one nuclear and four mitochondrial genes. *Cladistics* **19:** 496-511.

Goudy-Trainor A, Freeman PW (2002). Call parameters and facial features in bats: a surprising failure of form following function. *Acta Chiropt.* **4:** 1-16.

Gould E (1965). Evidence for echolocation in the Tenrecidae of Madagascar. *Proc. Am. Philos. Soc.* **109:** 352-360.

Gould E (1988). Wing-clapping sounds of *Eonycteris spelaea* (Pteropodidae) in Malaysia. *J. Mammal.* **69:** 378-379.

Gouy M, Guindon S, Gascuel O (2010). SeaView Version 4: A multiplatform graphical user interface for sequence alignment and phylogenetic tree building. *Mol. Biol. Evol.* **27:** 221-224.

Graf W, Vidal PP (1996). Semicircular canal size and upright stance are not interrelated. *J. Hum. Evol.* **30:** 175-181.

Gray AA (1905). Anatomical notes upon the membranous labyrinth of man and of the seal. *J. Anat.* **39:** 349 361.

Gray AA (1906). Observations on the labyrinth of certain animals. *J. Laryngol. Rhinol. Otol.* **21:** 365 - 377.

Gray O (1951). An introduction to the study of the comparative anatomy of the labyrinth. *J. Laryngol. Otol.* **65:** 681-703.

Graybeal A, Rosowski JJ, Ketten DR, Crompton AW (1989). Inner-ear structure in *Morganucodon*, an Early Jurassic mammal. *Zool. J. Linn. Soc.* **96:** 107-117.

Gregory WK (1910). The orders of mammals. *Bull. Am. Mus. Nat. Hist.* **24:** 1-524.

Griffin DR, Suthers RA (1970). Sensitivity of echolocation in cave swiftlets. *Biol. Bull.* **139:** 495-&.

Griffin DR, Thompson D (1982). Echolocation by cave swiftlets. *Behav. Ecol. Sociobiol.* **10:** 119-123.

Gunnell G, Fine Jacobs B, Herendeen PS, Head JJ, Kowalski E, Msuya CP *et al* (2003). Oldest placental mammal from Sub-Saharan Africa: Eocene Microbat from Tanzania - Evidence for early evolution of sophisticated echolocation. *Palaeontol. Electron.* **5:** 10.

Gunnell G, Simmons NB (2005). Fossil evidence and the origin of bats. *J. Mamm. Evol.* **12:** 209-246.

Habersetzer J, Richter G, Storch G (1994). Paleoecology of early middle Eocene bats from Messel, FRG. aspects of flight, feeding and echolocation. *Hist Biol* **8:** 235-260.

Habersetzer J, Storch G (1989). Ecology and echolocation of the Eocene Messel bats. In: Hanak V, Horacek I and Gaisler J (eds) *European bat research 1987*. Charles Univ. Press.: Prague, pp 213-233.

Habersetzer J, Storch G (1992). Cochlea size in extant Chiroptera and Middle Eocene microchiropterans from Messel. *Naturwissenschaften* **79:** 462-466.

Hadfield JD (2010). MCMC methods for multi-response generalized linear mixed models: The MCMCglmm R Package. *J. Stat. Softw.* **33:** 1-22.

Hadrys T, Braun T, Rinkwitz-Brandt S, Arnold HH, Bober E (1998). *Nkx5-1* controls semicircular canal formation in the mouse inner ear. *Development* **125:** 33-39.

Hall TA (1999). BioEdit: a user-friendly biological sequence alignment editor and analysis program for Windows 95/98/NT. *Nucl. Acids. Symp. Ser.* **41:** 95-98.

Halligan DL, Oliver F, Guthrie J, Stemshorn KC, Harr B, Keightley PD (2011). Positive and negative selection in murine ultra-conserved noncoding elements. *Mol. Biol. Evol.* **10.1093/molbev/msr093**.

Hammer Ø, Harper DAT, Ryan PD (2001). PAST: paleontological statistics software package for education and data analysis. *Palaeontol. Electron.* **4:** 9.

Hand S, Novacek M, Godthelp H, Archer M (1994). First Eocene bat from Australia. *J. Vertebr. Paleontol.* **14:** 375-381.

Harris DM, Rotche R, Freedom T (1990). Postnatal-growth of cochlear spiral in Mongolian gerbil. *Hear. Res.* **50:** 1-6.

Harvey PH, Pagel MD (1991). *The Comparative Method in Evolutionary Biology*. Oxford University Press: Oxford.

Haussler D, O'Brien SJ, Ryder OA, Barker FK, Clamp M, Crawford AJ *et al* (2009). Genome 10K: A proposal to obtain whole-genome sequence for 10,000 vertebrate species. *J. Hered.* **100:** 659-674.

Hayden S, Bekaert M, Crider TA, Mariani S, Murphy WJ, Teeling EC (2010). Ecological adaptation determines functional mammalian olfactory subgenomes. *Genome Res.* **20:** 1-9.

He DZZ, Zheng J, Kalinec F, Kakehata S, Santos-Sacchi J (2006). Tuning in to the amazing outer hair cell: Membrane wizardry with a twist and shout. *J. Membr. Biol.* **209:** 119-134.

Heanue TA, Davis RJ, Rowitch DH, Kispert A, McMahon AP, Mardon G *et al* (2002). *Dach1*, a vertebrate homologue of *Drosophila* dachshund, is expressed in the developing eye and ear of both chick and mouse and is regulated independently of *Pax* and *Eya* genes. *Mech. Dev.* **111:** 75-87.

Heffner HE, Heffner RS (2008). High-frequency hearing. In: Dallos P, Oertel D and Hoy R (eds) *Handbook of the senses: Audition*. Elsevier: New York, pp 55-60.
Heffner R, Heffner H (1980). Hearing in the elephant (*Elephas maximus*). *Science* **208:** 518-520.
Heffner RS, Heffner HE (1982). Hearing in the elephant (*Elephas maximus*) - absolute sensitivity, frequency, frequency discrimination, and sound localization. *J. Comp. Physiol. Psychol.* **96:** 926-944.
Heffner RS, Heffner HE, Contos C, Kearns D (1994). Hearing in prairie dogs - transistion between surface and subterranean rodents. *Hear. Res.* **73:** 185-189.
Hill JE (1974). A new family, genus and species of bat (Mammalia: Chiroptera) from Thailand. *Bull. Br. Mus. (Nat. Hist.) Zool.* **27:** 301-336.
Hopkins MA (1906). On the relative dimensions of the osseous semicircular canals of birds. *Biol. Bull. (Woods Hole)* **11:** 253-264.
Horowitz SS, Cheney CA, Simmons JA (2004). Interaction of vestibular, echolocation, and visual modalities guiding flight by the big brown bat, *Eptesicus fuscus*. *J. Vestibul. Res.-Equil.* **14:** 17-32.
Horvathova T, Nakagawa S, Uller T (2011). Strategic female reproductive investment in response to male attractiveness in birds. *Proc. R. Soc. Biol. Sci. B.***:** doi:10.1098/rspb.2011.0663.
Hosoya M, Fujioka M, Matsuda S, Ohba H, Shibata S, Nakagawa F *et al* (2011). Expression and function of *sox21* during mouse cochlea development. *Neurochem. Res.* **36:** 1261-1269.
Houston RD, Boonman A, Jones G (2004). Do echolocation signal parameters restrict bats' choice of prey? In: Thomas JA, Moss CF and Vater M (eds) *Echolocation in bats and dolphins*. University of Chicago Press: Chicago, Il, pp 339-345.
Huber KT, Langton M, Penny D, Moulton V, Hendy M (2002). Spectronet: a package for computing spectra and median networks. *Appl Bioinformatics* **1:** 159-161.
Hutcheon JM, Kirsch JAW (2004). Camping in a different tree: Results of molecular systematic studies of bats using DNA-DNA hybridization. *J. Mamm. Evol.* **11:** 17-47.
Hutcheon JM, Kirsch JAW, Pettigrew JD (1998). Base-compositional biases and the bat problem. III. The question of microchiropteran monophyly. *Phil. Trans. R. Soc. Lond. B* **353:** 607-617.
Hutcheon JM, Kirsch JW, Garland T (2002). A comparative analysis of brain size in relation to foraging ecology and phylogeny in the chiroptera. *Brain Behav. Evol.* **60:** 165-180.
Igarashi M, Yoshinob T (1966). Comparative observations of eminentia cruciata in birds and mammals. *Anat. Rec.* **155:** 269-&.
Illert C, Pickover CA (1992). Generating irregularly oscillating fossil seashells. *IEEE Comput. Graph.* **12:** 18-22.
Inselberg A (1978). Cochlear dynamics - evolution of a mathematical-model. *Siam Rev.* **20:** 301-351.
Ivanenko YP, Grasso R, Israel I, Berthoz A (1997). The contribution of otoliths and semicircular canals to the perception of two-dimensional passive whole-body motion in humans. *J. Physiol.-London* **502:** 223-233.
Iwaniuk AN, Clayton DH, Wylie DRW (2006). Echolocation, vocal learning, auditory localization and the relative size of the avian auditory midbrain nucleus (MLd). *Behav. Brain Res.* **167:** 305-317.
Jaeger R, Kondrachuk AV, Haslwanter T (2008). The distribution of otolith polarization vectors in mammals: Comparison between model predictions and single cell recordings. *Hear. Res.* **239:** 12-19.

Janes DE, Chapus C, Gondo Y, Clayton DF, Sinha S, Blatti CA *et al* (2011). Reptiles and mammals have differentially retained long conserved noncoding sequences from the amniote ancestor. *Genome Biol. Evol.* **3:** 102-113.

Jeffery N, Cox PG (2010). Do agility and skull architecture influence the geometry of the mammalian vestibulo-ocular reflex? *J. Anat.* **216:** 496 - 509.

Jeffery WR (2005). Adaptive evolution of eye degeneration in the Mexican blind cavefish. *J. Hered.* **96:** 185-196.

Jia SP, He DZZ (2005). Motility-associated hair-bundle motion in mammalian outer hair cells. *Nat. Neurosci.* **8:** 1028-1034.

Jones G (1999). Scaling of echolocation call parameters in bats. *J. Exp. Biol.* **202:** 3359-3367.

Jones G, Holderied MW (2007). Bat echolocation calls: adaptation and convergent evolution. *Proc. R. Soc. Biol. Sci. B.* **274:** 905-912.

Jones G, Teeling EC (2006). The evolution of echolocation in bats. *Trends Ecol. Evol.* **21:** 149-156.

Kandel BM, Hullar TE (2010). The relationship of head movements to semicircular canal size in cetaceans. *J. Exp. Biol.* **213:** 1175-1181.

Keats BJB, Nouri N, Huang JM, Money M, Webster DB, Berlin CI (1995). The deafness locus (dn) maps to mouse chromosome 19. *Mamm. Genome* **6:** 8-10.

Keresztes G, Mutai H, Heller S (2003). TMC and EVER genes belong to a larger novel family, the TMC gene family encoding transmembrane proteins. *BMC Genomics* **4:** 24-35.

Ketten DR (1994). Funtional analyses of whale ears - adaptations for underwater hearing. *Ocean 94 - Oceans Engineering for Today's Technology and Tomorrow's Preservation, Proceedings, Vol 1***:** A264-A270.

Ketten DR (1997). Structure and function in whale ears. *Bioacoustics* **8:** 103-135.

Ketten DR (2000). Cetacean Ears. In: Au WWL, Popper AN and Fay RR (eds) *Hearing by Whales and Dolphins*. Springer: New York, pp 43-108.

Ketten DR, Odell DK, Domning DP (1992). Structure, function, and adaptation of the manatee ear. In: Thomas JA, Kastelein RA and Supin AY (eds) *Marine Mammal Sensory Systems*. Plenum Press: New York, pp 77-95.

Khan FAA, Solari S, Swier VJ, Larsen PA, Abdullah MT, Baker RJ (2010). Systematics of Malaysian woolly bats (Vespertilionidae: *Kerivoula*) inferred from mitochondrial, nuclear, karyotypic, and morphological data. *J. Mammal.* **91:** 1058-1072.

Kiernan AE, Pelling AL, Leung KKH, Tang ASP, Bell DM, Tease C *et al* (2005). *Sox2* is required for sensory organ development in the mammalian inner ear. *Nature* **434:** 1031-1035.

Kim SY, Pritchard JK (2007). Adaptive evolution of conserved noncoding elements in mammals. *Plos Genetics* **3:** 1572-1586.

King MC, Wilson AC (1975). Evolution at 2 levels in humans and chimpanzees. *Science* **188:** 107-116.

Kingston T, Jones G, Zubaid A, Kunz TH (2000). Resource partitioning in rhinolophoid bats revisited. *Oecologia* **124:** 332-342.

Kingston T, Rossiter SJ (2004). Harmonic-hopping in Wallacea's bats. *Nature* **429:** 654-657.

Kirk EC, Gosselin-Ildari AD (2009). Cochlear labyrinth volume and hearing abilities in primates. *Anat. Rec.* **292:** 765-776.

Kirkegaard M, Jorgensen JM (2001). The inner ear macular sensory epithelia of the Daubenton's bat. *J. Comp. Neurol.* **438:** 433-444.

Kitajiri SI, McNamara R, Makishima T, Husnain T, Zafar AU, Kittles RA *et al* (2007). Identities, frequencies and origins of *TMC1* mutations causing DFNB7/B11 deafness in Pakistan. *Clin. Genet.* **72:** 546-550.

Knell RJ (2009). On the analysis of non-linear allometries. *Ecol. Entomol.* **34:** 1-11.

Koay G, Heffner RS, Heffner HE (1998). Hearing in a megachiropteran fruit bat (*Rousettus aegyptiacus*). *J. Comp. Psychol.* **112:** 371-382.

Konishi M, Knudsen EI (1979). Oilbird - hearing and echolocation. *Science* **204:** 425-427.

Kornhuber HH (1974). Introduction. In: Kornhuber HH (ed) *Vestibular System Part 1: Basic Mechanisms*. Springer Verlag: Berlin Vol. VI/1, pp 3-17.

Kossl M, Foeller E, Drexl M, Vater M, Mora E, Coro F *et al* (2003). Postnatal development of cochlear function in the mustached bat, *Pteronotus parnellii*. *J. Neurophysiol.* **90:** 2261-2273.

Kossl M, Foeller E, Faulstich M (2004). Otoacoustic emissions and cochlear mechanisms in echolocating bats. In: Thomas JA, Moss CF and Vater M (eds) *Echolocation in Bats and Dolphins*. The University of Chicago Press: Chicago and London, pp 104-108.

Kossl M, Mayer F, Frank G, Faulstich M, Russell IJ (1999). Evolutionary adaptations of cochlear function in Jamaican mormoopid bats. *J. Comp. Physiol. Sens. Neural. Behav. Physiol.* **185:** 217-228.

Kousathanas A, Oliver F, Halligan DL, Keightley PD (2011). Positive and negative selection on noncoding DNA close to protein-coding genes in wild house mice. *Mol. Biol. Evol.* **28:** 1183-1191.

Kruta I, Landman NH, Rouget I, Cecca F, Larson NL (2010). The jaw apparatus of the Late Cretaceous ammonite *Didymoceras*. *J. Paleontol.* **84:** 556-560.

Kuc R (2009). Model predicts bat pinna ridges focus high frequencies to form narrow sensitivity beams. *J. Acoust. Soc. Am.* **125:** 3454-3459.

Kucuk B, Abe K (1992). Microstructures of the osseous spiral laminae in the bat cochlea - a scanning electron-microscopic study. *Arch. Histol. Cytol.* **55:** 315-319.

Kurima K, Peters LM, Yang YD, Riazuddin S, Ahmed ZM, Naz S *et al* (2002). Dominant and recessive deafness caused by mutations of a novel gene, *TMC1*, required for cochlear hair-cell function. *Nat. Genet.* **30:** 277-284.

Lai CSL, Fisher SE, Hurst JA, Vargha-Khadem F, Monaco AP (2001). A forkhead-domain gene is mutated in a severe speech and language disorder. *Nature* **413:** 519-523.

Lande R (1978). Evolutionary mechanisms of limb loss in tetrapods. *Evolution* **32:** 73-92.

Lang M, Hadzhiev Y, Siegel N, Amemiya CT, Parada C, Strähle U *et al* (2010). Conservation of shh cis-regulatory architecture of the coelacanth is consistent with its ancestral phylogenetic position. *EvoDevo* **1:** 11.

Lange S, Stalleicken J, Burda H (2004). Functional morphology of the ear in fossorial rodents, *Microtus arvalis* and *Arvicola terrestris*. *J. Morphol.* **262:** 770-779.

Larkin MA, Blackshields G, Brown NP, Chenna R, McGettigan PA, McWilliam H *et al* (2007). Clustal W and Clustal X version 2.0. *Bioinformatics* **23:** 2947-2948.

Lee AP, Kerk SY, Tan YY, Brenner S, Venkatesh B (2011). Ancient Vertebrate Conserved Noncoding Elements Have Been Evolving Rapidly in Teleost Fishes. *Mol. Biol. Evol.* **28:** 1205-1215.

Leong TM, Teo SC, Lim KKP (2009). The naked bulldog bat, *Cheiromeles torquatus* in Singapore - past and present records, with highlight on its unique morphology (Microchiroptera: Molossidae). *Nature in Singapore* **2:** 215 - 230.

Li G, Wang JH, Rossiter SJ, Jones G, Cotton JA, Zhang SY (2008). The hearing gene *Prestin* reunites echolocating bats. *Proc. Natl. Acad. Sci. U. S. A.* **105:** 13959-13964.

Li W-H, Ellsworth DL, Krushkal J, Chang BH-J, Hewett-Emmett D (1996). Rates of nucleotide substitution in Primates and Rodents and the generation-time effect hypothesis. *Mol. Phylogenet. Evol.* **5:** 182-187.

Li Y, Liu Z, Shi P, Zhang JZ (2010). The hearing gene *Prestin* unites echolocating bats and whales. *Curr. Biol.* **20:** R55-R56.

Liang F (2000). Gene Index analysis estimates the human genome contains 120,000 genes. *Nat. Genet.* **25:** 501-501.

Lin Z, Cantos R, Patente M, Wu DK (2005). *Gbx2* is required for the morphogenesis of the mouse inner ear: a downstream candidate of hindbrain signaling. *Development* **132:** 2309-2318.

Lindenlaub T, Burda H, Nevo E (1995). Convergent evolution of the vestibular organ in the subterranean mole-rats, *Cryptomys* and *Spalax*, as compared with the aboveground rat, *Rattus*. *J. Morphol.* **224:** 303-311.

Lindenlaub T, Oelschlager HA (1999). Morphological, morphometric, and functional differences in the vestibular organ of different breeds of the rat (*Rattus norvegicus*). *Anat. Rec.* **255:** 15-19.

Liu W, Li G, Chien JS, S. R, Zhang H, Chiang C *et al* (2002). Sonic Hedgehog regulates otic capsule chondrogenesis and inner ear development in the mouse embryo. *Dev. Biol.* **248:** 240-250.

Liu Y, Cotton JA, Shen B, Han XQ, Rossiter SJ, Zhang SY (2010a). Convergent sequence evolution between echolocating bats and dolphins. *Curr. Biol.* **20:** R53-R54.

Liu Y, Rossiter SJ, Han X, Cotton JA, Zhang S (2010b). Cetaceans on a molecular fast track to ultrasonic hearing. *Curr. Biol.* **20:** 1834-1839.

Lohmann GP (1983). Eigenshape analysis of micro-fossils - a general morphometirc procedure for describing changes in shape. *J. Int. Ass. Math. Geol.* **15:** 659-672.

Longdon B, Hadfield JD, Webster CL, Obbard DJ, Jiggins FM (2011). Host phylogeny determines viral persistence and replication in novel hosts. *Plos Pathogens* **7:** e1002260. doi:1002210.1001371/journal.ppat.1002260.

Loots G, Ovcharenko I (2004). rVista 2.0: evolutionary analysis of transcription factor binding sites. *Nucleic Acids Res.***:** W217-W221.

Lowenstein OE (1974). Comparative morphology and physiology (of the vestibular system in vertebrates). In: Kornhuber HH (ed) *Vestibular System Part 1: Basic Mechanisms* Springer-Verlag: Berlin, pp 75 - 120.

Lucca G (2003). Representing seashells surface. *VisMath* **5**.

Lukats A, Szabo A, Rohlich P, Vigh B, Szel A (2005). Photopigment coexpression in mammals: comparative and developmental aspects. *Histol. Histopathol.* **20:** 551-574.

Luo ZX (2007). Transformation and diversification in early mammal evolution *Nature* **450:** 1011-1019.

Luo ZX, Ruf I, Schultz JA, Martin T (2011). Fossil evidence on evolution of inner ear cochlea in Jurassic mammals. *Proc. R. Soc. Biol. Sci. B.* **278:** 28-34.

Ma JG, Muller R (2011). A method for characterizing the biodiversity in bat pinnae as a basis for engineering analysis. *Bioinspir. Biomim.* **6**.

Maas SA, Fallon JF (2005). Single base pair change in the long-range Sonic hedgehog limb-specific enhancer is a genetic basis for preaxial polydactyly. *Dev. Dyn.* **232:** 345-348.

MacLeod N (1999). Generalizing and extending the eigenshape method of shape space visualization and analysis. *Paleobiology* **25:** 107-138.

MacLeod N (2002). Geometric morphometrics and geological shape-classification systems. *Earth-Sci. Rev.* **59:** 27-47.

Macrini TE, Flynn JJ, Croft DA, Wyss AR (2010). Inner ear of a notoungulate placental mammal: anatomical description and examination of potentially phylogenetically informative characters. *J. Anat.* **216:** 600-610.

Madsen O, Scally M, Douady CJ, Kao DJ, DeBry RW, Adkins R *et al* (2001). Parallel adaptive radiations in two major clades of placental mammals. *Nature* **409:** 610-614.

Malia Jr. MJ, Adkins RM, Allard MW (2002). Molecular support for Afrotheria and the polyphyly of Lipotyphla based on analyses of the growth hormone receptor gene *Mol. Phylogenet. Evol.* **24:** 91-101.

Manley GA (2000). Cochlear mechanisms from a phylogenetic viewpoint. *Proc. Natl. Acad. Sci. U. S. A.* **97:** 11736-11743.

Manley GA (2010). An evolutionary perspective on middle ears. *Hear. Res.* **263:** 3-8.

Manley GA, popper AN, Fay RR (eds) (2004). *Evolution of the Vertebrate Auditory System*. Springer: New York.

Manoussaki D, Chadwick RS, Ketten DR, Arruda J, Dimitriadis EK, O'Malley JT (2008). The influence of cochlear shape on low-frequency hearing. *Proc. Natl. Acad. Sci. U. S. A.* **105:** 6162-6166.

Manoussaki D, Dimitriadis EK, Chadwick RS (2006). Cochlea's graded curvature effect on low frequency waves. *Phys. Rev. Lett.* **96:** 088701.

Marcotti W, Erven A, Johnson SL, Steel KP, Kros CJ (2006). *Tmc1* is necessary for normal functional maturation and survival of inner and outer hair cells in the mouse cochlea. *J. Physiol.* **574:** 677-698.

Martin AP, Palumbi SR (1992). Body size, metabolic rate, generation time, and the molecular clock. *Proc. Natl. Acad. Sci. U. S. A.* **90:** 4087-4091.

McGowen MR, Spaulding M, Gatesy J (2009). Divergence date estimation and a comprehensive molecular tree of extant cetaceans. *Mol. Phylogenet. Evol.* **53:** 891-906.

McNab BK (1994). Energy-conservation and the evolution of flightlessness in birds. *Am. Nat.* **144:** 628-642.

McVean A (1999). Are the semicircular canals of the European mole, *Talpa europaea*, adapted to a subterranean habitat? *Comp. Biochem. Phys. A* **123:** 173-178.

Meng J, Fox RC (1995). Osseous inner ear structures and hearing in early marsupials and placentals. *Zool. J. Linn. Soc.* **115:** 47-71.

Merlo GR, Zerega B, Paleari L, Trombino S, Mantero S, Levi G (2000). Multiple functions of *Dlx* genes. *Int. J. Dev. Biol.* **44:** 619-626.

Mikkelsen TS, Hillier LW, Eichler EE, Zody MC, Jaffe DB, Yang SP *et al* (2005). Initial sequence of the chimpanzee genome and comparison with the human genome. *Nature* **437:** 69-87.

Mikkelsen TS, Wakefield MJ, Aken B, Amemiya CT, Chang JL, Duke S *et al* (2007). Genome of the marsupial *Monodelphis domestica* reveals innovation in non-coding sequences. *Nature* **447:** 167-U161.

Miller-Butterworth CM, Murphy WJ, O'Brien SJ, Jacobs DS, Springer MS, Teeling EC (2007). A family matter: Conclusive resolution of the taxonomic position of the long-fingered bats, Miniopterus. *Mol. Biol. Evol.* **24:** 1553-1561.

Miller JD (2007). Sex diffferences in the length of the organ of Corti in humans. *J. Acoust. Soc. Am.* **121:** EL151-EL155.

Mogdans J, Ostwald J, Schnitzler HU (1988). The role of pinna movement for the localization of vertical and horizontal wire obstacles in the greater horseshoe bat, *Rhinolophus ferrumequinum*. *J. Acoust. Soc. Am.* **84:** 1676-1679.

Morris A, Bowmaker JK, Hunt DM (1993). The molecular-basis of a spectral shift in the rhodopsins of 2 species of squid from different photic environments. *Proc. R. Soc. Biol. Sci. B.* **254:** 233-240.

Moss CF, Bohn K, Gilkenson H, Surlykke A (2006). Active listening for spatial orientation in a complex auditory scene. *PLoS Biol.* **4:** 615-626.

Murphy WJ, Eizirik E, Johnson WE, Zhang YP, Ryder OA, O'Brien SJ (2001a). Molecular phylogenetics and the origins of placental mammals. *Nature* **409:** 614-618.

Murphy WJ, Eizirik E, O'Brien SJ, Madsen O, Scally M, Douady CJ *et al* (2001b). Resolution of the early placental mammal radiation using Bayesian phylogenetics. *Science* **294:** 2348-2351.

Murphy WJ, O'Brien SJ (2007). Designing and optimizing comparative anchor primers for comparative gene mapping and phylogenetic inference. *Nat. Protoc.* **2:** 3022-3030.

Murphy WJ, Pringle TH, Crider TA, Springer MS, Miller W (2007). Using genomic data to unravel the root of the placental mammal phylogeny. *Genome Res.* **17:** 413-421.

Neuweiler G (1984). Foraging, echolocation and audition in bats. *Naturwissenschaften* **71:** 446-455.

Neuweiler G (2000). *The Biology of Bats*. Oxford University Press: New York and Oxford.

Neuweiler G (2003). Evolutionary aspects of bat echolocation. *J. Comp. Physiol. Sens. Neural. Behav. Physiol.* **189:** 245-256.

Nevo E (1979). Adaptive convergence and divergence of subterranean mammals. *Annu. Rev. Ecol. Syst.* **10:** 269-308.

Ni XJ, Flynn JJ, Wyss AR (2010). The bony labyrinth of the early platyrrhine primate *Chilecebus*. *J. Hum. Evol.* **59:** 595-607.

Nishihara H, Hasegawa M, Okada N (2006). Pegasoferae, an unexpected mammalian clade revealed by tracking ancient retroposon insertions. *Proc. Natl. Acad. Sci. U. S. A.* **103:** 9929-9934.

Nobrega MA, Zhu YW, Plajzer-Frick I, Afzal V, Rubin EM (2004). Megabase deletions of gene deserts result in viable mice. *Nature* **431:** 988-993.

Norberg UM (1981). Allometry of bat wings and legs and comparison with bird wings. *Phil. Trans. R. Soc. Lond. B* **292:** 359-398.

Norberg UM (1987). Wing form and flight mode in bats. *Fenton, M. B., P. Racey and J. M. V. Rayner (Ed.). Recent Advances in the Study of Bats; Joint Meeting of the Seventh International Bat Research Symposium, Aberdeen, Scotland, Uk, August 19-24, 1985. Xii+470p. Cambridge University Press: Cambridge, England, Uk; New York, New York, USA. Illus***:** 43-56.

Norberg UM, Rayner JMV (1987). Ecological morphology and flight in bats (Mammalia; Chiroptera): wing adaptations, flight performance, foraging strategy and echolocation. *Phil. Trans. R. Soc. Lond. B* **316:** 335-427.

Novacek MJ (1987). Auditory features and affinities of the Eocene bats *Icaronycteris* and *Palaeochiropteryx* (Microchiroptera, incertae sedis). *Am. Mus. Novit.* **2877:** 1-18.

Novacek MJ (1992). Mammalian phylogeny - shaking the tree. *Nature* **356:** 121-125.

Nummela S (1995). Scaling of the mammalian middle-ear. *Hear. Res.* **85:** 18-30.

Nummela S, Wagar T, Hemila S, Reuter T (1999). Scaling of the cetacean middle ear. *Hear. Res.* **133:** 71-81.

Obrist MK, Fenton MB, Eger JL, Schlegel PA (1993). What ears do for bats - a comparative-study of pinna sound pressure transformation in chiroptera. *J. Exp. Biol.* **180:** 119-152.

Odendaal LJ, Jacobs DS (2011). Morphological correlates of echolocation frequency in the endemic Cape horseshoe bat, *Rhinolophus capensis* (Chiroptera: Rhinolophidae). *J. Comp. Physiol. A.* **197:** 435-446.

Ofusori DA, Caxton-Martins EA, Komolafe OO, Oluyemi KA, Adeeyo OA, Ajayi SA *et al* (2008). A comparative study of the ileum in rat (*Rattus norvegicus*), bat (*Eidolon helvum*) and pangolin (*Manis tricuspis*) as investigated using histological method. *Int. J. Morphol.* **26:** 137-141.

Oman CM, Marcus EN, Curthoys IS (1987). The influence of semicircular canal morphology on endolymph flow dynamics - an anatomically descriptive mathematical model. *Acta Oto-Laryngol.* **103:** 1-13.

Orbach DN, Fenton B (2010). Vision impairs the abilities of bats to avoid colliding with stationary obstacles. *Plos One* **5**.

Oscar Sanchez-Guardado L, Luis Ferran J, Rodriguez-Gallardo L, Puelles L, Hidalgo-Sanchez M (2011). *Meis* gene expression patterns in the developing chicken inner ear. *J. Comp. Neurol.* **519:** 125-147.

Packard A (1972). Cephalopods and fish - limits of convergence. *Biol. Rev. Camb. Philos. Soc.* **47:** 241-&.

Parkinson N, Hardisty-Hughes RE, Tateossian H, Tsai H-T, Brooker D, Morse S *et al* (2006). Mutation at the *Evi1* locus in Junbo mice causes susceptibility to otitis media. *Plos Genetics* **2:** 1556-1564.

Payne RS (1971). Acoustic location of prey by barn owls. *J. Exp. Biol.***:** 535-573.

Pedersen SC (1993). Cephalometric correlates of echolocation in the Chiroptera. *J. Morphol.* **218:** 85-98.

Pedersen SC (2000). Skull growth and the acoustical axis of the head in bats. In: Adams RA and Pedersen SC (eds) *Ontogeny, functional ecology, and evolution of bats*. Cambridge University Press: Cambridge, pp 174-246.

Pereira MJR, Rebelo H, Teeling EC, O'Brien SJ, Mackie I, Bu SSH *et al* (2006). Status of the world's smallest mammal, the bumble-bee bat *Craseonycteris thonglongyai*, in Myanmar. *Oryx* **40:** 456-463.

Pierce GW, Griffin DR (1938). Experimental determination of supersonic notes emitted by bats. *J. Mammal.* **19:** 454-455.

Pitnick S, Jones KE, Wilkinson GS (2006). Mating system and brain size in bats. *Proc. R. Soc. Biol. Sci. B.* **273:** 719-724.

Polly PD, MacLeod N (2008). Locomotion in fossil Carnivora: An application of eigensurface analysis for morphometric comparison of 3D surfaces. *Palaeontol. Electron.* **11**.

Popadin K, Polishchuk LV, Mamirova L, Knorre D, Gunbin K (2007). Accumulation of slightly deleterious mutations in mitochondrial protein-coding genes of large versus small mammals. *Proc. Natl. Acad. Sci. U. S. A.* **104:** 13390-13395.

Posada D (2008). jModelTest: Phylogenetic model averaging. *Mol. Biol. Evol.* **25:** 1253-1256.

Prabhakar S, Noonan JP, Paeaebo S, Rubin EM (2006). Accelerated evolution of conserved noncoding sequences in humans. *Science* **314:** 786-786.

Pumo DE, Finamore PS, Franek WR, Phillips CJ, Tarzami S, Balzarano D (1998). Complete mitochondrial genome of a neotropical fruit bat, *Artibeus jamaicensis*, and a new hypothesis of the relationships of bats to other eutherian mammals. *J. Mol. Evol.* **47:** 709-717.

Puschel AW, Westerfield M, Dressler GR (1992). Comparative-analysis of Pax-2 protein distributions during neurulation in mice and zebrafish. *Mech. Dev.* **38:** 197-208.

Pye A (1966a). The megachiroptera and vespertilionoidea of the microchiroptera. *J. Morphol.* **119:** 101-119.

Pye A (1966b). The structure of the cochlea in chiroptera. I. Microchiroptera: Emballonuroidea and Rhinolophoidea. *J. Morphol.* **118:** 495-510.
Pye A (1967). The structure of the cochlea in chiroptera. III. Microchiroptera: Phyllostomatoidea. *J. Morphol.* **121:** 241-254.
Pye A (1980). Unique structural-changes in the cochlea of a bat (*Pteronotus parnelli*). *Clin. Otolaryngol.* **5:** 80-81.
Pye JD (1983). Echolocation and Countermeasures. In: Lewis B (ed) *Bioacoustics: A Comparative Approach*. Academic Press: New York, pp 407-429.
Pye JD, Pye A (1988). Echolocation sounds and hearing in the fruit bat *Rousettus*. In: Stephens SDG and Prasansuk S (eds) *Measurements in Hearing and Balance*. S. Karger AG Basel. Vol. 5, pp 1-12.
R Development Core Team (2011) R: A language and environment for statistical computing (Vienna, Austria.)
Ramprashad F, Landolt JP, Money KE, Laufer J (1980). Neuromorphometric features and dimensional analysis of the vestibular end organ in the little brown bat (*Myotis lucifugus*). *J. Comp. Neurol.* **192:** 883-902.
Ratcliffe JM, Raghuram H, Marimuthu G, Fullard JH, Fenton MB (2005). Hunting in unfamiliar space: echolocation in the Indian false vampire bat, *Megaderma lyra*, when gleaning prey. *Behav. Ecol. Sociobiol.* **58:** 157-164.
Reale D, Festa-Bianchet M, Jorgenson JT (1999). Heritability of body mass varies with age and season in wild bighorn sheep. *Heredity* **83:** 526-532.
Reeder DM, Helgen KM, Wilson DE (2007). Global trends and biases in new mammal species discoveries *Occas. Pap. Mus. Texas Tech Univ.* **269:** 1-36.
Renucci A, Zappavigna V, Zakany J, Izpisuabelmonte JC, Burki K, Duboule D (1992). Comparison of mouse and human *Hox-4* complexes defines conserved sequences involved in the regulation of *Hox-4.4*. *Embo Journal* **11:** 1459-1468.
Rhode WS, Recio A. (2003). *Biophysics of the Cochlea: from Molecules to Models, Proceedings of the International Symposium*: Titisee, Germany, pp 220-227.
Rhodes CR, Parkinson N, Tsai H, Brooker D, Mansell S, Spurr N *et al* (2003). The homeobox gene *Emx2* underlies middle ear and inner ear defects in the deaf mouse mutant pardon. *J. Neurocytol.* **32:** 1143-1154.
Richter CP, Evans BN, Edge R, Dallos P (1998). Basilar membrane vibration in the gerbil hemicochlea. *J. Neurophysiol.* **79:** 2255-2264.
Rinkwitzbrandt S, Justus M, Oldenettel I, Arnold HH, Bober E (1995). Distinct temporal expression of mouse *Nkx-5.1* and *Nkx-5.2* homeobox genes during brain and ear development. *Mech. Dev.* **52:** 371-381.
Riskin DK, Bahlman JW, Hubel TY, Ratcliffe JM, Kunz TH, Swartz SM (2009). Bats go head-under-heels: the biomechanics of landing on a ceiling. *J. Exp. Biol.* **212:** 945-953.
Riskin DK, Parsons S, Schutt WA, Carter GG, Hermanson JW (2006). Terrestrial locomotion of the New Zealand short-tailed bat *Mystacina tuberculata* and the common vampire bat *Desmodus rotundus*. *J. Exp. Biol.* **209:** 1725-1736.
Robinson M, Gouy M, Gautier C, Mouchiroud D (1998). Sensitivity of the relative-rate test to taxonomic sampling. *Mol. Biol. Evol.* **15:** 1091-1098.
Robinson MF (1996). A relationship between echolocation calls and noseleaf widths in bats of the genera *Rhinolophus* and *Hipposideros*. *J. Zool.* **239:** 389-393.
Robles L, Ruggero MA (2001). Mechanics of the mammalian cochlea. *Physiol. Rev.* **81:** 1305-1352.
Roelants K, Fry BG, Norman JA, Clynen E, Schoofs L, Bossuyt F (2010). Identical skin toxins by convergent molecular adaptation in frogs. *Curr. Biol.* **20:** 125-130.
Rokas A, Carroll SB (2008). Frequent and widespread parallel evolution of protein sequences. *Mol. Biol. Evol.* **25:** 1943-1953.

Romeroherrera AE, Lehmann H, Joysey KA, Friday AE (1978). On the evolution of myoglobin. *Phil. Trans. R. Soc. B* **283:** 61-&.

Ronquist F, Huelsenbeck JP (2003). MrBayes 3: Bayesian phylogenetic inference under mixed models. *Bioinformatics* **19:** 1572-1574.

Rosenbloom KR, Dreszer TR, Pheasant M, Barber GP, Meyer LR, Pohl A *et al* (2010). ENCODE whole-genome data in the UCSC Genome Browser. *Nucleic Acids Res.* **38:** D620-625.

Rosowski JJ (1996). Models of external- and middle-ear function. In: Hawkins HL, McMullen TA, Popper AN and Fay RR (eds) *Auditory Computation*. Springer. Vol. 6, pp 15-61.

Rosowski JJ, Graybeal A (1991). What did Morganucodon hear? *Zool. J. Linn. Soc.* **101:** 131-168.

Rossiter S. J. Unpublished data.

Rossiter SJ, Zhang S, Liu Y (2011). *Prestin* and high-frequency hearing in mammals. *Comm. Int. Biol.* **4:** 236-239.

Roth FP, Hughes JD, Estep PW, Church GM (1998). Finding DNA regulatory motifs within unaligned noncoding sequences clustered by whole-genome mRNA quantitation. *Nat. Biotechnol.* **16:** 939-945.

Rowe T, Frank LR (2011). The disappearing third dimension. *Science* **331:** 712-714.

Rozen S, Skaletsky H (2000). Primer3 on the WWW for general users and for biologist programmers. *Methods Mol. Biol.* **132:** 365-386.

Ruggero MA, Temchin AN (2002). The roles of the external, middle, and inner ears in determining the bandwidth of hearing. *Proc. Natl. Acad. Sci. U. S. A.* **99:** 13206-13210.

Russell IJ, Drexl M, Foeller E, Vater M, Kossl M (2003). The development of a single frequency place in the mammalian cochlea: The cochlear resonance in the mustached bat *Pteronotus parnellii*. *J. Neurosci.* **23:** 10971-10981.

Russo D, Mucedda M, Bello M, Biscardi S, Pidinchedda E, Jones G (2007). Divergent echolocation call frequencies in insular rhinolophids (Chiroptera): a case of character displacement? *J. Biogeogr.* **34:** 2129-2138.

Sajan SA, Warchol ME, Lovett M (2007). Towards a systems biology of mouse inner ear organogenesis: gene expression pathways, patterns and network analysis. *Genetics* **177:** 631-653.

Sandelin A, Wasserman WW, Lenhard B (2004). ConSite: web-based prediction of regulatory elements using cross-species comparison. *Nucleic Acids Res.* **32:** W249-W252.

Schmelzle T, Sanchez-Villagra MR, Maier W (2007). Vestibular labyrinth diversity in diprotodontian marsupial mammals. *Mamm. Study* **32:** 83-97.

Schmidt S, Gerasimova A, Kondrashov FA, Adzhubei IA, Kondrashov AS, Sunyaev S (2008). Hypermutable non-synonymous sites are under stronger negative selection. *Plos Genetics* **4:** e1000281.

Schmieder DA, Kingston T, Hashim R, Siemers BM (2010). Breaking the trade-off: rainforest bats maximize bandwidth and repetition rate of echolocation calls as they approach prey. *Biol. Lett.* **6:** 604-609.

Schnitzler HU, Kalko EKV (2001). Echolocation by insect-eating bats. *Bioscience* **51:** 557-569.

Schnitzler HU, Moss CF, Denzinger A (2003). From spatial orientation to food acquisition in echolocating bats. *Trends Ecol. Evol.* **18:** 386-394.

Schug J, Overton GC (1997). TESS: Transcription Element Search Software on the WWW. *Technical Report CBIL-TR-1997-1001-v0.0, Computational Biology and Informatics Laboratory, School of Medicine, University of Pennsylvania*

Schuller G, Pollak G (1979). Disproportionate frequency representation in the inferior colliculus of Doppler-compensating greater horseshoe bats: evidence for an acoustic fovea. *J. Comp. Physiol.* **132:** 47-54.

Schultz J, Milpetz F, Bork P, Ponting CP (1998). SMART, a Simple Modular Architecture Research Tool: Identification of signaling domains. *Proc. Natl. Acad. Sci. U. S. A.* **95:** 5857-5864.

Schusterman RJ (1981). Behavioral capabilities of the seals and sea lions - a review of their hearing, visual, learning and diving skills. *Psychol. Rec.* **31:** 125-143.

Schwander M, Sczaniecka A, Grillet N, Bailey JS, Avenarius M, Najmabadi H *et al* (2007). A forward genetics screen in mice identifies recessive deafness traits and reveals that pejvakin is essential for outer hair cell function. *J. Neurosci.* **27:** 2163-2175.

Scott SA, Carey JC (2006). Inner ear. In: Stevenson RE and Hall JG (eds) *Human malformations and related anomalies*, 2nd edn. Oxford University Press: New York, pp 366-369.

Shen YY, Liu J, Irwin DM, Zhang YP (2010). Parallel and convergent evolution of the dim-light vision gene *RH1* in bats (Order: Chiroptera). *Plos One* **5**.

Shimodaira H (2002). An approximately unbiased test of phylogenetic tree selection. *Syst. Biol.* **51:** 492-508.

Shimodaira H, Hasegawa M (2001). CONSEL: for assessing the confidence of phylogenetic tree selection. *Bioinformatics* **17:** 1246-1247.

Shoshani J, McKenna MC (1998). Higher taxonomic relationships among extant mammals based on morphology, with selected comparisons of results from molecular data. *Mol. Phylogenet. Evol.* **9:** 572-584.

Shu WG, Lu MM, Zhang YZ, Tucker PW, Zhou DY, Morrisey EE (2007). *Foxp2* and *Foxp1* cooperatively regulate lung and esophagus development. *Development* **134:** 1991-2000.

Siemers BM, Schauermann G, Turni H, von Merten S (2009). Why do shrews twitter? Communication or simple echo-based orientation. *Biol. Lett.* **5:** 593-596.

Silva M, Downing JA (1995). The allometric scaling of density and body-mass - a nonlinear relationship for terrestrial mammals. *Am. Nat.* **145:** 704-727.

Simmons N, Seymour K, Gunnell G (2007). A new primitive bat from the early Eocene of Wyoming: Fossils, phylogenetics, and the evolution of echolocation and flight. *J. Vertebr. Paleontol.* **27:** 147A-147A.

Simmons NB, Geisler JH (1998). Phylogenetic relationships of *Icaronycteris*, *Archaeonycteris*, *Hassianycteris*, and *Palaeochiropteryx* to extant bat lineages, with comments on the evolution of echolocation and foraging strategies in microchiroptera. *Bull. Am. Mus. Nat. Hist.***:** 4-182.

Simmons NB, Seymour KL, Habersetzer J, Gunnell GF (2008). Primitive Early Eocene bat from Wyoming and the evolution of flight and echolocation. *Nature* **451:** 818-821.

Simmons NB, Seymour KL, Habersetzer J, Gunnell GF (2010). Inferring echolocation in ancient bats. *Nature* **466:** E8-E9.

Sipla JS (2007). The semicircular canals of birds and non-avian theropod dinosaurs. Doctor of Philosophy thesis, Stony Brook University.

Skals N, Plepys D, Lofstedt C (2003). Foraging and mate-finding in the silver Y moth, *Autographa gamma* (Lepidoptera : Noctuidae) under the risk of predation. *Oikos* **102:** 351-357.

Smith HF, Fisher RE, Everett ML, Thomas AD, Bollinger RR, Parker W (2009). Comparative anatomy and phylogenetic distribution of the mammalian cecal appendix. *J. Evol. Biol.* **22:** 1984-1999.

Smotherman M, Guillen-Servent A (2008). Doppler-shift compensation behavior by Wagner's mustached bat, *Pteronotus personatus*. *J. Acoust. Soc. Am.* **123:** 4331-4339.

Snell LC, Rylander K (2001). Morphometric analysis of the superior vestibular nerve in ground and tree squirrels (Sciuridae). *J. Mammal.* **82:** 218-224.

Speakman JR (2001). The evolution of flight and echolocation in bats: another leap in the dark. *Mammal. Rev.* **31:** 111-130.

Speakman JR, Racey PA (1991). The energetics of echolocation. *Bat Res. News.* **33:** 86.

Spoor F (2003). The semicircular canal system and locomotor behaviour, with special reference to hominin evolution. *Cour. Forsch. Senckenberg.* **243:** 93-104.

Spoor F, Bajpal S, Hussaim ST, Kumar K, Thewissen JGM (2002). Vestibular evidence for the evolution of aquatic behaviour in early cetaceans. *Nature* **417:** 163-166.

Spoor F, Garland T, Krovitz G, Ryan TM, Silcox MT, Walker A (2007). The primate semicircular canal system and locomotion. *Proc. Natl. Acad. Sci. U. S. A.* **104:** 10808-10812.

Spoor F, Wood B, Zonneveld F (1994). Implications of early Hominid labyrinthine morphology for evolution of human bipedal locomotion. *Nature* **369:** 645-648.

Spoor F, Zonneveld F (1995). Morphometry of the primate bony labyrinth - a new method based on high-resolution computed-tomography. *J. Anat.* **186:** 271-286.

Spoor F, Zonneveld F (1998). Comparative review of the human bony labyrinth. *Am. J. Phys. Anthropol.* **Suppl 27:** 211-251.

Spotorno AE, Zuleta CA, Valladares JP, Deane AL, Jimenez JE (2004). *Chinchilla laniger*. *Mamm. Species* **758:** 1-9.

Springer MS, Cleven GC, Madsen O, de Jong WW, Waddell VG, Amrine HM *et al* (1997). Endemic African mammals shake the phylogenetic tree. *Nature* **388:** 61-64.

Springer MS, Stanhope MJ, Madsen O, de Jong WW (2004). Molecules consolidate the placental mammal tree. *Trends Ecol. Evol.* **19:** 430-438.

Springer MS, Teeling EC, Madsen O, Stanhope MJ, de Jong WW (2001). Integrated fossil and molecular data reconstruct bat echolocation. *Proc. Natl. Acad. Sci. U. S. A.* **98:** 6241-6246.

Stamatakis A (2006). RAxML-VI-HPC: Maximum likelihood-based phylogenetic analyses with thousands of taxa and mixed models. *Bioinformatics* **22:** 2688-2690.

Stanhope MJ, Czelusniak J, Si JS, Nickerson J, Goodman M (1992). A molecular perspective on mammalian evolution from the gene encoding Interphotoreceptor Retinoid Binding Protein, with convincing evidence for bat monophyly. *Mol. Phylogenet. Evol.* **1:** 148-160.

Stanhope MJ, Waddell VG, Madsen O, de Jong W, Hedges SB, Cleven GC *et al* (1998). Molecular evidence for multiple origins of Insectivora and for a new order of endemic African insectivore mammals. *Proc. Natl. Acad. Sci. U. S. A.* **95:** 9967-9972.

Stewart CB, Schilling JW, Wilson AC (1987). Adaptive evolution in the stomach lysozymes of foregut fermenters. *Nature* **330:** 401-404.

Storch G, Sige B, Habersetzer J (2002). *Tachypteron franzeni* n. gen., n. sp., earliest emballonurid bat from the Middle Eocene of Messel (Mammalia, Chiroptera). *Palaontol. Z.* **76:** 189–199.

Suthers RA, Suthers BJ (1972). Respiration, wing-beat and ultrasonic pulse emission in an echolocating bat. *J. Exp. Biol.* **56:** 37-&.

Suthers RA, Wallis NE (1970). Optics of eyes of echolocating bats. *Vision Res.* **10:** 1165-&.

Swartz JD, Daniels DL, Harnsberger HR, Shaffer A, Mark L (1996). Balance and equilibrium: 1. The vestibule and semicircular canals. *Am. J. Neuroradiol.* **17:** 17-21.

Swartz SM, Freeman PW, Stockwell EF (2003). Ecomorphology of bats: comparative and experimental approaches relating structural design to ecology. In: Kunz TH and Fenton B (eds) *Bat Ecology*. University of Chicago Press: Chicago and London, pp 257 - 300.

Swofford DL (2003) PAUP*. Phylogenetic Analysis Using Parsimony (*and other Methods). (Sinauer Associates, Sunderland, Massachusetts)

Tajima F (1993). Simple methods for testing the molecular evolutionary clock hypothesis. *Genetics* **135:** 599-607.

Tamura K, Peterson D, Peterson N, Stecher G, Nei M, Kumar S (2011). MEGA5: Molecular evolutionary genetics analysis using Maximum Likelihood, Evolutionary Distance, and Maximum Parsimony Methods. *Mol. Biol. Evol.* **10.1093/molbev/msr121**.

Teeling E (2009). Hear, hear: the convergent evolution of echolocation in bats? *Trends Ecol. Evol.* **24:** 351 - 354.

Teeling EC, Madsen O, Murphy WJ, Springer MS, O'Brien J (2003). Nuclear gene sequences confirm an ancient link between New Zealand's short-tailed bat and South American noctilionoid bats. *Mol. Phylogenet. Evol.* **28:** 308-319.

Teeling EC, Madsen O, Van den Bussche RA, de Jong WW, Stanhope MJ, Springer MS (2002). Microbat paraphyly and the convergent evolution of a key innovation in Old World rhinolophoid microbats. *Proc. Natl. Acad. Sci. U. S. A.* **99:** 1431-1436.

Teeling EC, Scally M, Kao DJ, Romagnoli ML, Springer MS, Stanhope MJ (2000). Molecular evidence regarding the origin of echolocation and flight in bats. *Nature* **403:** 188-192.

Teeling EC, Springer MS, Madsen O, Bates P, O'Brien SJ, Murphy WJ (2005). A molecular phylogeny for bats illuminates biogeography and the fossil record. *Science* **307:** 580-584.

Thabah A, Rossiter SJ, Kingston T, Zhang S, Parsons S, Mya K *et al* (2006). Genetic divergence and echolocation call frequency in cryptic species of *Hipposideros larvatus s.l.* (Chiroptera: Hipposideridae) from the Indo-Malayan region. *Biol. J. Linn. Soc.* **88:** 119-130.

The International HapMap Consortium (2010). Integrating common and rare genetic variation in diverse human populations. *Nature* **467:** 52-58.

Thewissen JGM, Etnier SA (1995). Adhesive devices on the thumb of vespertilionoid bats (Chiroptera). *J. Mammal.* **76:** 925-936.

Thewissen JGM, Williams EM, Roe LJ, Hussain ST (2001). Skeletons of terrestrial cetaceans and the relationship of whales to artiodactyls. *Nature* **413:** 277-281.

Thomas JA, Moss CF, Vater M (eds) (2004). *Echolocation in Bats and Dolphins*. The University of Chicago Press: Chicago and London.

Tian Q, Linthicum FH, Fayad JN (2006). Human cochleae with three turns: An unreported malformation. *Laryngoscope* **116:** 800-803.

Tobe SS, Kitchener AC, Linacre AMT (2010). Reconstructing mammalian phylogenies: a detailed comparison of the *Cytochrome b* and *Cytochrome Oxidase Subunit I* mitochondrial genes. *Plos One* **5**.

Ulfendahl M, Flock A (1998). Outer hair cells provide active tuning in the organ of Corti. *News Physiol. Sci.* **13:** 107-111.

Van den Bussche RA, Hoofer SR (2004). Phylogenetic relationships among recent chiropteran families and the importance of choosing appropriate out-group taxa. *J. Mammal.* **85:** 321-330.

Vater M, Kossl M (2004). Introduction: The ears of whales and bats. In: Thomas JA, Moss CF and Vater M (eds) *Echolocation in Bats and Dolphins*. The University of Chicago Press: Chicago and London, pp 89-98.

Vater M, Kossl M (2011). Comparative aspects of cochlear functional organization in mammals. *Hear. Res.* **273:** 89-99.

Veselka N, McErlain DD, Holdsworth DW, Eger JL, Chhem RK, Mason MJ *et al* (2010a). A bony connection signals laryngeal echolocation in bats. *Nature* **463:** 939-942.

Veselka N, McErlain DD, Holdsworth DW, Eger JL, Chhem RK, Mason MJ *et al* (2010b). Inferring echolocation in ancient bats Reply. *Nature* **466:** E9-E10.

Volleth M, Heller KG, Pfeiffer RA, Hameister H (2002). A comparative ZOO-FISH analysis in bats elucidates the phylogenetic relationships between megachiroptera and five microchiropteran families. *Chromosome Res.* **10:** 477-497.

Walsh SA, Barrett PM, Milner AC, Manley G, Witmer LM (2009). Inner ear anatomy is a proxy for deducing auditory capability and behaviour in reptiles and birds. *Proc. R. Soc. Biol. Sci. B.* **276:** 1355-1360.

Wang L, Li G, Wang JH, Ye SH, Jones G, Zhang SY (2009). Molecular cloning and evolutionary analysis of the *GJA1* (connexin43) gene from bats (Chiroptera). *Genet. Res.* **91:** 101-109.

Wang WD, Lufkin T (2005). Hmx homeobox gene function in inner ear and nervous system cell-type specification and development. *Exp. Cell Res.* **306:** 373-379.

Warner SJ, Hutson MR, Oh S-H, Gerlach-Bank LM, Lomax MI, Barald KF (2003). Expression of *ZIC* genes in the devlopment of the chick inner ear and nervous system. *Dev. Dyn.* **226:** 702-712.

Warrick DR, Bundle MW, Dial KP (2002). Bird maneuvering flight: Blurred bodies, clear heads. *Integr. Comp. Biol.* **42:** 141-148.

Wartzok D, Ketten DR (1999). Marine mammal sensory systems. In: Reynolds J and Rommel S (eds) *Biology of Marine Mammals*. Smithsonian Institution Press, pp 117-175.

Waters DA, Jones G (1995). Echolocation call structure and intensity in 5 species of insectivorous bats. *J. Exp. Biol.* **198:** 475-489.

Webster DB, Webster M (1980). Morphological adaptations of the ear in the rodent family Heteromyidae. *Am. Zool.* **20:** 247-254.

Welch JJ, Bininda-Emonds ORP, Bromham L (2008). Correlates of substitution rate variation in mammalian protein-coding sequences. *BMC Evol. Biol.* **8:** doi:10.1186/1471-2148-1188-1153.

Welker KL, Orkin JD, Ryan TM (2009). Analysis of intraindividual and intraspecific variation in semicircular canal dimensions using high-resolution x-ray computed tomography. *J. Anat.* **215:** 444-451.

Welscher PT, Zuniga A, Kuijper S, Drenth T, Goedemans HJ, Meijlink F *et al* (2002). Progression of vertebrate limb development through SHH-mediated counteraction of GLI3. *Science* **298:** 827-830.

West CD (1985). The relationship of the spiral turns of the cochlea and the length of the basilar membrane to the range of audible frequencies in ground dwelling mammals. *J. Acoust. Soc. Am.* **77:** 1091-1101.

Wiens JJ, Brandley MC, Reeder TW (2006). Why does a trait evolve multiple times within a clade? Repeated evolution of snakelike body form in squamate reptiles. *Evolution* **60:** 123-141.

Wiley DF (2007). Landmark *Institute for Data Analysis and Visualization, University of California, Davis (http://www.idav.ucdavis.edu/research/projects/EvoMorph).*

Wilson AJ, Pemberton JM, Pilkington JG, Coltman DW, Mifsud DV, Clutton-Brock TH *et al* (2006). Environmental coupling of selection and heritability limits evolution. *PLoS Biol.* **4:** 1270-1275.

Wilson AJ, Reale D, Clements MN, Morrissey MM, Postma E, Walling CA *et al* (2009). An ecologist's guide to the animal model. *J. Anim. Ecol.* **79:** 13-26.

Winter Y, Lopez J, von Helversen O (2003). Ultraviolet vision in a bat. *Nature* **425:** 612-614.

Witmer LM, Chatterjee S, Franzosa J, Rowe T (2003). Neuroanatomy of flying reptiles and implications for flight, posture and behaviour. *Nature* **425:** 950-953.

Witmer LM, Ridgely RC (eds) (2008). *Structure of the brain cavity and inner ear of the centrosaurine ceratopsid Pachyrhinosaurus based on CT scanning and 3D visualization.* National Research Council of Canada Monograph Series: Ottawa pp 117-144.

Wong JG, Waters DA (2001). The synchronisation of signal emission with wingbeat during the approach phase in soprano pipistrelles (*Pipistrellus pygmaeus*). *J. Exp. Biol.* **204:** 575-583.

Wood TE, Burke JM, Rieseberg LH (2005). Parallel genotypic adaptation: when evolution repeats itself. *Genetica* **123:** 157-170.

Woolfe A, Goode DK, Cooke J, Callaway H, Smith S, Snell P *et al* (2007). CONDOR: a database resource of developmentally associated conserved non-coding elements. *BMC Dev. Biol.* **7**.

Woolfe A, Goodson M, Goode DK, Snell P, McEwen GK, Vavouri T *et al* (2005). Highly conserved non-coding sequences are associated with vertebrate development. *PLoS Biol.* **3:** 116-130.

Xu PX, Adams J, Peters H, Brown MC, Heaney S, Mass R (1999). *Eya1*-deficient mice lack ears and kidneys and show abnormal apoptosis of organ primordia. *Nat. Genet.* **23:** 113-117.

Yang AZ, Hullar TE (2007). Relationship of semicircular canal size to vestibular-nerve afferent sensitivity in mammals. *J. Neurophysiol.* **98:** 3197-3205.

Yang ZH (2007). PAML 4: Phylogenetic analysis by maximum likelihood. *Mol. Biol. Evol.* **24:** 1586-1591.

Yang ZH, dos Reis M (2011). Statistical properties of the branch-site test of positive selection. *Mol. Biol. Evol.* **28:** 1217-1228.

Yang ZH, Swanson WJ (2002). Codon-substitution models to detect adaptive evolution that account for heterogeneous selective pressures among site classes. *Mol. Biol. Evol.* **19:** 49-57.

Yang ZH, Wong WSW, Nielsen R (2005). Bayes empirical Bayes inference of amino acid sites under positive selection. *Mol. Biol. Evol.* **22:** 1107-1118.

Yeager M, Hughes AL (1999). Evolution of the mammalian MHC: natural selection, recombination, and convergent evolution. *Immunol. Rev.* **167:** 45-58.

Yeager M, Kumar S, Hughes AL (1997). Sequence convergence in the peptide-binding region of primate and rodent MBC class Ib molecules. *Mol. Biol. Evol.* **14:** 1035-1041.

Zhang JZ, Nielsen R, Yang ZH (2005). Evaluation of an improved branch-site likelihood method for detecting positive selection at the molecular level. *Mol. Biol. Evol.* **22:** 2472-2479.

Zhao H, Xu D, Zhang S, Zhang J (2011). Widespread losses of vomeronasal signal transduction in bats. *Mol. Biol. Evol.* **28:** 7-12.

Zhao HB, Rossiter SJ, Teeling EC, Li CJ, Cotton JA, Zhang SY (2009a). The evolution of color vision in nocturnal mammals. *Proc. Natl. Acad. Sci. U. S. A.* **106:** 8980-8985.

Zhao HB, Ru BH, Teeling EC, Faulkes CG, Zhang SY, Rossiter SJ (2009b). Rhodopsin molecular evolution in mammals inhabiting low light environments. *Plos One* **4**.

Zhao HB, Yang JR, Xu HL, Zhang JZ (2010). Pseudogenization of the umami taste receptor gene *Tas1r1* in the giant panda coincided with its dietary switch to bamboo. *Mol. Biol. Evol.* **27:** 2669-2673.

Zhao HH, Zhang SY, Zuo MX, Zhou J (2003). Correlations between call frequency and ear length in bats belonging to the families Rhinolophidae and Hipposideridae. *J. Zool.* **259:** 189-195.

Zheng J, Shen WX, He DZZ, Kevin BL, Madison LD, Dallos P (2000). Prestin is the motor protein of cochlear outer hair cells. *Nature* **405:** 149-155.

Zhuang Q, Muller R (2006). Noseleaf furrows in a horseshoe bat act as resonance cavities shaping the biosonar beam. *Phys. Rev. Lett.* **97**.

Zuckerkandl E, Pauling LB (1962). Molecular disease evolution, and genetic heterogeneity. In: Kasha M and Pullman B (eds) *Horizons in Biochemistry*. Academic Press: New York, pp 189-225.

Electronic Appendices for:

A Comparative Study of the Evolution of Mammalian High-Frequency Hearing and Echolocation

Kalina Bętkowska-Davies

Contents:

Appendix A

Table A1 Taxonomic classification of species included in *in silico* study. Classification following Wilson and Reeder 2005; Jones and Teeling 2006; Miller- Butterworth et al. 2007.

Superorder			Source:	
Order	Family	Species	*Tmc1*	*Pjvk*
Laurasiatheria				
Chiroptera	Pteropodidae	*Eidolon helvum*	Solexa	Solexa
		Pteropus vampyrus	Ensembl	Ensembl
	Rhinolophidae	*Rhinolophus ferrumequinum*	Solexa	Solexa
	Mormoopidae	*Pteronotus parnellii*	Solexa	Solexa
	Vespertilionidae	*Myotis lucifugus*	GenBank	GenBank
Perissodactyla	Equidae	*Equus caballus*	Ensembl	Ensembl
Artiodactyla	Camelidae	*Vicugna pacos*	Ensembl	-
	Bovidae	*Bos Taurus*	Ensembl	Ensembl
	Suidae	*Sus scrofa*	-	Ensembl
Cetacea	Delphinidae	*Tursiops truncatus*	Ensembl	Ensembl
Carnivora	Canidae	*Canis familiaris*	Ensembl	
	Ursidae	*Ailuropoda melanoleuca*	GenBank	GenBank
	Felidae	*Felis cattus*	Ensembl	-
Euarchontoglires				
Primata	Hominidae	*Homo sapiens*	Ensembl	Ensembl
		Pan trogladytes	Ensembl	Ensembl
		Gorilla gorilla	Ensembl	Ensembl
		Pongo pygmaeus	Ensembl	Ensembl
	Cercopithecidae	*Macaca mulatta*	Ensembl	
	Cebidae	*Callithrix jacchus*	Ensembl	Ensembl
Lagomorpha	Leporidae	*Oryctolagus cuniculus*	Ensembl	Ensembl
Rodentia	Muridae	*Mus musculus*	Ensembl	Ensembl
	Caviidae	*Cavia porcellus*	Ensembl	Ensembl
	Heteromyidae	*Dipodomys ordii*	-	Ensembl
Afrotheria				
Proboscidea	Elephantidae	*Loxodonata africana*	-	Ensembl
Pilosa	Megalonychidae	*Choloepus hoffmanni*	Ensembl	-
Marsupialia				
Didelphimorphia	Didelphidae	*Monodelphis domestica*	-	Ensembl

Table A2 Taxonomic classification of the species included in wider taxonomic study, following Wilson and Reeder 2005; Jones and Teeling 2006; Miller-Butterworth et al. 2007. * Sequences not included in intron+exon analyses due to poor agreement of alignment.

Superorder				Source:	
Order	Family	Species	Common name	*Tmc1*	*Pjvk*
Laurasiatheria					
Chiroptera	Rhinolophidae	*Rhinolophus ferrumequinum*	Greater horseshoe bat	This study	This study
		Rhinolophus celebensis	Sulawesi horseshoe bat	This study	This study
		Rhinolophus trifoliatus	Trefoil horseshoe bat	-	This study
		Rhinolophus borneensis	Bornean horseshoe bat	This study	This study
		Rhinolophus creaghi	Creagh's horseshoe bat	This study	This study
		Rhinolophus pusillus	Least horseshoe bat	This study	-
		Rhinolophus acuminatus	Acuminate horseshoe bat	This study	-
		Rhinolophus affinis	Intermediate horseshoe bat	This study	-
		Rhinolophus euryotis	Broad-eared horseshoe bat	This study	This study
	Hipposideridae	*Hipposideros ridleyi*	Ridley's leafnosed bat	This study	This study
		Hipposideros cervinus	Fawn coloured roundleaf bat	This study	This study
		Hipposideros galeritus	Cantor's roundleaf bat	This study	This study
		Hipposideros bicolor	Bicoloured leaf-nosed bat	This study	This study
		Hipposideros dyacorum	Dayak roundleaf bat	This study	-
		Hipposideros cineraceus	Ashy roundleaf bat	This study	-
		Hipposideros diadema	Diadem roundleaf bat	This study	This study
	Craseonycteridae	*Craseonycteris thonglongyai*	Bumble bee bat	This study	-
	Megadermatidae	*Macroderma gigas*	Ghost bat	This study	This study
		Megaderma spasma	Lesser false vampire bat	-	This study
	Rhinopomatidae	*Rhinopoma hardwickii*	Lesser rat-tailed bat	This study	-
	Pteropodidae	*Macroglossus minimus*	Lesser long-tongued fruit bat	This study	This study
		Dobsonia viridis	Greenish Naked-backed fruit bat	This study	This study
		Eidolon helvum	Straw coloured fruit bat	This study	This study
		Cynopterus brachyotis	Lesser short nosed fruit bat	-	This study
		Nyctimene albiventer	Common tube nosed fruit bat	This study	This study
		Pteropus giganteus	Indian flying fox	-	This study
		Pteropus sp.	Fruit bat sp.	This study	This study
		Pteropus vampyrus	Large flying fox	Ensembl	Ensembl

		Rousettus lanosus	Long haired Rousette	This study	This study
		Rousettus celebensis	Sulawesi Rousette	This study	This study
		Rousettus amplexicaudatus	Geoffroy's Rousette	This study	This study
	Phyllostomidae	*Carollia perspicillata*	Seba's short tailed bat	This study	This study
		Desmodus rotundus	Common vampire bat	This study	This study
		Tonatia silvicola	White-throated round-eared bat	This study	-
		Artibeus jamaicensis	Jamaican fruit bat	This study	-
		Anoura geoffroyi	Geoffroy's tailess bat	This study	-
	Mormoopidae	*Pteronotus parnelli*	Parnell's moustached bat	This study	-
	Vespertilionidae	*Eptesicus serotinus*	Serotine bat	This study	-
		Kerivoula pellucida	Clear winged woolly bat	This study	This study
		Kerivoula hardwickii	Hardwicke's woolly bat	This study	This study
		Kerivoula minuta	Least woolly bat	This study	This study
		Murina cyclotis	Round eared tube nosed bat	This study	This study
		Murina rozendaali	Gilded tube nosed bat	This study	-
		Murina suilla	Brown tube nosed bat	This study	-
		Myotis lucifugus	Little brown bat	Ensembl	-
	Miniopteridae	*Miniopterus australis*	Little long-fingered bat	This study	-
	Molossidae	*Tadarida brasiliensis*	Mexican free-tailed bat	This study	This study
		Cheiromeles parcidens	Lesser naked bat	This study	-
	Nycteridae	*Nycteris tragata*	Malayan slit-faced bat	-	This study
	Emballonuridae	*Taphozous nudiventris*	Naked-rumped tomb bat	-	This study
		Emballonura atrata	Peter's sheath tailed bat	-	This study
Soricomorpha	Talpidae	*Condylura cristata*	Star nosed mole	This study	This study
		Talpa europaea	European mole	This study	-
	Soricidae	*Sorex araneus*	European shrew	Ensembl	-
Perissodactyla	Equidae	*Equus caballus*	Horse	Ensembl	Ensembl
Artiodactyla	Camelidae	*Lama pacos*	Alpaca	Ensembl	-
		Camelus bactrianus	Bactrian camel	This study	This study
	Bovidae	*Gazella thomsonii*	Thomson gazelle	This study	This study
		Tragelaphus eurycerus	Bongo	This study	This study
		Bos Taurus	Cow	Ensembl	Ensembl
	Suidae	*Sus scrofa*	Pig	-	Ensembl
Cetacea	Ziphiidae	*Hyperoodon ampullatus*	Northern bottle nosed whale	This study	This study
		Ziphius cavirostris	Cuvier's beaked whale	This study	This study

	Delphinidae	*Orcinus orca*	Killer whale	This study	This study
	Balaenopteridae	*Megaptera novaeangliae*	Humpback whale	This study	This study
	Delphinidae	*Tursiops truncatus*	Bottle nose dolphin	Ensembl	Ensembl
Carnivora	Canidae	*Canis familiaris*	Dog	Ensembl	Ensembl
	Mustelidae	*Meles meles*	European badger	-	This study
	Felidae	*Felis cattus*	Cat	Ensembl	-
	Herpestidae	*Suricata suricatta*	Meerkat	This study	This study
Euarchontoglires					
Primata	Hominidae	*Homo sapiens*	Human	Ensembl	Ensembl
		Pan trogladytes	Chimpanzee	Ensembl	Ensembl
		Pongo pygmaeus	Bornean orangutan	Ensembl	Ensembl
	Cercopithecidae	*Macaca mulatta*	Rhesus macaque	Ensembl	Ensembl*
	Cheirogaleidae	*Microcebus murinus*	Mouse lemur	Ensembl	-
	Tarsiidae	*Tarsius syrichta*	Tarsier	Ensembl	-
	Cebidae	*Callithrix jacchus*	Marmoset	-	Ensembl
	Galagidae	*Otolemur garnettii*	Bushbaby	Ensembl	-
Lagomorpha	Leporidae	*Oryctolagus cuniculus*	Rabbit	Ensembl	-
		Lepus europaeus	Hare	This study	This study
	Ochotonidae	*Ochotona princeps*	American pika	Ensembl	-
Rodentia	Muridae	*Rattus norvegicus*	Rat	Ensembl	-
		Mus musculus	Mouse	Ensembl	Ensembl*
	Cricetidae	*Clethrionomys glareolus*	Bank vole	This study	This study
	Caviidae	*Cavia porcellus*	Guinea pig	-	Ensembl
	Bathyergidae	*Heliophobius argenteocinereus*	Silvery mole rat	This study	This study
	Heteromyidae	*Dipodomys ordii*	Kangaroo rat	Ensembl	Ensembl*
Afrotheria					
Hyracoidea	Procaviidae	*Procavia capensis*	Rock Hyrax	Ensembl	-
Afrosoricida	Tenrecidae	*Echinops telfairi*	Madagascan hedgehog tenrec	Ensembl	-
Xenarthra					
Cingulata	Dasypodidae	*Dasypus novemcinctus*	Nine-banded armadillo	Ensembl	-
Marsupialia					
Diprotodontia	Phascolarctidae	*Phascolarctos cinereus*	Koala	-	This study*
Didelphimorphia	Didelphidae	*Monodelphis domestica*	Grey short-tailed opossum	-	Ensembl
	Macropodidae	*Macropus eugenii*	Wallaby	-	Ensembl

Table A3 Call type and estimated maximum call frequencies (kHz) used by the bat and cetacean species included in this study. * Indicates frequencies are estimated from the species shown in parentheses.

Family Species	Type of call:	Est. max freq. (kHz):	Ref.
Yinpterochiroptera:			
Rhinolophidae			
Rhinolophus ferrumequinum	Constant-frequency	83.00	(Jones and Rayner 1989)
Rhinolophus celebensis	Constant-frequency	83.00	www.batecho.eu
Rhinolophus trifoliatus	Constant-frequency	51.20	(Francis and Habersetzer 1998)
Rhinolophus borneensis	Constant-frequency	81.80	(Francis and Habersetzer 1998)
Rhinolophus creaghi	Constant-frequency	68.00	(Francis and Habersetzer 1998)
Rhinolophus pusillus	Constant-frequency	100.00	(Francis and Habersetzer 1998)
Rhinolophus acuminatus	Constant-frequency	89.00	(Francis and Habersetzer 1998)
Rhinolophus affinis	Constant-frequency	78.40	(Francis and Habersetzer 1998)
Rhinolophus euryotis	Constant-frequency	63.00	www.batecho.eu
Hipposideridae			
Hipposideros ridleyi	Constant-frequency	65.00	(Francis and Habersetzer 1998)
Hipposideros cervinus	Constant-frequency	128.80	(Francis and Habersetzer 1998)
Hipposideros galeritus	Constant-frequency	89.20	(Francis and Habersetzer 1998)
Hipposideros bicolor	Constant-frequency	132.00	(Francis and Habersetzer 1998)
Hipposideros dyacorum	Constant-frequency	161.9	(Francis and Habersetzer 1998)
Hipposideros cineraceus	Constant-frequency	>154.00	(Francis and Habersetzer 1998)
Hipposideros diadema	Constant-frequency	59.80	(Francis and Habersetzer 1998)
Craseonycteridae			
Craseonycteris thonglongyai	Constant-frequency	73.00	(Surlykke *et al.,* 1993)
Megadermatidae			
Macroderma gigas	Multiharmonic broadband	40.00-50.00	(Neuweiler 1990)
Megaderma spasma	Multiharmonic broadband	74.00	www.batecho.eu
Rhinopomatidae			
Rhinopoma hardwickii	Long quasi-CF	35.00	(Neuweiler 1990)
Pteropodidae			
Macroglossus minimus	None	-	
Dobsonia viridis	None	-	
Eidolon helvum	None	-	

Cynopterus brachyotis	None	-	
Nyctimene albiventer	None	-	
Pteropus giganteus	None	-	
Pteropus sp.	None	-	
Pteropus vampyrus	None	-	
Rousettus lanosus (*R. aegyptiacus*)	Tongue clicks	34.00*	(Holland *et al.,* 2004)
Rousettus celebensis (*R. aegyptiacus*)	Tongue clicks	34.00*	(Holland *et al.,* 2004)
Rousettus amplexicaudatus (*R. aegyptiacus*)	Tongue clicks	34.00*	(Holland *et al.,* 2004)
Yangochiroptera:			
Phyllostomidae			
Carollia perspicillata	Broadband	80.00	(Neuweiler 1990)
Desmodus rotundus	Broadband	72.50	(Schmidt *et al.,* 1991)
Tonatia silvicola (*T. saruphila*)	Broadband	56.5*	(Pio *et al.,* 2010)
Artibeus jamaicensis	Broadband	78.80	(Brinklov *et al.,* 2009)
Anoura geoffroyi	Broadband	92.00-112.00	(Pye 1967)
Mormoopidae			
Pteronotus parnelli	Constant-frequency	62.00	(Neuweiler 1990)
Vespertilionidae			
Eptesicus serotinus	Short, broadband calls, dominant fundamental harmonic	50.40	(Russo and Jones 2002)
Kerivoula pellucida	Broadband FM	178.50	(Kingston *et al.,* 1999)
Kerivoula hardwickii	Broadband FM	250.00	www.batecho.eu
Kerivoula minuta	Broadband FM	175.20	(Kingston *et al.,* 1999)
Murina cyclotis	Broadband FM	165.20	(Kingston *et al.,* 1999)
Murina rozendaali	Broadband FM	-	
Murina suilla	Broadband FM	165.00	(Kingston *et al.,* 1999)
Myotis lucifugus	Short, broadband calls, dominant fundamental harmonic	50.00	(Neuweiler 1990)
Miniopteridae			
Miniopterus australis (*M. schreibersii*)	Narrowband signals, with fundamental harmonic	52.40 *	(Russo and Jones 2002)
Molossidae			
Tadarida brasiliensis	Narrowband signals, with fundamental harmonic	42.00	(Neuweiler 1990)
Cheiromeles parvidens	Narrowband signals, with fundamental	45.00	www.batecho.eu

	harmonic		
Nycteridae			
Nycteris tragata	Short, broadband, multiharmonic	99.00	www.batecho.eu
Emballonuridae			
Taphozous nudiventris	Narrowband, multiharmonic	21.00-25.00	(Dietz 2005)
Emballonura atrata	Narrowband, multiharmonic	55.70	(Kofoky *et al.,* 2009)
Cetaceans:			
Ziphiidae			
Hyperoodon ampullatus	Clicks	24	(Hooker and Whitehead 2002)
Ziphius cavirostris	Clicks	45	(Zimmer *et al.,* 2005)
Delphinidae			
Orcinusorca	Scream	35	(Ketten 1994)
Tursiops truncatus	Click	150	(Ketten 1994)
	Whistle	20	(Ketten 1994)
Balaenopteridae			
Megaptera novaeangliae	Low-frequency song	10	(Ketten 1994)

Table A4 Site-model analyses using complete sequences, showing model parameters and model comparisons for *Tmc1* and *Pjvk*. Posterior probability values between 0.5 and 0.8 (plain text), between 0.8 and 0.95 (italics), and greater than 0.95 (boldface type)

Model	N^{o} P	-ln likelihood	dn/ds	Estimates of Parameters : (Positively selected sites)
Tmc1				
M0	45	11054.35	0.066	$\omega = 0.07$
M3	49	10860.36	0.074	$p_0 = 0.65$, $p_1 = 0.29$ ($p_2 = 0.06$), $\omega_0 = 0.00$, $\omega_1 = 0.12$, $\omega_2 = 0.63$
M1a	46	10904.12	0.100	$p_0 = 0.93$ ($p_1 = 0.07$)
M2a	48	10904.12	0.100	$p_0 = 0.93$, $p_1 = 0.07$ ($p_2 = 0.00$), $\omega_2 = 126.70$
				141, $\omega = 1.30 \pm 0.25$; 268, $\omega = 1.25 \pm 0.25$; 495, $\omega = 1.25 \pm 0.25$; *710*, $\omega = 1.42 \pm 0.19$
M7	46	10863.62	0.076	$p = 0.140$, $q = 1.578$
M8	48	10861.58	0.075	$p_0 = 0.99$ ($p_1 = 0.01$), $p = 0.16$, $q = 2.19$, $\omega = 1.00$
				26, $\omega = 1.18 \pm 0.45$; 50, $\omega = 1.191 \pm 0.42$; 55, $\omega = 1.16 \pm 0.45$; *141*, $\omega = 1.36 \pm 0.33$; 154, $\omega = 1.19 \pm 0.44$; 268, $\omega = 1.23 \pm 0.43$; 495, $\omega = 1.28 \pm 0.39$; **690**, $\omega = 1.49 \pm 0.09$; 736, $\omega = 1.05 \pm 0.50$
Pjvk				
M0	41	4506.06	0.061	$\omega = 0.06$
M3	45	4445.06	0.069	$p_0 = 0.29$, $p_1 = 0.58$ ($p_2 = 0.12$), $\omega_0 = 0.01$, $\omega_1 = 0.01$, $\omega_2 = 0.47$
M1a	42	4455.82	0.099	$p_0 = 0.92$ ($p_1 = 0.08$)
				$\omega_0 = 0.02$, $\omega_1 = 1.00$
M2a	44	4455.82	0.099	$p_0 = 0.92$, $p_1 = 0.08$, ($p_2 = 0.00$), $\omega_2 = 2.37$
				244, $\omega = 1.43 \pm 0.36$
M7	42	4445.47	0.070	$p = 0.10$, $q = 1.26$,
M8	44	4444.22	0.072	$p_0 = 1.00$ ($p_1 = 0.00$), $p = 0.11$, $q = 1.45$, $\omega = 2.92$
				105, $\omega = 1.18 \pm 0.44$; **244**, $\omega = 1.51 \pm 0.36$; 277, $\omega = 1.00 \pm 0.54$]

Table A5 Results of branch-site models along ancestral echolocating bat and echolocating tip species for *Tmc1* (a) and *Pjvk* (b). BEB estimates using Sloth as reference for *Tmc1*, and Elephant for *Pjvk*. Posterior probability values between 0.5 and 0.8 (plain text), between 0.8 and 0.95 (italics), and greater than 0.95 (boldface type).

a)

Branch	Model A Hypothesis	N° P	-ln likelihood	Estimates of Parameters: [Positively selected sites]
I Yangochiroptera	Null	47	10893.96	$p_0 = 0.73$, $p_1 = 0.05$, $p_{2a} = 0.21$, $p_{2b} = 0.01$ BG: $\omega_0 = 0.03$, $\omega_1 = 1.00$, $\omega_{2a} = 0.03$, $\omega_{2b} = 1.00$ FG: $\omega_0 = 0.03$, $\omega_1 = 1.00$, $\omega_{2a} = 1.00$, $\omega_{2b} = 1.00$
	Alternative	48	10891.55	$p_0 = 0.90$, $p_1 = 0.06$, $p_{2a} = 0.04$, $p_{2b} = 0.00$ BG: $\omega_0 = 0.03$, $\omega_1 = 1.00$, $\omega_{2a} = 0.03$, $\omega_{2b} = 1.00$ FG: $\omega_0 = 0.03$, $\omega_1 = 1.00$, $\omega_{2a} = 9.36$, $\omega_{2b} = 9.36$ [55, *72*, *73*, *74*, 76, *81*, *82*, *105*, *192*, **319**, **444**, *476*, *477*, *493*, 613, *731*]
II *Myotis lucifugus*	Null	47	10901.87	$p_0 = 0.90$, $p_1 = 0.06$, $p_{2a} = 0.03$, $p_{2b} = 0.00$ BG: $\omega_0 = 0.03$, $\omega_1 = 1.00$, $\omega_{2a} = 0.03$, $\omega_{2b} = 1.00$ FG: $\omega_0 = 0.03$, $\omega_1 = 1.00$, $\omega_{2a} = 1.00$, $\omega_{2b} = 1.00$
	Alternative	48	10899.11	$p_0 = 0.93$, $p_1 = 0.07$, $p_{2a} = 0.01$, $p_{2b} = 0.00$ BG: $\omega_0 = 0.03$, $\omega_1 = 1.00$, $\omega_{2a} = 0.03$, $\omega_{2b} = 1.00$ FG: $\omega_0 = 0.03$, $\omega_1 = 1.00$, $\omega_{2a} = 33.36$, $\omega_{2b} = 33.36$ [27, *54*, 273, **283**, 298, 462, 504, 725]
III *Pteronotus parnellii*	Null	47	10903.86	$p_0 = 0.92$, $p_1 = 0.07$, $p_{2a} = 0.02$, $p_{2b} = 0.00$ BG: $\omega_0 = 0.03$, $\omega_1 = 1.00$, $\omega_{2a} = 0.03$, $\omega_{2b} = 1.00$ FG: $\omega_0 = 0.03$, $\omega_1 = 1.00$, $\omega_{2a} = 1.00$, $\omega_{2b} = 1.00$
	Alternative	48	10903.86	$p_0 = 0.92$, $p_1 = 0.07$, $p_{2a} = 0.02$, $p_{2b} = 0.00$ BG: $\omega_0 = 0.03$, $\omega_1 = 1.00$, $\omega_{2a} = 0.03$, $\omega_{2b} = 1.00$ FG: $\omega_0 = 0.03$, $\omega_1 = 1.00$, $\omega_{2a} = 1.00$, $\omega_{2b} = 1.00$ [47, 64, 87, 191, 296, 343]
IV Yinpterochiroptera	Null	47	10904.12	$p_0 = 0.93$, $p_1 = 0.07$, $p_{2a} = 0.00$, $p_{2b} = 0.00$ BG: $\omega_0 = 0.03$, $\omega_1 = 1.00$, $\omega_{2a} = 0.03$, $\omega_{2b} = 1.00$ FG: $\omega_0 = 0.03$, $\omega_1 = 1.00$, $\omega_{2a} = 1.00$, $\omega_{2b} = 1.00$
	Alternative	48	10904.12	$p_0 = 0.93$, $p_1 = 0.07$, $p_{2a} = 0.00$, $p_{2b} = 0.00$

V Ancestral Pteropodidae	Null	47	10904.12	BG: $\omega_0 = 0.03$, $\omega_1 = 1.00$, $\omega_{2a} = 0.03$, $\omega_{2b} = 1.00$ FG: $\omega_0 = 0.03$, $\omega_1 = 1.00$, $\omega_{2a} = 1.00$, $\omega_{2b} = 1.00$ $p_0 = 0.93$, $p_1 = 0.07$, $p_{2a} = 0.00$, $p_{2b} = 0.00$
	Alternative	48	10904.12	BG: $\omega_0 = 0.03$, $\omega_1 = 1.00$, $\omega_{2a} = 0.03$, $\omega_{2b} = 1.00$ FG: $\omega_0 = 0.03$, $\omega_1 = 1.00$, $\omega_{2a} = 1.00$, $\omega_{2b} = 1.00$ $p_0 = 0.93$, $p_1 = 0.07$, $p_{2a} = 0.00$, $p_{2b} = 0.00$
VI *Rhinolophus ferrumequinum*	Null	47	10882.75	BG: $\omega_0 = 0.03$, $\omega_1 = 1.00$, $\omega_{2a} = 0.03$, $\omega_{2b} = 1.00$ FG: $\omega_0 = 0.03$, $\omega_1 = 1.00$, $\omega_{2a} = 1.00$, $\omega_{2b} = 1.00$ $p_0 = 0.81$, $p_1 = 0.06$, $p_{2a} = 0.13$, $p_{2b} = 0.01$
	Alternative	48	10880.15	BG: $\omega_0 = 0.03$, $\omega_1 = 1.00$, $\omega_{2a} = 0.03$, $\omega_{2b} = 1.00$ FG: $\omega_0 = 0.03$, $\omega_1 = 1.00$, $\omega_{2a} = 1.00$, $\omega_{2b} = 1.00$ $p_0 = 0.88$, $p_1 = 0.06$, $p_{2a} = 0.05$, $p_{2b} = 0.00$
VII *Tursiops truncatus*	Null	47	10900.72	BG: $\omega_0 = 0.03$, $\omega_1 = 1.00$, $\omega_{2a} = 0.03$, $\omega_{2b} = 1.00$ FG: $\omega_0 = 0.03$, $\omega_1 = 1.00$, $\omega_{2a} = 3.88$, $\omega_{2b} = 3.88$ [210, 223, 224, *235*, 261, 269, 282, **283**, 298, 323, 352, 352, 466, 492, 500, 541, 606, **607**, 629, 631, **632**, *634*, 657, 691, 692] $p_0 = 0.86$, $p_1 = 0.06$, $p_{2a} = 0.08$, $p_{2b} = 0.01$
	Alternative	48	10900.72	BG: $\omega_0 = 0.03$, $\omega_1 = 1.00$, $\omega_{2a} = 0.03$, $\omega_{2b} = 1.00$ FG: $\omega_0 = 0.03$, $\omega_1 = 1.00$, $\omega_{2a} = 1.00$, $\omega_{2b} = 1.00$ $p_0 = 0.86$, $p_1 = 0.06$, $p_{2a} = 0.08$, $p_{2b} = 0.01$
				BG: $\omega_0 = 0.03$, $\omega_1 = 1.00$, $\omega_{2a} = 0.03$, $\omega_{2b} = 1.00$ FG: $\omega_0 = 0.03$, $\omega_1 = 1.00$, $\omega_{2a} = 1.00$, $\omega_{2b} = 1.00$ [75, 79, 192, 295, 332, 333, 546, 689, 691, 718]

b)

Branch	Model A Hypothesis	N° P	-ln likelihood	Estimates of Parameters:Positively selected sites
I Yangochiroptera	Null	43	4455.82	$p_0 = 0.92$, $p_1 = 0.08$, $p_{2a} = 0.00$, $p_{2b} = 0.00$ BG: $\omega_0 = 0.02$, $\omega_1 = 1.00$, $\omega_{2a} = 0.02$, $\omega_{2b} = 1.00$ FG: $\omega_0 = 0.02$, $\omega_1 = 1.00$, $\omega_{2a} = 1.00$, $\omega_{2b} = 1.00$
	Alternative	44	4455.82	$p_0 = 0.92$, $p_1 = 0.08$, $p_{2a} = 0.00$, $p_{2b} = 0.00$ BG: $\omega_0 = 0.02$, $\omega_1 = 1.00$, $\omega_{2a} = 0.02$, $\omega_{2b} = 1.00$ FG: $\omega_0 = 0.02$, $\omega_1 = 1.00$, $\omega_{2a} = 1.00$, $\omega_{2b} = 1.00$
II *Myotis lucifugus*	Null	43	4455.79	$p_0 = 0.92$, $p_1 = 0.08$, $p_{2a} = 0.01$, $p_{2b} = 0.00$ BG: $\omega_0 = 0.02$, $\omega_1 = 1.00$, $\omega_{2a} = 0.02$, $\omega_{2b} = 1.00$ FG: $\omega_0 = 0.02$, $\omega_1 = 1.00$, $\omega_{2a} = 1.00$, $\omega_{2b} = 1.00$
	Alternative	44	4455.79	$p_0 = 0.92$, $p_1 = 0.08$, $p_{2a} = 0.01$, $p_{2b} = 0.00$ BG: $\omega_0 = 0.02$, $\omega_1 = 1.00$, $\omega_{2a} = 0.02$, $\omega_{2b} = 1.00$ FG: $\omega_0 = 0.02$, $\omega_1 = 1.00$, $\omega_{2a} = 1.12$, $\omega_{2b} = 1.12$
III *Pteronotus parnellii*	Null	43	4455.82	$p_0 = 0.92$, $p_1 = 0.08$, $p_{2a} = 0.00$, $p_{2b} = 0.00$ BG: $\omega_0 = 0.02$, $\omega_1 = 1.00$, $\omega_{2a} = 0.02$, $\omega_{2b} = 1.00$ FG: $\omega_0 = 0.02$, $\omega_1 = 1.00$, $\omega_{2a} = 1.00$, $\omega_{2b} = 1.00$
	Alternative	44	4455.82	$p_0 = 0.92$, $p_1 = 0.08$, $p_{2a} = 0.00$, $p_{2b} = 0.00$ BG: $\omega_0 = 0.02$, $\omega_1 = 1.00$, $\omega_{2a} = 0.02$, $\omega_{2b} = 1.00$ FG: $\omega_0 = 0.02$, $\omega_1 = 1.00$, $\omega_{2a} = 1.00$, $\omega_{2b} = 1.00$
IV Yinpterochiroptera	Null	43	4455.82	$p_0 = 0.92$, $p_1 = 0.08$, $p_{2a} = 0.00$, $p_{2b} = 0.00$ BG: $\omega_0 = 0.02$, $\omega_1 = 1.00$, $\omega_{2a} = 0.02$, $\omega_{2b} = 1.00$ FG: $\omega_0 = 0.02$, $\omega_1 = 1.00$, $\omega_{2a} = 1.00$, $\omega_{2b} = 1.00$
	Alternative	44	4455.82	$p_0 = 0.92$, $p_1 = 0.08$, $p_{2a} = 0.00$, $p_{2b} = 0.00$ BG: $\omega_0 = 0.02$, $\omega_1 = 1.00$, $\omega_{2a} = 0.02$, $\omega_{2b} = 1.00$ FG: $\omega_0 = 0.02$, $\omega_1 = 1.00$, $\omega_{2a} = 1.00$, $\omega_{2b} = 1.00$
V Ancestral Pteropodidae	Null	43	4455.82	$p_0 = 0.92$, $p_1 = 0.08$, $p_{2a} = 0.00$, $p_{2b} = 0.00$ BG: $\omega_0 = 0.02$, $\omega_1 = 1.00$, $\omega_{2a} = 0.02$, $\omega_{2b} = 1.00$ FG: $\omega_0 = 0.02$, $\omega_1 = 1.00$, $\omega_{2a} = 1.00$, $\omega_{2b} = 1.00$
	Alternative	44	4455.82	$p_0 = 0.92$, $p_1 = 0.08$, $p_{2a} = 0.00$, $p_{2b} = 0.00$ BG: $\omega_0 = 0.02$, $\omega_1 = 1.00$, $\omega_{2a} = 0.02$, $\omega_{2b} = 1.00$ FG: $\omega_0 = 0.02$, $\omega_1 = 1.00$, $\omega_{2a} = 1.00$, $\omega_{2b} = 1.00$

VI *Rhinolophus ferrumequinum*	Null	43	4455.17	$p_0 = 0.89$, $p_1 = 0.07$, $p_{2a} = 0.04$, $p_{2b} = 0.00$ BG: $\omega_0 = 0.02$, $\omega_1 = 1.00$, $\omega_{2a} = 0.02$, $\omega_{2b} = 1.00$ FG: $\omega_0 = 0.02$, $\omega_1 = 1.00$, $\omega_{2a} = 1.00$, $\omega_{2b} = 1.00$
	Alternative	44	4455.17	$p_0 = 0.89$, $p_1 = 0.07$, $p_{2a} = 0.04$, $p_{2b} = 0.00$ BG: $\omega_0 = 0.02$, $\omega_1 = 1.00$, $\omega_{2a} = 0.02$, $\omega_{2b} = 1.00$ FG: $\omega_0 = 0.02$, $\omega_1 = 1.00$, $\omega_{2a} = 1.00$, $\omega_{2b} = 1.00$ [3, 72, 230]
VII *Tursiops truncatus*	Null	43	4450.94	$p_0 = 0.79$, $p_1 = 0.06$, $p_{2a} = 0.14$, $p_{2b} = 0.01$ BG: $\omega_0 = 0.02$, $\omega_1 = 1.00$, $\omega_{2a} = 0.02$, $\omega_{2b} = 1.00$ FG: $\omega_0 = 0.02$, $\omega_1 = 1.00$, $\omega_{2a} = 1.00$, $\omega_{2b} = 1.00$
	Alternative	44	4450.88	$p_0 = 0.83$, $p_1 = 0.06$, $p_{2a} = 0.10$, $p_{2b} = 0.01$ BG: $\omega_0 = 0.02$, $\omega_1 = 1.00$, $\omega_{2a} = 0.02$, $\omega_{2b} = 1.00$ FG: $\omega_0 = 0.02$, $\omega_1 = 1.00$, $\omega_{2a} = 1.59$, $\omega_{2b} = 1.59$ [72, 110, 192, 209, 236, 281, 303, 316, 330]

Table A6 Clade model estimates a) *Tmc1* and b) *Pjvk* . (BG – background; FG – foreground).

a)

Clade	Model	-ln likelihood	Estimates of Parameters:
Null hypothesis	M1a	3020.90	$p_0 = 0.87$ ($p_1 = 0.13$), $\omega_0 = 0.03$, $\omega_1 = 1.00$
I Rhinolophidae and Hipposideridae	C	2990.25	$p_0 = 0.82$, $p_1 = 0.02$, $p_2 = 0.16$, BG: $\omega_0 = 0.02$, $\omega_1 = 1.00$, $\omega_2 = 0.29$, FG: $\omega_0 = 0.02$, $\omega_1 = 1.00$, $\omega_2 = 2.48$
II Hipposideridae	C	2989.56	$p_0 = 0.82$, $p_1 = 0.02$, $p_2 = 0.16$, BG: $\omega_0 = 0.02$, $\omega_1 = 1.00$, $\omega_2 = 0.30$, FG: $\omega_0 = 0.02$, $\omega_1 = 1.00$, $\omega_2 = 4.76$
III Pteropodidae	C	3002.15	$p_0 = 0.81$, $p_1 = 0.03$, $p_2 = 0.16$, BG: $\omega_0 = 0.02$, $\omega_1 = 1.00$, $\omega_2 = 0.35$, FG: $\omega_0 = 0.02$, $\omega_1 = 1.00$, $\omega_2 = 0.00$
IV Yangochiroptera	C	2997.87	$p_0 = 0.82$, $p_1 = 0.02$, $p_2 = 0.16$, BG: $\omega_0 = 0.02$, $\omega_1 = 1.00$, $\omega_2 = 0.30$, FG: $\omega_0 = 0.02$, $\omega_1 = 1.00$, $\omega_2 = 0.86$
V Kerivoulinae	C	2998.12	$p_0 = 0.82$, $p_1 = 0.03$, $p_2 = 0.15$, BG: $\omega_0 = 0.02$, $\omega_1 = 1.00$, $\omega_2 = 0.32$, FG: $\omega_0 = 0.02$, $\omega_1 = 1.00$, $\omega_2 = 2.41$,
VI Vespertilionidae	C	3000.08	$p_0 = 0.83$, $p_1 = 0.02$, $p_2 = 0.15$, BG: $\omega_0 = 0.02$, $\omega_1 = 1.00$, $\omega_2 = 0.34$, FG: $\omega_0 = 0.02$, $\omega_1 = 1.00$, $\omega_2 = 1.02$,
VII Phyllostomidae	C	3002.72	$p_0 = 0.83$, $p_1 = 0.00$, $p_2 = 0.17$, BG: $\omega_0 = 0.02$, $\omega_1 = 1.00$, $\omega_2 = 0.42$, FG: $\omega_0 = 0.02$, $\omega_1 = 1.00$, $\omega_2 = 0.84$
VII Odontoceti	C	3004.18	$p_0 = 0.83$, $p_1 = 0.02$, $p_2 = 0.16$, BG: $\omega_0 = 0.02$, $\omega_1 = 1.00$, $\omega_2 = 0.40$, FG: $\omega_0 = 0.02$, $\omega_1 = 1.00$, $\omega_2 = 1.13$

b)

Hypothesis	Model	-ln likelihood	Estimates of Parameters:
Null hypothesis.	M1a	1732.76	$p_0 =$ 0.95 ($p_1 = 0.05$), $\omega_0 = 0.06$, $\omega_1 = 1.00$
I Rhinolophidae and Hipposideridae	C	1722.89	$p_0 =$ 0.83, $p_1 =$ 0.02, $p_2 = 0.16$,
			BG: $\omega_0 = 0.04$, $\omega_1 = 1.00$, $\omega_2 = 0.24$, FG: $\omega_0 = 0.04$, $\omega_1 = 1.00$, $\omega_2 = 0.97$
II Hipposideridae	C	1722.98	$p_0 =$ 0.81, $p_1 = 0.02$, $p_2 = 0.18$
			BG: $\omega_0 = 0.03$, $\omega_1 = 1.00$, $\omega_2 = 0.24$, FG: $\omega_0 = 0.03$, $\omega_1 = 1.00$, $\omega_2 = 1.05$
III Pteropodidae	C	1724.60	$p_0 =$ 0.77, $p_1 =$ 0.02, $p_2 = 0.21$,
			BG: $\omega_0 = 0.03$, $\omega_1 = 1.00$, $\omega_2 = 0.23$, FG: $\omega_0 = 0.03$, $\omega_1 = 1.00$, $\omega_2 = 0.18$
IV Yangochiroptera	C	1722.66	$p_0 =$ 0.80, $p_1 =$ 0.02, $p_2 = 0.19$
			BG: $\omega_0 = 0.03$, $\omega_1 = 1.00$, $\omega_2 = 0.20$, FG: $\omega_0 = 0.03$, $\omega_1 = 1.00$, $\omega_2 = 0.42$
V Kerivoulinae	C	1723.61	$p_0 =$ 0.76, $p_1 =$ 0.02, $p_2 = 0.23$
			BG: $\omega_0 = 0.03$, $\omega_1 = 1.00$, $\omega_2 = 0.21$, FG: $\omega_0 = 0.03$, $\omega_1 = 1.00$, $\omega_2 = 0.46$
VI Vespertilionoidae	C	1722.31	$p_0 =$ 0.77, $p_1 =$ 0.02, $p_2 = 0.22$
			BG: $\omega_0 = 0.03$, $\omega_1 = 1.00$, $\omega_2 = 0.20$, FG: $\omega_0 = 0.03$, $\omega_1 = 1.00$, $\omega_2 = 0.61$
VII Phyllostomidae	C	1723.30	$p_0 =$ 0.81, $p_1 =$ 0.02, $p_2 = 0.17$,
			BG: $\omega_0 = 0.03$, $\omega_1 = 1.00$, $\omega_2 = 0.24$, FG: $\omega_0 = 0.03$, $\omega_1 = 1.00$, $\omega_2 = 0.64$
VIII Odontoceti	C	1719.37	$p_0 =$ 0.82, $p_1 =$ 0.02, $p_2 = 0.16$
			BG: $\omega_0 = 0.03$, $\omega_1 = 1.00$, $\omega_2 = 0.24$, FG: $\omega_0 = 0.03$, $\omega_1 = 1.00$, $\omega_2 = 7.40$

Table A7 Branch-Site model along the Old World CF bat branch in *Pjvk*. BEB estimates use Opossum as reference. LRT = 4.28, DF = 1, P = 0.04. Posterior probability values between 0.5 and 0.8 (plain text), between 0.8 and 0.95 (italics), and greater than 0.95 (boldface type).

Branch	Model A Hypothesis	N° P	-ln likelihood	Estimates of Parameters:Positively selected sites
I Rhinolophidae and Hipposideridae	Null	128	1732.14	$p_0 = 0.95$, $p_1 = 0.05$, $p_{2a} = 0.00$, $p_{2b} = 0.00$ BG: $\omega_0 = 0.06$, $\omega_1 = 1.00$, $\omega_{2a} = 0.06$, $\omega_{2b} = 1.00$, FG: $\omega_0 = 0.06$, $\omega_1 = 1.00$, $\omega_{2a} = 1.00$, $\omega_{2b} = 1.00$
	Alternative	129	1730.01	$p_0 = 0.94$, $p_1 = 0.04$, $p_{2a} = 0.02$, $p_{2b} = 0.00$ BG: $\omega_0 = 0.06$, $\omega_1 = 1.00$, $\omega_{2a} = 0.06$, $\omega_{2b} = 1.00$, FG: $\omega_0 = 0.06$, $\omega_1 = 1.00$, $\omega_{2a} = 115.81$, $\omega_{2b} = 115.81$ 3 V, 21 A

Appendix B

Table B1 Results of Tajima's Rate Test for concatenated ear development CNEs. Tests compared species to *E. caballus* with *H. sapiens* as outgroup. The X^2 test statistic given with 1 degree of freedom, *P*-values significant if < 0.007 (following Bonferroni corrections).

Gene:	Focal species:	Sites in sequences: Ident.	Div.	Unique differences: *Equus caballus*	Focal species	*Homo sapiens*	X^2 (1 d.f.)	*P*
Shh	*B. taurus*	2925	7	60	89	75	5.64	0.018
	T. truncatus	2790	5	54	78	70	4.36	0.037
	E. helvum	2764	11	38	119	62	41.79	<0.001
	P. vampyrus	2788	9	41	105	60	28.05	<0.001
	R. ferrumequinum	3004	14	53	95	75	11.92	0.001
	M. lucifugus	2572	11	40	96	57	23.06	<0.001
	P. parnellii	1654	5	26	90	38	35.31	<0.001
Tshz1	*B. taurus*	7755	1	55	83	92	5.68	0.017
	T. truncatus	7285	4	50	142	91	44.08	<0.001
	E. helvum	6552	4	42	88	60	16.28	<0.001
	P. vampyrus	6518	6	40	129	65	46.87	<0.001
	R. ferrumequinum	7833	4	52	89	97	9.71	0.002
	M. lucifugus	7681	6	56	120	89	23.27	<0.001
	P. parnellii	6320	7	36	150	54	69.87	<0.001
Hmx2/3	*B. taurus*	5026	1	35	59	58	6.13	0.013
	T. truncatus	4830	3	31	85	57	25.14	<0.001
	E. helvum	4924	1	34	53	63	4.15	0.042
	P. vampyrus	4344	2	31	55	51	6.70	0.010
	R. ferrumequinum	4900	2	29	55	65	8.05	0.005
	M. lucifugus	3443	4	17	151	29	106.88	<0.001
	P. parnellii	4836	4	40	85	51	16.20	<0.001
Dlx1	*B. taurus*	3812	4	26	30	33	0.29	0.593
	T. truncatus	4541	7	32	37	43	0.36	0.547
	E. helvum	4754	6	25	42	54	4.31	0.038
	P. vampyrus	4647	4	25	53	55	10.05	0.002
	R. ferrumequinum	4695	3	33	54	50	5.07	0.024
	M. lucifugus	4653	5	32	82	43	21.93	<0.001
	P. parnellii	4615	3	23	37	41	3.27	0.071
Meis2	*B. taurus*	5047	5	32	38	37	0.21	0.649
	T. truncatus	4624	3	62	28	40	7.28	0.007
	E. helvum	5369	1	38	33	42	0.00	0.948
	P. vampyrus	4847	1	34	35	41	1.52	0.217
	R. ferrumequinum	5335	3	36	38	45	1.20	0.273
	M. lucifugus	5336	3	34	59	46	35.68	<0.001
	P. parnellii	5292	3	37	57	44	12.75	<0.001
Bhlhb5	*B. taurus*	4715	2	34	86	55	22.53	<0.001
	T. truncatus	4433	2	71	31	44	15.69	<0.001
	E. helvum	4794	5	34	48	56	2.39	0.122
	P. vampyrus	4452	4	27	42	51	3.26	0.071
	R. ferrumequinum	4772	4	33	57	55	6.40	0.011
	M. lucifugus	4749	3	36	66	53	8.82	0.003
	P. parnellii	4667	7	30	61	55	10.56	0.001
Emx2	*B. taurus*	6617	3	58	49	72	0.76	0.384
	T. truncatus	6185	4	58	67	63	0.65	0.421
	E. helvum	6627	3	68	62	70	0.28	0.598

	P. vampyrus	6517	2	63	61	75	0.03	0.857
	R. ferrumequinum	6611	4	64	68	74	0.12	0.728
	M. lucifugus	6490	5	64	143	62	30.15	<0.001
	P. parnellii	6406	4	61	100	69	9.45	0.002)
Zic2	*B. taurus*	5365	5	64	116	83	15.02	<0.001
	T. truncatus	5256	2	63	87	80	3.84	0.050
	E. helvum	5564	6	62	59	95	0.07	0.785
	P. vampyrus	5162	3	51	37	80	2.23	0.136
	R. ferrumequinum	5456	7	55	61	94	0.31	0.577
	M. lucifugus	5514	4	61	95	97	7.41	0.006
	P. parnellii	5410	4	62	111	93	13.88	<0.001
Sox21	*B. taurus*	4045	4	45	51	55	0.38	0.540
	T. truncatus	4154	3	50	85	68	9.07	0.003
	E. helvum	4259	1	52	38	70	2.18	0.140
	P. vampyrus	3626	4	47	55	61	0.63	0.428
	R. ferrumequinum	4241	2	54	50	67	0.15	0.695
	M. lucifugus	4202	2	50	81	71	7.34	0.007
	P. parnellii	4123	5	56	108	60	16.49	<0.001
Dach1	*B. taurus*	9848	2	30	59	61	9.45	0.002
	T. truncatus	9470	4	35	89	55	23.52	<0.001
	E. helvum	9642	3	35	49	51	2.33	0.127
	P. vampyrus	9527	2	37	54	50	3.18	0.075
	R. ferrumequinum	9775	2	37	63	57	6.76	0.009
	M. lucifugus	9772	2	40	64	54	5.54	0.019
	P. parnellii	9385	2	34	66	52	10.24	0.001
Gli3	*B. taurus*	2161	0	38	36	29	0.05	0.816
	T. truncatus	2137	0	39	43	28	0.20	0.659
	E. helvum	2036	0	35	62	25	7.52	0.006
	P. vampyrus	1815	0	32	61	20	9.04	0.003
	R. ferrumequinum	2048	2	30	49	25	4.57	0.033
	M. lucifugus	2137	1	36	47	29	1.46	0.227
	P. parnellii	2103	3	33	59	26	7.35	0.007
Esrrb	*B. taurus*	3222	3	25	30	48	0.45	0.500
	T. truncatus	3177	6	23	37	45	3.27	0.071
	E. helvum	3180	3	27	39	43	2.18	0.140
	P. vampyrus	2424	1	23	27	34	0.32	0.572
	R. ferrumequinum	3197	3	25	38	47	2.68	0.101
	M. lucifugus	3197	3	25	46	48	6.21	0.013
	P. parnellii	3067	2	25	48	44	7.25	0.007
Sox2	*B. taurus*	2588	0	7	10	11	0.53	0.467
	T. truncatus	2570	1	6	14	11	3.20	0.074
	E. helvum	2405	0	6	11	9	1.47	0.225
	P. vampyrus	2358	1	7	13	10	1.80	0.180
	R. ferrumequinum	2406	1	6	8	7	0.29	0.593
	M. lucifugus	2581	0	9	22	9	5.45	0.020
	P. parnellii	2468	0	7	27	8	11.76	0.001
Zic1	*B. taurus*	5382	4	61	75	68	1.44	0.230
	T. truncatus	5787	4	66	94	70	4.90	0.027
	E. helvum	5869	2	72	93	69	2.67	0.102
	P. vampyrus	5758	2	67	79	74	0.99	0.321
	R. ferrumequinum	5879	4	66	66	73	0.00	1.000
	M. lucifugus	5484	6	61	180	65	58.76	<0.001
	P. parnellii	5820	5	65	77	74	1.01	0.314
Eya1	*B. taurus*	3561	4	78	89	76	0.72	0.395
	T. truncatus	3419	3	65	62	71	0.07	0.790

	E. helvum	3512	3	81	114	71	5.58	0.018
	P. vampyrus	3346	5	81	106	67	3.34	0.068
	R. ferrumequinum	3590	1	82	91	66	0.47	0.494
	M. lucifugus	3594	7	69	89	69	2.53	0.112
	P. parnellii	3667	1	85	61	71	3.95	0.047
Evi1	*B. taurus*	2587	1	16	20	15	0.44	0.505
	T. truncatus	2583	1	17	24	14	1.20	0.274
	E. helvum	2451	0	16	12	15	0.57	0.450
	P. vampyrus	2428	0	14	17	15	0.29	0.590
	R. ferrumequinum	2589	1	17	16	13	0.03	0.862
	M. lucifugus	2590	0	17	22	15	0.64	0.423
	P. parnellii	2490	0	15	23	16	1.68	0.194
Fign	*B. taurus*	8799	1	40	56	47	2.67	0.102
	T. truncatus	8232	2	34	81	52	19.21	<0.001
	E. helvum	8844	3	56	58	33	0.04	0.851
	P. vampyrus	8210	4	54	70	32	2.06	0.151
	R. ferrumequinum	8833	2	53	55	35	0.04	0.847
	M. lucifugus	8826	2	53	76	35	4.10	0.043
	P. parnellii	8818	3	54	69	33	1.83	0.176
Gbx2	*B. taurus*	1393	1	12	10	10	0.18	0.670
	T. truncatus	1339	0	15	29	6	4.45	0.035
	E. helvum	1383	0	13	28	10	5.49	0.019
	P. vampyrus	1394	0	12	25	12	4.57	0.033
	R. ferrumequinum	1360	0	12	19	12	1.58	0.209
	M. lucifugus	1389	0	12	16	10	0.57	0.450
	P. parnellii	8818	3	54	69	33	0.36	0.549
Lhx1	*B. taurus*	2650	1	14	24	30	2.63	0.105
	T. truncatus	2829	2	13	36	32	10.80	0.001
	E. helvum	2852	0	14	16	31	0.13	0.715
	P. vampyrus	2858	0	14	10	31	0.67	0.414
	R. ferrumequinum	2672	1	13	14	29	0.04	0.847
	M. lucifugus	2747	0	10	14	24	0.67	0.414
	P. parnellii	2748	0	15	16	29	0.03	0.857
Meis1	*B. taurus*	5047	5	32	38	37	0.51	0.473
	T. truncatus	4624	3	28	62	40	12.84	<0.001
	E. helvum	5369	1	38	33	42	0.35	0.553
	P. vampyrus	4847	1	34	35	41	0.01	0.904
	R. ferrumequinum	5335	3	36	38	45	0.05	0.816
	M. lucifugus	5336	3	34	59	46	6.72	0.010
	P. parnellii	5292	3	37	57	44	4.26	0.039
Pax2	*B. taurus*	8272	2	34	24	36	1.72	0.189
	T. truncatus	7224	2	21	83	34	36.96	<0.001
	E. helvum	7955	2	23	34	37	2.12	0.145
	P. vampyrus	7660	1	31	39	40	0.91	0.339
	R. ferrumequinum	8300	5	18	33	34	4.41	0.036
	M. lucifugus	8006	3	31	38	37	0.71	0.399
	P. parnellii	7245	2	17	26	37	1.88	0.170
Pax3	*B. taurus*	957	1	14	9	8	1.09	0.297
	T. truncatus	822	0	11	8	10	0.47	0.491
	E. helvum	954	0	13	12	10	0.04	0.841
	P. vampyrus	766	0	8	10	6	0.22	0.637
	R. ferrumequinum	950	0	15	10	8	1.00	0.317
	M. lucifugus	955	0	13	11	10	0.17	0.683
	P. parnellii	947	0	13	10	10	0.39	0.532
Pax5	*B. taurus*	291	0	2	0	1	2.00	0.157

T. truncatus	289	0	2	2	1	0.00	1.000
E. helvum	289	0	1	2	2	0.33	0.564
P. vampyrus	291	0	1	0	2	1.00	0.317
R. ferrumequinum	291	0	1	0	2	1.00	0.317
M. lucifugus	291	0	1	0	2	1.00	0.317
P. parnellii	261	0	1	1	2	0.00	1.000

Table B2 i) PCA loadings, correlations and ii) variance expressed by PC1 and PC2.
a) Complete CNE dataset
i)

Gene	PC1		PC2	
region:	Coefficient	Correlation	Coefficient	Correlation
ARX	0.00	-0.01	0.01	0.37
ATBF1	0.07	0.81	-0.07	-0.34
AUTS2	0.13	0.79	-0.12	-0.31
BARHL2	0.11	0.93	-0.04	-0.15
BCL11A	0.04	0.74	0.00	-0.03
BCL11B	0.49	0.93	-0.30	-0.24
BHLHB5	0.08	0.83	-0.07	-0.30
BNC2	0.11	0.38	-0.07	-0.09
CST	0.01	0.40	0.01	0.09
DACH1	0.06	0.89	-0.03	-0.21
DLX1	0.07	0.92	0.00	-0.02
EBF1	0.05	0.74	-0.07	-0.42
EBF3	0.07	0.58	0.19	0.62
EMX2	0.09	0.93	0.01	0.03
EN1	0.03	0.36	-0.05	-0.23
ESRRB	0.04	0.54	-0.04	-0.23
ESRRG	0.12	0.82	0.16	0.45
EVI1	0.10	0.93	-0.04	-0.17
EYA1	0.16	0.90	-0.05	-0.12
FIGN	0.05	0.87	-0.02	-0.15
FOG2	0.08	0.78	0.01	0.02
FOXD3	0.09	0.60	-0.02	-0.07
FOXP1	0.14	0.79	0.13	0.31
FOXP2	0.08	0.83	0.11	0.44
GBX2	0.04	0.36	0.05	0.19
GLI3	0.09	0.67	0.11	0.35
HLX1	0.32	0.77	0.32	0.32
HMX2	0.08	0.68	0.08	0.27
HOXD9	0.08	0.91	-0.03	-0.16
IRX2	0.09	0.56	-0.06	-0.15
IRX5	0.13	0.73	0.16	0.38
LHX1	0.02	0.54	-0.02	-0.22
LMO1	0.01	0.30	0.02	0.26
LMO4	0.07	0.86	-0.06	-0.31
MAB21L1	0.17	0.55	0.46	0.63
MAB21L2	0.08	0.86	-0.02	-0.10
MAF	0.13	0.82	-0.16	-0.44
MEIS1	0.09	0.90	-0.05	-0.19
MEIS2	0.06	0.93	-0.01	-0.09
NKX6_1	0.08	0.93	-0.02	-0.09
NR2F1	0.10	0.93	-0.06	-0.22
NR2F2	0.12	0.56	0.33	0.64
NR4A2	0.07	0.85	-0.06	-0.32
OTP	0.06	0.83	-0.05	-0.29
PAX1	0.12	0.71	-0.01	-0.02
PAX2	0.01	0.21	-0.04	-0.36
PAX3	0.07	0.79	-0.04	-0.18
PAX5	0.01	0.26	0.02	0.18
PAX6	0.08	0.80	-0.04	-0.19

PAX7	0.14	0.90	-0.11	-0.29
PAX8	-0.01	-0.07	0.04	0.15
PAX9	0.03	0.69	-0.01	-0.06
PBX3	0.06	0.90	-0.05	-0.27
PHOX2B	0.08	0.86	-0.04	-0.17
PITX2	0.08	0.92	-0.01	-0.03
POU3F1	0.00	0.09	0.00	-0.05
POU3F2	0.04	0.85	-0.01	-0.08
POU3F3	0.11	0.90	-0.03	-0.11
POU4F2	0.17	0.96	-0.02	-0.04
POU6F2	0.05	0.61	0.05	0.24
SALL3	0.14	0.61	0.17	0.32
SATB1	0.06	0.81	-0.07	-0.40
SHH	0.09	0.44	0.31	0.68
SHOX2	0.04	0.46	0.00	0.00
SOX1	0.06	0.40	-0.09	-0.24
SOX2	0.13	0.83	-0.08	-0.22
SOX3	0.02	0.28	0.03	0.20
SOX4	0.07	0.73	-0.09	-0.40
SOX6	0.08	0.89	-0.03	-0.12
SOX14	0.06	0.73	-0.04	-0.20
SOX21	0.15	0.87	-0.08	-0.19
SP8	0.06	0.80	0.00	0.02
TCF7L2	0.10	0.91	-0.07	-0.28
TFAP2A	0.12	0.93	-0.09	-0.29
TSHZ1	0.06	0.65	0.04	0.17
TSHZ2	0.18	0.96	-0.05	-0.12
TSHZ3	0.07	0.66	0.15	0.57
ZFHX1B	0.05	0.95	-0.02	-0.15
ZFHX4	0.07	0.85	0.08	0.40
ZIC1	0.12	0.89	0.04	0.12
ZIC2	0.15	0.86	-0.07	-0.16
ZNF503	0.07	0.90	-0.06	-0.31
ZNF703	0.03	0.45	-0.09	-0.56

ii)

PC	Eigenvalue	% variance	% cumulative variance
1	0.0044	59.58	59.58
2	0.0008	10.38	69.96
3	0.0005	6.85	76.80
4	0.0004	6.05	82.86
5	0.0004	5.07	87.93
6	0.0003	3.91	91.84
7	0.0002	2.62	94.46
8	0.0001	1.43	95.89
9	0.0001	1.04	96.93
10	0.0001	0.86	97.79
11	0.0000	0.57	98.37
12	0.0000	0.52	98.89
13	0.0000	0.24	99.13
14	0.0000	0.21	99.34
15	0.0000	0.19	99.54
16	0.0000	0.15	99.68

17	0.0000	0.14	99.82
18	0.0000	0.08	99.90
19	0.0000	0.05	99.94
20	0.0000	0.04	99.98
21	0.0000	0.02	100.00

b) Ear development CNEs
i)

Gene	PC1		PC2	
region:	Coefficient	Correlation	Coefficient	Correlation
BHLHB5	0.181	0.86	-0.088	-0.19
DACH1	0.136	0.93	-0.044	-0.14
DLX1	0.173	0.94	-0.060	-0.15
EMX2	0.212	0.94	-0.042	-0.09
ESRRB	0.097	0.58	-0.144	-0.40
EVI1	0.228	0.95	-0.027	-0.05
EYA1	0.373	0.92	0.064	0.07
FIGN	0.121	0.89	0.007	0.02
GBX2	0.088	0.36	0.223	0.42
GLI3	0.185	0.62	0.411	0.64
HMX2	0.184	0.66	0.000	0.00
LHX1	0.045	0.52	0.025	0.13
MEIS1	0.219	0.95	-0.080	-0.16
MEIS2	0.129	0.95	-0.022	-0.07
PAX2	0.012	0.11	-0.083	-0.36
PAX3	0.153	0.74	-0.012	-0.03
PAX5	0.017	0.18	0.040	0.19
SHH	0.191	0.44	0.757	0.81
SOX2	0.324	0.90	-0.194	-0.25
SOX21	0.372	0.93	-0.219	-0.25
TSHZ1	0.137	0.64	0.184	0.40
ZIC1	0.263	0.88	0.002	0.00
ZIC2	0.356	0.89	-0.180	-0.21

ii)

PC	Eigenvalue	% variance	% cumulative variance
1	0.0009	64.19	64.19
2	0.0002	13.75	77.94
3	0.0001	5.88	83.82
4	0.0001	4.64	88.46
5	0.0001	3.94	92.40
6	0.0000	2.29	94.69
7	0.0000	1.52	96.22
8	0.0000	1.37	97.59
9	0.0000	0.80	98.39
10	0.0000	0.52	98.90
11	0.0000	0.37	99.27
12	0.0000	0.25	99.52
13	0.0000	0.14	99.66
14	0.0000	0.12	99.79
15	0.0000	0.08	99.87
16	0.0000	0.05	99.91
17	0.0000	0.04	99.95
18	0.0000	0.03	99.98
19	0.0000	0.01	99.99
20	0.0000	0.01	100.00
21	0.0000	0.00	100.00

Appendix C

Table C1 Specimen details and measurements of the bats species included in this study. Origin of specimens: 1 Natural History Museum, London; 2 The Harrison Institute, Sevenoaks; 3 Museum Zoology Bogor, Indonesia; 4 Dr Steven Le Comber, Queen Mary University of London. * Denotes spirit specimen, otherwise all specimens were prepared skulls.

Family	Specimen code	Species	Voxel size	Basilar membrane	Number of turns
Pteropodidae	NHM. 76.3.15.14[1]	*Pteropus rodricensis*	0.017539	-	1.75
	N/A	*Pteropus sp.*	0.0167	16.237	1.75
	HZM.16.36082[2]	*Rousettus lanosus*	0.0118	12.517	1.75
	HZM.107.11626[2]	*Rousettus aegyptiacus*	0.0101	11.014	1.75
	HZM.1.3518[2]	*Hypsignathus monstrosus*	0.0126	13.080	2.25
Rhinolophidae	MZB22913[3]	*Rhinolophus philippensis (Small)*	0.0064	12.978	3.25
	MZB22897[3]	*Rhinolophus philippensis (Medium)*	0.0073	24.666	3.25
	MZB22910[3]	*Rhinolophus philippensis (Large)*	0.0101	29.958	3.25
	NHM.67.1427[1]	*Rhinolophus philippensis*	0.0063	-	-
	HZM.58.20697[2]	*Rhinolophus ferrumequinum*	0.0073	18.488	3.25
	NHM.1903.8.3.3[1]	*Rhinolophus megaphyllus*	0.0087	28.642	3.75
	HZM.B035FBEN25[2]*	*Rhinolophus pearsonii*	0.0081	21.403	3.5
	HZM.14.35.110[2]	*Rhinolophus pearsonii*	0.0083	21.419	3.25
	HZM.F42600[2]*	*Rhinolophus marshalli*	0.0106	21.535	3.25
	HZM.29.35223[2]	*Rhinolophus affinis*	0.0088	21.990	3.5
Hipposideridae	NHM.1983.423[1]	*Hipposideros ridleyi*	0.0076	13.861	2.75
	HZM.3.28778[2]	*Hipposideros fulvus*	0.007	10.417	2.75
	HZM.3.1164[2]	*Hipposideros gigas*	0.0108	22.580	3.25
	HZM.13.4765[2]	*Cleotis percivali*	0.0069	9.405	2.75
	NHM.66.5456[1]	*Cleotis percivali*	0.0049	-	2.75
Rhinopomatidae	NHM.1968.453[1]	*Rhinopoma microphyllum*	0.0082	12.974	2.25
	HZM.37.9152[2]	*Rhinopoma hardwickii*	0.0073	12.667	2.5
Megadermatidae	NHM.1892.5.20.2[1]	*Macroderma gigas*	0.0083	6.161	2.25
	NHM.1975.2453[1]	*Cardioderma cor*	0.0124	14.903	2
	NHM.1912.11.28.32[1]	*Megaderma spasma*	0.0069	9.664	2.25
	HZM.30.25025[2]	*Lavia frons*	0.0085	12.601	2.25
Craseonycteridae	HZM.1.34982[2]	*Craseonycteris thonglongyai*	0.0057	10.536	2.5
Miniopteridae	NHM.62.1443[1]	*Miniopterus schreibersii*	0.0049	10.332	2.25

	HZM.247.22505[2]	*Miniopterus schreibersii*	0.0085	10.499	2.25
Vespertilionidae	HZM.0001-A1[2]*	*Murina tubinaris*	0.0106	11.806	2.75
	HZM.24454[2]*	*Myotis muricola*	0.0097	10.228	2.5
	NHM.18.79.11.15.16[1]	*Murina suilla*	0.0069	10.559	2.75
	NHM.16.3.25.29[1]	*Murina cyclotis*	0.0118	9.642	2.5
	NHM.7.7.7.3359[1]	*Myotis lucifugus*	0.005188	8.210	2.25
	HZM. T11[2]*	*Scotophilus kuhlii*	0.0118	13.421	2.75
	HZM.TD78[2]*	*Scotomanes ornatus*	0.0097	12.041	2.25
	HZM.4.3341[2]	*Lasiurus borealis*	0.0057	10.829	2.5
	SLC.0001.NMS[4]	*Plecotus auritus*	0.0055	9.192	2
	SLC.0002.NMS[4]	*Plecotus auritus*	0.0055	8.763	2
	SLC.0003.NMS[4]	*Plecotus auritus*	0.0058	9.304	2
	P.PIP.001.DO[4]	*Pipistrellus pipistrellus*	0.005	8.871	2.5
	P.PIP.005.DO[4]	*Pipistrellus pipistrellus*	0.005	9.231	2.5
	P.PIP.002.STC[4]	*Pipistrellus pipistrellus*	0.0049	8.473	2.5
	P.PIP.004.STC[4]	*Pipistrellus pipistrellus*	0.0047	8.999	2.5
Noctilionidae	NHM.1928.7.21.35[1]	*Noctilio leporinus*	0.0118	16.030	2.75
	HZM.12.15977[2]	*Noctilio leporinus*	0.0107	16.518	2.75
Thyropteridae	N/A*	*Thyroptera sp.*	0.007	13.422	2.5
Mormoopidae	NHM.65.3990[1]	*Pteronotus (chilonycteris) macleayi grisea*	0.004548	11.770	3
	HZM.5.21236[2]	*Pteronotus parnellii*	0.0112	16.470	2.5
	HZM.8.16031[2]	*Pteronotus davyi*	0.0083	11.418	2.75
	HZM.2.16030[2]	*Mormoops megaphylla*	0.0074	13.205	2.5
Phyllostomidae	NHM.1907.1.1.684[1]	*Artibeus jamaicensis*	0.0118	12.958	2.75
	NHM.1954.322[1]	*Tonatia silvicola*	0.0101	14.145	2.75
	NHM.1924.3.1.33[1]	*Trachops cirrhosus*	0.0101	17.503	3.25
	HZM.41.11631[2]	*Desmodus rotundus*	0.0099	15.245	3
	NHM.1914.5.21.4[1]	*Anoura geoffroyi*	0.0063	7.595	2.75
	HZM.140.29127[2]	*Carollia perspicillata perspicillata*	0.0079	10.131	2.25
	HZM.1.13198[2]	*Centurio senex*	0.0088	11.949	2.75
Molossidae	NHM.1844.10.17.7[1]	*Cheiromeles torquatus*	0.0186	28.532	2.75
	HZM.61.28841[2]	*Molossus molossus*	0.0096	14.073	2.75
	NHM.1960.482[1]	*Tadarida brasiliensis*	0.006	10.012	2.25
Nycteridae	HZM.214.35929[2]	*Nycteris thebaica*	0.0085	9.170	2
Natalidae	HZM.8.7055[2]	*Natalus stramineus saturates*	0.0065	9.020	2.5

Emballonuridae	HZM.2.18450[2]	*Taphozous peli*	0.0186	23.424	3.25
	HZM.18.30235[2]	*Taphozous melanopogon*	0.0086	14.600	2.25
	HZM.3.18512[2]	*Peropteryx macrotis*	0.0059	12.024	2.5
	HZM.8.16002[2]	*Saccopteryx bilineata*	0.0087	12.559	2.5
	HZM.34.5860[2]	*Rhynchonycteris naso*	0.0057	10.337	2.75

Table C2 Basilar membrane lengths and body mass used in this study. (Published basilar membrane values indicated by *)

Species	Basilar membrane length (mm) Mean ± SD, Min – Max (n)	Body mass (g)	Source: Basilar membrane[1], Body mass[2]
Pteropus sp.	16.24	1175	(Spoor *et al.,* 2007) [2]
Rousettus lanosus	12.52	140	(Norberg and Rayner 1987) [2]
Rousettus aegyptiacus	11.01	140	(Norberg and Rayner 1987) [2]
Hypsignathus monstrous	13.08	427	(Norberg and Rayner 1987) [2]
Rhinolophus ferrumequinum	17.29 ± 1.69	21.30 ± 1.84	(Norberg and Rayner 1987) [2]
	16.10* - 18.49 (2)	20 – 22.6 (2)	(Kirk and Gosselin-Ildari 2009)[1]
Rhinolophus rouxi	15.6*	12.57	(Melzer 1985) [1,2]
Rhinolophus philippensis (Medium)	24.67	7	SJ Rossiter, T Kingston [2]
Rhinolophus philippensis (Small)	12.98	6.5	SJ Rossiter, T Kingston [2]
Rhinolophus philippensis (Large)	29.96	12	SJ Rossiter, T Kingston [2]
Rhinolophus megaphyllus	28.64	9.8	(Norberg and Rayner 1987) [2]
Rhinolophus pearsonii	21.42 ± 0.01	8.8	HZM [2]
	21.40 – 21.42 (2)		
Rhinolophus marshalli	21.53	6.4	(Zhang *et al.,* 2009) [2]
Rhinolophus affinis	21.99	12.6	HZM [2]
Hipposideros ridleyi	13.86	9.3	(Struebig 2005) [2]
Cleotis percivali	9.41	4.05	(Barclay and Brigham 1991) [2]
Hipposideros fulvus	9.61 ± 1.14	9.25 ± 1.06	(Smith and Xie 2008) [2]
	8.80* - 10.41 (2)	8.50 – 10.00 (2)	(Kirk and Gosselin-Ildari 2009) [1,2]
Hipposideros speoris	9.55 ± 0.50	11.53 ± 2.17	
	9.20*- 9.90* (2)	10.00 - 13.07 (2)	(Neuweiler 2000; Kirk and Gosselin-Ildari 2009)[1,2]
Hipposideros gigas	22.58	89	(Norberg and Rayner 1987) [2]
Hipposideros bicolor	8.8*	13.29	(Neuweiler 2000)[1,2]
Rhinopoma microphyllum	12.97	32	(Norberg and Rayner 1987) [2]
Rhinopoma hardwickii	12.23 ± 0.613	12.93 ± 4.77	(Norberg and Rayner 1987) [2]
	11.8* – 12.67 (2)	9.56 – 16.30 (2)	(Neuweiler 2000)[1,2]
Macroderma gigas	6.16	123	(Norberg and Rayner 1987) [2]
Cardioderma cor	14.90	28	(Csada 1996) [2]

Megederma spasma	9.66	27	(Struebig 2005) [2]
Megaderma lyra	9.9*	41.38 ± 8.94	(Neuweiler 2000)[1], (Kirk and Gosselin-Ildari 2009) [2]
		35.36 – 48.00 (2)	
Lavia frons	12.60	34.8	HZM [2]
Craseonycteris thonglongyai	10.54	2.5	HZM [2]
Nyctalus noctula	11.8*	5.19	(Neuweiler 2000) [1,2]
Eptesicus serotinus	8.9*	22.30	(Neuweiler 2000) [1,2]
Myotis lucifugus	8.45 ± 0.93	8.06 ± 0.09	(Spoor *et al.,* 2007) [2]
	6.90* – 8.21 (2)	8.00 – 8.13 (2)	(Kirk and Gosselin-Ildari 2009) [1]
Myotis muricola	10.23	4.85	(Borisenko and Kruskop 2003) [2]
Miniopterus schreibersii	10.42 ± 0.12	14.20	(Norberg and Rayner 1987) [2]
	10.33 – 10.50 (2)		
Scotophilus kuhlii	13.42	34.50	(Norberg and Rayner 1987) [2]
Murina suilla	10.56	3.90	(Struebig 2005) [2]
Murina cyclotis	9.64	11.30	(Struebig 2005) [2]
Murina tubinaris	11.81	4.75	(Struebig 2005) [2]
Scotomanes ornatus	12.04	21.8	(Cox and Jeffery 2010) [2]
Lasiurus borealis	10.83	16.7	(Norberg and Rayner 1987) [2]
Plecotus auritus	9.09 ± 0.29	9.00	(Norberg and Rayner 1987) [2]
	8.76 – 9.30 (3)		(Norberg and Rayner 1987) [2]
Pipistrellus pipistrellus	8.89 ± 0.32	6.55	(Spoor *et al.,* 2007) [2]
	8.47 – 9.23 (4)		
Noctilio leporinus	16.27 ± 0.35	59.00	(Norberg and Rayner 1987) [2]
	16.03 – 16.52 (2)		(Norberg and Rayner 1987) [2]
Pteronotus macleayi grisea	11.77	5.35	(Mancina 2005) [2]
Pteronotus parnellii	15.75 ± 1.27	14.57 ± 2.51	(Rydell *et al.,* 2002) [2]
	14.30* – 16.69 (3)	12.00 – 17.02 (3)	(Neuweiler 2000) [1,2]
Pteronotus davyi	11.42	10.90	(Norberg and Rayner 1987) [2]
Mormoops megaphylla	13.21	17.00	(Norberg and Rayner 1987) [2]
Artibeus jamaicensis	12.96	47.00	(Norberg and Rayner 1987) [2]
Tonatia silvicola	14.15	32.85	(Mendellin and Arita 1989) [2]
Trachops cirrhosus	16.00 ± 2.12	43.87 ± 0.09	(Norberg and Rayner 1987) [2]

	14.50* – 17.50 (2)	43.80 – 43.93 (2)	(Neuweiler 2000) [1,2]
Desmodus rotundus	15.25	28.5	(Norberg and Rayner 1987) [2]
Anoura geoffroyi	7.60	14.1	(Norberg and Rayner 1987) [2]
Carollia perspicillata perspicillata	10.13	19.1	(Norberg and Rayner 1987) [2]
Centurio senex	11.95	22	(Norberg and Rayner 1987) [2]
Cheiromeles torquatus	28.53	135.5	(Norberg and Rayner 1987) [2]
Molossus molossus	14.07	16.2	(Norberg and Rayner 1987) [2]
Molossus ater	14.6*	37.23 ± 0.32	(Kirk and Gosselin-Ildari 2009)[1,2]
		37.00 – 37.45 (2)	(Neuweiler 2000) [1,2]
Tadarida brasiliensis	11.11 ± 1.55	12.5	(Norberg and Rayner 1987) [2]
	10.01 – 12.20* (2)		(Vater and Siefer 1995) [1]
Nycteris thebaica	9.17	11.00	(Norberg and Rayner 1987) [2]
Natalus stramineus saturates	9.02	3.9	(Norberg and Rayner 1987) [2]
Taphozous melanopogon	14.60	24.00	HZM [2]
Taphozous peli	23.42	95.00	(Norberg 1981) [2]
Taphozous kachensis	13.25* ± 1.63	49.20 ± 1.13	(Kirk and Gosselin-Ildari 2009)[1,2]
	12.10 – 14.40 (2)	48.40 – 50.00 (2)	(Neuweiler 2000)[1]
Peropteryx macrotis	12.02	4.4	(Yee 2000) [2]
Saccopteryx bilineata	12.56	7.5	(Norberg and Rayner 1987) [2]
Rhynchonycteris naso	10.34	3.9	(Norberg and Rayner 1987) [2]
Thyroptera sp.	13.42	19.5	Body mass recorded
Phocoena phocoena	25.97* ± 0.05	337,500 ± 403051	(Ketten 1994; Kirk and Gosselin-Ildari 2009)[1,2]
	25.93 – 26.00 (2)	52,500 – 622,500 (2)	
Eubalaena glacialis	52.55* ± 4.31	39,512,500 ± 24059308	(Ketten 1994; Kirk and Gosselin-Ildari 2009)[1,2]
	49.50 – 55.60 (2)	22,500,000 – 56,525,000 (2)	
Balaena mysticetus	61.3*	105,000,000 ± 7071067	(Ketten 1994; Kirk and Gosselin-Ildari 2009)[1,2]
		100,000,000 - 110,000,000 (2)	
Balaenoptera acutorstrata	55*	8,044,000	(Ketten 1994) [1,2]
Megaptera noveangliae	54*	48,350,000	(Ketten 1994) [1,2]
Physeter catodon	54*	27,500,000	(Ketten 1994) [1,2]
Grampus griseus	40.75* ± 0.35	468,750 ± 61872	(Ketten 1994; Kirk and Gosselin-Ildari 2009)[1,2]
	40.50 – 41.00 (2)	425,000 – 512500 (2)	

Lagenorhynchus albirostris	34.95* ± 0.07	127,350 ± 34436	(Ketten 1994; Kirk and Gosselin-Ildari 2009)[1,2]
	34.90 – 35.00 (2)	103,000 - 151,700 (2)	
Lagenorhynchus obliquidensis	36.9*	120,000	(Ketten 1997) [1,2]
Stenella attenuata	36.95* ± 0.07	103,050 ± 13364	(Ketten 1994; Kirk and Gosselin-Ildari 2009)[1,2]
	36.90 – 37.00 (2)	93,600 – 112,500 (2)	
Tursiops truncatus	40.83* ± 0.25	182,438 ± 10518	(Ketten 1994; Kirk and Gosselin-Ildari 2009)[1,2]
	40.65 – 41.00 (2)	175,000 - 189,875 (2)	
Inia geoffrensis	38*	128,250	(Ketten 1994) [1,2]
Delphinapterus leucas	42*	1,400,000	(Ketten 1997) [1,2]
Dephinus delphis	34.9*	70,000	(Ketten 1997) [1,2]
Rattus norvegicus	10.2* ± 0.71	325	(West 1985; Kirk and Gosselin-Ildari 2009) [1,2]
	9.70 – 10.70 (2)		
Rattus rattus	12.1*	200	(Kirk and Gosselin-Ildari 2009) [1,2]
Mus musculus	6.9* ± 0.14	10	(Kirk and Gosselin-Ildari 2009)*
	6.80 – 7.00 (2)		(West 1985)*
Spalacopus cyanus	11.68*	90	(Kirk and Gosselin-Ildari 2009)*
Spalax ehrenbergi	12.6*	143	(Kirk and Gosselin-Ildari 2009)*
Pachyuromys duprasi	10.75*	90	(Kirk and Gosselin-Ildari 2009)*
Meriones unguiculatus	12.1*	50	(Manoussaki *et al.,* 2008)*
Microtus arvalis	8.5*	27	(Kirk and Gosselin-Ildari 2009)*
Cavia porcellus	19.5* ± 1.41	406	(Kirk and Gosselin-Ildari 2009)*
	18.50 – 20.50 (2)		(West 1985)*
Chinchilla laniger	18.5*	490	(West 1985)*
Ctenomys talarum	10.58*	140	(Kirk and Gosselin-Ildari 2009)*
Dipodomys merriami	9.83*	50	(Kirk and Gosselin-Ildari 2009)*
Arvicola terrestris	10.5*	130	(Kirk and Gosselin-Ildari 2009)*
Fukomys anselli	11.1*	80	(Kirk and Gosselin-Ildari 2009)*
Oryctolagus cuniculus	15.25*	2,000	(West 1985)*
Panthera onca	33.3*	90,000	(Kirk and Gosselin-Ildari 2009)*
Panthera tigris	35.5*	106,300	(Kirk and Gosselin-Ildari 2009)*
Bos taurus	38*	500,000	(Kirk and Gosselin-Ildari 2009)*
Felis catus	22.5*	2,500	(Kirk and Gosselin-Ildari 2009)*

			(West 1985)*
Zalophus californianus	54.3*	24,250	(Manoussaki *et al.,* 2008)*
Macaca nemestrina	25.6*	8,850	(Kirk and Gosselin-Ildari 2009)*
Homo sapiens	34.63* ± 0.53	75,000	(West 1985)*
	34.25 – 35.00 (2)		(Kirk and Gosselin-Ildari 2009)*
Saimiri sciureus	15.4*	759	(Manoussaki *et al.,* 2008)*
Elephas maximus	60*	40,00,000	(West 1985)*
Monodelphis domestica	6.4*	110	(Kirk and Gosselin-Ildari 2009)*
Didelphis viriginiana	15*	3,000	(Fernandez and Schmidt 1963)*

Table C3 Number of cochlear spirals taken from literature sources.

Species:	Turns (n):	Source:
Pteropus giganteus	2	(Pye 1966a)
Hipposideros pomona	3	(Pye 1966b)
Myotis albescens	2.5	(Pye 1966a)
Chilonycteris rubiginosa	3	(Pye 1967)
Artibeus cinereus	2.5	(Pye 1967)
Glossophaga longirostris	2.5	(Pye 1967)
Glossophaga soricina	2.5	(Pye 1967)
Phyllostomus discolor	2.5	(Pye 1967)
Phylloderma stenops	2.5	(Pye 1967)
Micronycteris hirsuta	2.5	(Pye 1967)
Carollia perspicillata perspicillata	2.5	(Pye 1967)
Sturnira tildae	2.5	(Pye 1967)
Artibeus lituratus	3	(Pye 1967)
Diaemus youngi	3	(Pye 1967)
Phyllostomus hastatus	3	(Pye 1967)
Sturnira lilium	3	(Pye 1967)
Vampyrops helleri	3	(Pye 1967)
Chiroderma villosum	3	(Pye 1967)
Tadarida brasiliensis	2.5	(Vater and Siefer 1995)
Molossus ater	3	(Pye 1966a)
Molossus major	3	(Pye 1966a)
Molossus coebensis	3	(Pye 1966a)
Natalus tumidirostris	2.5	(Pye 1966a)
Saccopteryx bilineata	2.5	(Pye 1966b)
Saimiri sciureus	2.25	(Manoussaki *et al.,* 2008)
Homo sapiens	2.5	(West 1985)
Hapale jacchus	2.75	(West 1985)
Procyon lotor	2.5	(West 1985)
Felis catus	3	(West 1985)
Canis familiaris	3.25	(West 1985)
Ovis aries	2.25	(West 1985)
Equus caballus	2.5	(West 1985)
Bos taurus	3.5	(West 1985)
Mus musculus	2	(West 1985)
Rattus norvegicus	2.25	(West 1985)
Oryctolagus cuniculus	2.5	(West 1985)
Chincilla langer	3	(West 1985)
Dipodymus merriam	3.25	(West 1985)
Meriones unguiculatis	3.25	(Manoussaki *et al.,* 2008)
Cavia porcellus	4.25	(West 1985)
Elephas maximus	2.25	(West 1985)
Trichechus mantus	1.75	(Ketten *et al.,* 1992)
Inia geoffrensis	1.5	(Ketten 1994)
Phocoena phocoena	1.5	(Ketten 1994)
Physeter catodon	1.75	(Ketten 1994)
Tursiops truncatus	2.25	(Ketten 1994)
Grampus griseus	2.5	(Ketten 1994)
Lagenorhynchus albirostris	2.5	(Ketten 1994)
Stenella attenuata	2.5	(Ketten 1994)
Balaena mysticetus	2.25	(Ketten 1994)
Eubalaena glacialis	2.5	(Ketten 1994)
Megaptera novaeanglia	2.5	(Ketten 1994)

Phoca vitulina	2.25	(West 1985)
Zalophus californianus	1.75	(Manoussaki *et al.,* 2008)

Table C4 Fossil calibration points for species phylogeny.

Fossil Constraint	Approx. age: (million years)	Source:
Split of placental and marsupial mammals	131.0	(Benton and Donoghue 2007)
Carnivores	57.5	(Benton and Donoghue 2007)
Primates	58.5	(Gingerich 1984)
Artiodactyla	60.0	(Gatesy and O'Leary 2001)
Cetartiodactyla	55.0	References within (McGowen *et al.,* 2009)
Base of cetaceans	32.0	References within (McGowen *et al.,* 2009)
Baleen whales	29.0	References within (McGowen *et al.,* 2009)
Base of Felidae	16.0	(Johnson *et al.,* 2006)
Split of *Mus* and *Rattus*	13.0	References within (Chevret *et al.,* 2005)
Minimum oldest bat	52.5	(Simmons *et al.,* 2008)
Maximum base of Rhinolophoidea	53.5	(Teeling *et al.,* 2005)
Split of Rhinolophidae and Hipposideridae	37.0	(Teeling *et al.,* 2005)
Minimum for split of Mormoopidae and Phyllostomidae	32.0	(Teeling *et al.,* 2005)
Maximum for base of Phyllostomidae	34.0	(Teeling *et al.,* 2005)
Minimum for base of Emballonuridae	37.0	(Teeling *et al.,* 2005)
Minimum for split of Vespertilionidae and Molossidae	37.0	(Teeling *et al.,* 2005)

Table C5 Prior testing.

i) G=list(G1 = list(V=matrix(BM.var/2), n=1)), R= list(V=matrix(BM.var/2), n=1)
ii) G=list(G1 = list(V=matrix(BM.var*0.95), n=1)),R=list(V=matrix(BM.var*0.05), n=1)
iii) G=list(G1 = list(V=matrix(BM.var/2), n=1)), R=list(V=matrix(BM.var/2), n=1)
iv) G=list(G1 = list(V=matrix(BM.var/2), n=10)), R=list(V=matrix(BM.var/2), n=10)

Prior	Variance	Belief	DIC	Equation	Animal	Residual
i	50:50	1	-197.3	logY = 0.38 logX + 0.71	0.024	0.006
ii	95:5	1	-205.0	logY = 0.39 logX + 0.71	0.026	0.005
iii	50:50	1	-197.3	logY = 0.38 logX + 0.71	0.024	0.006
iv	50:50	10	-170.1	logY = 0.38 logX+ 0.73	0.024	0.010

Table C6 Results of phylogenetic correction of the relationship between echolocation ability, basilar membrane length and body mass.

a) Tree A

	Model and parameters	DIC
1.	log basilar membrane = 0.44 log body mass$^{0.33}$ + 0.66 p(intercept) <0.0004x10^{-4}, p(body mass$^{0.33}$) <0.0004x10$^{-4,}$ (animal) = 0.024, (units) = 0.006,	-160.05
2.	log basilar membrane = 0.46 log body mass$^{0.33}$ + 0.07 Size + 0.58 p(intercept) = 0.003, p(body mass$^{0.33}$)<0.0004x10^{-4}, p(size) = 0.59, (animal) = 0.025, (units) = 0.006,	-159.55
3.	log basilar membrane = 0.52 log body mass$^{0.33}$ + 0.22 Echolocation + 0.57 p(intercept) <0.0004x10^{-4}, p(body mass$^{0.33}$) <0.0004x10^{-4}, p(Echolocation) = 0.01, (animal) = 0.020, (units) = 0.006,	-160.54
4.	log basilar membrane = 0.52 log body mass$^{0.33}$ + (0.19, 0.30) Echolocation + 0.57 p(intercept) <0.0004x10^{-4}, p(body mass$^{0.33}$) <0.0004x10^{-4}, p(Echolocation) = (0.013, 0.001), (animal) = 0.017, (units) = 0.007,	-159.42
5.	log basilar membrane = 0.46 log body mass$^{0.33}$ + 0.13 CF + 0.65 p(intercept) <0.0004x10^{-4}, p(body mass$^{0.33}$) <0.0004x10^{-4}, p(CF) = 0.03, (animal) = 0.021, (units) = 0.006,	-159.17

b) Tree B

	Model and parameters	DIC
1.	log basilar membrane = 0.44 log body mass$^{0.33}$ + 0.66 p(intercept) <0.0004x10^{-4}, p(body mass$^{0.33}$) <0.0004x10^{-4}, (animal) = 0.024, (units) = 0.006,	-159.94
2.	log basilar membrane = 0.46 log body mass$^{0.33}$ + 0.06 Size + 0.60 p(intercept) = 0.001, p(body mass$^{0.33}$) <0.0004x10^{-4}, p(size) = 0.59, p(Size) = 0.69, (animal) = 0.025, (units) = 0.006	-159.60
3.	log basilar membrane = 0.53 log body mass$^{0.33}$ + 0.22 Echolocation + 0.56 p(intercept) <0.0004x10^{-4}, p(body mass$^{0.33}$) <0.0004x10^{-4}, p(Echolocation) = 0.003, (animal) = 0.020, (units) = 0.006,	-161.03
4.	log basilar membrane = 0.53 log body mass$^{0.33}$ + (0.19, 0.31) Echolocation + 0.56 p(intercept) <0.0004x10^{-4}, p(body mass$^{0.33}$) <0.0004x10^{-4}, p(Echolocation) = (0.010, 0.001), (animal) = 0.017, (units) = 0.007	-160.25
5.	log basilar membrane = 0.45 log body mass$^{0.33}$ + 0.14 CF + 0.65 p(intercept) <0.0004x10^{-4}, p(body mass$^{0.33}$) <0.0004x10^{-4}, p(CF) = 0.02, (animal) = 0.021, (units) = 0.006,	-159.86

Table C7 The relationship between echolocation ability, basilar membrane length, body mass and number of turns.

a) Without correcting for phylogenetic relatedness

	Model and parameters	AIC
1.	log basilar membrane = 0.32 log body mass$^{0.33}$ + 0.96 p(Intercept)<2 x 10^{-16}, p(log body mass$^{0.33}$)<2 x 10^{-16} Mult. R^2 = 0.67, Adj. R^2 = 0.67, F = 188.8 (1, 93 DF),	-89.48
2.	log basilar membrane = 0.35 log body mass$^{0.33}$ + N^o turns + 0.39 p(Intercept) = 0.002, p(log body mass$^{0.33}$) < 2 x 10^{-16}, p(N^o turns) = (0.002, 0.0004, 0.013, 7.65 x 10^{-5}, 1.79 x 10^{-5}, 1.16 x 10^{-6}, 9.19 x 10^{-6}), Mult. R^2 = 0.79, Adj. R^2 = 0.77, F = 39.87 (8, 86 DF), p <2 x 10^{-16}	-117.37
3.	log basilar membrane = 0.44 log body mass$^{0.33}$ + Bat + 0.75 p(Intercept)<2 x 10^{-16}, p(log body mass$^{0.33}$) < 2 x 10^{-16}, p(Echo) = 1.32 x 10^{-6}, Mult. R^2 = 0.74, Adj. R^2 = 0.74, F = 134 (2, 92 DF), p < 2 x 10^{-16}	-111.77
4.	log basilar membrane = 0.46 log body mass$^{0.33}$ + N^o turns + Echo + 0.31 p(Intercept) = 0.006, p(log body mass$^{0.33}$) < 2 x 10^{-16}, p(N^o turns) = (0.006, 0.001, 0.003, 0.001, 0.0003, 5.10 x 10^{-6}, 3.63 x 10^{-6}), p(Bat) = 6.11x10^{-7} , Mult. R^2 = 0.842, Adj. R^2 = 0.825, F = 50.25 (9, 85 DF), p <2 x 10^{-16}	-143.33
5.	log basilar membrane = 0.42 log body mass$^{0.33}$ + N^o turns + Echo + N^o turns:Echo + 0.33 p(Intercept) = 0.001, p(log body mass$^{0.33}$) < 2 x 10^{-16}, p(N^o turns) = (0.001, 4.00 x 10^{-5}, 0.001, 5.35 x 10^{-5}, 8.63 x 10^{-6}, 4.15 x 10^{-5}, 2.32 x 10^{-5}), p(Echo) = (0.0002), p(N^o turns:Echo) = (0.004, 0.008, 0.005, 0.391), Mult. R^2 = 0.879, Adj. R^2 = 0.86, F = 45.42 (13, 81 DF), p <2 x 10^{-16}	-161.09

b) Correcting for phylogenetic relatedness

i) Tree A

	Model and parameters	DIC
1	log basilar membrane = 0.38 log body mass$^{0.33}$ + 0.72 p(Intercept) <0.0004, p(body mass$^{0.33}$) <0.0004, (animal) = 0.025, (units) = 0.006,	-176.98
2	log basilar membrane = 0.43 log body mass$^{0.33}$ + Echo + 0.65 p(Intercept) <0.0004, p(body mass$^{0.33}$) <0.0004, p(Echo) = 0.019, (animal) = 0.022, (units) = 0.006,	-177.54
3	log basilar membrane = 0.37 log body mass$^{0.33}$ + N^{o} turns + 0.37 p(Intercept) = 0.015, p(body mass$^{0.33}$) < 0.0004, p(N^{o} turns) = (0.055, 0.018, 0.030, 0.017, 0.009, 0.004, 0.002), (animal) = 0.018, (units) = 0.006,	-176.07
4	log basilar membrane = 0.42 log body mass$^{0.33}$ + N^{o} turns + Echo + 0.33 p(Intercept) = 0.027, p(body mass$^{0.33}$) < 0.0004, p(N^{o} turns) = (0.059, 0.024, 0.027, 0.024, 0.013, 0.006, 0.001), p(Bat) = 0.019, (animal) = 0.015, (units) = 0.007)	-175.50

ii) Tree B

	Model and parameters	DIC
1	log basilar membrane = 0.38 log body mass$^{0.33}$ + 0.72 p(Intercept) <0.0004, p(body mass$^{0.33}$) <0.0004, (animal) = 0.024, (units) = 0.006,	-177.33
2	log basilar membrane = 0.44 log body mass$^{0.33}$ + Echo + 0.64 p(Intercept) <0.0004, p(body mass$^{0.33}$) <0.0004, p(Echo) = 0.030, (animal) = 0.021, (units) = 0.006,	-177.38
3	log basilar membrane = 0.37 log body mass$^{0.33}$ + N^{o} turns + 0.37 p(Intercept) = 0.014, p(body mass$^{0.33}$) < 0.0004, p(N^{o} turns) = (0.057, 0.021, 0.033, 0.013, 0.010, 0.004, 0.001), (animal) = 0.018, (units) = 0.006,	-175.77
4	log basilar membrane = 0.42 log body mass$^{0.33}$ + N^{o} turns + Echo + 0.33 p(Intercept) = 0.031, p(body mass$^{0.33}$) < 0.0004, p(N^{o} turns) = (0.047, 0.018, 0.021, 0.017, 0.009, 0.003, 0.001), p(Bat) = 0.027, (animal) = 0.015, (units) = 0.007)	-175.17

Table C8 Values used for PCA. Class: T = terrestrial, V = volant, SA = semi-aquatic, S = subterranean, A = aquatic

	Hearing (kHz)				Basilar membrane		
Species	Min.	Max.	Opt.	No. of Turns	length (mm)	Body mass (g)	Class
Ornithorhynchus anatinus	1	15	4	0.500	4.426	1752	T
Didelphis virginiana	0.5	64	32	2.250	15	3,000	T
Monodelphis domestica	4.2	80	16	1.800	6.4	110	T
Artibeus jamaicensis	2.8	130	16	2.750	12.96	47	V
Carollia perspicillata	5.2	150	25	2.375	10.13	19.1	V
Carollia perspicillata	5.2	150	71	2.375	10.13	19.1	V
Tadarida brasiliensis	3	80	41.5	2.375	11.11	12.5	V
Plecotus auritus	12	50	12	2.000	9.09	9	V
Pteronotus parnellii	10	111	62	2.500	15.75	14.57	V
Noctilio leporinus	7.5	111	44.5	2.833	16.27	59	V
Trachops cirrhosus	5	90	5	3.250	16	43.87	V
Desmodus rotundus	15	74	22.5	3.000	15.25	28.5	V
Taphozous melanopogon	1	80	27	2.250	14.6	24	V
Lasiurus cinereus	10	50	27.5	2.500	10.83	16.7	V
Myotis lucifugus	10.3	115	40	2.250	8.45	8.06	V
Megaderma lyra	1.7	160	38	2.250	9.9	41.38	V
Megaderma spasma	5	50	15	2.250	9.66	27	V
Rhinolophus ferrumequinum	4.3	103	81.426	3.375	17.29	21.3	V
Rhinolophus rouxi	15	77.5	77.138	*3.250*	15.6	12.57	V
Rhinopoma hardwickii	1	70	33.8	2.500	12.23	12.93	V
Rousettus aegyptiacus	2.25	64	26.5	1.750	11.01	140	V
Pteropus pumilus	2	50	15	1.750	16.24	1175	V
Rousettus leschenaultii	2.25	64	26.5	1.750	12.52	140	V
Arvicola terrestris	1.2	51	10	2.300	10.5	130	SA
Zalophus californianus	0.18	33	14.5	1.750	54.3	24,250	SA
Cavia porcellus	0.086	46.5	8	4.250	19.5	406	T
Chinchilla lanigera	0.05	32.5	4	3.000	18.5	490	T
Meriones unguiculatus	0.07	58	8.5	3.250	12.1	50	T
Microtus arvalis	1.95	59	11	2.300	8.5	27	T

Mus musculus	2.3	92	16	2.000	6.9	10	T
Dipodomys merriami melanurus	0.05	52	8.5	3.250	9.83	50	T
Bos taurus	0.023	35	8	3.500	38	500,000	T
Canis familiaris	0.067	45	8	3.250	24	13,850	T
Elephas maximus	0.017	10.5	1	2.250	60	4000000	T
Felis catus	0.045	64	8	3.000	22.5	2,500	T
Homo sapiens	0.031	17.6	4	2.500	34.63	75,000	T
Oryctolagus cuniculus	0.096	49	8.5	2.500	15.25	2,000	T
Ovis aries musimon	0.1	30	9	2.250	35	33750	T
Rattus norvegicus	0.53	68	24	2.250	10.2	325	T
Rattus rattus	0.2	76	24	2.125	12.1	200	T
Saimiri sciureus collinsi	0.1	43	8	2.250	15.4	759	T
Spalacopus cyanus	0.25	20	1.425	3.500	11.68	90	S
Spalax ehrenbergi	0.05	5.9	1	4.000	12.6	143	S
Trichechus manatus	0.41	45	17	1.750	35	400000	A
Megaptera novaeangliae	0.02	8	2.06	2.500	54	48,350,000	A
Balaena mysticetus	0.02	5	0.3	2.250	61.3	105,000,000	A
Balaenoptera acutorostrata	0.06	7.5	0.15	2.250	55	8,044,000	A
Delphinapterus leucas	2	130	55	2.000	42	1,400,000	A
Tursiops truncatus	8	152	45	2.250	40.83	182,438	A
Stenella attenuata	0.5	160	64	2.500	36.95	103,050	A
Phocoena phocoena	16	180	120	1.500	25.97	337,500	A
Grampus griseus	4	150	56.25	2.500	40.75	468,750	A
Inia geoffrensis	1	105	82.5	1.500	38	128,250	A
Physeter catodon	2.5	40	12.5	1.750	54	27,500,000	A
Lagenorhynchus albirostris	18	181	57	2.500	34.95	127,350	A
Delphinus delphis	12	128	64	1.750	34.9	70,000	A

Table C9 Multiple regression analyses of minimum, maximum and peak-energy call frequency parameters versus body mass, basilar membrane length and number of cochlear turns. Coefficients and significance values, in brackets, are given for each variable.

a) Without correcting for phylogenetic relatedness

	Call frequency:		
	Min.	Max.	Peak
AIC	-19.16	-25.46	-13.11
RSE	0.19 (56 DF)	0.19 (56 DF)	0.20 (56 DF)
Mult. R^2	0.46	0.34	0.40
Adj. R^2	0.41	0.27	0.34
F	8.03 (6, 56 DF)	4.84 (6, 56 DF)	6.27 (6, 56 DF)
Overall *P*	2.85×10^{-6}	5.00×10^{-4}	4.37×10^{-5}
P(Intercept)	2.47 (6.49×10^{-13})	2.84 (6.04×10^{-16})	2.60 (5.33×10^{-13})
P(log body mass$^{0.33}$)	-0.70 (0.0001)	-0.30 (0.11)	-0.64 (0.003)
P(log basilar memb.)	-0.68 (0.01)	-0.80 (0.002)	-0.57 (0.04)
P(Turns 2)	0.06 (0.52)	-0.11 (0.24)	-0.12 (0.24)
P(Turns 3)	0.29 (0.01)	0.09 (0.37)	0.15 (0.18)
P(Turns 4)	0.34 (0.01)	0.09 (0.46)	0.09 (0.50)
P(Turns 5)	0.58 (0.02)	0.28 (0.24)	0.28 (0.29)

b) Correcting for phylogenetic relatedness

		Model and parameters	DIC
Min.	1	log min. = -0.97 log body mass$^{0.33}$ + 2.01	-
			65.23
		(animal) = 0.034, (units) = 0.013 p(Intercept) <0.0004x10^{-4}, p(log body mass$^{0.33}$) <0.0004x10^{-4}	
	2	log min. = -0.61 log membrane + 2.28	-
			66.68
		(animal) = 0.049, (units) = 0.012, p(Intercept)< 0.0004x10^{-4}, p(log membrane) = 0.003	
	3	log min. = -0.25 log membrane -0.84 log body mass$^{0.33}$ + 2.23	-
			67.67
		(animal) = 0.035, (units) = 0.012, p(Intercept)< 0.0004x10^{-4}, p(log body mass$^{0.33}$)< 0.0004x10^{-4}, p(log membrane) = 0.229	
	4	log min. = -0.62 log membrane -0.70 log body mass$^{0.33}$ + N^{o} turns + 2.43	-
			81.26
		(animal) = 0.033, (units) = 0.009, p(Intercept)< 0.0004x10^{-4}, p(log body mass$^{0.33}$) = 0.001, p(log membrane) = 0.007 p(N^{o} turns) = 0.334, 0.06, 0.039, 0.002, N^{o} turns = 0.101, 0.218, 0.297, 0.591,	
Max	1	log max. = -0.67 log body mass$^{0.33}$ + 2.09	-
			63.19
		(animal) = 0.041, (units) = 0.013, p(Intercept)< 0.0004x10^{-4}, p(log body mass$^{0.33}$) = 0.004,	
	2	log max. = -0.59 log membrane + 2.47	-
			58.93
		(animal) = 0.039, (units) = 0.015, p(Intercept)< 0.0004x10^{-4}, p(log membrane) = 0.003	
	3	log max. = -0.39 log membrane -0.47 log body mass$^{0.33}$ + 2.44	-
			63.22
		(animal) = 0.038, (units) = 0.013, p(Intercept)< 0.0004x10^{-4}, p(log body mass$^{0.33}$) =0.054, p(log membrane) = 0.087	
	4	log max. = -0.74 log membrane -0.37 log body mass$^{0.33}$ + N^{o} turns + 2.68	-
			85.76
		(animal) = 0.038, (units) = 0.009, p(Intercept)< 0.0004x10^{-4}, p(log body mass$^{0.33}$) = 0.102, p(log membrane) = 0.001 p(N^{o} turns) = 0.856, 0.146, 0.080, 0.008, N^{o} turns = 0.021, 0.171, 0.255, 0.552	
Peak	1	log Peak = -0.95 log body mass$^{0.33}$ + 2.11	-
			59.75
		(animal) = 0.043, (units) = 0.014, p(Intercept)< 0.0004x10^{-4}, p(log body mass$^{0.33}$)< 0.0004x10^{-4}	

2	log Peak = -0.62 log membrane + 2.40	-57.31
	(animal) = 0.054, (units) = 0.014, p(Intercept)< 0.0004x10^{-4}, p(log membrane) = 0.003	
3	log Peak = -0.28 log membrane -0.79 log body mass$^{0.33}$ + 2.35	-62.60
	(animal) = 0.044, (units) = 0.013, p(Intercept)< 0.0004x10^{-4}, p(log membrane) = 0.198, p(log body mass$^{0.33}$) = 0.002,	
4	log Peak = -0.61 log membrane -0.70 log body mass$^{0.33}$ + N^{o} turns + 2.63	-79.54
	(animal) = 0.042, (units) = 0.010, p(Intercept)< 0.0004x10^{-4}, p(log membrane) = 0.011, p(log body mass$^{0.33}$) = 0.006, p(N^{o} turns) = 0.750, 0.373, 0.207, 0.031, N^{o} turns = -0.035, 0.111, 0.190, 0.483,	

Figure C1 Hearing parameters. a) Old World fruit bats, b) laryngeally echolocating bats, c) Baleen whales, d) Toothed whales. 1 *Ornithorhynchus anatinus,* 2 *Didelphis virginiana*, 3 *Monodelphis domestica,* 4 *Elephas maximus,* 5 *Trichechus manatus,* 6 *Hapale jacchus,* 7 *Saimiri sciureus collinsi,* 8 *Homo sapiens,* 9 *Oryctolagus cuniculus,* 10 *Cavia porcellus,* 11 *Chinchilla lanigera,* 12 *Meriones unguiculatus,* 13 *Microtus arvalis,* 14 *Rattus norvegicus,* 15 *Rattus rattus,* 16 *Mus musculus,* 17 *Dipodomys merriami melanurus,* 18 *Spalacopus cyanus,* 19 *Spalax ehrenbergi,* 20 *Arvicola terrestris,* 21 *Bos taurus,* 22 *Ovis aries musimon,* 23 *Canis familiaris,* 24 *Procyon lotor,* 25 *Felis catus,* 26 *Zalophus californianus,* 27 *Phoca vitulina,* 28 *Equus caballus,* 29 *Rousettus aegyptiacus,* 30 *Pteropus pumilus,* 31 *Rousettus leschenaultia,* 32 *Rhinolophus ferrumequinum,* 33 *Rhinolophus rouxi*, 34 *Rhinopoma hardwickei,* 35 *Megaderma lyra,* 36 *Megaderma spasma,* 37 *Artibeus jamaicensis,* 38 *Carollia perspicillata,* 39 *Carollia perspicillata,* 40 *Desmodus rotundus,* 41 *Trachops cirrhosus,* 42 *Tadarida brasiliensis,* 43 *Taphozous melanopogon,* 44 *Lasiurus cinereus,* 45 *Myotis lucifugus,* 46 *Plecotus auritus,* 47 *Pteronotus parnellii,* 48 *Noctilio leporinus,* 49 *Balaena mysticetes,* 50 *Megaptera novaeangliae,* 51 *Balaenoptera acutorostrata,* 52 *Eubalaena glacialis,* 53 *Delphinapterus leucas,* 54 *Delphinus delphis,* 55 *Grampus griseus,* 56 *Inia geoffrensis,* 57 *Lagenorhynchus albirostris,* 58 *Phocoena phocoena,* 59 *Physeter catodon,* 60 *Stenella attenuate,* 61 *Tursiops truncatus*

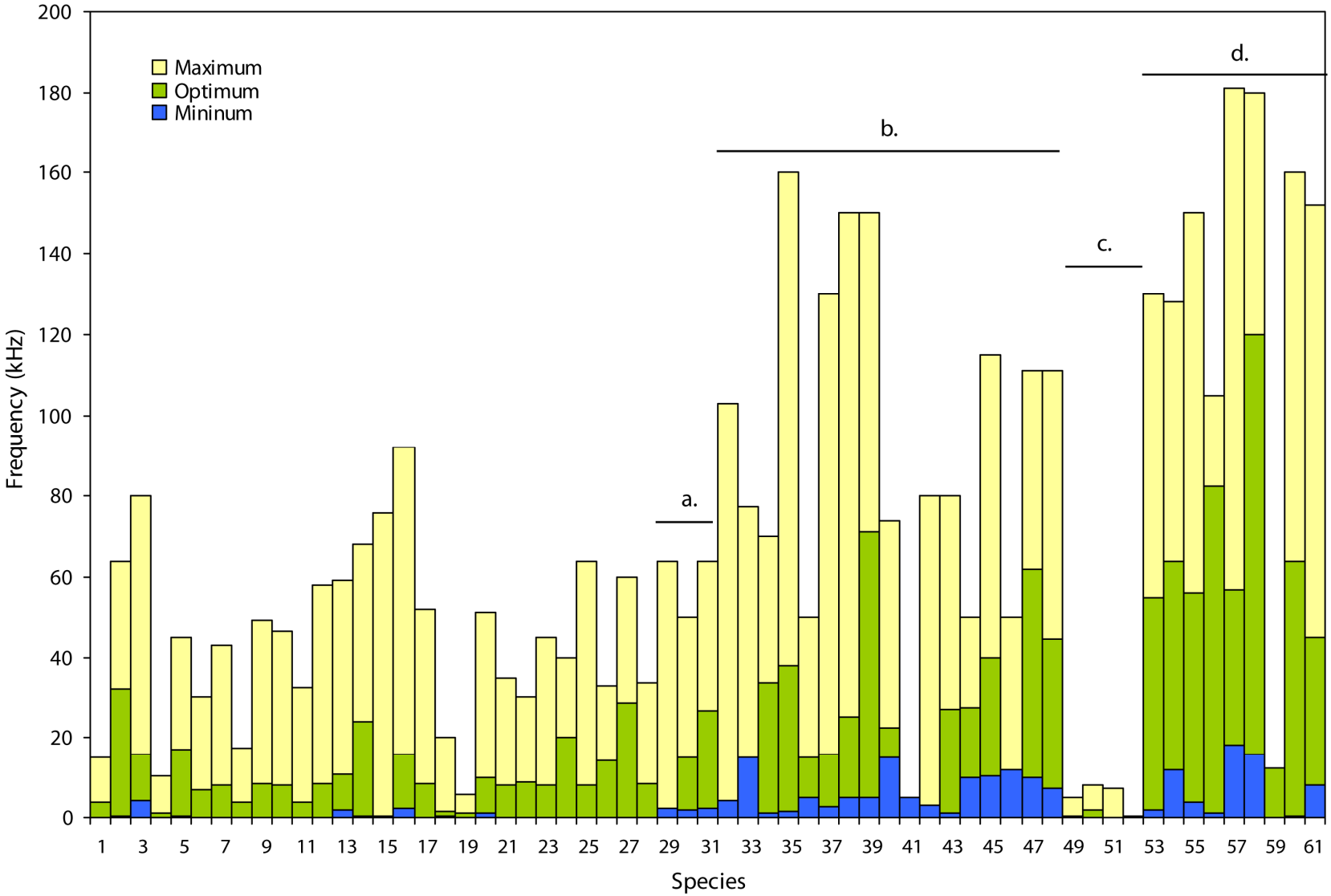
Maximum
Optimum
Mininum
Frequency (kHz)
Species
a.
b.
c.
d.
0
20
40
60
80
100
120
140
160
180
200
1
3
5
7
9
11
13
15
17
19
21
23
25
27
29
31
33
35
37
39
41
43
45
47
49
51
53
55
57
59
61

Appendix D

Table D1 Average bat semicircular radii of curvature (R), average cochlea size, angle between lateral and anterior semicircular canal and call emission categories used in this study. (Spoor *et al.,* 2007)[1]**,** (Cox and Jeffery 2010)[2].

		Semicircular canal R			Cochlear measure					
Specimen number:	Species	Posterior	Anterior	Lateral	Slant height	1st d	2nd d	Ave.	Angle (n)	Call emission
	Pteropus sp.	1.578	1.785	1.540	2.70	3.81	2.24	2.92	85.44 (1)	None
	Pteropus giganteus [1]	1.328	1.531	1.313	-	-	-	-	-	-
	Pteropus rodricensis [2]	1.170	1.400	1.030	-	-	-	-	75.19 (1)	None
HZM.1.3518	*Hypsignathus monstrosus*	1.198	1.478	1.263	2.29	3.04	1.83	2.39	101.49 (1)	None
HZM.107.11626	*Rousettus aegyptiacus*	1.120	1.313	1.065	2.52	2.66	1.67	2.28	76.51 (1)	None
HZM.16.36082	*Rousettus lanosus*	1.210	1.508	1.128	2.52	3.01	2.02	2.52	94.03 (1)	None
	Epomophorus gambianus[2]	1.280	1.290	1.080	-	-	-	-	-	-
HZM.F42600	*Rhinolophus marshallii*	0.758	0.815	0.938	3.44	4.09	2.71	3.41	76.02 (1)	Nasal
HZM.B035FBEN25	*Rhinolophus pearsonii*	0.783	0.840	0.936	3.20	4.11	2.93	3.41	74.79 (2)	Nasal
HZM.1435110	*Rhinolophus pearsonii*				2.29	4.16	2.70	3.05		
HZM.29.35223	*Rhinolophus affinis*	0.883	0.838	0.883	3.30	3.41	2.25	2.99	77.65 (1)	Nasal
MZB22897	*Rhinolophus philippinensis*	0.885	0.963	1.023	3.58	4.46	2.98	3.67	55.87 (1)	Nasal
MZB22913	*Rhinolophus philippinensis*	0.478	0.500	0.510	1.99	2.38	1.59	1.99	59.97 (1)	Nasal
MZB22910	*Rhinolophus philippinensis*	-	-	1.195	4.22	5.49	3.69	4.47	72.61 (1)	Nasal
NHM.1903.8.3.3	*Rhinolophus megaphyllus*	1.070	1.125	1.280	4.55	5.27	3.51	4.44	64.02 (1)	Nasal
HZM.58.20697	*Rhinolophus ferrumequinum*	0.763	0.793	0.813	2.89	3.59	2.36	2.95	78.36 (1)	Nasal
	Rhinolophus cornutus[1]	0.570	0.648	0.631	-	-	-	-	-	-
HZM.3.1164	*Hipposideros gigas*	1.015	1.140	1.058	3.59	4.30	3.28	3.72	81.63 (1)	Nasal
HZM.3.28778	*Hipposideros fulvus*	0.533	0.588	0.513	1.99	2.25	1.57	1.94	60.69 (1)	Nasal
NHM.1983.423	*Hipposideros ridleyi*	0.733	0.720	0.603	2.30	2.83	2.01	2.38	61.58 (1)	Nasal
HZM.13.4765	*Cleotis percivali*	0.363	0.390	0.363	1.91	1.90	1.61	1.81	66.86 (2)	Nasal
NHM.1968.453	*Rhinopoma microphyllum*	0.863	0.998	0.875	2.11	2.69	1.76	2.19	80.09 (1)	Nasal
HZM.37.9152	*Rhinopoma hardwickii*	0.825	0.955	0.873	2.45	2.37	1.90	2.24	78.31 (1)	Nasal
NHM.1975.2453	*Cardioderma cor*	1.235	1.540	1.288	3.12	3.49	2.32	2.98	61.48 (1)	Nasal
NHM.1892.5.20.2	*Macroderma gigas*	0.510	0.608	0.570	1.18	1.42	0.94	1.18	71.78 (1)	Nasal
NHM.1912.11.28.32	*Megaderma spasma*	0.675	0.785	0.688	1.86	2.01	1.35	1.74	81.24 (1)	Nasal
HZM.30.25025	*Lavia frons*	0.863	1.008	0.855	2.19	2.59	1.78	2.19	79.44 (1)	Nasal

HZM.1.34982	*Craseonycteris thonglongyai*	0.640	0.683	0.640	1.79	2.27	1.58	1.88	87.09 (1)	Oral
HZM.140.29127	*Carollia perspicillata*	0.683	0.783	0.650	2.05	2.11	1.37	1.84	75.03 (2)	Nasal
HZM.41.11631	*Desmodus rotundus*	1.008	1.150	0.840	2.33	2.46	1.83	2.21	66.95 (1)	Nasal
NHM.1954.322	*Tonatia silvicola*	0.788	0.923	0.800	2.71	2.78	1.69	2.39	78.37 (1)	Nasal
NHM.1924.3.1.33	*Trachops cirrhosus*	0.870	1.050	0.908	2.70	2.74	2.04	2.49	65.72 (1)	Nasal
HZM.1.13198	*Centurio senex*	0.635	0.753	0.605	2.12	2.39	1.60	2.04	75.61 (1)	Nasal
NHM.1907.1.1.684	*Artibeus jamaicensis*	0.768	0.905	0.848	2.61	2.77	1.88	2.42	75.28 (1)	Nasal
NHM.1914.5.21.4	*Anoura geoffroyi*	0.575	0.650	0.545	1.44	1.68	1.07	1.40	57.24 (1)	Nasal
NHM.1928.7.21.35	*Noctilio leporinus*	0.768	0.939	0.865	2.37	3.25	2.49	2.70	73.74 (2)	Oral
HZM.12.15977	*Noctilio leporinus*				2.99	3.37	2.55	2.97		
NA	*Thyroptera sp.*	0.540	0.685	0.653	2.00	2.79	1.78	2.19	88.16 (1)	Oral
HZM.61.28841	*Molossus molossus*	0.655	0.770	0.620	2.34	2.74	1.85	2.31	72.35 (1)	Oral
	Molossus molossus [2]	0.490	0.950	0.490	-	-	-	-	-	-
NHM.1844.10.17.7	*Cheiromeles torquatus*	1.698	2.003	1.738	5.07	5.58	3.94	4.86	71.57 (1)	Oral
NHM.1960.482	*Tadarida brasiliensis*	-	0.748	0.693	1.61	2.22	1.44	1.76	76.85 (1)	Oral
HZM.4.3341	*Lasiurus borealis*	0.645	0.760	0.658	1.92	2.20	1.58	1.90	68.33 (1)	Oral
HZM. T11	*Scotophilus kuhlii*	0.690	0.898	0.853	2.10	2.50	1.91	2.17	76.63 (1)	Oral
	Scotophilus robustus [2]	0.790	1.060	0.760	-	-	-	-	-	-
HZM.TD78	*Scotomanes ornatus*	0.778	0.938	0.768	1.95	2.50	1.92	2.12	74.83 (1)	Oral
NHM.7.7.7.3359	*Myotis lucifugus*	0.578	0.705	0.565	1.43	1.90	1.29	1.54	63.57 (1)	Oral
HZM.24454	*Myotis muricola*	0.583	0.738	0.578	2.08	2.60	1.65	2.11	76.08 (1)	Oral
	Myotis macrodactylus[1]	0.569	0.743	0.561	-	-	-	-	-	-
	Myotis lucifugus [1]	0.671	0.884	0.689	-	-	-	-	-	-
	Eptesicus fuscus[1]	0.670	0.865	0.770	-	-	-	-	-	-
SLC.0001.NMS	*Plecotus auritus*	0.732	0.911	0.673	1.83	2.15	1.44	1.81	79.76 (3)	Oral
SLC.0002.NMS	*Plecotus auritus*				1.79	2.07	1.39	1.75		
SLC.0003.NMS	*Plecotus auritus*				1.80	2.19	1.41	1.80		
HZM.0001-A1	*Murina tubinaris*	0.615	0.920	0.635	2.21	2.52	1.80	2.18	70.54 (1)	Oral
NHM.16.3.25.29	*Murina cyclotis*	0.670	-	0.632	1.78	2.19	1.49	1.82	75.80 (1)	Oral
NHM.18.79.11.15.16	*Murina suilla*	0.623	0.748	0.645	1.86	2.18	1.62	1.89	74.18 (1)	Oral
	Nyctalus lasiopterus aviator r[1]	0.854	1.008	0.985	-	-	-	-	-	-
P.PIP.001.DO	*Pipistrellus pipistrellus*	0.561	0.679	0.573	1.56	1.83	1.41	1.60		
P.PIP.005.DO	*Pipistrellus pipistrellus*				1.46	1.92	1.40	1.59		
P.PIP.002.STC	*Pipistrellus pipistrellus*				1.50	1.89	1.36	1.58		
P.PIP.004.STC	*Pipistrellus pipistrellus*				1.63	1.87	1.56	1.69	66.34 (4)	Oral

	Pipistrellus pipistrellus [1]	0.625	0.875	0.594	-	-	-	-	-	-
NHM.62.1443	*Miniopterus schreibersii*	0.733	0.841	0.728	1.61	2.38	1.59	1.86	70.91 (2)	Oral
HZM.247.22505	*Miniopterus schreibersii*				1.67	2.42	1.64	1.91		
HZM.214.35929	*Nycteris thebaica*	0.643	0.798	0.698	1.93	2.29	1.47	1.90	66.03 (1)	Nasal
HZM.18.30235	*Taphozous melanopogon*	0.853	1.003	0.903	2.30	2.75	1.80	2.28	70.50 (1)	Oral
HZM.2.18450	*Taphozous peli*	1.075	1.208	1.068	3.05	3.62	2.35	3.01	76.65 (1)	Oral
HZM.8.16002	*Saccopteryx bilineata*	0.593	0.710	0.628	2.02	2.68	1.73	2.14	78.20 (1)	Oral
HZM.34.5860	*Rhynchonycteris naso*	0.528	0.608	0.530	1.77	1.96	1.50	1.74	65.71 (1)	Oral
HZM.3.18512	*Pteropteryx macrotis*	0.648	0.728	0.680	1.91	2.48	1.50	1.96	90.30 (1)	Oral
NHM.65.3990	*Pteronotus macleayii grisea*	0.633	0.788	0.643	2.01	2.17	1.57	1.92	73.64 (1)	Oral
HZM.5.21236	*Pteronotus parnellii*	0.778	0.984	0.905	3.16	3.96	2.04	3.05	79.47 (2)	Oral
	Pteronotus parnellii				2.98	3.72	2.01	2.90		
HZM.8.16031	*Pteronotus davyii*	0.600	0.688	0.610	1.83	2.24	1.47	1.85	80.05 (1)	Oral
HZM.2.16030	*Mormoops megaphylla*	0.700	0.908	0.713	1.88	2.24	1.67	1.93	71.17 (1)	Oral
HZM.8.7055	*Natalus stramineus saturates*	0.526	0.753	0.611	1.68	2.11	1.42	1.74	74.83 (1)	Oral

Table D2 Body mass and wing morphology parameters used in this study. * denotes substitute species.

Species	Body mass (g)		WAR		WL		WTS index		Wingspan		Wing area		Comments:
Pteropodidae													
Pteropus rodricensis	338	1	6.3	1	46.6	1	1.01	1	0.67	1	0.0710	1	
Pteropus sp.	1175*	9	5.3*	2	20.3*	2	1.24**	3	1.25*	3	0.168*	2	*P. giganteus, **P. vampyrus
Pteropus giganteus	1175	9	5.3	2	20.3	2	1.24*	3	1.25	3	0.168	2	*P. vampyrus
Rousettus lanosus	140	3	5.9*	3	24.6*	3	1.45*	3	0.572*	3	0.0558*	3	*R. aegyptiacus
Rousettus aegyptiacus	140	3	5.9	3	24.6	3	1.45	3	0.572	3	0.0558	3	
Hypsignathus monstrous	427	3	6.7	3	36.3	3	1.76	3	0.882	3	0.115	3	
Epomophorus gambianus	158	3	5.9	3	27.0	3	-	-	0.584	3	0.0575	3	
Rhinolophidae													
Rhinolophus philippinensis (Small)	6.5	4	6.7	5	4.6	5	3.34	5	0.303	5	0.014	5	
Rhinolophus philippinensis (Medium)	7	4	6.7	5	4.6	5	3.34	5	0.303	5	0.014	5	
Rhinolophus philippinensis (Large)	12	4	9.0	5	7.9	5	2.53	5	0.366	5	0.015	5	
Rhinolophus ferrumequinum	22.6	3	6.1	3	12.2	3	2.13	3	0.332	3	0.0182	3	
Rhinolophus megaphyllus	9.8	3	6.1	3	7.4	3	2.15	3	0.281	3	0.013	3	
Rhinolophus pearsonii	8.8	7	4.4	13	9.4	13	4.17	13	0.200	13	0.009	13	
Rhinolophus marshalli	6.4	27	6.4	13	12.4	13	3.16*	23	0.23	13	0.008	13	* R. macrotis
Rhinolophus affinis	12.6	7	8.1	9	8.6	22	1.27	22	0.312	22	0.012	22	
Rhinolophus cornutus	6.1	9	5.2	6	13.9	13	1.63	13	0.16	13	0.004	13	
Hipposideridae													
Hipposideros ridleyi	9.3	10	6.0	10	6.1	10	2.25	10	0.2997	10	0.015	10	
Hipposideros fulvus	8.5	12	5.5	13	14.1	13	1.80	13	0.1800	13	0.0059	13	
Hipposideros gigas	89	3	7.7*	3	15.7*	3	3.1*	26	0.654*	3	0.0556*	3	*H. commersoni
Cleotis percivali	4.0	30	4.8	13	11.2	13	1.01	13	0.13	13	0.004	13	
Rhinopomatidae													
Rhinopoma microphyllum	32	3	8.0	3	20.5	3	1.24	3	0.35	3	0.0153	3	
Rhinopoma hardwickii	16.3	3	6.9	3	14.0	3	2.56	3	0.28	3	0.0114	3	
Megadermatidae													
Macroderma gigas	123	3	6.1	3	16.8	3	0.83	3	0.66	3	0.0717	3	
Cardioderma cor	28	11	5.7	11	9.6	3	1.7	11	0.328	3	0.058	29	
Megaderma spasma	27	10	5.0	3	7.8	10	1.83	3	0.344	3	0.0688	29	

Lavia frons	34.8	7	5.4	3	12.0	3	1.69	3	0.34	3	0.0213	3	
Craseonycteridae													
Craseonycteris thonglongyai	2.5	7t	7.1	3	5.2	3	1.14	3	0.16	3	0.0036	3	
Miniopteridae													
Miniopterus schreibersii	14.2	3	7.0	3	10.2	3	1.03	3	0.309	3	0.0137	3	
Vespertilionidae													
Murina tubinaris	4.75	19	5.2	13	7.0	13	0.62	13	0.17	13	0.0056	13	
Murina suilla	3.9	10	6.0	10	5.1	10	1.607	10	0.2117	10	0.0075	10	
Murina cyclotis	11.3	10	6.0	10	7.5	10	1.337	10	0.2959	10	0.0147	10	
Myotis lucifugus	8.1	9	6.0	3	7.5	3	3.2	3	0.237	3	0.0093	3	
Myotis muricola	4.85	28	4.8	13	6.3	13	2.26*	3	0.19	13	0.0075	13	**M. mystacinus*
Myotis macrodactylus	6.5	9	6.3*	3	7*	3	2.05*	3	0.248*	3	0.0098*	3	**M. daubentonii*
Scotophilus kuhlii	34.5*	3	5.8	13	15.0*	3	-	-	0.339	3	0.0091	13	**S. heathii*
Scotophilus robustus	83	17	6.9	13	-	-	-	-	0.26	13	0.0108	13	
Scotomanes ornatus	21.8	17	5.9	13	21.8	13	-	-	0.24	13	0.0098	13	
Lasiurus borealis	16.7	3	6.7	3	14.0	3	1.26	3	0.281	3	0.0117	3	
Plecotus auritus	9	3	5.7	3	7.1	3	1.43	3	0.267	3	0.0124	3	
Pipistrellus pipistrellus	6.55	9	7.5	3	8.1	3	1.74	3	0.218	3	0.0063	3	
Eptesicus fuscus	18.79	9	6.4	3	9.4	3	1.09	3	0.325	3	0.0166	3	
Nyctalus lasiopterus aviator	34.8	9	7.2	14	19.7	14	0.99*	24	0.441	20	0.06125	29	**N. noctula*
Noctilionidae													
Noctilio leporinus	59	3	9.0	3	15.2	3	2.23	3	0.584	3	0.038	3	
Thyropteridae													
Thyroptera sp.	19.5	13	5.9*	3	4.1*	3	1.75*	3	0.211*	3	0.0075*	3	**T. discifera*
Mormoopidae													
Pteronotus macleayi grisea	5.35	15	7.6	15	4.6	15	-	-	0.289	29	0.011	29	
Pteronotus parnellii	14.7	16	6.7	16	7.9	16	1.54	3	0.349	29	0.0182	29	
Pteronotus davyi	10.9	3	8.3	3	8.0	3	1.36	3	0.334	3	0.0134	3	
Mormoops megaphylla	17	3	7.1	3	11.2	3	1.1	3	0.325	3	0.0149	3	
Phyllostomidae													
Artibeus jamaicensis	47	3	6.4	3	16.6	3	1.27*	3	0.42	3	0.0277	3	**A. lituratus*
Tonatia silvicola	32.85	18	5.0	25	15.7	25	-	-	0.320	29	0.0205	29	
Trachops cirrhosus	43.8	3	6.3	3	15.3	3	-	-	0.422	3	0.0281	3	
Desmodus rotundus	28.5	3	6.7	3	14.0	3	1.38	3	0.366	3	0.02	3	

Anoura geoffroyi	14.1	3	7.2	3	12.5	3	3	3	0.282	3	0.0111	3	
Carollia perspicillata perspicillata	19.1	3	6.1	3	11.4	3	2.22	3	0.316	3	0.0165	3	
Centurio senex	22	3	-	-	-	-	0.93	3	-	-	-	-	
Molossidae													
Cheiromeles torquatus	135.5	3	8.6*	3	35.7	3	-	-	0.330	29	0.0384	3	**Cheiromeles sp*
Molossus molossus	16.2	3	8.7	3	16.0	3	-	-	0.294	3	0.0099	3	
Tadarida brasiliensis	12.5	3	8.2	3	11.5	3	1.48	3	0.295	3	0.0106	3	
Nycteridae													
Nycteris thebaica	11	3	5.5	3	6.3	3	4.5	26	0.307	3	0.0171	3	
Natalidae													
Natalus stramineus saturates	3.9	3	5.8	3	3.9	3	2.83	3	0.24	3	0.0099	3	
Emballonuridae													
Taphozous peli	95	2	10.2*	13	69.5*	13	-	-	0.685	3	0.0134*	13	** T. saccolaimus*
Taphozous melanopogon	24	7	10.0	3	25.9	3	1.1*	26	0.385	3	0.0148	3	** T. mauritanus*
Peropteryx macrotis	4.4	21	6.8	13	10.1	13	0.78	13	0.17	13	0.004	13	
Saccopteryx bilineata	7.5	3	6.1	3	5.9	3	1.53	3	0.275	3	0.0125	3	
Rhynchonycteris naso	3.9	3	6.5	3	4.3	3	-	-	0.239	3	0.0088	3	

Sources:

1. A Walsh, (Lubee Bat Conservancy); 2. UM Norberg (1981); 3. UM Norberg, JMV Rayner (1987); 4. Body mass recorded by SJ Rossiter, T Kingston; 5. Calculated from wing traces; 6. KJ Olival (Submitted); 7. Body mass recorded by HZM; 8. T Kingston (2000); 9. F Spoor *et al*. (2007); 10. MJ Struebig (2005); 11. R Csada (1996); 12. AT Smith and Y Xie (2008); 13. Calculated from specimen; 14. A. Thabah *et al*. (2007); 15. CA Mancina (2005); 16. J Rydell *et al.* (2002); 17. PG Cox and N Jeffery (2010); 18. RA Medellin and HT Arita (1989); 19. MJ Struebig *et al*. (2005); 20. N Yigit *et al.* (2008); 21. DA Yee (2000); 22. MJ Struebig (Unpublished data); 23. KP Sun *et al*. (2008)**;** 24. M Thollesson & UM Norberg (1991); 25. UM Norberg and MB Fenton (1988); 26. HDJN Aldridge and IL Rautenbach (1987); 27. LB Zhang *et al.* (2009); 28. AV Borisenko and SV Kruskop (2003); 29. Estimated from several sources; 30. Sources within (Barclay and Brigham 1991).

Table D3 Fossil calibration points used for construction of the dated phylogenies used in this study.

Fossil Constraint	Approx. age: (million years)	Source:
Placental mammals	131.0	(Benton and Donoghue 2007)
Carnivores	57.5	(Benton and Donoghue 2007)
Primates	58.5	(Gingerich 1984)
Artiodactyla	60.0	(Gatesy and O'Leary 2001)
Leporidae	53.0	(Rose *et al.,* 2008)
Dermoptera	35.5	(Ducrocq *et al.,* 1992)
Base of Felidae	16.0	(Johnson *et al.,* 2006)
Split of Lorisidae and Galagidae	41.2–36.9	(Seiffert *et al.,* 2003)
Split of *Mus* and *Rattus*	12.0 - 14.0	References within (Chevret *et al.,* 2005)
Oldest bat	52.5	(Simmons *et al.,* 2008)
Maximum for base of Rhinolophoidea	55.0	(Teeling *et al.,* 2005)
Minimum for base of Emballonuridae	37.0	(Teeling *et al.,* 2005)
Minimum for base of Rhinolophidae	37.0	(Teeling *et al.,* 2005)
Minimum for split of Mormoopidae and Phyllostomidae	30.0	(Teeling *et al.,* 2005)
Maximum for base of Phyllostomidae	34.0	(Teeling *et al.,* 2005)
Minimum for split of Vespertilionidae and Molossidae	37.0	(Teeling *et al.,* 2005)

Table D4 Prior testing.

i) G=list(G1 = list(V=matrix(SCC.var/2), n=1)), R= list(V=matrix(SCC.var/2), n=1)
ii) G=list(G1 = list(V=matrix(SCC.var*0.95), n=1)), R=list(V=matrix(SCC.var*0.05), n=1)
iii) G=list(G1 = list(V=matrix(SCC.var/2), n=1)), R=list(V=matrix(SCC.var/2), n=1)
iv) G=list(G1 = list(V=matrix(SCC.var/2), n=10)), R=list(V=matrix(SCC.var/2), n=10)

Prior	Variance	Belief	DIC	Equation	Animal	Residual
i	50:50	1	-592.3	log Y = 0.44 X - 0.29	0.0052	0.0034
ii	95:5	1	-597.2	log Y = 0.44 X - 0.29	0.0061	0.0031
iii	50:50	1	-589.7	log Y = 0.44 X - 0.29	0.0050	0.0035
iv	50:50	10	-565.9	log Y = 0.44 X - 0.29	0.0074	0.0044

Table D5 Repeated anterior semicircular canal radius of curvature measures; mean values, standard deviation and minimum minus maximum difference expressed as a percentage of the mean were calculated.

a) Degree of error in repeated measures.

Specimen code	Species	Mean ± SD	Min - Max	% diff. of mean
Pteropus_sp	*Pteropus sp.*	1.81 ± 0.03	1.785 - 1.833	2.63
HZM.16.36082	*Rousettus lanosus*	1.51 ± 0.00	1.503 - 1.508	0.33
HZM.107.11626	*Rousettus aegyptiacus*	1.30 ± 0.02	1.283 - 1.313	2.31
HZM.1.3518	*Hypsignathus monstrosus*	1.46 ± 0.02	1.450 - 1.478	1.88
HZM.58.20697	*Rhinolophus ferrumequinum*	0.80 ± 0.00	0.793 - 0.798	0.63
MZB22897	*Rhinolophus philippinensis*	0.94 ± 0.03	0.925 - 0.963	3.97
MZB22913	*Rhinolophus philippinensis*	0.50 ± 0.00	0.500 - 0.503	0.50
NHM.1903.8.3.3	*Rhinolophus megaphyllus*	1.13 ± 0.00	1.125 - 1.125	0.00
HZM.1435110_L	*Rhinolophus pearsonii*	0.84 ± 0.00	0.838 - 0.843	0.60
HZM.1435110_R	*Rhinolophus pearsonii*	0.84 ± 0.00	0.838 - 0.843	0.60
HZM.B035FBEN25	*Rhinolophus pearsonii*	0.79 ± 0.02	0.775 - 0.808	4.11
HZM.F42600	*Rhinolophus marshallii*	0.82 ± 0.01	0.815 - 0.828	1.52
HZM.29.35223	*Rhinolophus affinis*	0.85 ± 0.01	0.838 - 0.858	2.36
NHM.1983.423	*Hipposideros ridleyi*	0.72 ± 0.01	0.720 - 0.728	1.04
HZM.13.4765	*Cleotis percivali*	0.39 ± 0.00	0.390 - 0.395	1.27
HZM.3.28778	*Hipposideros fulvus*	0.59 ± 0.01	0.588 - 0.598	1.69
HZM.3.1164	*Hipposideros gigas*	1.13 ± 0.01	1.125 - 1.140	1.32
NHM.1968.453	*Rhinopoma microphyllum*	0.99 ± 0.01	0.990 - 0.998	0.75
HZM.37.9152	*Rhinopoma hardwickii*	0.96 ± 0.00	0.955 - 0.958	0.26
NHM.1892.5.20.2	*Macroderma gigas*	0.61 ± 0.00	0.608 - 0.613	0.82
NHM.1975.2453	*Cardioderma cor*	1.53 ± 0.01	1.523 - 1.540	1.14
NHM.1912.11.28.32	*Megaderma spasma*	0.78 ± 0.00	0.783 - 0.785	0.32
HZM.30.25025	*Lavia frons*	1.00 ± 0.01	0.995 - 1.008	1.25
HZM.1.34982	*Craseonycteris thonglongyai*	0.66 ± 0.03	0.638 - 0.683	6.82
NHM.7.7.7.3359	*Myotis lucifugus*	0.70 ± 0.01	0.698 - 0.705	1.07
NHM.62.1443	*Miniopterus schreibersii*	0.82 ± 0.02	0.803 - 0.830	3.37
HZM.247.22505	*Miniopterus schreibersii*	0.86 ± 0.01	0.853 - 0.860	0.88
HZM.0001-A1	*Murina tubinaris*	0.94 ± 0.02	0.920 - 0.955	3.73
HZM. T11	*Scotophilus kuhlii*	0.90 ± 0.01	0.898 - 0.905	0.83
NHM.18.79.11.15.16	*Murina suilla*	0.75 ± 0.00	0.748 - 0.753	0.67
HZM.TD78	*Scotomanes ornatus*	0.95 ± 0.01	0.938 - 0.953	1.59
HZM.24454	*Myotis muricola*	0.74 ± 0.01	0.738 - 0.748	1.35
HZM.4.3341	*Lasiurus borealis*	0.75 ± 0.02	0.733 - 0.760	3.69
SLC.0001.NMS	*Plecotus auritus*	0.94 ± 0.01	0.933 - 0.953	2.12
SLC.0002.NMS	*Plecotus auritus*	0.87 ± 0.01	0.865 - 0.875	1.15
SLC.0003.NMS	*Plecotus auritus*	0.91 ± 0.00	0.905 - 0.905	0.00
P.PIP.001.DO	*Pipistrellus pipistrellus*	0.66 ± 0.02	0.645 - 0.670	3.80
P.PIP.005.DO	*Pipistrellus pipistrellus*	0.67 ± 0.00	0.673 - 0.675	0.37
P.PIP.002.STC	*Pipistrellus pipistrellus*	0.67 ± 0.01	0.665 - 0.673	1.12
P.PIP.004.STC	*Pipistrellus pipistrellus*	0.70 ± 0.01	0.698 - 0.705	1.07
NHM.1928.7.21.35	*Noctilio leporinus*	0.90 ± 0.04	0.870 - 0.923	5.86
HZM.12.15977	*Noctilio leporinus*	0.92 ± 0.05	0.890 - 0.955	7.05
NHM.65.3990	*Pteronotus macleayii grisea*	0.76 ± 0.03	0.740 - 0.788	6.22
HZM.5.21236_L	*Pteronotus parnellii*	0.97 ± 0.03	0.945 - 0.988	4.40
HZM.5.21236_R	*Pteronotus parnellii*	0.97 ± 0.02	0.955 - 0.980	2.58
HZM.8.16031	*Pteronotus davyii*	0.67 ± 0.03	0.645 - 0.688	6.38

HZM.2.16030	*Mormoops megaphylla*	0.91 ± 0.00	0.903 - 0.908	0.55
NHM.1907.1.1.684	*Artibeus jamaicensis*	0.89 ± 0.02	0.878 - 0.905	3.09
NHM.1954.322	*Tonatia silvicola*	0.89 ± 0.05	0.855 - 0.923	7.59
NHM.1924.3.1.33	*Trachops cirrhosus*	1.02 ± 0.04	0.990 - 1.050	5.88
HZM.41.11631	*Desmodus rotundus*	1.12 ± 0.04	1.093 - 1.150	5.13
NHM.1914.5.21.4	*Anoura geoffroyi*	0.65 ± 0.00	0.648 - 0.650	0.39
HZM.140.29127_R	*Carolia perspicillata*	0.76 ± 0.03	0.745 - 0.783	4.91
HZM.140.29127_L	*Carolia perspicillata*	0.76 ± 0.00	0.755 - 0.760	0.66
HZM.1.13198	*Centurio senex*	0.73 ± 0.03	0.713 - 0.753	5.46
NHM.1844.10.17.7	*Cheiromeles torquatus*	1.97 ± 0.05	1.935 - 2.003	3.43
HZM.61.28841	*Molossus molossus*	0.75 ± 0.03	0.723 - 0.770	6.37
NHM.1960.482	*Tadarida brasiliensis*	0.75 ± 0.00	0.748 - 0.750	0.33
HZM.214.35929	*Nycteris thebaica*	0.76 ± 0.05	0.730 - 0.798	8.84
HZM.8.7055_R	*Natalus stramineus saturates*	0.75 ± 0.00	0.748 - 0.753	0.67
HZM.3.18512	*Pteropteryx macrotis*	0.73 ± 0.01	0.728 - 0.735	1.03
HZM.18.30235	*Taphozous melanopogon*	0.97 ± 0.05	0.933 - 1.003	7.24
HZM.2.18450	*Taphozous peli*	1.18 ± 0.05	1.143 - 1.208	5.53
HZM.8.16002	*Saccopteryx bilineata*	0.69 ± 0.04	0.660 - 0.710	7.30
HZM.34.5860	*Rhynchonycteris naso*	0.61 ± 0.01	0.608 - 0.620	2.04
ID.BAM.THO1	*Thyroptera sp.*	0.67 ± 0.02	0.650 - 0.685	5.24

b) Individual and intra-specific deviation in radius of curvature measured for the anterior semicircular canal.

Specimen code	Species	Mean R ± SD	Min – Max (n)
HZM.1435110	*Rhinolophus pearsonii*	0.840 ± 0.004	0.838 - 0.843 (2)
HZM.5.21236	*Pteronotus parnellii*	0.984 ± 0.001	0.980 - 0.988 (2)
HZM.140.29127	*Carollia perspicillata*	0.771 ± 0.004	0.760 - 0.783 (2)
N/A	*Rhinolophus pearsonii*	0.778 ± 0.084	0.718 - 0.838 (2)
N/A	*Miniopteris schreibersii*	0.841 ± 0.02	0.830 - 0.853 (2)
N/A	*Plecotus auritus*	0.911 ± 0.05	0.875 - 0.953 (3)
N/A	*Pipistrellus pipistrellus*	0.679 ± 0.02	0.670 - 0.705 (4)
N/A	*Noctilio leporinus*	0.939 ± 0.02	0.923 - 0.955 (2)

Table D6 Model comparison and selection based on AIC values. Significance levels: p = 0 < *** < 0.001 < ** < 0.01 < * < 0.05

Linear: log Semicircular canal R = a[log(Body mass^{033})] + c							
	a	c	R	R^2	Adj. R^2	SEE	AIC
Anterior OLS	0.42	-0.16		0.74	0.74	0.08	-333.30
Anterior RMA	0.49	-0.23	0.86	0.74			
Lateral OLS	0.44	-0.27		0.74	0.74	0.08	-323.94
Lateral RMA	0.51	-0.34	0.86	0.74			
Posterior OLS	0.46	-0.24		0.80	0.80	0.07	-366.85
Posterior RMA	0.51	-0.30	0.90	0.80			

Polynomial: log Semicircular canal R = Y_0 + a[log(Body mass^{033})] + b[log(Body mass^{033})^2]								
	a	b	Y_0	R	R^2	Adj. R^2	SEE	AIC
Anterior	0.91	-0.25	-0.37	0.88	0.78	0.77	0.08	-356.02
Lateral	1.03	-0.30	-0.53	0.89	0.80	0.79	0.08	-357.10
Posterior	0.87	-0.21	-0.43	0.91	0.83	0.83	0.07	-387.46

Hyperbola: log Semicircular canal R = Y_0 + a[log(Body mass^{033})] / [b+log(Body mass^{033})]								
	a	b	Y_0	R	R^2	Adj. R^2	SEE	AIC
Anterior	1.56	1.08	-0.46	0.88	0.78	0.77	0.08	-354.77
Lateral	1.61	0.82	-0.68	0.89	0.80	0.79	0.08	-356.33
Posterior	1.80	1.53	-0.48	0.91	0.83	0.83	0.07	-385.99

log Semicircular canal R = log Body mass^{033} + Size Category 1								
	a_1	c_1	a_2	c_2	R^2	Adj. R^2	RSE	AIC
Anterior	0.33***	-0.15	0.33***	-0.05	0.77	0.77	0.08	-351.52
Lateral	0.36***	-0.26***	0.36***	-0.16***	0.77	0.77	0.08	-338.37
Posterior	0.38***	-0.24***	0.38***	-0.15***	0.82	0.82	0.07	-380.58
log Semicircular canal R = log Body mass^{033} * Size Category 1								
	a1	c1	a2	c2	R2	Adj. R2	RSE	AIC
Anterior	0.58**	-0.29***	0.31***	-0.02	0.78	0.78	0.075	-356.18
Lateral	0.78***	-0.43***	0.32***	-0.13***	0.79	0.79	0.076	-354.28
Posterior	0.62***	-0.37***	0.36**	-0.13***	0.83	0.83	0.068	-385.73

log(Semicircular canal R) = log(Body mass033) + Size Category 2.								
	a1	c1	a2	c2	R2	Adj. R2	RSE	AIC
Anterior	0.34***	-0.20***	0.34***	-0.06*	0.79	0.79	0.07	-364.63
Lateral	0.34***	-0.32***	0.34***	-0.14***	0.81	0.81	0.07	-369.96
Posterior	0.38***	-0.28***	0.38***	-0.15***	0.85	0.84	0.07	-402.45
log(Semicircular canal R) = log(Body mass033) * Size Category 2.								
	a1	c1	a2	c2	R2	Adj. R2	RSE	AIC
Anterior	0.39	-0.22*	0.34***	-0.05*	0.79	0.79	0.07	-362.82
Lateral	0.52***	-0.40	0.33***	-0.14***	0.82	0.81	0.07	-370.29
Posterior	0.39	-0.29*	0.37***	-0.15***	0.85	0.08	0.07	-400.47

Figure D1 Standard diagnostic plots exploring variance in semicircular canal size and body mass within a of 156 non-bat species (Spoor *et al.,* 2002; Spoor *et al.,* 2007; Cox and Jeffery 2010). Plots revealed that the data was left-skewed and not strictly uni-modal and so simple linear models were rejected.

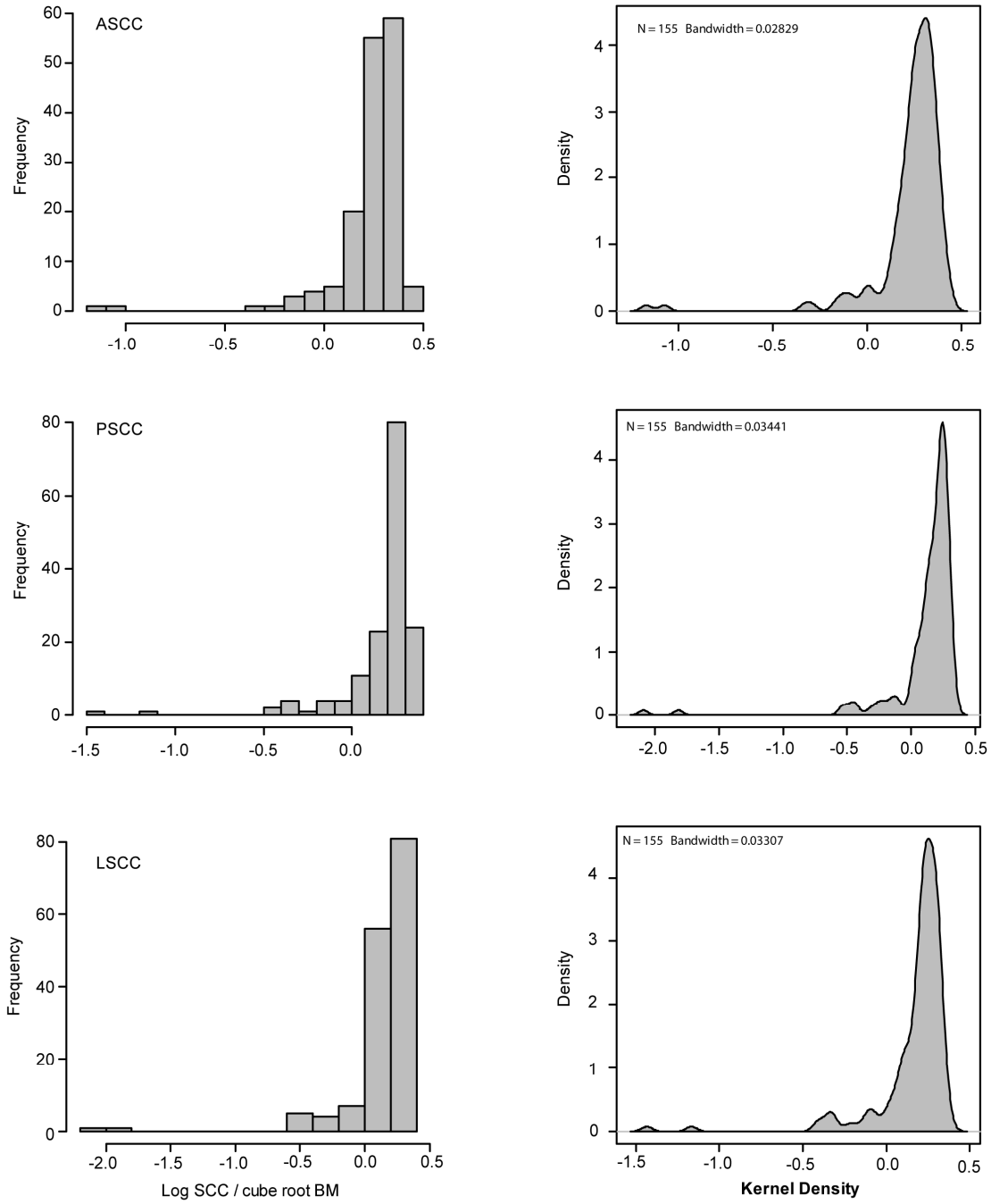

Figures D2 Plots of log_{10} semicircular canal size vs. log body mass$^{0.33}$ for 156 non-bat mammals, data are modelled using linear and non-linear methods. Non-linear models were favoured over simple linear models based on AIC values, however, they is a poor fit at the two extremes of the dataset, furthermore, these models are purely mathematical and there is no physiological basis to assume a non-linear relationship.

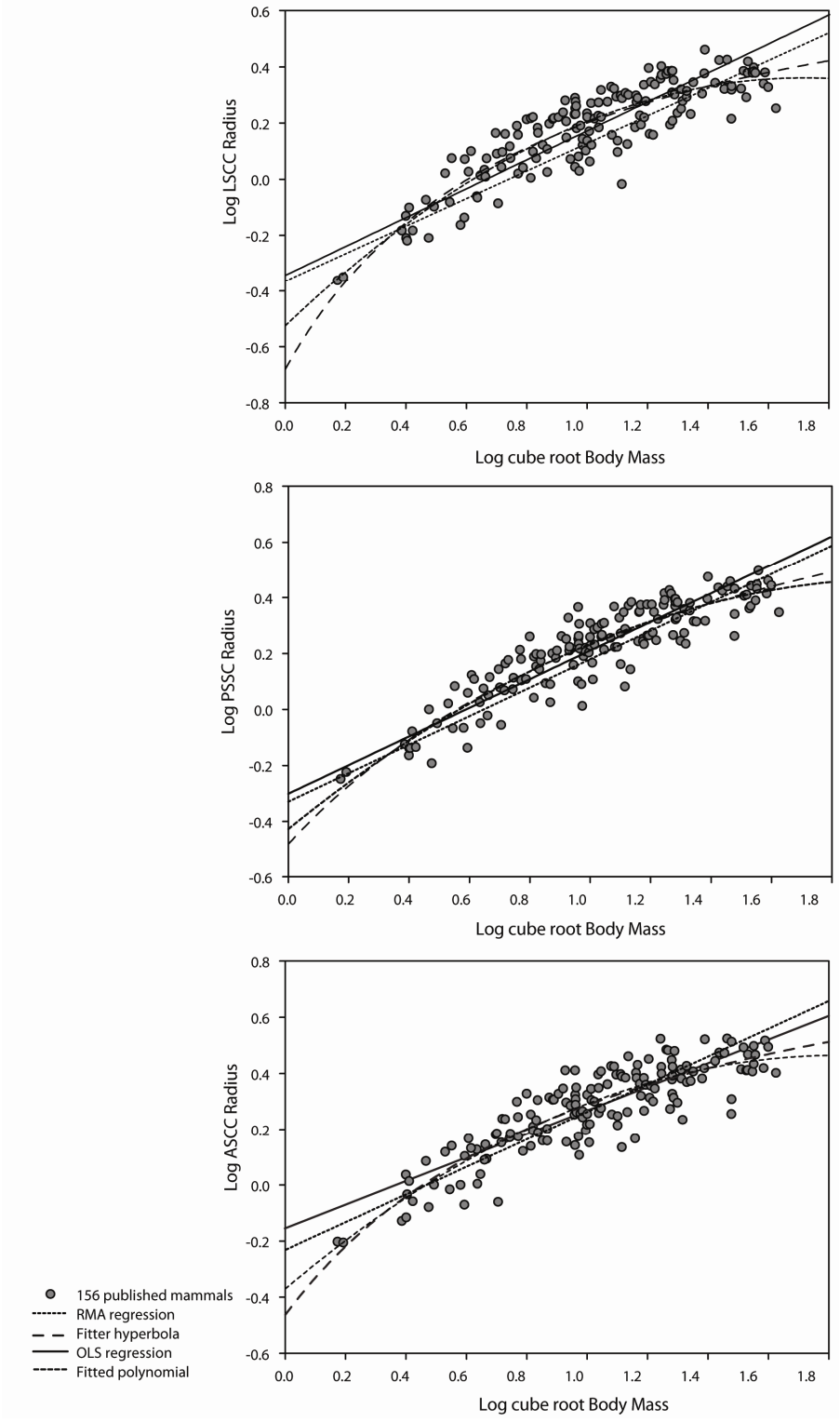

Figures D3 Plots of $\log_{10}$ semicircular canal size vs. log body mass$^{0.33}$ for 156 non-bat mammals, data are modelled using two discontinuous linear models. Firstly, one with a body mass cut-off of 130g and secondly, one that follows the natural grouping particularly evident in the lateral semicircular canal data. Lines with dash-dots and long dashes model the small size category, with and without an interaction; solid and dotted lines model the large category with and without an interaction respectively.

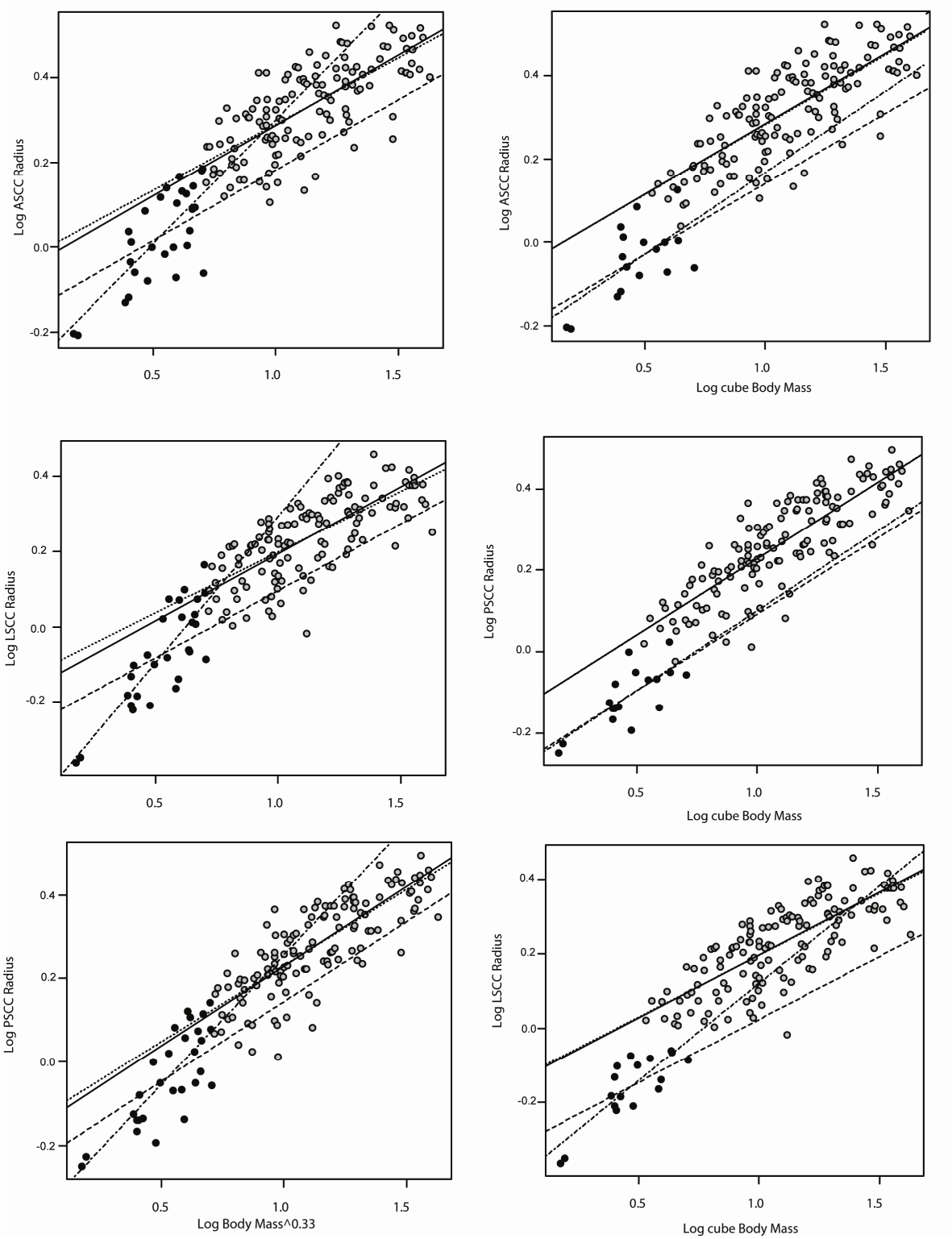

REFERENCES:

Aldridge HDJN, Rautenbach IL (1987). Morphology, echolocation and resource partitioning in insectivorous bats. *J. Anim. Ecol.* **56:** 763-778.

Barclay RMR, Brigham RM (1991). Prey detection, dietary niche breadth, and body size in bats - why are aerial insectivorous bats so small? *Am. Nat.* **137:** 693-703.

Benton MJ, Donoghue PCJ (2007). Paleontological evidence to date the tree of life. *Mol. Biol. Evol.* **24:** 26-53.

Borisenko A, Kruskop S (2003). *Bats of Vietnam and adjacent territories. An identification manual*. Geos.

Brinklov S, Kalko EKV, Surlykke A (2009). Intense echolocation calls from two 'whispering' bats, *Artibeus jamaicensis* and *Macrophyllum macrophyllum* (Phyllostomidae). *J. Exp. Biol.* **212:** 11-20.

Chevret P, Veyrunes F, Britton-Davidian J (2005). Molecular phylogeny of the genus *Mus* (Rodentia: Murinae) based on mitochondrial and nuclear data. *Biol. J. Linn. Soc.* **84:** 417-427.

Cox PG, Jeffery N (2010). Semicircular canals and agility: the influence of size and shape measures. *J. Anat.* **216:** 37-47.

Csada R (1996). *Cardioderma cor. Mamm. Species* **519:** 1-4.

Dietz C (2005). *Illustrated identification key to the bats of Eqypt*, Vol Version 1.0.

Ducrocq S, Buffetaut E, Buffetauttong H, Jaeger JJ, Jongkanjanasoontorn Y, Suteethorn V (1992). 1st fossil flying lemur - a Dermopteran from the Late Eocene of Thailand. *Palaeontology* **35:** 373-380.

Fernandez C, Schmidt RS (1963). Opossum ear and evolution of coiled cochlea. *J. Comp. Neurol.* **121:** 151-&.

Francis CM, Habersetzer J (1998). Interspecific and intraspecific variation in echolocation call frequency and morphology of horseshoe bats, *Rhinolophus* and *Hipposideros*. In: Kunz TH and Racey P (eds) *Bat Biology and Conservation* Smithsonian Institution Press: Washington and London.

Gatesy J, O'Leary MA (2001). Deciphering whale origins with molecules and fossils. *Trends Ecol. Evol.* **16:** 562-570.

Gingerich PD (1984). Primate evolution - evidence from the fossil record, comparative morphology, and molecular biology. *Yearb. Phys. Anthropol.* **27:** 57-72.

Holland RA, Waters DA, Rayner JMV (2004). Echolocation signal structure in the Megachiropteran bat *Rousettus aegyptiacus* Geoffroy 1810. *J. Exp. Biol.* **207:** 4361-4369.

Hooker SK, Whitehead H (2002). Click characteristics of northern bottlenose whales (*Hyperoodon ampullatus*). *Mar. Mamm. Sci.* **18:** 69-80.

Johnson WE, Eizirik E, Pecon-Slattery J, Murphy WJ, Antunes A, Teeling E *et al* (2006). The Late Miocene radiation of modern Felidae: A genetic assessment. *Science* **311:** 73-77.

Jones G, Rayner JMV (1989). Foraging behavior and echolocation of wild horseshoe bats *Rhinolophus ferrumequinum* and *Rhinolophus hipposideros* (Chiroptera, Rhinolophidae). *Behav. Ecol. Sociobiol.* **25:** 183-191.

Ketten DR (1994). Funtional analyses of whale ears - adaptations for underwater hearing. *Ocean 94 - Oceans Engineering for Today's Technology and Tomorrow's Preservation, Proceedings, Vol 1***:** A264-A270.

Ketten DR (1997). Structure and function in whale ears. *Bioacoustics* **8:** 103-135.

Ketten DR, Odell DK, Domning DP (1992). Structure, function, and adaptation of the manatee ear. In: Thomas JA, Kastelein RA and Supin AY (eds) *Marine Mammal Sensory Systems*. Plenum Press: New York, pp 77-95.

Kingston T, Jones G, Akbar Z, Kunz TH (1999). Echolocation signal design in Kerivoulinae and Murininae (Chiroptera: Vespertilionidae) from Malaysia. *J. Zool.* **249:** 359-374.
Kingston T, Jones G, Zubaid A, Kunz TH (2000). Resource partitioning in rhinolophoid bats revisited. *Oecologia* **124:** 332-342.
Kirk EC, Gosselin-Ildari AD (2009). Cochlear labyrinth volume and hearing abilities in primates. *Anat. Rec.* **292:** 765-776.
Kofoky AF, Randrianandrianina F, Russ J, Raharinantenaina I, Cardiff SG, Jenkins RKB *et al* (2009). Forest bats of Madagascar: results of acoustic surveys. *Acta Chiropt.* **11:** 375-392.
Mancina CA (2005). *Pteronotus macleayii*. *Mamm. Species* **778:** 1-3.
Manoussaki D, Chadwick RS, Ketten DR, Arruda J, Dimitriadis EK, O'Malley JT (2008). The influence of cochlear shape on low-frequency hearing. *Proc. Natl. Acad. Sci. U. S. A.* **105:** 6162-6166.
McGowen MR, Spaulding M, Gatesy J (2009). Divergence date estimation and a comprehensive molecular tree of extant cetaceans. *Mol. Phylogenet. Evol.* **53:** 891-906.
Melzer P (1985). A deoxyglucose study on auditory responses in the bat *Rhinolophus rouxi*. *Brain Res. Bull.* **15:** 677-681.
Mendellin RA, Arita HT (1989). *Tonatia evotis* and *Tonatia silvicola*. *Mamm. Species* **334:** 1-5.
Neuweiler G (1990). Auditory adaptations for prey capture in echolocating bats. *Physiol. Rev.* **70:** 615-641.
Neuweiler G (2000). *The Biology of Bats*. Oxford University Press: New York and Oxford.
Norberg UM (1981). Allometry of bat wings and legs and comparison with bird wings. *Phil. Trans. R. Soc. B* **292:** 359-398.
Norberg UM, Fenton MB (1988). Carnivorous bats. *Biol. J. Linn. Soc.* **33:** 383-394.
Norberg UM, Rayner JMV (1987). Ecological morphology and flight in bats (Mammalia; Chiroptera): wing adaptations, flight performance, foraging strategy and echolocation. *Phil. Trans. R. Soc. B* **316:** 335-427.
Olival KJ (Submitted). Correlates and evolutionary consequences of population genetic structure in bats. In: Gunnell GF and Simmons N (eds) *Evolutionary History of Bats: Fossils, Molecules and Morphology*: Cambridge.
Pio DV, Clarke FM, Mackie I, Racey PA (2010). Echolocation calls of the bats of Trinidad, West Indies: is guild membership reflected in echolocation signal design? *Acta Chiropt.* **12:** 217-229.
Pye A (1966a). The megachiroptera and vespertilionoidea of the microchiroptera. *J. Morphol.* **119:** 101-119.
Pye A (1966b). The structure of the cochlea in chiroptera. I. Microchiroptera: Emballonuroidea and Rhinolophoidea. *J. Morphol.* **118:** 495-510.
Pye A (1967). The structure of the cochlea in chiroptera. III. Microchiroptera: Phyllostomatoidea. *J. Morphol.* **121:** 241-254.
Rose KD, DeLeon VB, Missiaen P, Rana RS, Sahni A, Singh L *et al* (2008). Early Eocene lagomorph (Mammalia) from Western India and the early diversification of Lagomorpha. *Proc. R. Soc. B* **275:** 1203-1208.
Russo D, Jones G (2002). Identification of twenty-two bat species (Mammalia : Chiroptera) from Italy by analysis of time-expanded recordings of echolocation calls. *J. Zool.* **258:** 91-103.
Rydell J, Arita HT, Santos M, Granados J (2002). Acoustic identification of insectivorous bats (order Chiroptera) of Yucatan, Mexico. *J. Zool.* **257:** 27-36.

Schmidt U, Schlegel P, Schweizer H, Neuweiler G (1991). Audition in vampire bats, *Desmodus rotundus*. *J. Comp. Physiol. Sens. Neural. Behav. Physiol.* **168:** 45-51.
Seiffert ER, Simons EL, Attia Y (2003). Fossil evidence for an ancient divergence of lorises and galagos. *Nature* **422:** 421-424.
Simmons NB, Seymour KL, Habersetzer J, Gunnell GF (2008). Primitive Early Eocene bat from Wyoming and the evolution of flight and echolocation. *Nature* **451:** 818-821.
Smith AT, Xie Y (eds) (2008). *A guide to the mammals of China.* Princeton University Press: Princeton, pp 576.
Spoor F, Bajpal S, Hussaim ST, Kumar K, Thewissen JGM (2002). Vestibular evidence for the evolution of aquatic behaviour in early cetaceans. *Nature* **417:** 163-166.
Spoor F, Garland T, Krovitz G, Ryan TM, Silcox MT, Walker A (2007). The primate semicircular canal system and locomotion. *Proc. Natl. Acad. Sci. U. S. A.* **104:** 10808-10812.
Struebig MJ (2005). Bat diversity and ecology in lowland forest, southern Borneo. Final report of the UEA Kalimantan Bat Expedition, 2004 1-19.
Struebig MJ, Rossiter SJ, Bates PJJ, Kingston T, Oo SSL, Nwe AA *et al* (2005). Results of a recent bat survey in Upper Myanmar including new records from the Kachin forests. *Acta Chiropt.* **7:** 147-163.
Sun KP, Feng J, Jiang TL, Ma J, Zhang ZZ, Jin LR (2008). A new cryptic species of *Rhinolophus macrotis* (Chiroptera: Rhinolophidae) from Jiangxi Province, China *Acta Chiropt.* **10:** 1-10.
Surlykke A, Miller LA, Mohl B, Andersen BB, Christensendalsgaard J, Jorgensen MB (1993). Echolocation in 2 very small bats from Thailand - *Craseonycteris thonglongyai* and *Myotis siligorensis*. *Behav. Ecol. Sociobiol.* **33:** 1-12.
Teeling EC, Springer MS, Madsen O, Bates P, O'Brien SJ, Murphy WJ (2005). A molecular phylogeny for bats illuminates biogeography and the fossil record. *Science* **307:** 580-584.
Thabah A, Li G, Wang YN, Liang B, Hu KL, Zhang SY *et al* (2007). Diet, echolocation calls, and phylogenetic affinities of the great evening bat (*Ia IO;* Vespertilionidae): Another carnivorous bat. *J. Mammal.* **88:** 728-735.
Thollesson M, Norberg UM (1991). Moments of inertia of bat wings and body. *J. Exp. Biol.* **158:** 19-35.
Vater M, Siefer W (1995). The cochlea of *Tadarida brasiliensis*: Specialized functional organization in a generalized bat. *Hear. Res.* **91:** 178-195.
West CD (1985). The relationship of the spiral turns of the cochlea and the length of the basilar membrane to the range of audible frequencies in ground dwelling mammals. *J. Acoust. Soc. Am.* **77:** 1091-1101.
Yee D (2000). *Peropteryx macrotis Mamm. Species* **643:** 1-4.
Yigit N, Bulut S, Karatas A, Cam P, Saygili F (2008). Contribution the the distribution, morphological peculiarities, and karyology of the greater noctule, *Nyctalus lasioptrus* (Chiroptera: Vespertilionidae), in Southwestern Turkey. *Turk. J. Zool.* **32:** 53-58.
Zhang LB, Jones G, Zhang JS, Zhu GJ, Parsons S, Rossiter SJ *et al* (2009). Recent surveys of bats (Mammalia: Chiroptera) from China. I. Rhinolophidae and Hipposideridae. *Acta Chiropt.* **11:** 71-88.
Zimmer WMX, Johnson MP, Madsen PT, Tyack PL (2005). Echolocation clicks of free-ranging Cuvier's beaked whales (*Ziphius cavirostris*). *J. Acoust. Soc. Am.* **117:** 3919-3927.